IL
NUOVO CIMENTO
ORGANO DELLA SOCIETÀ ITALIANA DI FISICA
SOTTO GLI AUSPICI DEL CONSIGLIO NAZIONALE DELLE RICERCHE

VOL. XII, N. 3 *Serie nona* 1° Settembre 1954

On the Universal Fermi Interaction.

O. HARA, T. MARUMORI, Y. OHNUKI and H. SHIMODAIRA
Institute of Theoretical Physics, Nagoya University

(ricevuto il 25 Maggio 1954)

Summary. — It is shown that, by introducing the interaction in the form of the interaction of Urmaterie, a substance of higher level than elementary particles, the universal Fermi interaction with the combination $f_1(S - T + P) + f_2(S - A - P)$, where f_1 and f_2 are arbitrary constants, follows uniquely.

1. – Introduction.

Considerable evidence has been found in recent years to suggest that the coupling constants of various Fermi interactions are nearly equal. In the current theory of the theory of elementary particles, however, the introduction of the mutual interaction is done ad hoc, and this remarkable fact cannot help being regarded as entirely accidental.

It seems also the feeling of recent years that the specific combination $(aS - bT + cP)$ where a, b, and c are positive numbers of the order of unity [1], is most favoured, and several authors have pointed out that this combination is closely related to some symmetry properties of the interaction Hamiltonian

[1] D. PURSEY: *Physica*, **18**, 101 (1952); D. C. PEASLEE: *Phys. Rev.*, **91**, 1447 (1953); M. MORITA, J. FUJITA and M. YAMADA: *Prog. Theor. Phys.*, **10**, 630 (1953); E. J. KONOPINSKI and H. M. MAHMOUD: *Phys. Rev.*, **92**, 1045 (1953); R. FINKELSTEIN and P. KAUS: *Phys. Rev.*, **92**, 1316 (1953); L. MICHEL and A. WHIGHTMAN: *Phys. Rev.*, **93**, 314 (1954).

under the exchange of participating field variables ([2]). It is clear, however, that, in the current theory, any symmetry condition cannot claim more than an æsthetic reason.

Recently, we proposed the theory of Urmaterie, a substance of higher level than elementary particles, and by regarding elementary particles as phenomenal forms of Urmaterie, tried to grasp them in a unified way and more positively ([3]). We want to show in this paper that, by introducing the interaction in the form of the interaction of Urmaterie, a way is given of introducing the interaction in a unified way, which leads uniquely to the universal Fermi interaction with the combination $f_1(S-T+P)+f_2(S-A-P)$.

2. – The Derivation of the Universal Fermi Interaction.

We assume that various Fermi particles correspond to respective mass levels of spinor Urmaterie. We further assume that this Urmaterie is described by a spinor non-local field $\psi(X_\mu r_\mu)_\varrho$, $(\varrho = 1, 2, 3, 4)$. What is essential in our discussion is, however, the notion of Urmaterie, and the use of non-local field is only as a convention of materializing it. Indeed, our result is completely independent upon details of the way of describing Urmaterie.

The equation of motion of $\psi(X_\mu r_\mu)_\varrho$, was proposed by many authors. For example, the one proposed by YUKAWA ([4]) is

$$(\gamma_\mu \partial/\partial X_\mu + M)\psi(X_\mu r_\mu) = 0 \qquad (2.1)$$
$$(\beta_\mu r_\mu - \lambda)\psi(X_\mu r_\mu) = 0 \,,$$

which is derivable from a suitable Lagrangian.

It is clear, however, that the linear equation of such type would not hold except for the simplest case of zero order approximation, where the effect of the interaction is completely neglected. At the present, we know nothing of the interaction of Urmaterie. Under this circumstance, it seems reasonable to try to include it phenomenologically by adding a non-linear term L' to the original Lagrangian. This is analogous to the introduction of viscosity term in hydrodynamics.

The form of L' is restricted by the condition of Lorentz-invariance and that of beeing hermitic. The simplest one is the product of four ψ's:

$$(x'_\mu|L'|x''_\mu) = \sum_{i=1}^{5} g^i \int (x'_\mu|\bar{\psi}|x^{(1)}_\mu) O^i (x^{(1)}_\mu|\psi|x^{(2)}_\mu) \cdot \qquad (2.2)$$
$$\cdot (x^{(2)}_\mu|\bar{\psi}|x^{(3)}_\mu) O^i (x^{(3)}_\mu|\psi|x''_\mu)(\mathrm{d}x^{(1)})(\mathrm{d}x^{(2)})(\mathrm{d}x^{(3)}) \,, \qquad (g^i\text{'s are real})$$

([2]) M. FIERZ: *Zeits. f. Phys.*, **104**, 553 (1937); R. FINKELSTEIN and P. KAUS: loc. cit.; C. L. CRICTHFIELD: *Phys. Rev.*, **63**, 417 (1943).

([3]) O. HARA, T. MARUMORI, Y. OHNUKI and H. SHIMODAIRA: *Prog. Theor. Phys.* (in press). This is refered to as I.

([4]) H. YUKAWA: *Phys. Rev.*, **77**, 219 (1950).

where O^i mean Bethe's five covariants, and $i = 1, 2, 3, 4$ and 5 corresponds to S, V, T, A and P respectively.

As discussed in (1), $\psi(X_\mu r_\mu)_\varrho$ is a superposition of local fields with various rest masses;

$$\psi(X_\mu r_\mu)_\varrho = \sum_m \varphi_m\left((1/i)(\partial/\partial X_\mu), r_\mu\right) \psi_m(X_\mu)_\varrho \,. \tag{2.3}$$ (*)

From (2.1) it follows

$$(\gamma_\mu \partial/\partial X_\mu + m)\, \psi_m(X_\mu) = 0 \,,$$

and in this expanded form $\psi_m(X_\mu)$ corresponds to the local field of rest mass m, where $\varphi_m((1/i)(\partial/\partial X_\mu)r_\mu)$ is the eigenfunction of the internal motion belonging to the eigenvalue m of the mass operator.

We assume that the former is subjected to the usual procedure of the second quantization to yield creation and anihilation operators, while $\varphi_m((1/i)(\partial/\partial X_\mu)r_\mu)$ will be responsible to form factors when the interaction is introduced.

Substituting (2.3) into (2.2),

$$(x'_\mu \,|\, L' \,|\, x''_\mu) = \sum_{i=1}^{5} \sum_{\substack{m, m' \\ m'', m'''}} g^i \int \bar{\psi}_m(X_\mu) O^i \psi_{m'}(X'_\mu) \cdot \bar{\psi}_{m''}(X''_\mu) O^i \psi_{m'''}(X'''_\mu) \cdot$$

$$\cdot (\text{form factor}) \cdot (\mathrm{d}x) \,. \tag{2.4}$$

(2.4) represents various interactions of Fermi particles according to which Urmaterie takes the eigenvalue of the mass operator. It gives for example, the interaction of the nucleon and the μ-meson, of the μ-meson and the electron, or of the μ-meson and the nucleon .... according to the eigenvalue of m. Here an important fact is that they all appear with the same coupling constant g. This explains at once the equality of coupling constants of various Fermi interactions, since form factors are expected to reduce to δ-functions in low energy region. (By low energy region we mean energy region below approximately $(\hbar c/\lambda)$, λ beeing expected to be of the order of the Compton wave lenght of the nucleon, this corresponds to about 1 GeV).

(*) This form of φ_m corresponds to the restriction that M be a function of r_μ, $(1/i)\partial/\partial X_\mu$ and $(1/i)\partial/\partial r_\mu$, which is imposed by the requirement that M must be invariant under translations. For simplicity φ_m is assumed as scalar, and we do not touch the difficulty of infinite degeneracy pointed out by YUKAWA [5].

[5] H. YUKAXA: *Phys. Rev.*, **91**, 416, 416 (1953).

3. – The Derivation of $f_1(S-T+P)+f_2(S-A-P)$ Combination.

In § 2 we introduced the interaction in the form of (2.4), the essential part of which in low energy region is given by

$$(3.1)\qquad L'=\sum_{i=1}^{5}\sum_{\substack{m,m'\\ m'',m'''}} g^i\,\bar{\psi}_m(X_\mu)O^i\,\psi_{m'}(X'_\mu)\cdot\bar{\psi}_{m''}(X''_\mu)O^i\psi_{m'''}(X'''_\mu)\cdot \\ \cdot\,\delta(X_\mu-X'_\mu)\,\delta(X'_\mu-X''_\mu)\,\delta(X''_\mu-X'''_\mu)\,.$$

It is our basic assumption that the universal Fermi interaction corresponding to a specified process is given by the sum of terms of (3.1) contributing to it. Suppose, for example, $m=P, N, e$, and ν corresponds to the proton, neutron, electron and neutrino respectively. Then terms contributing to the β-disintegration are given by

$$(3.2)\qquad \sum_{i=1}^{5} g^i\big\{\bar{\psi}_{\mathrm{P}}(X_\mu)\,O^i\psi_{\mathrm{N}}(X'_\mu)\cdot\bar{\psi}_{\mathrm{e}}(X''_\mu)\,O^i\psi_{\nu}(X'''_\mu)+ \\ +\bar{\psi}_{\mathrm{P}}(X_\mu)O^i\psi_{\nu}(X'''_\mu)\cdot\bar{\psi}_{\mathrm{e}}(X''_\mu)O^i\psi_{\mathrm{N}}(X'_\mu)+\bar{\psi}_{\mathrm{e}}(X''_\mu)O^i\psi_{\mathrm{N}}(X'_\mu)\cdot\bar{\psi}_{\mathrm{P}}(X_\mu)O^i\psi_{\nu}(X'''_\mu)+ \\ +\bar{\psi}_{\mathrm{e}}(X''_\mu)O^i\psi_{\nu}(X'''_\mu)\cdot\bar{\psi}_{\mathrm{P}}(X_\mu)O^i\psi_{\mathrm{N}}(X'_\mu)\big\}\cdot\,\delta(X_\mu-X'_\mu)\,\delta(X'_\mu-X''_\mu)\,\delta(X''_\mu-X'''_\mu)\,.$$

Corresponding interaction of the current theory

$$(3.3)\qquad \sum_{i=1}^{5} G^i\,\bar{\psi}_{\mathrm{P}}O^i\psi_{\mathrm{N}}\cdot\bar{\psi}_{\mathrm{e}}O^i\psi_{\nu}\,,$$

is obtained by rewriting it using Fierz's formula ([2]);

$$\begin{aligned}
4S'&=S+V+T+A+P,\\
4V'&=4S-2V+2A-4P,\\
4T'&=6S-2T+6P,\\
4A'&=4S+2V-2A-4P,\\
4P'&=S-V+T-A+P,
\end{aligned}$$

where for example

$$S'=\bar{\psi}_{\mathrm{P}}\psi_{\nu}\cdot\bar{\psi}_{\mathrm{e}}\psi_{\mathrm{N}}\,,$$

or

$$=\bar{\psi}_{\mathrm{e}}\psi_{\mathrm{N}}\cdot\bar{\psi}_{\mathrm{P}}\psi_{\nu}\,.$$

(3.2) is obviously invariant under the exchange of $\bar{\psi}_{\mathrm{P}}(X_\mu)$ and $\bar{\psi}_{\mathrm{e}}(X''_\mu)$, as well as of $\psi_{\mathrm{N}}(X'_\mu)$ and $\psi_{\nu}(X'''_\mu)$. Therefore, (3.3) must have the same symmetry.

This is an important consequence of introducing the interaction in the form of (3.1), and it is the purpose of this section to show that this symmetry condition determines the possible form of $\sum_i O^i$ to $f_1(S-T+P)+f_2(S-A-P)$ uniquely.

In what follows we return to the general form, and start from

$$(3.5)\quad \sum_{i=1}^{5} g^i \{\bar{\psi}_m(X_\mu)O^i\psi_{m'}(X'_\mu)\cdot\bar{\psi}_{m''}(X''_\mu)O^i\psi(X'''_\mu)+\bar{\psi}_m(X_\mu)O^i\psi_{m'''}(X'''_\mu)\cdot\bar{\psi}_{m''}(X''_\mu)O^i\psi_{m'}(X'_\mu)\}\cdot \\ \cdot\,\delta(X_\mu-X'_\mu)\,\delta(X'_\mu-X''_\mu)\,\delta(X''_\mu-X'''_\mu)\,,$$

where we fix the position of bared variables, since nothing new is added by the exchange of them.

What is needed first is the commutation relations. We assume

$$(3.6)\quad \{\psi_m(X_\mu)_\alpha\,,\ \psi_{m'}(X'_\mu)_\beta\}=\{\bar{\psi}_m(X_\mu)_\alpha\,,\ \bar{\psi}_{m'}(X'_\mu)_\beta\}=0\,,$$

and

$$\{\psi_m(X_\mu)_\alpha\,,\ \bar{\psi}_{m'}(X'_\mu)_\beta\}=(1/i)\delta_{mm'}S_{m'}(X_\mu-X'_\mu)\,,$$

where $\{\}$ means anti-commutator, and $S_m(X_\mu-X'_\mu)$ is the usual S-function for particles of rest mass m.

Using (3.6), the rewriting of the second term of (3.5) can be performed explicitely:

$$(3.7)\quad \sum_{i=1}^{5} g^i\,\bar{\psi}_m(X_\mu)O^i\psi_{m''}(X'''_\mu)\cdot\bar{\psi}_{m''}(X''_\mu)O^i\psi_{m'}(X'_\mu)= \\ =\sum_{i=1}^{5} a^i\,\bar{\psi}_m(X_\mu)O^i\psi_{m'}(X'_\mu)\cdot\bar{\psi}_{m''}(X''_\mu)O^i\psi_{m'''}(X'''_\mu)+ \\ +(1/i)\,\delta_{m''m'''}\sum_{i=1}^{5} g^i\bar{\psi}_m(X_\mu)O^iS_{m''}(X'''_\mu-X''_\mu)O^i\psi_{m'}(X'_\mu)+ \\ +(1/i)\,\delta_{m'm''}\sum_{i=1}^{5} g^i\bar{\psi}_m(X_\mu)O^i\psi_{m''}(X'''_\mu)\cdot\mathrm{Sp}\{O^iS_{m'}(X'_\mu-X''_\mu)\}\,,$$

where a^i's are some constants. The first term is opposite signed to the one obtained when $\psi_m(X_\mu)$'s are treated as c-number, which is the consequence of three times exchanges of $\psi(X_\mu)$'s.

The appearing of bilinear terms in (3.7) imposes a condition to O^i of (2.2), which we have hitherto regarded as entirely arbitrary except for the condition of Lorentz-invariance and that of being hermitic. Bilinear terms in the Lagrangian give linear ones in the equation of motion. They express, for example,

the mass correction of the nucleon due to virtual leptons. As mentioned in § 2, however, our standpoint was a phenomenological one as far as the interaction of Urmaterie was concerned. This implies that, so long as we stand on this standpoint, all linear effects must be understood to be taken in the free equation whatever its origin may be, and the introduction of non-linear terms must be understood to include effects not expressible in the free equation. We assume that our free equation is already constructed in accordance with this requirement, and therefore the effects of bilinear terms are already included in it. Thus, L' of (2.2) must be so chosen that it is essentially non-linear. This restricts O^i to some extent. To formulate this condition here precisely is not necessary, and it is sufficient to assume that O^i's are so chosen that bilinear terms do not appear in (3.7). The consistency of this assumption will be checked later.

Under this assumption, we get as the rewriting of (3.5)

$$\sum_i G^i\, \bar{\psi}_m(X_\mu) O^i \psi_{m'}(X'_\mu) \cdot \bar{\psi}_{m''}(X''_\mu) O^i \psi_{m'''}(X'''_\mu)\,, \qquad (G^i = a^i + 1) \tag{3.7'}$$

which symmetry condition must be satisfied as before. The exchange of $\psi_m(X'_\mu)$ and $\psi_{m'''}(X'''_\mu)$ yields

$$\begin{aligned} \sum_{l=1}^{5} G^i\, \bar{\psi}_m(X_\mu) O^i \psi_{m'''}(X'''_\mu) \cdot \bar{\psi}_{m''}(X''_\mu) O^i \psi_{m'}(X'_\mu) = \\ = \sum_{i=1}^{5} G^{i\prime} \bar{\psi}_m(X_\mu) O^i \psi_{m'}(X'_\mu) \cdot \bar{\psi}_m(X''_\mu) O^i \psi_{m'''}(X'''_\mu) + \\ + (1/i)\, \delta_{m''m'''} \sum_{i=1}^{5} G^i \bar{\psi}_m(X_\mu) O^i S_{m''}(X''_\mu - X''_\mu) O^i \psi_{m'}(X'_\mu) + \\ + (1/i)\, \delta_{m'm''} \sum_{i=1}^{5} G^i\, \bar{\psi}_m(X_\mu) O^i\, \psi_{\mu'''}(X'''_\mu) \cdot \mathrm{Sp}\left\{ O^i S_{m'}(X'_\mu - X''_\mu) \right\}. \end{aligned} \tag{3.8}$$

Therefore, the symmetry condition requires

i) The restoration of the first term to the original form (3.7'), and

ii) The vanishing of bilinear terms.

i) corresponds to the condition of antisymmetry in the c-number theory. This restricts $\sum_i O^i$ to be one of

$$\begin{cases} a) \quad S - T + P, \\ b) \quad A - V, \\ c) \quad S - A - P, \end{cases} \tag{3.9}$$

or a linear combination of them. Of solutions of (3.9), only those that satisfy ii) are admissible ones. The vanishing of bilinear terms requires first

$$\mathrm{Sp}\left\{O^i S_{m'}(X'_\mu - X''_\mu)\right\} \cdot \delta(X'_\mu - X''_\mu) = 0 ,$$

where $\delta(X'_\mu - X''_\mu)$ comes from (3.1). Substituting explicit form for $S_{m'}(X'_\mu - X''_\mu)$

$$S_{m'}(X'_\mu - X''_\mu) = (\gamma_\mu \partial/\partial X'_\mu - m)\Delta(X'_\mu - X''_\mu) ,$$

(3.10) is reduced to

$$\mathrm{Sp}\ \{ O^i \gamma_4 \} = 0 ,$$

since

$$\Delta(X'_\mu - X''_\mu) \cdot \delta(X'_\mu - X''_\mu) = 0 ,$$

and

$$\partial_k \Delta(X'_\mu - X''_\mu) \cdot \delta(X'_\mu - X''_\mu) = 0 \qquad \text{for } k = 1, 2, 3 .$$

(3.11) selects out $(S - T + P)$ and $(S - A - P)$ from (3.9). It is clear that these combinations annullate another bilinear term;

$$\sum_{i=1}^{5} G^i O^i S_{m'}(X'''_\mu - X''_\mu) O^i \cdot \delta(X'''_\mu - X''_\mu) = 0 .$$

This is seen from

$$O^i \gamma_\mu O^i = \begin{cases} \gamma_\mu & \text{for } S, \\ -2\gamma_\mu & \text{for } V, \\ 0 & \text{for } T, \\ 2\gamma_\mu & \text{for } A, \\ -\gamma_\mu & \text{for } P. \end{cases} \tag{3.12}$$

Therefore, the combination of (3.7) is determined to

$$f_1(S - T + P) + f_2(S - A - P) , \tag{3.13}$$

where f_1 and f_2 are arbitrary (real) constants. This is effectively equivalent to restrict at the beginning $\sum_i O^i$ of (2.2) to (3.13).

It is also clear that this combination satisfies the condition of beeing essentially non-linear. The consistency of our discussion is therefore assured, and we see that an apparently artificial appearing of the specific combination is closely related to the rewriting of the second term of (3.5).

4. – Discussion.

Thus, we see that the universal Fermi interaction of the type of (3.13) follows as an immediate consequence of introducing the interaction in the form of the interaction of Urmaterie. If the universal interaction of this type is established, therefore, it may be regarded as a strong support for assuming Urmaterie.

Recent data suggest $f_2 = 0$. It would be an important problem in the next stage of our theory to examine how this fact restricts the type or the mechanism of the interaction of Urmaterie.

A remarkable conclusion suggested by our model is that the universal Fermi interaction will fail to hold in high energy region. This is because the approximation of replacing form factors by δ-functions is not permitted there. The critical energy will be of the order of GeV as discussed in § 2.

It must of course be stressed that many problems remain untouched in this paper. For example, we gave no attention to unwanted processes contained in our formalism. That the coupling constants of various Fermi interactions are nealry equal, and that they appear in a specific combination are, however, the most essential features of the universal Fermi interaction, and our main purpose is to show that they can be reproduced to considerable extent by introducing the interaction in the form of the interaction of Urmaterie. In particular, it should be noted that this follows as an immediate consequence, not depending upon details of the way of describing Urmaterie, of treating the interaction of non-local fields, or upon the form of the mass operator.

In conclusion, we wish to express our sincere gratitude to Prof. S. SAKATA for his interest in this work.

RIASSUNTO (*)

Si dimostra che, introducendo l'interazione sotto forma di interazione dell' « Urmaterie », sostanza di livello superiore a quello delle particelle elementari, ne consegue univocamente l'interazione universale di Fermi con la combinazione $f_1(S - T) + P) + f_2(S - A - P)$, dove f_1 e f_2 sono costanti arbitrarie.

(*) *Traduzione a cura della Redazione.*

IL NUOVO CIMENTO Vol. XII, N. 3 1° Settembre 1954

Normal Products of Heisenberg Operators.

J. C. Polkinghorne

Trinity College - Cambridge, England

(ricevuto il 14 Giugno 1954)

Summary. — The properties required of a normal product are discussed and a definition of the normal product of Heisenberg operators that fulfils these requirements is given. Rules for obtaining the differential equations satisfied by these products are stated.

1. – Introduction.

Interaction representation operators may be decomposed into positive and negative frequency parts in a Lorentz invariant manner and normal (N–) products defined in terms of them. This is not possible for Heisenberg operators. In this paper we seek to define a normal (N'–) product of Heisenberg operators that possesses the analogous properties to those that make the N-product important in the interaction representation.

The two most important properties of N-products are:

i) The vacuum expectation value of any N-product is zero.

ii) N-products obey the equations of motion; for example

$$\mathcal{D}_x N(\psi(x)\ldots) = 0\,, \tag{1}$$

where $\mathcal{D}_x$ is the Dirac operator for the coordinate x.

We shall require our N'-products to satisfy the Heisenberg analogues of these two conditions. In addition they must satisfy the condition:

iii) The N'-product becomes the N-product when the coupling constant tends to zero.

Several authors have given definitions of normal products that do not satisfy these conditions ([1,2,3]).

2. – Functional Equations.

We shall consider the case of nucleons interacting with pseudoscalar mesons. In order to state the Heisenberg analogue of condition ii) it is necessary to use the functional technique of SCHWINGER ([4]). This requires us to work in terms of matrix elements. We shall use the notation

$$\langle F(x)\rangle = \frac{\langle \Psi_0 | F(x) | \Psi \rangle}{\langle \Psi_0 | \Psi_0 \rangle} , \tag{2}$$

where $F(x)$ is any function of Heisenberg operators, Ψ_0 is the state vector of the true vacuum, and Ψ is the state vector of the state we are considering. Source functions, η and $\bar{\eta}$ for the nucleon field and K for the meson field, are introduced and play an important part in the theory. The following relations hold as simple generalisations of equations given by SCHWINGER for the functional derivatives of matrix elements with respect to the source functions:

$$\frac{\delta}{\delta\bar{\eta}(x)} \langle T(x_i \ldots; y_j \ldots; z_k \ldots)\rangle = i\langle T(x x_i \ldots; y_j \ldots; z_k \ldots)\rangle - \tag{3}$$
$$- i\langle T(x_i \ldots; y_j \ldots; z_k)\rangle \langle \psi(x)\rangle_0 ,$$

$$\frac{\delta}{\delta\eta(y)} \langle T(x_i \ldots; y_j \ldots; z_k \ldots)\rangle = i\langle T(x_i \ldots; y_j \ldots y; z_k \ldots)\rangle - \tag{4}$$
$$- i\langle T(x_i \ldots; y_j \ldots y; z_k \ldots)\rangle \langle \bar{\psi}(y)\rangle_0 ,$$

$$\frac{\delta}{\delta K(z)} \langle T(x_i \ldots; y_j \ldots; z_k \ldots)\rangle = i\langle T(x_i \ldots; y_j \ldots; z z_k \ldots)\rangle - \tag{5}$$
$$- i\langle T(x_i \ldots; y_j \ldots; z_k \ldots)\rangle \langle \varphi(z)\rangle_0 ,$$

$\langle T(x_i \ldots; y_j \ldots; z_k)\rangle$ denotes the matrix element of the product $T(\psi(x_i) \ldots \bar{\psi}(y_j) \ldots \varphi(z_k) \ldots)$ defined by WICK ([5]), and $\rangle_0$ denotes that Ψ is replaced by Ψ_0. The functional derivatives are defined by

$$\delta F = \int \mathrm{d}x' \, \delta\bar{\eta}(x') \frac{\delta F}{\delta\bar{\eta}(x')} , \tag{6}$$

$$\delta F = \int \mathrm{d}y' \frac{\delta F}{\delta\eta(y')} \delta\eta(y') , \tag{7}$$

$$\delta F = \int \mathrm{d}z' \delta K(z') \frac{\delta F}{\delta K(z')} . \tag{8}$$

([1]) P. T. MATTHEWS and A. SALAM: *Proc. Roy. Soc.*, A **221**, 128 (1953).
([2]) K. NISHIJIMA: *Prog. Theor. Phys.*, **10**, 549 (1953).
([3]) E. FREESE: *Zeits. f. Naturfor.*, **8***a*, 775 (1953).
([4]) J. SCHWINGER: *Proc. Nat. Acad. Sci.*, **37**, 452 (1951).
([5]) G. C. WICK: *Phys. Rev.*, **80**, 268 (1950).

Other operators in this theory that are important are the mass correction operators M_x, $\overline{M}_y$, K_z^2. These are defined by the equations

$$M_x\langle T(x\ldots;\ \ldots;\ \ldots)\rangle = -\,g\gamma_5(x)\langle T(x\ldots;\ \ldots;\ x\ldots)\rangle\,, \tag{9}$$

$$\overline{M}_y\langle T(\ldots;\ y\ldots;\ \ldots)\rangle = -\,g\gamma_5(y)\langle T(\ldots;\ y\ldots;\ y\ldots)\rangle\,, \tag{10}$$

$$K_z^2\langle T(\ldots;\ \ldots;\ z\ldots)\rangle = -\,g\gamma_5(z)\langle T(\ldots z;\ z\ldots;\ \ldots)\rangle\,. \tag{11}$$

The simbol $\gamma_5(x)$ has the meaning defined by MATTHEW and SALAM [1] and is just a device to obtain the correct spinor suffices. Operating on T-products that do not contain the appropriate field operator at the appropriate space time point these operators are defined to give zero. The Heisenberg analogues of the Dirac and Klein-Gordon operators are

$$\mathcal{D}_x' = \mathcal{D}_x + M_x\,, \tag{12}$$

$$\overline{\mathcal{D}}_y' = \mathcal{D}_y + \overline{M}_y\,, \tag{13}$$

$$\mathcal{K}_z' = \mathcal{K}_z + K_z^2\,. \tag{14}$$

Of particular importance are the functions defined by

$$G(x\ldots;\ y\ldots;\ z\ldots) = \langle T(x\ldots;\ y\ldots;\ z\ldots)\rangle_0\,. \tag{15}$$

They satisfy the equations

$$\mathcal{D}_x'G(x\ldots;\ y_j\ldots;\ \ldots) = \sum_j \delta(x-y_j)G(x^{-1}\ldots;\ y_j^{-1}\ldots;\ \ldots)\,, \tag{16}$$

$$\overline{\mathcal{D}}_y G(x_i\ldots;\ y\ldots;\ \ldots) = \sum_i \delta(y-x_i)G(x_i^{-1}\ldots;\ y^{-1};\ \ldots)\,, \tag{17}$$

$$\mathcal{K}_z'G(\ldots;\ \ldots;\ zz_k\ \ldots) = \sum_k \delta(z-z_k)G(\ldots;\ \ldots;\ z^{-1}z_k^{-1}\ldots)\,, \tag{18}$$

where, for example, $G(x^{-1}\ldots;\ y_j^{-1};\ \ldots)$ is the G function with x and y_j omitted from its arguments and the function multiplied by $(-)^n$, where n is the number of nucleon operators between $\psi(x)$ and $\overline{\psi}(y_j)$ in the corresponding T-product. These equations follow from some given by MATTHEWS and SALAM [1, 6]. Equations analogous to equations (3)-(5) hold for the effect of functional derivatives on the G's.

---

[6] An error in sign has been corrected.

3. – N'-products.

We define N'-products implicitly by the set of equations

$$T(x_1x_2\ldots;\ y_1y_2\ldots;\ z_1z_2\ldots) = \tag{19}$$
$$= N'(x_1x_2\ldots;\ y_1y_2\ldots;\ z_1z_2\ldots) + \sum \varepsilon G(x_1\ldots;\ y_1\ldots;\ z_1\ldots)N'(x_2\ldots;\ y_2\ldots;\ z_2\ldots)\ .$$

The sum on the right hand side is taken over all ways of dividing the x's y's and z's between the G functions and the N'-products, and ε is the signature of the permutation of the nucleon factors from their order in the T-product to their order in the sum. If Heisenberg operators are replaced by interaction representation operators, and the true vacuum by the bare vacuum in the definition of the G functions, equation (19) becomes Wick's theorem ([5]). Therefore the definition (19) certainly satisfies the condition iii) of section 1.

In principle it is possible to solve the set of equations for the N'-products in terms of the T-products. However the general result is too complicated to be worth considering in detail. Another method for obtaining this result will be given below.

The N'-products satisfy the equations

$$\langle N'(x\ldots;\ y\ldots;\ z\ldots)\rangle_0 = 0\ . \tag{20}$$

This is the analogue of property i). It is readily obtained by verifying that (20) makes $\langle(19)\rangle_0$ true for all T-products. All the properties of N'-products that we shall state in this paper are most easily obtained in this indirect fashion by performing suitable operations on equations (19) and using the properties of T-products given in section 2. The actual labour of verifying that they are correct is both trivial to perform and tedious to state and so will be omitted.

Equations (16)-(18) together with the definitions of the mass correction operators enable us to prove the property of N'-products analogous to property ii). This is that the following relations hold:

$$\mathscr{D}'_x\langle N'(x\ldots;\ \ldots;\ \ldots)\rangle = 0\ , \tag{21}$$

$$\mathscr{D}'_y\langle N'(\ldots;\ y\ldots;\ \ldots)\rangle = 0\ , \tag{22}$$

$$\mathscr{K}'_z\langle N'(\ldots;\ \ldots;\ z\ldots)\rangle = 0\ . \tag{23}$$

Another interesting property possessed by N'-products is concerned with their functional derivatives with respect to the source functions. These satisfy

the relations:

$$\frac{\delta}{\delta\bar{\eta}(x)}\langle N'(\ldots;\ \ldots;\ \ldots)\rangle = i\langle N'(x\ldots;\ \ldots;\ \ldots)\rangle\ , \tag{24}$$

$$\frac{\delta}{\delta\eta(y)}\langle N'(\ldots;\ \ldots;\ \ldots)\rangle = i\langle N'(\ldots\ ;\ \ldots y;\ \ldots)\rangle\ , \tag{25}$$

$$\frac{\delta}{\delta K(z)}\langle N'(\ldots;\ \ldots;\ \ldots)\rangle = i\langle N'(\ldots;\ \ldots;\ z\ldots)\rangle\ . \tag{26}$$

This implies that the set of matrix elements of all N'-products can be obtained by applying all combinations of source-functional derivatives to

$$\frac{\Psi_0\ \Psi}{\langle\Psi_0|\Psi_0\rangle}\ .$$

This provides the simplest way of expressing N'-products in terms of T-products. This definition of N'-products has also been given, *inter alia*, by FREESE (7). If source functions are introduced for non-interacting fields a similar definition may be given for the normal product of interaction representation operators.

4. – Differential Equations.

The equations (21)-(23) are not very convenient to work with and so we shall gives rules for determining a more tractable set of differential equations satisfied by the N'-products. We take as our starting point the definition given at the end of the last section. This shows that

$$\mathcal{D}_x\langle N'(xx_i\ldots;\ y_j\ldots;\ z_k\ldots) = (-)^{N-1}\left(-i\frac{\delta}{\delta\bar{\eta}(x_i)}\right)\ldots\left(-i\frac{\delta}{\delta\eta(y_j)}\right)\ldots\left(-i\frac{\delta}{\delta K(z_k)}\right)\ldots \mathcal{D}_x\langle N'(x,,)\rangle\ , \tag{27}$$

where N is the number of nucleon factors and the term $(-)^{N-1}$ arises from the fact that the derivatives with respect to the nucleon source functions anti-commute. Similar equations hold for the effect of $\mathcal{D}_y$ and K_z. These equations, together with the equations

$$\mathcal{D}_x\langle N'(x,,)\rangle = \left[\langle\varphi(x)\rangle_0 - i\frac{\delta}{\delta K(x)}\right] g\gamma^5\langle N'(x,,)\rangle + \bar{\eta}(x)[\langle\ \rangle - \langle\ \rangle_0]\ , \tag{28}$$

$$\overline{\mathcal{D}}_y\langle N'(,y,)\rangle = \left[\langle\varphi(y)\rangle_0 - i\frac{\delta}{\delta K(y)}\right]\langle N'(,y,)\rangle g\gamma^5 + \eta(y)[\langle\ \rangle - \langle\ \rangle_0]\ , \tag{29}$$

$$\mathcal{K}_z\langle N'(,,z)\rangle = \left[\langle\psi(z)\rangle_0 - i\frac{\delta}{\delta\bar{\eta}(z)}\right] g\gamma^5\left[\langle\bar{\psi}(z)\rangle_0 - i\frac{\delta}{\delta\eta(z)}\right][\langle\ \rangle - \langle\ \rangle_0] + K(z)[\quad - \quad_0]\ . \tag{30}$$

(7) E. FREESE: *Nuovo Cimento*, **11**, 312 (1954).

enable us to determine the effect of a Dirac or Klein-Gordon operator upon any N'-product. (The source functions are put equal to zero after the differentiations have been performed). The result is a series of coupled equations for the N'-products. These are of great complexity in the general case and we shall be content to illustrate their form by the following examples:

$$\mathcal{D}_x\langle N'(xx',,)\rangle = g\gamma_5\langle N'(xx',, x)\rangle\,, \tag{31}$$

$$\mathcal{D}_x\langle N'(xx',, z)\rangle = g\gamma_5\langle N'(xx',, xz)\rangle + ig\gamma_5 G(,, xz)\langle N'(xx',,)\rangle\,. \tag{32}$$

RIASSUNTO (*)

Si discutono le proprietà che si richiedono da un prodotto normale e si dà una definizione del prodotto normale degli operatori di Heisenberg che soddisfa tali esigenze. Si danno regole per ricavare le equazioni differenziali soddisfatte da questi prodotti.

(*) *Traduzione a cura della Redazione.*

No-Pair Terms in the Adiabatic Nuclear Potential.

E. A. Power (*)

Laboratory of Nuclear Studies Cornell University - Ithaca, N.Y.

(ricevuto il 18 Giugno 1954)

Summary. – A critical analysis is made of the controversial no-pair and non-adiabatic terms in the nuclear force problem. As a specific example the scalar theory is examined carefully. It is shown that the non-static corrections are required to the adiabatic local potential to give the correct phase shifts in Born approximation.

1. – Introduction.

The investigation of higher order effects in the meson theory of nuclear forces was initiated by Bethe [1] who demonstrated that, due to the properties of the pseudoscalar coupling, large contributions to the potential energy of interaction between two nucleons are to be expected from the exchange of two mesons. Detailed computations using S-matrix theory were carried through by Watson and Lepore [2], who included radiative corrections, and by Taketani, Machida and Onuma [3] for the non-divergent terms of the pseudovector coupling theory. With the recent development initiated by Lévy [4] the non-adiabatic method of Tamm [5] and Dancoff [6] has led to a field

(*) On leave of absence from the Department of Mathematics, University College, London, England.

(1) H. A. Bethe: *Phys. Rev.*, **76**, 191 (1949).

(2) K. M. Watson and J. V. Lepore: *Phys. Rev.*, **76**, 1157 (1949).

(3) M. Taketani, S. Machida and S. Onuma: *Prog. Theor. Phys.* (Japan), **7**, 45 (1952).

(4) M. M. Lévy: *Phys. Rev.*, **88**, 72 and 725 (1952).

(5) I. Tamm : *Journ. Phys.* (*USSR*), **9**, 449 (1945).

(6) S. Dancoff: *Phys. Rev.*, **78**, 382 (1950).

theoretical deduction of a Schrödinger-like equation for the two particle amplitude up to a certain order in G^2 (7). That this equation is not of the conventional form, since the amplitude is not the exact wavefunction and since the kernel contains the total energy eigenvalue W, has been emphasized by FELDMAN (8). It was recognized by TAMM and by DANCOFF that the interaction kernel is energy dependent. No one has succeeded in solving exactly the integral equation which arises and it is usual to make approximations resulting in an adiabatic kernel. The new Tamm-Dancoff theory has been considered by KURŞUNOĞLU (9) with the resulting adiabatic potential equivalent to that of KLEIN (7). BRUECKNER and WATSON (10) initiated their own method for solving the field theoretical Schrödinger equation and have obtained an adiabatic potential distinct from KLEIN; so also have HENLEY and RUDERMAN (11). Both pairs of authors consider multiple scattering effects of the virtual mesons; the resulting potential given by the latter authors differs little from that of TAKETANI *et al.*, the resonance (12) which occurs in real scattering of p-wave mesons is not reproduced on account of the different energy-momentum relationship for virtual mesons.

It is now agreed that the sum of the two-pair and one-pair contributions to the potential, being of attractive and repulsive character respectively, gives insufficient binding and becomes strongly repulsive for $\mu r \sim 0.5$. The no-pair term contribution is thus of major importance. The scattering matrix teory (13) gives

$$
\begin{aligned}
(1) \qquad V_4^{(0)} = -\left(\frac{G^2}{4\pi}\right)^2 \left(\frac{\mu}{2M}\right)^4 \mu \frac{1}{\mu^4 r^4} \frac{2}{\pi} \{ & [(23 + 4\mu^2 r^2)\mu r K_0(2\mu r) + \\
& + (23 + 12\mu^2 r^2) K_1(2\mu r)] \boldsymbol{\tau}_1 \cdot \boldsymbol{\tau}_2 - [12\mu r K_0(2\mu r) + \\
& + (12 + 8\mu^2 r^2) K_1(2\mu r)] \underline{\sigma}_1 \cdot \underline{\sigma}_2 + [12\mu r K_0(2\mu r) + \\
& + (15 + 4\mu^2 r^2) K_1(2\mu r)] S_{12} \} .
\end{aligned}
$$

The central potential is attractive for the singlet s-state and allows a fit to experiment; for the triplet state the central part is repulsive and, unless a cut-off is chosen to give sufficient binding for the tensor force, it gives no fit

(7) A. KLEIN: *Phys. Rev.*, **90**, 1101 (1953).
(8) D. FELDMAN: *Bull. Am. Phys. Soc.*, **28**, 6, 31 (1953).
(9) B. KURŞUNOĞLU: *Phys. Rev.* (in cours of publication).
(10) K. A. BRUECKNER and K. M. WATSON: *Phys. Rev.*, **92**, 1023 (1953).
(11) E. M. HENLEY and M. A. RUDERMAN: *Phys. Rev.*, **92**, 1036 (1953).
(12) G. CHEW: *Phys. Rev.*, **89**, 591 (1953); S. FUBINI: *Nuovo Cimento*, **10**, 564 (1953); H. A. BETHE and F. J. DYSON: *Phys. Rev.*, **90**, 372 (1953).
(13) Reference (3); there are two misprints. The factors U_σ should contain $3/x^3 k_0(2x)$ and U_τ should contain $(3/x^2 + 23/4x^4) k_1(2x)$.

to the deuteron data. Recently FUJII, IWADARE, OTSUKI, TAKETANI, TANI and WATARI [14] have applied this potential to the 40 MeV and 90 MeV nucleon-nucleon scattering with fair agreement subject again to the central potential being cut-off at $\mu r \sim 0.5$. The correction due to multiple scattering found by HENLEY and RUDERMAN is repulsive in all states and is of magnitude 20% of the perturbation theory energy. In the method of Tamm and Dancoff the fourth order irreducible kernel consists of contributions from the eight graphs:

(2) 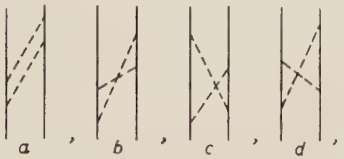 + reflections;

it excludes the reducible orderings of emission and absorption represented by the four graphs:

(3) 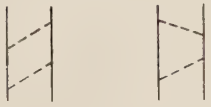 + reflections.

This irreducible contribution in the adiabatic limit gives [10] a potential

$$V^{(0)}_{4,I} = V^{(0)}_{4} - V^{(0)}_{4,R}, \tag{4}$$

where

$$V^{(0)}_{4,R} = \left(\frac{G^2}{4\pi}\right)^2 \left(\frac{\mu}{2M}\right)^4 \mu \frac{2(3 - 2\boldsymbol{\tau}_1\cdot\boldsymbol{\tau}_2)}{\pi} \frac{e^{-\mu r}}{\mu^4 r^4} \Big\{ (2 + 2\mu r + \mu^2 r^2)\mu r K_0(\mu r) + \tag{5}$$

$$+ (4 + 4\mu r + \mu^2 r^2) K_1(\mu r) + \frac{2}{3}[(1 + \mu r)\mu r K_0(\mu r) + (2 + 2\mu r + \mu^2 r^2) K_1(\mu r)]\underline{\sigma}_1\cdot\underline{\sigma}_2 -$$

$$- \frac{1}{3}[(1 + \mu r)\mu r K_0(\mu r) + (5 + 5\mu r + \mu^2 r^2) K_1(\mu r)] S_{12} \Big\}.$$

The central part of $V^{(0)}_{4,R}$ is repulsive for all triplet states. When this potential is subtracted from $V^{(0)}_{4}$ it leaves an attractive potential in both singlet and triplet s-states. This final potential $V^{(0)}_{4,I}$, together with a repulsive core, is the one considered by BRUECKNER and WATSON which fits the low energy

---

[14] S. FUJII, J. IWADARE, S. OTSUKI, M. TAKETANI, S. TARI and W. WATARI: *Prog. Theor. Phys.* (*Japan*), **11**, 11 (1954).

data to about 10% including a large quadruple moment $2.83 \cdot 10^{-28}$ cm^2. The controversy concerning the no-pair term lies just in the four-graph contribution (5) or, in the Tamm-Dancoff formalism, the similar terms arising from non-adiabatic corrections to the G^2 kernel. This note is an attempt to clarify the no-pair contribution to the fourth order adiabatic nuclear potential by considering various perturbation approximations possible on the field theoretical Schrödinger equation and also the iteration and uniteration procedures used in the Tamm-Dancoff method.

2. – No-Pair Terms.

In the Tamm-Dancoff theory used by LÉVY and KLEIN and also in the approach used by BRUECKNER and WATSON the kernels in the integral equation for the two-particle amplitude are energy dependent and contain recoil effects. We distinguish two approximations made in the kernel. The first is to consider ε, the difference between the total energy W and the rest mass of the two nucleons $2M$, as small compared with the rest mass of the meson. The second, which we will call the static approximation, is to consider the recoil energy of the nucleons in the intermediate states as small compared with the meson energy. The adiabatic limit is that obtained by going to the extreme limit in both these approximations. Neutral scalar meson theory can enlighten us on the static approximation since here the two body problem is exactly soluble for fixed nucleon sources giving as the interaction energy the Yukawa potential.

The second order kernel, in the non-relativistic approximation for the nucleons, is

$$K^{(2)}(\underline{p}, \underline{p}') = \frac{G^2 Q}{\omega(k)\left\{\varepsilon - \frac{p^2}{2M} - \frac{p'^2}{2M} - \omega(k)\right\}}, \tag{6}$$

where $\underline{k} = \underline{p} - \underline{p}'$ and

$$\begin{aligned} Q &= 1 && \text{scalar neutral} \\ &= \boldsymbol{\tau}_1 \cdot \boldsymbol{\tau}_2 && \text{scalar symmetric} \\ &= \frac{1}{4M^2} \boldsymbol{\tau}_1 \cdot \boldsymbol{\tau}_2 \underline{\sigma}_1 \cdot \underline{k}\, \underline{\sigma}_2 \cdot \underline{k} && \text{pseudoscalar symmetric.} \end{aligned} \tag{7}$$

The error in the kernel due to the neglect of ε with respect to $\omega(k)$ is less than 2% for the deuteron and reaches 15% for the scattering problem at 20 MeV. If p is small in a scattering event the error in the static approximation reaches

15 % for $K \sim \sqrt{M\mu} \sim 2.7\ \mu$, but here the momentum wave function may be small. That these errors are of the same order of magnitude as the fourth order static corrections was pointed out by NAMBU [15] and by SALPETER and BETHE [16]. LÉVY [4] and KLEIN [7] obtain an estimate of the non-static corrections to the adiabatic potential by an expansion of the energy denominators in the kernel in powers of $1/\omega(k)$. The lowest order integral equation is used to iterate these terms to bring them into the form of adiabatic fourth order potentials. In fact potentials whith equal parts of those arising from fourth order adiabatic Tamm-Dancoff irreducible kernels cancelling with them completely in neutral scalar theory and with $-V_{4,R}^{(0)}$ in pseudoscalar theory. A similar result is obtained in the next section by a perturbation expansion using the kinetic energy of the nucleons in the presence of a meson as a perturbation together with the meson-nucleon coupling energy. This is suggested by the comments of SALPETER and BETHE on the approximate equality in magnitude ($\sim 15\,\%$) of the non-adiabatic corrections and those of next higher order in G^2. Since the cancellation occurs amongst the fourth-order no-pair terms it is important in a pair-suppressed theory such as that used by BRUECKNER and WATSON. That this damping is a consequence of radiative corrections has been suggested by KLEIN [17] where the two-pair terms have been shown to give the perturbation results with a renormalized coupling constant $g_s^2/4\pi$ which may well be small $\sim 1/3$. The method of renormalization is that of DESER, THIRRING and GOLDBERGER [18]. It is also suggestive that the combined one and two pair terms of KLEIN, $V_4^{(1)}+V_4^{(2)}$, give little effect in the region of deuteron separations due to their approximate cancellation. BRUECKNER and WATSON point out that it is precisely these terms which lead to the differences between their final potential and that of TAKETANI *et al.* [3].

3. – Scalar Theory.

SALPETER and BETHE [16] show, by means of an argument similar to that used by FEYNMAN [19] in dealing with longitudinal photons, that the G^2 contribution for neutral scalar theory, vanishes to order $(\mu/M)^2$ in the case of a perturbation calculation between plane wave states [20]. However, if an

---

[15] Y. NAMBU: *Prog. Theor. Phys.* (*Japan*), **5**, 614 (1950).

[16] E. SALPETER and H. A. BETHE: *Phys. Rev.*, **84**, 1232 (1951).

[17] A. KLEIN: *Phys. Rev.* (in course of publication).

[18] S. DESER, W. E. THIRRING and M. L. GOLDBERGER: *Phys. Rev.*, **94**, 711 (1954).

[19] R. P. FEYNMAN: *Phys. Rev.*, **76**, 769 (1949).

[20] Alternatively this may be seen by carrying through two successive Møller-Rosenfeld transformations (C. MØLLER and L. ROSENFELD: *Kgl. Danske Videnskab. Selskab*, **17**, 8 (1940)). The first eliminates the static interaction $G\bar{\psi}\psi p$ leaving the

iteration procedure is to be used in the ladder approximation, the final two nucleon states defining the kernel may have an energy p'^2/M not too small compared with $\omega(k)$. This two nucleon state being coupled back to a state of low energy by an iteration and the resulting kernel contributing to the static G^4 potential. That this is indeed the case is demonstrated if we compute the contribution to the static potential from two meson graphs. From the Tamm-Dancoff non-crossed graphs (2*a*) we obtain the contribution to the potential

$$-\frac{G^4}{(2\pi)^3}\int\frac{\exp[-i(\underline{k}_1+\underline{k}_2)\cdot\underline{r}]}{2\omega_1^2\omega_2^2(\omega_1+\omega_2)}\mathrm{d}^3\underline{k}_1\mathrm{d}^3\underline{k}_2\,, \tag{8}$$

while the non-adiabatic correction to the G^2 potential gives, as we show below,

$$\frac{G^4}{(2\pi)^3}\int\frac{\exp[-i(\underline{k}_1+\underline{k}_2)\cdot\underline{r}]}{\omega_1^3\omega_2^2}\mathrm{d}^3\underline{k}_1\,\mathrm{d}^3\underline{k}_2\,. \tag{9}$$

These do not cancel unless the contributions from two meson crossed graphs, the irreducible contributions in the Salpeter and Bethe formalism, are added. These are, from (2 *b*, *c* and *d*),

$$-\frac{G^4}{(2\pi)^3}\int\frac{\exp[-i(\underline{k}_1-\underline{k}_2)\cdot\underline{r}]}{2\omega_1^2\omega_2(\omega_1-\omega_2)}\left(\frac{2}{\omega_1}-\frac{1}{\omega_2}\right)\mathrm{d}^3\underline{k}_1\,\mathrm{d}^3\underline{k}_2\,. \tag{10}$$

It has been recently emphasized by KLEIN ([21]) that any procedure which sets adiabatic limits in first order terms while including other higher order terms is inconsistent. KLEIN ([22]) has also pointed out that such an adiabatic limit has been made in the work of CINI and FUBINI ([23]). One may easily show that a further partial integration made in the manner of these authors (equation (5) of reference ([23])) and ignoring the second derivative of $\Phi(t)$, the interaction representation state vector for the two nucleons, leads to a correction to the CINI and FUBINI potential equal to (9). Of course this makes no difference to their variational approach which has as yet not been subject to detailed testing against the low energy experimental data.

Yukawa potential and a trilinear but dynamic interaction. The second transformation eliminates this latter leaving an energy dependent two body interaction together with a smaller trilinear recoil term. The resultant potential is then the Yukawa potential plus an exponential potential depending on the square of the energy exchanged.

([21]) A. KLEIN: *Phys. Rev.*, **94**, 195 (1954).

([22]) Private communication to S. FUBINI. I am especially indebted to Dr. FUBINI for his guidance in this section.

([23]) M. CINI and S. FUBINI: *Nuovo Cimento*, **10**, 12 (1953).

We consider the non-static corrections, in a manner somewhat different from LÉVY and KLEIN, by a Wigner-Brillouin perturbation theory based on taking the kinetic energy of the nucleons in the presence of a meson to be a perturbation. For the unperturbed Hamiltonian density we take

$$H_0 = \frac{1}{2}\{\mu^2\varphi^2 + (\underline{\nabla}\varphi)^2 + \pi^2\} + M\bar{\psi}\psi + \eta\,\bar{\psi}\left(-\frac{\nabla^2}{2M}\right)\psi\,, \tag{11}$$

while as the perturbation energy density we have

$$H_1 = G\bar{\psi}\psi\varphi + (1-\eta)\bar{\psi}\left(-\frac{\nabla^2}{2M}\right)\psi\,, \tag{12}$$

where we have used the usual notation for the field operators and where

$$\eta = \begin{cases} 1 & \text{two nucleon state} \\ \\ 0 & \text{otherwise.} \end{cases}$$

The Wigner-Brillouin perturbation expansion for the Schrödinger equation

$$(W - H_0)\Psi = H_1\Psi \tag{13}$$

gives

$$(W - H_0)\Phi = \eta H_1 \frac{(1-\eta)}{W - H_0} H_1\Phi + \eta H_1 \frac{(1-\eta)}{W - H_0} H_1 \frac{(1-\eta)}{W - H_0} H_1\Phi - \tag{14}$$

$$- \eta H_1 \frac{(1-\eta)}{W - H_0} H_1 \frac{(1-\eta)}{W - H_0} H_1 \frac{(1-\eta)}{W - H_0} H_1\Phi + \dots\,,$$

where $\Phi = \eta\Psi$.

The lowest order equation for the amplitude

$$a_{\alpha\beta}(\underline{p}) = \sum_{u\,v} (\Phi_0,\, b_u^{(1)}(\underline{p}) b_v^{(2)}(-\underline{p})\Phi)\, u_\alpha v_\beta\,, \tag{15}$$

is

$$\left(\varepsilon - \frac{p^2}{M}\right) a^{(1)}(\underline{p}) = -\frac{G^2}{(2\pi)^3}\int \frac{a^{(1)}(\underline{p} - \underline{k})}{\omega(k)[\omega(k) - \varepsilon]}\,\mathrm{d}^3\underline{k}\,. \tag{16}$$

Which is an excellent approximation to the Schrödinger equation for two particles moving under the Yukawa potential. We admit that $a^{(1)}(\underline{p})$ is not a

conventional wave function but for the two body problem equation (16) should lead to a good S-matrix though not to an amplitude with which to compute expectation values ([24]).

The next order contributions lead to two types of contributions, those considered above in equations (8) and (10) namely the Tamm-Dancoff irreducible adiabatic fourth order terms, though of course now there is no static limit to perform, and four contributions arising from the perturbation $(1-\eta)\bar{\psi}\cdot(-\nabla^2/2M)\psi$ acting on each nucleon line during the transit of the meson. At zero energy the equation becomes

$$(17)\qquad -\frac{p^2}{M}a^{(2)}(\underline{p}) = -\frac{G^2}{(2\pi)^3}\int\frac{a^{(2)}(\underline{p}-\underline{k})}{\omega^2(k)}\,\mathrm{d}^3\underline{k} - \\ -\frac{G^4}{(2\pi)^3}\int\frac{a^{(2)}(\underline{p}-\underline{k}_1-\underline{k}_2)}{\omega^3(k_1)\omega^2(k_2)}\,\mathrm{d}^3\underline{k}_1\,\mathrm{d}^3\underline{k}_2 + \frac{G^2}{(2\pi)^3}\int\frac{(\underline{p}-\underline{k})^2}{\omega^3(k)M}\,a^{(2)}(\underline{p}-\underline{k})\,\mathrm{d}^3\underline{k}\,;$$

we have used a theorem by Lévy concerning kernels of the form $\{(\underline{p}-\underline{k})^2 - p^2\}/2M$. If we use equation (16) to iterate the term we obtain to order G^4

$$(18)\qquad -\frac{p^2}{M}a^{(2)}(\underline{p}) = -\frac{G^2}{(2\pi)^3}\int\frac{a^{(2)}(\underline{p}-\underline{k})}{\omega^2(k)}\,\mathrm{d}^3\underline{k}\,.$$

For symmetric scalar theory a similar procedure is possible. There is no complete cancellation in this case due to the non-commutativity of the τ matrices. The fourth-order kernel can be written down by inspection of (2): it is

$$(19)\qquad -\frac{G^4}{(2\pi)^3}\,\frac{1}{4\omega_1\omega_2}\left\{\frac{2U\omega_1 + 2C\omega_1 + 4C\omega_2 - 4U(\omega_1+\omega_2)}{\omega_1^2\omega_2(\omega_1+\omega_2)}\right\}.$$

C is the isotopic factor $(3+2\boldsymbol{\tau}_1\cdot\boldsymbol{\tau}_2)$ for crossed graphs and U the corresponding factor $(3-2\boldsymbol{\tau}_1\cdot\boldsymbol{\tau}_2)$ for uncrossed graphs. The final fourth order potential is

$$(20)\qquad -\left(\frac{G^2}{4\pi}\right)^2\mu\boldsymbol{\tau}_1\cdot\boldsymbol{\tau}_2\,\frac{8}{\pi}\,\frac{K_0(2\mu r)}{\mu r}\,.$$

It is clear that we have supposed that the high order corrections are small so that (16) gives a useful lowest order amplitude with which to compute the non-static correction in equation (17).

([24]) A. M. Sessler: *Phys. Rev.*, (in course of publication).

4. – Adiabatic Kernels and Potentials.

Reducible and irreducible kernels are defined relative to the wave function under consideration. In general we define a reducible kernel of an integral equation as one which may be obtained by iteration of another equivalent integral equation in which this kernel does not appear. Reducible kernels can be obtained for any integral equation by iteration; the converse operation is uniteration and it is clear that an integral equation which can be uniterated contains reducible kernels. It we had collected the second order term into the fourth order by iteration we would obtain an equation similar to that of KLEIN ([7]) and would then have to uniterate that part corresponding to the adiabatic second order term. KLEIN uniterates the total Tamm-Dancoff reducible part to give non-adiabatic second order terms the strictly non-adiabatic part of which he again iterates. It is not surprising that reducible kernels in the adiabatic limit are different from iterated irreducible adiabatic kernels. The higher order terms obtained by iteration of adiabatic kernels are, save for radiation damping corrections, those with near energy conservation in the two nucleon intermediate state. Thus fourth order contributions to the kernel arise not only from Tamm-Dancoff irreducible graphs but from the four Tamm-Dancoff reducible graphs in which the intermediate state contains two nucleons with energy different from that of the actual system. Taking the adiabatic limit and iteration are not commutative operations.

Similar considerations to those outlined in the previous section are possible for the $(G/2M)\underline{\sigma}\cdot\underline{\nabla}\boldsymbol{\varphi}\cdot\boldsymbol{\tau}$ theory of BRUECKNER and WATSON ([10]). The cancellation which occurs is such as to lead to $V_4^{(0)}$. BRUECKNER and WATSON consider that the iteration procedure is invalid and that a correct estimate of the order of magnitude of the non-static correction is that it is less than 1% of $V_2 + V_{4,I}$. The reason for this is that due to the repulsive core of radius $.300\cdot 10^{-13}$ cm which is added to the predicted potential to fit the low energy data the momentum wave function is considerably damped in the regions where the non-static corrections to the kernel become important.

It is instructive to consider the problem of the adiabatic limit in the following way. We consider the low energy scattering of the two-nucleon system. The Tamm-Dancoff amplitude in the center of mass system satisfies the equation

$$\left(\varepsilon - \frac{\underline{p}^2}{M}\right) a(\underline{p}) = (2\pi)^{-3} \int K(\underline{p}, \underline{p}') a(\underline{p}') \, \mathrm{d}^3\underline{p}' \,, \tag{21}$$

and so the integral equation for $f(\underline{p})$ defined by

$$a(\underline{p}) = \delta(\sqrt{M\varepsilon} - p) + \frac{1}{\sqrt{M\varepsilon} - p} f(\underline{p}) \,, \tag{22}$$

is

$$f(\underline{p}) = f_B(\underline{p}) + (2\pi)^{-3} \int K(\underline{p}, \underline{p}') \frac{1}{\sqrt{M\varepsilon} - p'} f(\underline{p}')\, \mathrm{d}^3\underline{p}' \,. \tag{23}$$

The tangent of the phase shift for scattering is linearly related to $f(\underline{p})$ ior p on the energy shell, i.e. $|\underline{p}| = q\sqrt{M\varepsilon}$. The first Born approximatfon to $f(\underline{p})$ is

$$f_B(\underline{p}) = (2\pi)^{-3} \int K(\underline{p}, \underline{p}')\, \delta(q - p')\, \mathrm{d}^3\underline{p}' \,. \tag{24}$$

We require that any approximation to equation (21) due to an adiabatic kernel $L(\underline{p} - p')$ replacing $K(\underline{p}, \underline{p}')$ must give rise to the identical phase shifts to some required order. In configuration space the problem is to obtain a local potential $V(r)$ which gives rise to the same S-matrix at a given non-local potential.

It is clear that to order G^2 alone, $L^{(2)}(\underline{p} - \underline{p}')$ is merely the adiabatic limit of $K^{(2)}(\underline{p}, \underline{p}')$ but that corrections are required to high orders. If we consider the S-matrix to order G^4 in the case of the Yukawa potential this is but a computational exercise since of course the second Born approximation makes very little physical sense with the known existence of low lying virtual resonances. However demanding equality of the S-matrix in this order it is easy to see that an extra local potential is required and that the obvious choice is just that obtained by the previously considered iterative procedure

$$\frac{G^4}{(2\pi)^5} \int \frac{\exp[-i(\underline{k}_1 + \underline{k}_2)\cdot\underline{r}]}{\omega_1^3 \omega_2^2}\, \mathrm{d}^3\underline{k}_1\, \mathrm{d}^3\underline{k}_2 = \left(\frac{G^2}{4\pi}\right) \mu\, \frac{2}{\pi}\, \frac{\exp[-\pi r]}{\pi r} K_0(\mu r) \,. \tag{25}$$

It is more useful to consider the general $f(p)$ function not confined to the energy shell. For the Yukawa potential we have the second Born approximation

$$f_2(\underline{p}) = -\frac{G^2}{4\pi} \frac{2M q^2}{q + p} \frac{1}{\pi} \cdot \left\{ \int \frac{\mathrm{d}\Omega_q / 4\pi}{(\mu^2 + |\underline{p} - \underline{q}|^2)} - \frac{G^2}{4\pi} \frac{M}{2\pi^2} \int \frac{\mathrm{d}^3\underline{r}\, \mathrm{d}\Omega_q / 4\pi}{(\mu^2 + |\underline{p} + \underline{r}|^2)(\mu^2 + |\underline{r} - \underline{q}|^2)(q^2 - r^2)} \right\} , \tag{26}$$

which can be integrated to give the scattering length at zero energy

$$a = -\frac{G^2}{4\pi} \frac{M}{\mu^2} \left\{ 1 + \frac{1}{4} \frac{G^2}{4\pi} \left(\frac{2M}{\mu}\right) + \ldots \right\} \,. \tag{27}$$

For the exact kernel (6) the corresponding $f(\underline{p})$ is

$$(28)\qquad f(\underline{p}) = -\frac{G^2}{4\pi}\,\frac{2Mq^2}{q+p}\,\frac{1}{\pi}\left\{\int \frac{\mathrm{d}\Omega_q/4\pi}{(\mu^2+|\underline{p}-\underline{q}|^2)} - \right.$$

$$\left. -\frac{G^2}{4\pi}\,\frac{M}{2\pi^2}\int \frac{\mathrm{d}^3\underline{v}\,\mathrm{d}\Omega_q/4\pi}{\sqrt{\mu^2+|\underline{p}+\underline{r}|^2}\left[\sqrt{\mu^2+|\underline{p}+\underline{r}|^2}-\dfrac{q^2-r^2}{M}\right](\mu^2+|\underline{r}-\underline{q}|^2)(q^2-r^2)}\right\}.$$

The difference is to a good approximation

$$(29)\qquad \frac{M}{q+p}\,\frac{G^4}{(4\pi)^2}\,\frac{q^2}{\pi^3}\int \frac{\mathrm{d}^3v\,\mathrm{d}\Omega_q/4\pi}{(\mu^2+\underline{r}-\underline{q}^2)(\mu^2+\underline{p}+\underline{r}^2)^{\frac{1}{2}}}\,.$$

Thus to obtain the correct phase shift to order G^4 we require to add to the adiabatic limit of $K^{(2)}(\underline{p},\underline{p}') + K^{(4)}(\underline{p},\underline{p}')$ a local potential which gives, in first Born approximation, an $f(\underline{p})$ equal to (29). The obvious potential for this purpose is (25) above since the first Born approximation for the amplitude under this potential is

$$(30)\qquad \frac{M}{q+p}\,\frac{G^4}{(2\pi)^5}\int \frac{\delta(q-|\underline{p}-\underline{k}_1|)}{(\mu^2+|\underline{k}_1-\underline{k}_2|^2)^{\frac{1}{2}}(\mu^2+k_2^2)}\,\mathrm{d}^3\underline{k}_1\,\mathrm{d}^3\underline{k}_2\,,$$

which is exactly equal to (29).

Formally similar considerations are possible for pseudoscalar theory. The added potential is

$$(31)\qquad V^{(0)}_{4,R} = \frac{G^4}{(2\pi)^5}\,\frac{3-2\boldsymbol{\tau}_1\cdot\boldsymbol{\tau}_2}{(2M)^4}\cdot$$

$$\cdot\int \frac{\exp\left[-i(\underline{k}_1+\underline{k}_2)\cdot\underline{r}\right]}{\omega_1^3\omega_2^2}\,\underline{\sigma}_1\cdot\underline{k}_1\,\underline{\sigma}_1\cdot\underline{k}_2\,\underline{\sigma}_2\cdot\underline{k}_1\,\underline{\sigma}_2\cdot\underline{k}_2\,\mathrm{d}^3\underline{k}_1\,\mathrm{d}^3\underline{k}_2\,.$$

The final local potential is $V^{(0)}_4$. The reason for the formal nature of this result in pseudoscalar theory lies in the fact that the first order equation does not give an adequate approximation to the potential for the remainder to be considered small. For example one hopes that the nuclear potential contains a hard core. BRUECKNER and WATSON take phenomenological hard cores of radius $0.328\cdot10^{-13}$ cm $\sim .23/\mu$ for the singlet state and 10% smaller for the triplet state. They then compute the expected value of $V^{(0)}_{4,R}$ by the iteration procedure using the ground state wave function given by $V_2 + V^{(0)}_{4,I} + V^{(1)}_4 - V^{(2)}_4 - -$(hard core). They find the correction is less than 1%. It appears that in each method of obtaining a local potential from field theory some similar ar-

guments will appear thus, insofar as a series of Born approximations or a series of large iteration corrections cannot be trusted, the correct evaluation of the nuclear force problem will await the solution of the integral equation with the exact kernel; an attempt of this kind in the G^2 order is being made by SUNDARESAN ([25]).

The author wishes to express his gratitude to Professor H. A. BETHE and the Laboratory of Nuclear Studies for their kind hospitality and to the Commonwealth Fund of New York for financial assistance. He is also grateful to Drs. S. P. FUBINI and B. KURŞUNOĞLU for many discussions.

([25]) M. K. SUNDARESAN: private communication.

RIASSUNTO

Si procede ad uno studio critico dei contributi senza coppie e non adiabatici nel problema delle forze nucleari. Tali contributi sono attualmente oggetto di controversia. Si esamina con cura l'esempio specifico della teoria scalare. Si dimostra che è necessario tener conto delle correzioni non statiche al potenziale locale adiabatico per ottenere gli sfasamenti esatti in approssimazione di Born.

IL NUOVO CIMENTO Vol. XII, N. 3 1° Settembre 1954

Temperate Distributions Associated with the Klein-Gordon Equation.

A. Deprit

Christ's College - Cambridge

(ricevuto il 21 Giugno 1954)

Summary. — A distribution treatment is applied to the Klein-Gordon equation. The function $\Delta(\boldsymbol{x}, t)$ is found to be the *resolving distribution* of the Klein-Gordon equation, considered as an evolution equation connected with the space convolution product. $\Delta_{\text{ret}}(\boldsymbol{x}, t)$ is the *elementary kernel* in the one-parameter algebra of operators which is associated with the Klein-Gordon differential operator. Finally $\overline{\Delta}(\boldsymbol{x}, t)$ is shown to be one of the *elementary solutions* of the Klein-Gordon equation, which is now regarded as a space-time convolution equation.

In order to solve the Klein-Gordon partial differential equation, two methods are available. Either, we can, by an exponential transformation, reduce this evolution equation into an elliptic differential equation, which we solve by separation of the variables and expansion of the solution in eigenfunctions. Or we can use a Green function treatment. R. P. Feynman's papers [1] have largely showed how this last method is powerful in Quantum Electrodynamics.

However, both methods — Green function treatment and expansion in eigenfunctions — lead to the same difficulties. But according to W. Güttinger [2], E. C. G. Stückelberg and A. Petermann [3], we can get rid of some of the divergences, if we revise the Green function method in the light of distribution analysis. At the end of his paper, W. Güttinger suggested

(1) R. P. Feynman: *Phys. Rev.*, **76**, 749 and 769 (1949).
(2) W. Güttinger: *Phys. Rev.*, **89**, 1004 (1953).
(3) E. C. G. Stueckelberg et A. Petermann: *Helv. Phys. Acta*, **26**, 499 (1953).

that a valuable improvement could be acquired if the local and causal structure of invariant propagation functions were investigated. Of course, the singular nature of the Green functions $\bar{\Delta}$, Δ_{ret}, Δ_{adv}, etc., had already caught the attention of the mathematical physicists. After a first attempt (4), in which he deduced systematically the various Green functions, — although still by means of unjustified functional artifices — M. SCHÖNBERG came back on this subject (5) and, after having used a Stieltjes transformation, suggested to treat the problem by a *resolvent operator* treatment. But, what is true for the whole of partial differential equations, is a fortiori true for the Klein-Gordon equation: the Cauchy problem, if it has to be solved in the set of numerical functions, does not find its complete solution; the *Green functions* do not reveal their algebraic and topological structures if they are to be found only in the set of numerical functions.

Applying straightforward ideas as developed in L. Schwartz's most valuable contribution to the evolution equations (6), we show that the *Green functions* Δ, $\Delta^{(+)}$, $\Delta^{(-)}$, etc., actually are *temperate distributions*. They belong to three distinct kinds according to three ways of considering this partial differential equation.

(i) We can look on it as an evolution equation associated with the convolution in the space R^3. Its solutions form a subspace of the complex topological vector-space of temperate distributions with carrier in R^3. The *function* $-\Delta(\boldsymbol{x}, t)$ is the *resolving distribution*; other *functions*, such as $\Delta^{(+)}(\boldsymbol{x}, t)$ and $\Delta^{(-)}(\boldsymbol{x}, t)$ are also temperate distributions, solutions of this evolution equation.

(ii) To the Klein-Gordon equation is associated a one-parameter operator algebra: its elements are the continuous mappings of the time interval $]a, b[$ into the set $(O'_c)_x$ of quickly decreasing distributions. The *elementary kernel* of this algebra is the *Green function* $\Delta_{ret}(\boldsymbol{x}, t)$; other operators define other Green functions, such as $\Delta_{adv}(\boldsymbol{x}, t)$.

(iii) Finally, the Klein-Gordon equation can also be regarded as a convolution equation in space-time. To solve this convolution equation is tantamount to studying a division problem in the vector-space of temperate distributions whose carrier is contained in space-time R^4. There exists an infinite set of *elementary solutions*; among them are the so called *Green functions* $\bar{\Delta}(\boldsymbol{x}, t)$ and $\Delta_{(+)}(\boldsymbol{x}, t)$.

(4) M. SCHÖNBERG: *Rev. Union matem. Argent.*, **12**, 238 (1947).
(5) M. SCHÖNBERG: *Il Nuovo Cimento*, **8**, 651 (1951).
(6) L. SCHWARTZ: *Ann. Inst. Fourier*, **2**, 19 (1950).

1. – Heisenberg [7] Distributions $\delta_{(+)}$ and $\delta_{(-)}$.

Let us consider the two multiplication equations

$$xT_x = \mp \frac{1}{2\pi i}, \tag{1}$$

where T_x is a distribution $\in (\mathcal{D}')_x$, the support of which is contained in the real axis ($x \in R$).

Each of them possesses an infinite number of solutions:

$$T_{(\pm)x} = \mp \frac{1}{2\pi i} \text{ v.p.} \frac{1}{x} + \lambda \, \delta_x . \tag{2}$$

v.p. $1/x$ is the pseudo-function distribution $Pf(1/x)$, which is defined by L. SCHWARTZ [8]; δ_x is the Dirac measure and λ is an *arbitrary* complex constant.

For $\lambda = \frac{1}{2}$, we find the distributions $\delta_{(+)x}$ and $\delta_{(-)x}$ that Heisenberg introduced.

We must emphasize that, according to W. GÜTTINGER, there is a great resource for the Quantum Field theory, in the fact that the Distribution Theory corrected the usual expressions for $\delta_{(\pm)}$ by introducing the symbol Pf: Quantum Field Theory may benefit from the property that the distribution $Pf(1/x)$ is not invariant with respect to a variable transformation.

$$\delta_{(+)x} = -\frac{1}{2\pi i} \text{ v.p.} \frac{1}{x} + \frac{1}{2} \delta_x . \tag{3_1}$$

$$\delta_{(-)x} = \frac{1}{2\pi i} \text{ v.p.} \frac{1}{x} + \frac{1}{2} \delta_x . \tag{3_2}$$

Both are made up of a distribution carried by the complement of the origin on the real axis, and a measure caused by a mass $\frac{1}{2}$, placed at the origin.

As δ_x and v.p. $1/x$ are temperate distributions, we can apply to (3_1) and (3_2) the Fourier transformation, which gives

$$\mathcal{F}_x(\delta_{(+)x}) = Y_y , \tag{4_1}$$

$$\mathcal{F}_x(\delta_{(-)x}) = \overset{\vee}{Y}_y . \tag{4_2}$$

---

[7] W. HEISENBERG: *Zeits. f. Phys.*, **120**, 513 (1943).

Y_y represents the distribution associated with the Heaviside function $Y(y)$

$$Y(y) = \begin{cases} 1 & y > 0\,, \\ 0 & y < 0\,. \end{cases}$$

$\overset{\vee}{Y}_y$ is Y_y transformed by a symmetry with respect to the origin [8].

If we start from the relation

$$\log x = \log|x| + i \arg x + ik\pi\,,$$

where k is an arbitrary integer, we can define a distribution associated with the function $\log x$, by the linear mapping $\varphi(x) \to \log x \cdot \varphi(x)$ of the set$(\mathcal{D})_x$ of indefinitely differentiable numerical functions which vanish outside a compact, into the set of complex numbers, such that

$$\log x \cdot \varphi(x) = \{\log|x| + i\pi[Y(x) - 1] + ik\pi\} \cdot \varphi(x)\,. \tag{5}$$

Because, in terms of *distribution derivatives*, we have

$$\frac{\mathrm{d}}{\mathrm{d}x} \log|x| = Pf\frac{1}{x} = \text{v.p.}\,\frac{1}{x}\,, \qquad \frac{\mathrm{d}}{\mathrm{d}x}\, Y(x) = -\,\delta_x\,,$$

we can get from the definition (5) an identity which was found by Dirac [9].

$$\frac{\mathrm{d}}{\mathrm{d}x} \log x = \text{v.p.}\,\frac{1}{x} - i\pi\delta_x\,. \tag{6}$$

According to (3_1), we can also write

$$\frac{\mathrm{d}}{\mathrm{d}x} \log x = -\,2\pi i\, \delta_{(+)x}\,. \tag{7}$$

A straightforward application of the definition given by L. Schwartz [8] provides the identities

$$\delta_{(+)x-a} = \tau_a \delta_{(+)x}\,, \tag{8_1}$$

$$\delta_{(-)x-a} = \tau_a \delta_{(-)x}\,, \tag{8_2}$$

where τ_a is the mapping $\varphi(x) \to \tau_a(\varphi(x)) = \varphi(x - a)$.

If we perform the variable substitution $x \to x^2 - a^2$ according to [10],

[8] L. Schwartz: *Théorie des distributions*, (Paris A.S.I.), 1091 (1950) and 1122 (1951).

[9] P. A. M. Dirac: *Principles of Quantum Mechanics* (Oxford, 1947), 3rd ed.

we find in the set $(\mathcal{D}')_x$ of distributions, the following identities

$$\delta_{(x^2-a^2)} = \frac{1}{2a}\left[\delta_{(x-a)} + \delta_{-(x+a)}\right] \qquad (a \in R,\ a \neq 0);$$

$$\text{v.p.}\,\frac{1}{x^2-a^2} = \frac{1}{2a}\left[\text{v.p.}\,\frac{1}{x-a} + \text{v.p.}\,\frac{1}{-x-a}\right] \qquad (a \in R,\ a \neq 0).$$

From here we deduce

$$(9_1) \qquad \delta_{(+)(x^2-a^2)} = \frac{1}{2a}\left[\delta_{(+)(x-a)} + \delta_{(+)(-x-a)}\right] \qquad (a \in R,\ a \neq 0);$$

$$(9_2) \qquad \delta_{(-)(x^2-a^2)} = \frac{1}{2a}\left[\delta_{(-)(x-a)} + \delta_{(-)(-x-a)}\right] \qquad (a \in R,\ a \neq 0).$$

Formulas (8_1) and (8_2), (9_1) and (9_2) are to be compared with the corresponding expressions for δ. Furthermore, by (3_1) and (3_2), we have

$$\delta_x = \delta_{(+)x} + \delta_{(-)x}\,.$$

However we must emphasize, beyond these resemblances and this « decomposition » of δ_x, that δ_x on one side and $\delta_{(\pm)x}$, on the other side are of an essentially distinct nature. While $\delta_{(\pm)x}$ are *distributions* carried by the real axis, and are solutions of (1), the Dirac *measure* δ_x has a point for support and is not a solution of (1).

2. – The Resolving Distribution of the Klein-Gordon Equation.

The homogeneous convolution equation

$$(10) \qquad \frac{\mathrm{d}^2}{\mathrm{d}t^2}\,U_x(t) - \Delta_{x\,(x)}^{*}\,U_x(t) + m^2 U_x(t) = 0\,,$$

belongs to the general type of evolution equations associated with the convolution, which L. SCHWARTZ analysed (6). The general theorems drawn by L. SCHWARTZ have been applied to this particular equation. The spatial Fourier transformation $\mathcal{F}_x$, between x^3 and its dual X^3 performed for any t, transforms the convolution equation (10) into the multiplication equation

$$(11) \qquad \frac{\mathrm{d}^2}{\mathrm{d}t^2}\,\mathcal{U}_y(t) + \left[4\pi^2|y|^2 + m^2\right]\mathcal{U}_y(t) = 0\,,$$

where $|\boldsymbol{y}|$ represents the Euclidean norm $\sqrt{y_1^2 + y_2^2 + y_3^2}$ in Y^3. It is a second order differential equation which has for general solution

$$\mathcal{U}_{\boldsymbol{y}}(t) = (\cos t\sqrt{4\pi^2|\boldsymbol{y}|^2 + m^2})\,\mathcal{U}_{\boldsymbol{y}}(0) + \frac{\sin t\sqrt{4\pi^2|\boldsymbol{y}|^2 + m^2}}{\sqrt{4\pi^2|\boldsymbol{y}|^2 + m^2}} \cdot \frac{\mathrm{d}\mathcal{U}_{\boldsymbol{y}}(0)}{\mathrm{d}t}\,. \tag{12}$$

L. SCHWARTZ ([6]) uses the name of a *resolving distribution* of (10), for an application – if it exists – $(t, \tau) \to R_{\boldsymbol{x}}(t, \tau)$ of the triangle $a \leqslant \tau \leqslant t \leqslant b$ of $[a, b]\times[a, b]$ into the set $(\mathcal{O}_c')_{\boldsymbol{x}}$ of the *quickly decreasing* distributions, such that it is a solution of (10), viz.

$$\frac{\partial^2}{\partial t^2} R_{\boldsymbol{x}}(t, \tau) - \Delta_{\boldsymbol{x}} \overset{*}{}_{(\boldsymbol{x})} R_{\boldsymbol{x}}(t, \tau) + m^2 R_{\boldsymbol{x}}(t, \tau) = 0\,, \tag{13}$$

for the initial conditions,

$$R_{\boldsymbol{x}}(\tau, \tau) = 0\,, \tag{14_1}$$

$$\left(\frac{\mathrm{d}}{\mathrm{d}t} R_{\boldsymbol{x}}\right)(\tau, \tau) = \delta_{\boldsymbol{x}}\,. \tag{14_2}$$

It has been proved ([10]) that $R_{\boldsymbol{x}}(t, \tau)$ exists and is unique for any t and τ. If we define $R_{\boldsymbol{x}}(t) = R_{\boldsymbol{x}}(t, 0)$, then from (12) and the initial conditions (14_1) and (14_2), we obtain for the Fourier transform $\mathcal{R}_{\boldsymbol{y}}(t) = \mathcal{F}_{\boldsymbol{x}}\,\mathcal{R}_{\boldsymbol{x}}(t)$

$$\mathcal{R}_{\boldsymbol{y}}(t) = \mathcal{R}(\boldsymbol{y}; t) = \frac{\sin t\sqrt{4\pi^2|\boldsymbol{y}|^2 + m^2}}{\sqrt{4\pi^2|\boldsymbol{y}|^2 + m^2}}\,.$$

$\mathcal{R}(\boldsymbol{y}; t_2)$. is an indefinitely differentiable, slowly increasing function: $\mathcal{R}(\boldsymbol{y}; t) \in \in (\mathcal{O}_M)_{\boldsymbol{y}}$.

Using L. SCHWARTZ's kernel theorem ([11]), we may write

$$\mathcal{R}_{\boldsymbol{x}}(t) = \int_{Y^3} \mathrm{d}^3\boldsymbol{y} \exp\left[2\pi i(\boldsymbol{x}\cdot\boldsymbol{y})\right] \frac{\sin t\sqrt{4\pi^2|\boldsymbol{y}|^2 + m^2}}{\sqrt{4\pi^2|\boldsymbol{y}|^2 + m^2}}\,. \tag{15}$$

The substitutions $\boldsymbol{y} = \boldsymbol{k}/2\pi$ and $\omega^2 = |\boldsymbol{k}|^2 + m^2$ give to (15) the usual form

$$R_{\boldsymbol{x}}(t) = \frac{1}{(2\pi)^3} \int_{E^3} \mathrm{d}^3\boldsymbol{k} \exp\left[i\boldsymbol{k}\cdot\boldsymbol{x}\right] \frac{\sin \omega t}{\omega}\,,$$

([10]) S. ALBERTONI and M. CUGIANI: *Nuovo Cimento*, **8**, 874 (1951).
([11]) A. DEPRIT: *Ann. Soc. Scientif. Brux.*, **68**, 119 (1954),

where we recognize the $\Delta(\boldsymbol{x}, t)$ already introduced into Quantum Field Theory.

$$R_{\boldsymbol{x}}(t) = -\Delta(\boldsymbol{x}, t)\,. \tag{16}$$

The Distribution Theory gives to $\Delta(\boldsymbol{x}, t)$ its true mathematical meaning: it is — save on the sign, — the *resolving distribution* of the Klein-Gordon equation: $\Delta(\boldsymbol{x}, t) \in (\mathcal{O}_c')_{\boldsymbol{x}}$.

Any Cauchy problem, as it is defined by L. SCHWARZ ([6]), is solved by the formula

$$U_{\boldsymbol{x}}(t) = R_{\boldsymbol{x}}(t - t_0) \overset{*}{_{(\boldsymbol{x})}} \left(\frac{\partial U_{\boldsymbol{x}}}{\partial t}\right)_{t=t_0} - \frac{\partial R_{\boldsymbol{x}}}{\partial t}(t - t_0) \overset{*}{_{(\boldsymbol{x})}} U(t_0)\,,$$

which can be written according to the kernel theorem ([12]), as

$$U_{\boldsymbol{x}}(t) = \int_{\dot{x}^3} \mathrm{d}^3\boldsymbol{\xi}\, R_{\boldsymbol{x}-\boldsymbol{\xi}}(t - t_0) \left(\frac{\partial U_{\boldsymbol{\xi}}}{\partial t}\right)_{t=t_0} - \int_{\dot{x}^3} \mathrm{d}^3\boldsymbol{\xi}\, \frac{\partial R_{\boldsymbol{x}-\boldsymbol{\xi}}}{\partial t}(t - t_0) U_{\boldsymbol{\xi}}(t_0)\,.$$

H. G. GARNIR ([13]) found, by a direct calculation, in a closed form, the resolving distribution of the Klein-Gordon equation. His result, restricted to a distribution carried by the half space-time $t > 0$, can be extended to the whole space-time and will give

$$R_{\boldsymbol{x}}(t) = \frac{\delta_{r-t} - \delta_{r+t}}{4\pi r} - m\,\frac{\varepsilon(t + r) + \varepsilon(t - r)}{8\pi\sqrt{t^2 - r^2}}\, J_1(m\sqrt{t^2 - r^2}) \tag{17}$$

$$r^2 = x_1^2 + x_2^2 + x_3^2\,.$$

$\varepsilon(z)$ is the function, regular in sections ([8]) given by $\varepsilon(z) = Y(z) - \dot{Y}(z)$.

If we define the function

$$F(r, t) = \frac{1}{2}\left[\varepsilon(t + r) + \varepsilon(t - r)\right] J_0(m\sqrt{t^2 - r^2})\,,$$

a straightforward computation, which implies the distribution derivative of $\varepsilon(z)$, i.e. $(\mathrm{d}/\mathrm{d}z)\varepsilon(z) = 2\delta_z$ and some elementary properties of the change of variables in distributions ([14]), will afford the concise result

$$R_{\boldsymbol{x}}(t) = \frac{1}{4\pi r}\,\frac{\partial}{\partial r} F(r, t)\,.$$

([12]) L. SCHWARTZ: *Proc. Intern. Congr. Math. Cambridge (Mass.)*, **1**, 220 (1950).
([13]) H. G. GARNIR: *Bull. Soc. Roy. Sc. Liège*, **60**, 271 (1951).
([14]) S. ALBERTONI and M. CUGIANI: *Nuovo Cimento*, **10**, 157 (1953).

3. – The Distributions $\Delta^{(+)}(x, t)$, $\Delta^{(-)}(x, t)$ and $\Delta^{(1)}(x, t)$.

The convolution equation [10] possesses other solutions than $R_x(t)$, for other initial conditions than (14_1) and (14_2). In other words, there exist for the differential multiplication equation (11), solutions other than $\mathcal{R}(y, t)$ for other initial conditions. Among them we take

$$\mathcal{R}^{(+)}(y, t) = -\frac{1}{2i}\,\frac{\exp\left[-it\sqrt{4\pi^2|y|^2+m^2}\right]}{\sqrt{4\pi^2|y|^2+m^2}}\,; \tag{18_1}$$

$$\mathcal{R}^{(-)}(y, t) = \frac{1}{2i}\,\frac{\exp\left[it\sqrt{4\pi^2|y|^2+m^2}\right]}{\sqrt{4\pi^2|y|^2+m^2}}\,, \tag{18_2}$$

which are *functions* $\in (\mathcal{O}_M)_y$. Their Fourier transforms are distributions $\in (\mathcal{O}'_c)_x$

$$R_x^{(+)}(t) = -\frac{1}{2i(2\pi)^3}\int_{K^3} d^3k\,\frac{1}{\omega}\exp\left[i\boldsymbol{k}\cdot\boldsymbol{x} - \omega t)\right]\,; \tag{19_1}$$

$$R_x^{(-)}(t) = \frac{1}{2i(2\pi)^3}\int_{K^3} d^3k\,\frac{1}{\omega}\exp\left[i(\boldsymbol{k}\cdot\boldsymbol{x} + \omega t)\right]. \tag{19_2}$$

M. Schönberg [4] obtained the Fourier transforms of (18_1) and (18_2). If we put

$$F^{(+)}(r, t) = \frac{1}{2}\,\varepsilon(t-r)J_0(m\sqrt{t^2-r^2}) - \frac{i}{2}\,N_0(m\sqrt{t^2-r^2})\,;$$

$$F^{(-)}(r, t) = -\frac{1}{2}\,\varepsilon(t-r)J_0(m\sqrt{t^2-r^2}) - \frac{i}{2}\,N_0(m\sqrt{t^2-r^2})\,;$$

we get

$$R_x^{(+)}(t) = -\frac{1}{4\pi r}\,\frac{\partial}{\partial r}\,F^{(+)}(r, t)\,,$$

$$R_x^{(-)}(t) = \frac{1}{4\pi r}\,\frac{\partial}{\partial r}\,F^{(-)}(r, t)\,,$$

where $\partial/\partial r$ is understood as a *distribution derivative*. The only trouble in performing these derivations comes from the Neumann function N_0. But, because the distribution derivative of a convergent series is the series of the distribution derivatives of each term [8], from the expansion [15]

$$\pi N_0(z) = 2J_0(z)\ln\frac{\gamma z}{2} - C_0 - (B_0 - D_0)\,,$$

[15] E. Janke and F. Emde: *Tables of Functions* (New York, 1945), p. 130.

we arrive through (7) at

$$\frac{\mathrm{d}}{\mathrm{d}z} N_0(z) = - N_1(z) - 2i\delta(z) .$$

Hence we come to the formulas given by M. SCHÖNBERG:

$$R_x^{(+)}(t) = \frac{\delta(t-r)}{4\pi r} - \frac{\delta(t^2-r^2)}{4\pi} -$$

$$- m \frac{\varepsilon(t-r)}{8\pi\sqrt{t^2-r^2}} J_1(m\sqrt{t^2-r^2}) + mi \frac{1}{8\pi\sqrt{t^2-r^2}} N_1(m\sqrt{t^2-r^2}) ,$$

$$R_x^{(-)}(t) = -\frac{\delta(t+r)}{4\pi r} + \frac{\delta(t^2-r^2)}{4\pi} -$$

$$- m \frac{\varepsilon(t+r)}{8\pi\sqrt{t^2-r^2}} J_1(m\sqrt{t^2-r^2}) - mi \frac{1}{8\pi\sqrt{t^2-r^2}} N_1(m\sqrt{t^2-r^2}) .$$

The distributions (19_1) and (19_2) are the «functions» $-\Delta^{(+)}(\boldsymbol{x}, t)$ and $-\Delta^{(-)}(\boldsymbol{x}, t)$ and the relations

$$R_x(t) = R_x^{(+)}(t) + R_x^{(-)}(t) , \tag{20}$$

$$\frac{\partial^2}{\partial t^2} R_x^{(\pm)}(t) - \Delta_{x(x)}^{*} R_x^{(\pm)}(t) + m^2 R_x^{(\pm)}(t) = 0 . \tag{21}$$

express correctly the usual identities:

$$\Delta(\boldsymbol{x}, t) = \Delta^{(+)}(\boldsymbol{x}, t) + \Delta^{(-)}(\boldsymbol{x}, t) ,$$

$$(\Box - m^2)\Delta^{(\pm)}(\boldsymbol{x}, t) = 0 \qquad \text{with} \qquad \Box = \Delta_x - \frac{\partial^2}{\partial t^2} .$$

Every linear combination of (18_1) and (18_2) is also a solution of (11); in particular

$$\mathscr{R}^{(1)}(\boldsymbol{y}; t) = i\left[\mathscr{R}^{(-)}(\boldsymbol{y}; t) - \mathscr{R}^{(+)}(\boldsymbol{y}; t)\right] = \frac{\cos t\sqrt{4\pi^2|\boldsymbol{y}|^2 + m^2}}{\sqrt{4\pi^2|\boldsymbol{y}|^2 + m^2}} .$$

Obviously $\mathscr{R}^{(1)}(\boldsymbol{y}, t) \in (\mathcal{O}_M)_{\boldsymbol{y}}$; then $R_x^{(1)}(t) \in (\mathcal{O}_C')_x$ and the kernel theorem allows us to write

$$R_x^{(1)}(t) = \frac{1}{(2\pi)^3} \int_{K^3} \mathrm{d}^3\boldsymbol{k} \exp[i\boldsymbol{k}\cdot\boldsymbol{x}] \frac{\cos \omega t}{\omega} . \tag{22}$$

We recognize in (22) the « function » $\Delta^{(1)}(\boldsymbol{x}, t)$.

Because

$$R^{(1)}(\boldsymbol{x}, t) = i\left[R_x^{(-)}(t) - R_x^{(+)}(t)\right],$$

$$\frac{\partial^2}{\partial t^2} R_x^{(1)}(t) - \Delta_{x\,(x)}^{*} R_x^{(1)}(t) + m^2 R_x^{(1)}(t) = 0,$$

we find again the classical formulas

$$\Delta^{(1)}(\boldsymbol{x}, t) = i\left[\Delta^{(+)}(\boldsymbol{x}, t) - \Delta^{(-)}(\boldsymbol{x}, t)\right],$$

$$(\Box - m^2)\Delta^{(1)}(\boldsymbol{x}, t) = 0.$$

Using M. Schönberg's transforms, we have

$$R_x^{(1)}(t) = m\frac{1}{4\pi\sqrt{t^2 - r^2}} N_1(m\sqrt{t^2 - r^2}) - mi\frac{\varepsilon(t + r) - \varepsilon(t - r)}{8\pi\sqrt{t^2 - r^2}} J_1(m\sqrt{t^2 - r^2}).$$

4. – Elementary Kernel Associated with the Klein-Gordon Differential Operator.

. The differential operator $\partial^2/\partial t^2 - \Delta_x + m^2$ defines a continuous linear application of $(\mathcal{D})_{x,t}$ into $(\mathcal{D}')_{x,t}$. The kernel theorem associates to it a *kernel distribution* L

$$L = L_{x,\xi,t,\tau} = \delta_{x-\xi} \times \frac{\partial^2}{\partial t^2}\delta_{t-\tau} - \delta_{t-\tau} \times \Delta_x \delta_{x-\xi} + m^2 \delta_{x-\xi} \times \delta_{t-\tau}.$$

Let us define a continuous application $R_x^{\mathrm{ret}}(t)$ of $]a, b[$ into $(\mathcal{O}_c')_x$ by the condition

$$R_x^{\mathrm{ret}}(t) = \begin{cases} R_x(t) & t > 0, \\ 0 & t < 0. \end{cases} \tag{23}$$

Because the resolving distribution $R_x(t)$ is defined for any $t \in R$, we shall write

$$R_x^{\mathrm{ret}}(t) = Y(t) R_x(t). \tag{24}$$

L. Schwartz [6] showed that

$$R^{\mathrm{rte}} \circ L = L \circ R^{\mathrm{ret}} = \delta_x \times \delta_t. \tag{25}$$

In other words, R^{ret} is the bilateral inverse of the kernel L; it is the *elementary kernel* associated with L. We identify in (23) the « Green function » $\Delta_{\text{ret}}(\boldsymbol{x}, t)$. (24) and (25) restate exactly, but in terms of distributions, the usual formulas

$$\Delta_{\text{ret}}(\boldsymbol{x}, t) = -\, Y(t)\,\Delta(\boldsymbol{x}, t)\,,$$

$$(\Box - m^2)\,\Delta_{\text{ret}}(\boldsymbol{x}, t) = -\,\delta(\boldsymbol{x}, t)\,.$$

Following the same pattern as L. SCHWARTZ's deduction, we can also define a continuous application $R_x^{\text{adv}}(t)$ of $]a, b[$ into $(\mathcal{O}_c')_x$ by the condition

$$R_x^{\text{adv}}(t) = \begin{cases} 0 & t > 0\,, \\ R_x(t) & t < 0\,, \end{cases} \tag{26}$$

or

$$R_x^{\text{adv}}(t) = \overset{\vee}{Y}(t) R_x(t) \tag{27}$$

and we can also prove that

$$R_x^{\text{adv}}(t) \circ L = L \circ R_x^{\text{adv}}(t) = -\,\delta_x \times \delta_t\,. \tag{28}$$

(26) defines rigorously the so-called « Green function » $-\Delta_{\text{adv}}(\boldsymbol{x}, t)$; (27) and (28) justify rigorously the symbolical formulas

$$\Delta^{\text{adv}}(\boldsymbol{x}, t) = \overset{\vee}{Y}(t)\,\Delta(\boldsymbol{x}, t)\,,$$

$$(\Box - m^2)\Delta_{\text{adv}}(\boldsymbol{x}, t) = -\,\delta(\boldsymbol{x}, t)\,.$$

$R_x^{\text{adv}}(t)$ and $R_x^{\text{ret}}(t)$ belong to the one-parameter (t) algebra of operators, which is defined by the Klein-Gordon differential operator L. By the usual properties of an algebra, we deduce

$$R_x^{\text{ret}}(t) + R_x^{\text{adv}}(t) = \left[Y(t) + \overset{\vee}{Y}(t)\right] R_x(t) = R_x(t)$$

and, in transposing,

$$\Delta(\boldsymbol{x}, t) = \Delta_{\text{adv}}(\boldsymbol{x}, t) - \Delta_{\text{ret}}(\boldsymbol{x}, t)\,.$$

(17) shows that

$$R_x(t) = \overset{\vee}{R}_x(t) = -\,R_x(-t) = -\,\overset{\vee}{R}_x(-t)$$

where $\vee$ represent the symmetry with respect to the origin in R^3. Then by (24) and (27)

$$\overset{\vee}{R}_x^{\text{ret}}(t) = Y(-t)\overset{\vee}{R}_x(-t) = -\,Y(-t)R_x(t) = -\,R_x^{\text{adv}}(t)\,.$$

These identities express well known properties of the « functions » $\Delta(\boldsymbol{x}, t)$, $\Delta_{\text{ret}}(\boldsymbol{x}, t)$ and $\Delta_{\text{adv}}(\boldsymbol{x}, t)$.

Comparing (17), (24) and (27), we get

$$R_{\boldsymbol{x}}^{\text{ret}}(t) = \frac{1}{4\pi r}\,\delta(t-r) - m\,\frac{Y(t-r)}{4\pi\sqrt{t^2-r^2}}\,J_1(m\sqrt{t^2-r^2})\,,$$

a result already brought up by H. G. Garnir ([13]) and corrected by L. Schwartz ([16]), and

$$R_{\boldsymbol{x}}^{\text{adv}}(t) = -\frac{1}{4\pi r}\,\delta(t+r) + m\,\frac{Y(t+r)}{4\pi\sqrt{t^2-r^2}}\,J_1(m\sqrt{t^2-r^2})\,.$$

Finally, we can also find the relations between

$$R_{\boldsymbol{x}}^{(+)}(t) = R_{\boldsymbol{x}}^{\text{ret}}(t) + \frac{m}{8\pi}\,\frac{1}{\sqrt{t^2-r^2}}\,H_1^{(1)}(m\sqrt{t^2-r^2}) - \frac{\delta(t^2-r^2)}{4\pi}\,,$$

$$R_{\boldsymbol{x}}^{(-)}(t) = R_{\boldsymbol{x}}^{\text{adv}}(t) - \frac{m}{8\pi}\,\frac{1}{\sqrt{t^2-r^2}}\,H_1^{(1)}(m\sqrt{t^2-r^2}) + \frac{\delta(t^2-r^2)}{4\pi}\,.$$

5. – The " Green Function " $\Delta(\boldsymbol{x}, t)$.

We considered the Klein-Gordon equation as a convolution equation in the set of distributions with carrier in $X^3 = R^3$. However we can also look on it as a convolution equation in the set $(\mathcal{D}')_{\boldsymbol{x},t}$ of the distributions which are carried in $X^3 \times \{t\} = R^4$

$$A_{\boldsymbol{x},t} \underset{(\boldsymbol{x},t)}{*} U_{\boldsymbol{x},t} = 0\,. \tag{29}$$

$A_{\boldsymbol{x},t}$ is a distribution $\in (\mathcal{O}_c')_{(\boldsymbol{x},t)}$, defined by

$$A_{\boldsymbol{x},t} = \frac{\partial^2}{\partial t^2}\,\delta_{(\boldsymbol{x},t)} - \Delta_{\boldsymbol{x}}\,\delta_{(\boldsymbol{x},t)} + m^2.$$

$U_{\boldsymbol{x},t}$ is assumed to belong to $(\mathcal{S}')_{\boldsymbol{x},t}^{\boldsymbol{\Gamma}}$.

If the two spaces $X^4 = \{(\boldsymbol{x}, t)\}$ and $Y^4 = \{(\boldsymbol{y}, y_0)\}$ are put in duality by the scalar product $x \cdot y = \boldsymbol{x} \cdot \boldsymbol{y} + t y_0 = x_1 y_1 + x_2 y_2 + x_3 y_3 + t y_0$, because $A_{\boldsymbol{x},t} \in \in (\mathcal{O}_c')_{(\boldsymbol{x},t)}$ and $U_{\boldsymbol{x},t}$ is assumed to be in $(\mathcal{S}')_{(\boldsymbol{x},t)}$, we can apply to (29) the Fourier transformation $\mathcal{F}_{\boldsymbol{x},t}$ which is performed between X^4 and its dual Y^4. This changes the convolution equation (29) into the multiplication equation

$$(4\pi^2\sigma^2 + m^2)\,\mathcal{U}_{\boldsymbol{y},y_0} = 0 \qquad \sigma^2 = |\boldsymbol{y}|^2 - y_0^2. \tag{30}$$

([16]) L. Schwartz: *Math. Rev.*, **13**, 352 (1952).

In order to study the evolution equation (10) we have to study the division by the function $(4\pi^2\sigma^2 - m^2) \in (\mathcal{O}_M)_{(\mathbf{y}, y_0)}$ in the topological modulus $(\mathcal{S}')_{\mathbf{y}, y_0}$ on $(\mathcal{O}_M)_{\mathbf{y}, y_0}$.

The function $4\pi^2\sigma^2 + m^2$ is singular on the hyperboloid $4\pi^2|\mathbf{y}|^2 - 4\pi^2 y^2 + m^2 = 0$ in Y^4. Hence the multiplication equation in $(\mathcal{S}')_{\mathbf{y}, y_0}$

$$(4\pi^2\sigma^2 + m^2)\mathcal{U}_{\mathbf{y}, y_0} = 1 \tag{31}$$

possesses an infinite number of solutions $\in (\mathcal{S}')_{\mathbf{y}, y_0}$, viz.

$$\mathcal{U}_{\mathbf{y}, y_0} = Pf \frac{1}{4\pi^2\sigma^2 + m^2} + \lambda \delta_{(4\pi^2\sigma^2 + m^2)}. \tag{32}$$

λ is an arbitrary complex-constant and $\delta_{(4\pi^2\sigma^2 + m^2)}$ is the Dirac measure produced by masses spread on the hyperboloid $4\pi^2\sigma^2 + m^2 = 0$ with a surface density -1. The pseudo-function distribution represented by Pf must still be defined. For every $\varphi(\mathbf{y}, y_0) \in (\mathcal{E})_{\mathbf{y}, y_0}$

$$Pf \frac{1}{4\pi^2\sigma^2 + m^2} \cdot \varphi(\mathbf{y}, y_0) = \int_{Y^3} \mathrm{d}^3\mathbf{y} \left[\text{v.p.} \int_{-\infty}^{+\infty} \mathrm{d}y_0 \frac{1}{4\pi^2\sigma^2 + m^2} \varphi(\mathbf{y}, y_0) \right]. \tag{33}$$

$\overline{\mathcal{U}}_{\mathbf{y}, y_0}$ is the particular solution for $\lambda = 0$.

The kernel theorem and the convention (33) give

$$\overline{\mathcal{U}}_{\mathbf{x}, t} = \int_{Y^3} \mathrm{d}\mathbf{y} \exp(2\pi i \mathbf{x}\cdot\mathbf{y}) \left[\text{v.p.} \int_{-\infty}^{+\infty} \exp[2\pi i t y_0] \frac{1}{4\pi^2\sigma^2 - m^2} \mathrm{d}y_0 \right].$$

or

$$U_{\mathbf{x}, t} = \begin{cases} \dfrac{1}{2} \displaystyle\int_{Y^3} \mathrm{d}\mathbf{y} \exp[2\pi i \mathbf{x}\cdot\mathbf{y}] \frac{\sin \omega t}{\omega} & \text{for any } t > 0 \\ -\dfrac{1}{2} \displaystyle\int_{Y^3} \mathrm{d}\mathbf{y} \exp[2\pi i \mathbf{x}\cdot\mathbf{y}] \frac{\sin \omega t}{\omega} & \text{for any } t < 0 . \end{cases} \tag{34}$$

From (15), the distribution $R_x(t) \in (\mathcal{S}')_x$ is a function of t, which is indefinitely differentiable and slowly decreasing; moreover, it is measurable for the Lebesgue measure on the t-axis; hence, to $R_x(t)$ is associated a distribution $\in (\mathcal{S}')_{x, t}$ which, by an *abus de langage*, we still represent by $R_x(t)$. If we compare (16) and (34), we learn that

$$U_{x, t} = \begin{cases} \frac{1}{2} R_x(t) & \text{for any } t > 0 , \\ -\frac{1}{2} R_x(t) & \text{for any } t < 0 . \end{cases}$$

Because $R_x(t)$ is defined for any $t \in R$, we are allowed to write

$$\overline{U}_{x,t} = \tfrac{1}{2}\varepsilon(t) R_x(t) . \tag{35}$$

In (35), we can identify $\overline{U}_x$; it is the « Green function » $\Delta(x, t)$.

By the inverse Fourier transform on (31) and (32) where $\lambda = 0$, we get

$$A_{x,t} \overset{*}{_{(x,t)}} \overline{U}_{x,t} = \delta_{(x,t)} , \tag{36}$$

$$\overline{U}_{x,t} = Pf \int_{V^4} \mathrm{d}^4 y \exp[2\pi i x \cdot y] \frac{1}{4\pi^2\sigma^2 + m^2} , \tag{37}$$

which justifies the classical formulas

$$(\Box - m^2)\overline{\Delta}(x, t) = -\delta(x, t) ,$$

$$\overline{\Delta}(x, t) = \frac{1}{(2\pi)^4} \text{v.p.} \int_{K^4} \mathrm{d}^4 k \frac{\exp[ikx]}{k^2 + m^2} .$$

(23) and (26) show that, as well as $R_x(t)$, $R_x^{\text{ret}}(t)$ and $R_x^{\text{adv}}(t)$ belong to $(\mathcal{S}')_{(x,t)}$. Hence, by (35), (23) and (26),

$$\overline{U}_{x,t} = \begin{cases} + \tfrac{1}{2} R_x^{\text{ret}}(t) & t > 0 \\ - \tfrac{1}{2} R_x^{\text{adv}}(t) & t < 0 \end{cases}$$

which justifies the well known corresponding result.

(17) and (35) give

$$\overline{U}_{x,t} = \frac{1}{4\pi r} \delta(t^2 - r^2) - m \frac{Y(t^2 - r^2)}{8\pi\sqrt{t^2 - r^2}} J_1(m\sqrt{t^2 - r^2}) .$$

If $\vee$ now designates the symmetry in X^4 with respect to the origin, we find that $\overset{\vee}{\overline{U}}_{x,t} = \overline{U}_{x,t}$ which is the usual property $\overline{\Delta}(x, t) = \overline{\Delta}(-x, -t)$.

By the way, we must notice that we could have reached $\overline{U}_{x,t}$ by another method. The elementary solution of the equation (10) is not unique: any other distribution which is obtained by adding to $R_x^{\text{ret}}(t)$ a solution of the homogeneous equation (10) is also an elementary solution. A particularly interesting form is the one which consists in adding to $R_x^{\text{ret}}(t)$, the solution $-R_x(t)$ of the homogeneous problem; and so we meet again the elementary solution

$$\overline{U}_{x,t} = R_x^{\text{ret}}(t) - \tfrac{1}{2} R_x(t) .$$

6. – The Distributions $\Delta_{(+)}(x, t)$ and $\Delta_{(-)}(x, t)$.

The equation (31) possesses other solutions than $\overline{U}_{x,t}$. For $\lambda = \pi i$, we get from (32)

$$\mathcal{U}_{(+)\mathbf{y},y_0} = 2\pi i \delta_{(-)(4\pi^2\sigma^2+m^2)} \cdot \tag{38}$$

The inverse Fourier transformation and the convention authorized by the kernel theorem give

$$A_{x,t\,(x,t)}^{*}\, U_{(+)(x,t)} = \delta_{(x,t)} , \tag{39}$$

$$U_{(x,t)} = 2\pi i \int_{Y^4} \mathrm{d}^4 y \exp\left[2\pi i x \cdot y\right] \delta_{(-)(4\pi^2\sigma^2+m^2)} \cdot \tag{40}$$

(38) shows that $U_{(+)x} = \Delta_{(-)}(x, t)$, a Green function which has been defined by J. SCHWINGER ([17]).

Besides the multiplication equation (31), we can also consider

$$(4\pi^2\sigma^2 + m^2)\, \mathcal{U}_{\mathbf{y},y_0} = -1 . \tag{41}$$

It possesses an infinite number of solutions $\in (\mathcal{S}')_{\mathbf{y},y_0}$,

$$\mathcal{U}_{\mathbf{y},y_0} = -Pf \frac{1}{4\pi^2\sigma^2 + m^2} + \lambda\delta_{(4\pi^2\sigma^2+m^2)} , \tag{42}$$

where the symbols Pf, λ and δ have the same meaning as in § 1. For $\lambda = \pi i$, we have the particular solution

$$\mathcal{U}_{(-)\mathbf{y},y_0} = 2\pi i\, \delta_{(+)(4\pi^2\sigma^2+m^2)} \cdot \tag{43}$$

Once more, by the inverse Fourier transformation,

$$A_{x,t\,(x,t)}^{*}\, U_{(-)(x,t)} = -\delta_{x,t} , \tag{44}$$

$$U_{(-)(x,t)} = 2\pi i \int_{Y^4} \mathrm{d}^4 y \exp\left[2\pi i x \cdot y\right] \delta_{(+)(4\pi^2\sigma^2+m^2)} \cdot \tag{45}$$

From (38) and (43),

$$\overline{U}_{(x\,t)} = \tfrac{1}{2}\left[U_{(+)(x,t)} - U_{(-)(x,t)}\right] . \tag{46}$$

([17]) J. SCHWINGER: *Phys. Rev.*, **76**, 790 (1949).

In (43), we recognize the temperate distribution $\Delta_{(\ )}(\boldsymbol{x}, t)$, as it has been defined by J. SCHWINGER ([17]).

T. TAKAHASHI ([18]) analysed the singularities of these distributions $\Delta^{(1)}$, $\Delta_{(+)}$ and $\Delta_{(-)}$ on the light cone.

([18]) T. TAKAHASHI: *Prog. Theor. Phys.*, **11**, 1 (1954).

RIASSUNTO (*)

Si applica una distribuzione all'equazione di Klein-Gordon. Si trova che la funzione $\Delta(\boldsymbol{x}, t)$ è la *distribuzione che risolve* l'equazione di Klein-Gordon considerata come equazione di evoluzione connessa col prodotto di convoluzione spaziale. $\Delta_{\text{ret}}(\boldsymbol{x}, t)$ è il *nocciolo elementare* nell'algebra degli operatori a un parametro, associato coll'operatore differenziale di Klein-Gordon. Finalmente, si dimostra che $\bar{\Delta}(\boldsymbol{x}, t)$ è una delle *soluzioni elementari* dell'equazione di Klein-Gordon che si considera ora come un'equazione di convoluzione spazio-temporale.

(*) *Traduzione a cura della Redazione.*

Variazione della sensbilità delle emulsioni nucleari in funzione della temperatura.

G. Alvial C.

Departemento de Física, Facultad de Filosofía y Educación, Universidad de Chile

(ricevuto il 23 Giugno 1954)

Riassunto. — Si studia la variazione della sensibilità delle emulsioni nucleari in funzione della temperatura tra i 20 °C ed i 90 °C. Tale variazione si misura dalla variazione della densità granulare media delle tracce di particelle α di 4,18 MeV. Si dà anche la variazione della densità del «fog» in funzione della temperatura. Si trovano due massimi di sensibilità: uno intorno ai 30 °C, l'altro intorno ai 70 °C.

1. – Lo studio della sensibilità delle emulsioni fotografiche ordinarie e nucleari, a temperature relativamente basse, si è particolarmente orientato in due direzioni: 1) ricerca delle variazioni delle leggi fotochimiche e della formazione dell'immagine latente; 2) conoscenza del comportamento delle emulsioni come strumento di lavoro.

Un notevole esempio del primo tipo d'indagini è il lavoro di Webb e Evans [1] nel quale — secondo la teoria di Gurney e Mott — la variazione della sensibilità delle emulsioni fotografiche è attribuita alla diminuzione della velocità degli ioni argento che si muovono verso gli «specks» per neutralizzare gli elettroni presi in essi.

Del secondo tipo si debbono ricordare due lavori: uno di Cosyns, Dilworth e Occhialini [2], in cui i ricercatori utilizzano la bassa sensibilità delle emulsioni nucleari come un «otturatore termico» per ottenere che esse non siano

[1] J. H. Webb e C. H. Evans: *Journ. Opt. Soc. Am.*, **28**, 249 (1938).

[2] M. Cosyns, C. Dilworth e G. P. S. Occhialini: *Bull. C. de Phys. Nucl. Bruxelles*, n. 6 (1949); C. Dilworth: *Bristol Symposium Cosmic Ray* (1948). Butterukth. London.

impressionate, o lo siano debolmente, prima di essere esposte alla radiazione in istudio; un altro di DOLLMANN [3], nel quale si stabilisce chiaramente la variazione della densità granulare (sensibilità) dei protoni di rinculo fra i — 66 °C ed i 25 °C. Questo comportamento fu determinato per dar conto dell'incompatibilità che si trovò nel misurare rapporti di massa di particelle elementari con il metodo del conteggio dei granuli.

L'autore del presente lavoro determina la variazione della densità granulare media — in granuli per micron — delle tracce di particelle α di 4,18 MeV e la densità dei granuli del fondo delle emulsioni nucleari in funzione della temperatura.

2. – Le emulsioni nucleari usate furono Eastman Kodak, NTA, NTB ed NTB3.

Di ogni tipo si prese una serie di dodici lastre di ugual fabbricazione. Ogni lastra di una serie determinata fu irradiata con particelle α di 4,18 MeV a una temperatura fissa. Tale temperatura d'esposizione fu diversa per ogni lastra d'una serie, variando tra i 20 °C ed i 90 °C, di 10 °C in 10 °C approssimativamente.

Si usò un campione radioattivo di ossido d'uranio. Particolare interesse si mise nel determinare la possibile esistenza della radiazione γ proveniente da sostanze estranee; ma le diverse misure eseguite con la camera di ionizzazione e con i contatori non rivelarono la presenza di radiazione γ nel materiale campione. In ogni caso, a certe temperature si riscaldò prima una lastra senza esporla a radiazione alcuna, onde confrontare il fondo di essa con quello della lastra esposta alle particelle α alla stessa temperatura. In una serie di otto lastre del tipo NTA, ogni lastra fu semplicemente scaldata alla temperatura corrispondente dell'intervallo già indicato, senza che la lastra stessa venisse esposta alla sorgente radioattiva. Il tempo d'esposizione per tutte le lastre fu di un'ora, eccezion fatta delle lastre NTA, la cui esposizione alle particelle α fu di mezz'ora.

Tutte le lastre di una serie furono sviluppate simultaneamente. Per ogni serie si usò il metodo di sviluppo che l'autore del presente lavoro, in una pubblicazione anteriore [4], discusse ed indicò come più conveniente per ottenere un fondo uniforme in profondità. E cioè, le lastre del tipo NTA ed NTB furono sviluppate seguendo il metodo di « hot-plate » con D-19b indicato da DAINTON, GATTIKER e LOCK [5], e quelle del tipo NTB3, seguendo il metodo in « due temperature » con D-19 indicato da WILSON e VANSELOW [6].

[3] E. M. DOLLMANN: *Rev. Scient. Instr.*, **21**, 118 (1950).
[4] G. ALVIAL C.: *Nuovo Cimento*, **10**, 1616 (1953).
[5] A. D. DAINTON, A. R. GATTIKER e W. O. LOCK: *Phil. Mag.*, **42**, 396 (1951).
[6] M. J. WILSON e W. VANSELOW: *Phys. Rev.*, **75**, 1144 (1949).

Tutte le lastre vennero sottoposte ad un lavaggio preliminare durante 30 minuti; poi, al corrispondente processo di sviluppo; quindi, ad un bagno di acido acetico al $\frac{1}{2}$ %; il fissaggio si effettuò in una soluzione di tiosolfato di sodio al 40%; infine, prima d'esser asciugate, le lastre furono immerse durante un'ora in una soluzione di glicerina al 10% secondo il metodo indicato da MIGNONE (7) e si asciugarono poi senza corrente d'aria.

Il «fog» delle emulsioni nucleari fu osservato in immersione in un microscopio universale Galileo con un ingrandimento totale di 3 700 diametri, corrispondente ad una superficie d'osservazione di 1344 μ^2.

La densità granulare media delle tracce α fu determinata in immersione usando un aumento totale di 1000 diametri ed illuminando le emulsioni nucleari con luce di sodio.

Per poter ottenere una miglior discriminazione delle singole immagini dei granuli d'argento che costituiscono le tracce, si collocò un obiettivo da microscopio nel sistema ottico del condensatore e si diaframmò convenientemente: in tal maniera si ottennero immagini diffratte e differenziabili dei granuli di argento. Le misure si realizzarono su un totale di 48 lastre.

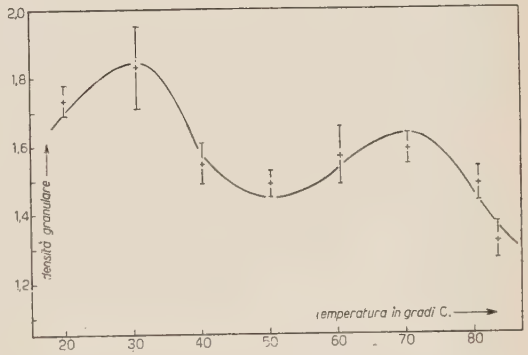

Fig. 1.

3. – Le misure della densità granulare media si realizzarono su tracce α rette per poter facilitare la determinazione della loro lunghezza.

Le curve delle fig. 1, 2 e 3 rappresentano la densità granulare media delle tracce α in funzione della temperatura per emulsioni rispettivamente del tipo NTA, NTB ed NTB3.

Ognuna delle curve fu misurata da un osservatore differente; inoltre esistono altre tre curve della stessa serie misurate da altri osservatori e che hanno lo stesso comportamento.

Le misure della densità dei granuli del fondo si effettuarono in due o tre strati equidistanti e paralleli alla superficie della emulsione. Per evitare il conteggio del «fog» spurio, il primo strato si prese a 5 μ sotto la superficie e l'ultimo a 5 μ sopra il vetro.

Le curve della fig. 4 danno il comportamento della densità granulare del fondo secondo la temperatura. Le lastre che s'impiegarono qui furono solo

(7) G. MIGNONE: *Nuovo Cimento*, **8**, 896 (1951).

riscaldate e non furono esposte ad alcuna radiazione. Le curve *a*, *b* e *c* corrispondono rispettivamente al primo, al secondo ed al terzo strato in ogni lastra del tipo NTA. In esse uno stesso osservatore ha esaminato 8 lastre. Di questa stessa serie esistono altri due gruppi di curve ottenute da altri osservatori e che presentano lo stesso andamento e numericamente sono quasi uguali. La densità si misurò dal numero di granuli per ogni 1 344 μ^2.

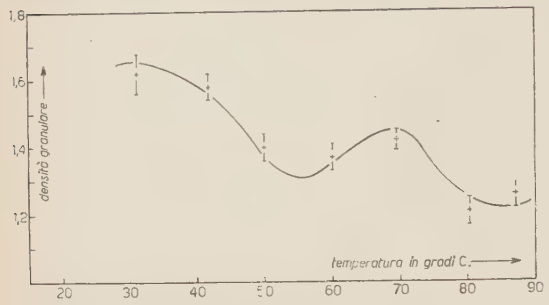

Fig. 2.

La fig. 5 confronta l'andamento della densità dei granuli del fondo con la densità granulare delle tracce α in funzione della temperatura. Le 8 lastre rappresentate, del tipo NTA e differenti da quelle rappresentate nella fig. 4, sono state irradiate con il campione di ossido d'uranio e misurate da uno stesso osservatore. Le curve *a* e *b* dànno la densità del « fog » rispettivamente del primo e del secondo strato. La curva *s* corrisponde al comportamento della densità granulare delle tracce α ed è la stessa della fig. 1.

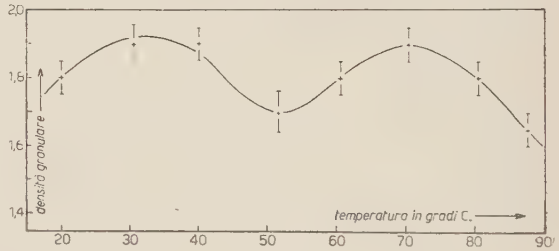

Fig. 3.

Nelle lastre del tipo NTB3 si osservò lo stesso comportamento descritto per la densità dei granuli del fondo. Le 8 lastre del tipo NTB non accusarono un comportamento definito: la densità dei granuli del fondo del primo strato di ogni lastra coincide esattamente con le curve descritte; il secondo e terzo strato presentano due massimi poco pronunciati e il quarto si comporta in forma completamente irregolare.

4. – Nella misura della densità granulare delle tracce radioattive e della densità dei granuli del fondo, le fluttuazioni statistiche furono gaussiane. Dato che le lastre di una stessa serie furono sviluppate simultaneamente, risultando approssimativamente tutte del medesimo spessore dopo d'essere state sviluppate, si può assicurare che i risultati esposti sono indipendenti dalla contrazione della gelatina.

Le curve sensibilità-temperatura delle fig. 1, 2 e 3 corrispondono a serie d'emulsioni di diverso tipo; inoltre, quelle delle fig. 1 e 2 furono sviluppate

con un metodo diverso di quello usato per sviluppare le emulsioni della fig. 3. Esattamente lo stesso si fece con le lastre corrispondenti alla densità di fondo in funzione della temperatura. Di conseguenza i risultati che si riportano, ed altri ottenuti in questo laboratorio, sono indipendenti dai metodi di sviluppo usati e dal tipo delle emulsioni.

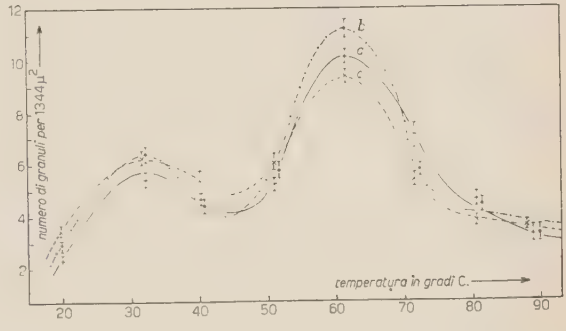

Fig. 4.

La densità di fondo dei tre strati di ogni lastra si aggruppa intorno ad uno stesso valore per una temperatura data, così come lo indica la fig. 4. Ciò significa che nel conteggio dei granuli del fondo non sono intervenuti sensibilmente granuli spuri, cioè che il fenomeno corrisponde essenzialmente ad un effetto di temperatura ed inoltre che la densità del « fog » è quasi uniforme in profondità in ogni lastra, come si indica e discute nel lavoro già citato [4].

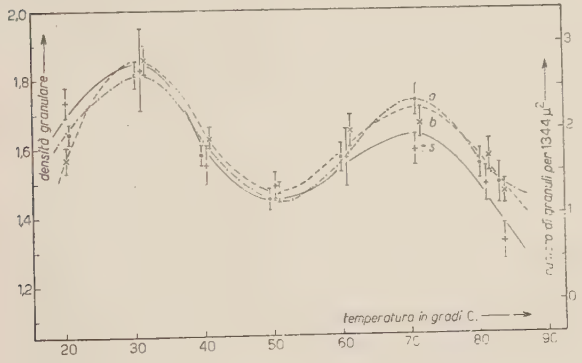

Fig. 5.

Una conferma del comportamento secondo la temperatura, tanto della densità dei granuli delle tracce come del fondo lo dànno le curve della fig. 5.

Il quoziente tra le densità medie delle tracce α a 30 °C e 50 °C varia tra 1,2 ed 1,3; tra 70 °C e 50 °C varia tra 1,1 ed 1, 2. Evidentemente, come strumento di lavoro, interessa solo il primo quoziente. C'è da considerare che DOLLMANN [3] trova per le lastre Ilford C2 un valore vicino a 3 per il quoziente tra le densità dei protoni di rinculo a 25 °C ed a — 66 °C, temperature alle quali misura le densità medie sopra settori corrispondenti delle tracce protoniche. È da supporre dunque che le nostre curve decrescano a mano a mano che diminuisce la temperatura.

I quozienti tra le densità dei granuli di fondo a 30 °C ed a 50 °C e tra le densità a 70 °C ed a 50 °C variano tra 1,5 e 2,5 e fra 1,5 e 3 per le diverse serie.

5. – L'interpretazione dell'esperimento esposto presenta molteplici difficoltà. L'autore di questo lavoro stima che una interpretazione esatta si otterrà solo con la determinazione di altre grandezze in funzione della temperatura. D'altra parte, qualunque sia l'interpretazione, deve mettersi in diretta relazione con una teoria della formazione dell'immagine latente.

MATHER ([8]) propone un meccanismo fondato sulla liberazione termica di elettroni e sull'evaporazione di atomi dello « speck » d'argento per spiegare il « fading » non dovuto ad agenti chimici. Il predominio della liberazione elettronica sull'evaporazione faciliterebbe la formazione dell'immagine; al contrario, se l'evaporazione fosse più intensa della liberazione di elettroni, si distruggerebbe l'immagine latente.

BEISER ([9]) ha proposto anche un meccanismo termico che consiste nel lancio di elettroni dallo « speck » d'argento per spiegare il « fading » d'origine non chimica.

È conveniente tener presente alcuni lavori sperimentali per analizzare le considerazioni precedenti. L'affinità elettronica degli alogeni è intorno a 3 eV; l'energia di legame di un elettrone di un centro F non è ancora determinata con precisione, ma oscilla tra 2,5 e 3,5 eV. Accettando una piccola differenza tra le affinità elettroniche del Br^- e dello I^- e prendendo in considerazione che il Br costituisce il 31,15% e lo I l'1,30% della composizione totale delle emulsioni usate, non è possibile far intervenire in uno dei massimi il Br^- e nell'altro lo I^- dato che entrambi i massimi sono quasi della stessa altezza.

Finalmente, è necessario considerare alcune reazioni chimiche del Br con la gelatina proposte da alcuni autori e che produrrebbero ioni OH^-.

Le proposte di MATHER e di BEISER sono basate sull'accettazione della ipotesi di GURNEY e MOTT relativa alla formazione dell'immagine latente. D'altro canto, è difficile ammettere a priori una fluttuazione della liberazione elettronica o dell'evaporazione atomica in intervalli di solo 20 °C. Una liberazione elettronica degli ioni Br o dei centri F richiederebbe temperature assai più elevate ed in tal caso si otterrebbe solo a spese dell'energia di vibrazione della rete dell'AgBr.

Un'altra possibile spiegazione viene data dalla teoria di Mitchell ([10]) sulla formazione dell'immagine latente. Secondo questa, è evidente che l'aumento della temperatura implica una probabilità maggiore di formare associazioni di centri F dato il meccanismo termico proposto per spiegare il movimento dei posti vacanti degli ioni Br. D'altra parte, la vita media d'un aggregato dei centri F diminuisce con la temperatura secondo l'espressione

$$t = t_0 \exp[W/KT],$$

([8]) K. B. MATHER: *Phys. Rev.*, **76**, 486 (1949).
([9]) A. BEISER: *Phys. Rev.*, **80**, 112 (1950).
([10]) J. W. MITCHELL: *Phil. Mag.*, **40**, 249 (1949).

in cui W è l'energia necessaria per separare un centro F dall'aggregato; K, la costante di Boltzmann e T, la temperatura assoluta. Si ricordi che a partire dalla prima grandezza critica l'aggregato è stabile.

La maggior probabilità di formare aggregati e la minore vita media di essi potrebbero dare il comportamento osservato nell'esperimento che si espone.

Finalmente, per definire l'intervento della gelatina o anche considerare la possibilità di un effetto quantico, mancano esperimenti che contribuiscano autonomamente ad una spiegazione. Vari di essi sono attualmente in corso in questo laboratorio.

Ringrazio il Rettore Magnifico dell'Università del Cile, Prof. JUAN GOMEZ MILLAS, ed il Decano della Facoltà di Filosofia ed Educazione, Prof. EUGENIO PEREIRA SALAS, per il costante interesse che hanno dimostrato durante lo sviluppo del presente lavoro. Esprimo anche la mia gratitudine alle mie assistenti, Signorine SILVIA STANTIC A. e LUISA FERNANDEZ M. per la loro preziosa collaborazione nell'esecuzione sperimentale di questo lavoro, all'aiutante Signorina ELISA SILVA M. ed alle laureande Signore ROSA JIMENEZ V. ed ELENA DUMONT M. per il loro aiuto nel corso delle esperienze.

Ringrazio il Prof. G. VALLI per la traduzione dallo spagnolo in italiano del presente lavoro.

SUMMARY

Variation of the sensibility of nuclear emulsions as a function of temperature between 20 °C and 90 °C is herein investigated. This variation is measured by means of the change in the average grain density of tracks of α particles of 4.18 MeV. Density variation of the fog as a function of the temperature is also given. Two maxima of sensibility are found: one at about 30 °C; the other at about 70 °C.

On the Decay Scheme of $^{214}_{84}$Po.

F. Demichelis and R. Malvano

Istituto di Fisica Sperimentale del Politecnico - Torino

(ricevuto il 27 Giugno 1954)

Summary. — New researches have been accomplished on the decay scheme of $^{214}_{84}$Po, and we have now used as well a photographic method as a method of opportunely discriminated coincidence countings. These methods have brought to the individuation of γ-γ cascades existing in the $^{214}_{84}$Po decay spectrum. In consequence it has been possible to establish the energy level scheme for the γ-rays according to the known γ-ray spectrum and the cascades. The resulting scheme shows remarkable differences from those proposed in the past by other authors.

1. – Introduction.

We have quite recently studied [1], with an absorption method, the energies and the intensities of $^{214}_{84}$Po cascade γ-rays.

However, owing to the poor approximation of our experimental method, we could not establish if among the various decay schemes built taking into account the data of the long range α-particles [2] and the γ-ray energies [3] there is one that satisfies univocally the experimental results.

Indeed the various decay schemes [2,4] do not present such a different behaviour in the absorption, to be revealed through our experimental results.

The mentioned decay schemes show a (1.76; 1.12) MeV γ-γ cascade whose

[1] F. Demichelis and R. Malvano: *Nuovo Cimento*, **10**, 405 (1953).

[2] E. Rutherford, W. B. Lewis and B. V. Bowden: *Proc. Roy. Soc.*, A **142**, 347 (1933); W. B. Lewis and B. V. Bowden: *Proc. Roy. Soc.*, A **145**, 235 (1934); G. H. Briggs: *Rev. Mod. Phys.*, **26**, 1 (1954).

[3] C. D. Ellis and G. H. Aston: *Proc. Roy. Soc.*, A **129**, 180 (1930); C. D. Ellis: *Proc. Roy. Soc.*, A **143**, 350 (1935); G. D. Latyshev: *Rev. Mod. Phys.*, **19**, 132 (1947).

[4] J. Surugue: *Journ. de Phys. et le Rad.*, (8) **7**, 145 (1946).

intensity is ≈ 0.20 per every β disintegration of $^{214}_{83}$Bi; otherwise the 0.61 MeV γ-ray, that decays with an intensity of 0.66 from the first excited to the ground state ([5]), appears partially as a member of a γ-ray cascade only in the scheme suggested by J. SURUGUE.

At the same time of our paper, a new report by A. H. WAPSTRA ([6]) appeared on some experimental investigations about the β-decay from $^{214}_{83}$Bi.

The author did not experimentally find a β-ray whose energy corresponds to a direct transition to the 0.61 MeV energy level; but he was brought to admit of its existence as he suggests in his partial decay scheme.

In this scheme the (1.76; 1.12) MeV γ-γ ray cascade was no longer considered, because a β-ray with energy and intensity which could justify this cascade was not experimentally found.

All these results cannot be considered in agreement with each other.

Therefore we have been induced to study again the $^{214}_{84}$Po decay spectrum by means of experimental methods more suitable to the complexity of this problem.

2. – Experimental Apparatus.

In our measurements we have made use of the following apparatus, whose block-diagram is sketched in Fig. 1.

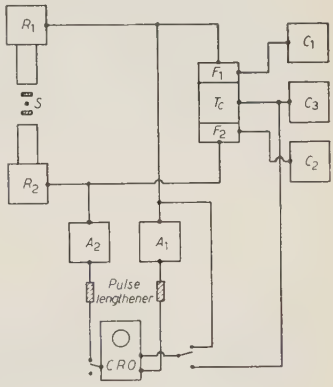

Fig. 1.

R_1 and R_2 are two γ-rays scintillation crystal (NaI-Tl)-phototube devices acting as γ-ray proportional counters with good resolving power.

The voltage pulses at the output of the phototubes, through a convenient preamplifier are applied to the grids of two pulse shapers F_1 and F_2 (asymmetrical univibrators).

The pulses, after a process of differentiation, are applied to the grids of a twin triode T_c which reveals the coincidence of two pulses [resolving time: $\tau = (1.72 \pm 0.05)\ 10^{-7}$ s].

C_1 and C_2 count the total numbers of γ-rays detected by R_1 and R_2, after having triggered the pulse shapers. These shapers are also used as integral discriminators.

C_3 counts the total number of coincidences.

To obtain a good ratio between the effective and the accidental coincidence

([5]) G. SCHARFF-GOLDHABER: *Phys. Rev.*, **90**, 587 (1953).
([6]) A. H. WAPSTRA: *Akademisch Proefschrift* (Amsterdam, 1953).

counting rate, the radioactive source intensity is reduced to few microcuries (≈ 5 μc).

We get, however, a good counting rate by placing the scintillation crystals and their phototubes so that the solid angle between each crystal and the source be as wide as possible.

The Compton backscattered photons do not interfere with the measurements because the pulse shapers F_1 and F_2 are constantly biased to detect only those pulses produced by γ-rays whose energy is greater than 0.3 MeV.

The source (radium bromide in equilibrium with its decay products) is contained inside a small aluminium enclosure with thin walls (thickness ≈ 0.5 mm); it is hermetically closed and is placed between two lead discs (thickness 1 mm), which are fit to stop completely the most energetic β-rays (3.17 MeV) emitted in the decay of $^{214}_{83}$Bi.

The pulses, at the output of one detector, feed at the same time the coincidence circuit and a conveniently triggered differential discriminator.

The discriminator is used in the following *a*) and *b*) ways:

a) The pulse from the preamplifier passes through a further linear amplifier (amplification ≈ 50) and is lengthened ([7]) so that the pulse flat top lasts for ≈ 4 μs; at last the pulse is applied to the vertical deflection plates of a wide-band cathode ray oscillograph (C.R.O.), which has a very linear deflection, a very thin trace and a fine and uniformly distributed grain screen.

The horizontal deflection is obtained through the deflection generator used as a syncroscope: the grid that drives the intensity of the cathode ray beam is normally biased to cut-off (in this case the oscillograph screen is dark), and is triggered above cut-off only by an external pulse.

The screen of the cathode ray oscillograph is photographed ($f = 5.8$ cm) on a fine grain film (32 mm).

The differential discriminator can be used to record all pulses from only one crystal device; in this case the pulse to the driving grid of the oscillograph is taken from one of the pulse shapers.

In Fig. 2 we can observe the spectrogram of RdTh ($\approx 500\,000$ pulses) (*); we may observe, incidentally, that the writing speed on the cathode ray screen does not depend upon the pulse amplitude and produces therefore on the photographic film a blackening that is a function only of the number, not of the amplitude, of the traces.

If we want to record only the coincidence pulses (*coincidence spectrum with one side discrimination*) the brightening driving grid is triggered by the output pulse from the coincidence circuit ([8]).

([7]) J. CRAIB: *Electronics*, **24**, 6, 129 (1951).

(*) The high number of pulses in every spectrogram is necessary to reduce the statistical errors.

([8]) S. A. E. JOHANSSON and S. ALMQUIST: *Ark. för Fysik*, **5**, 20, 427 (1952).

Fig. 2.

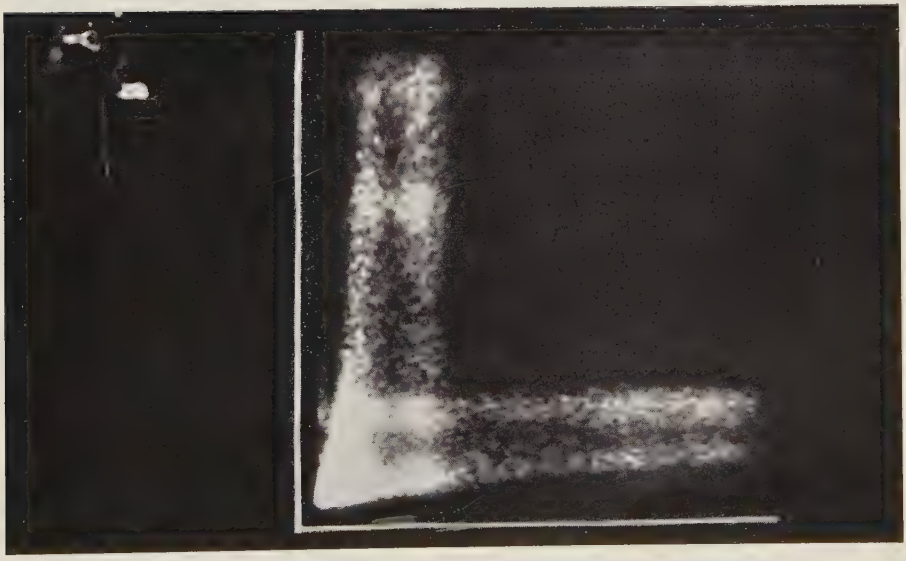

Fig. 3.

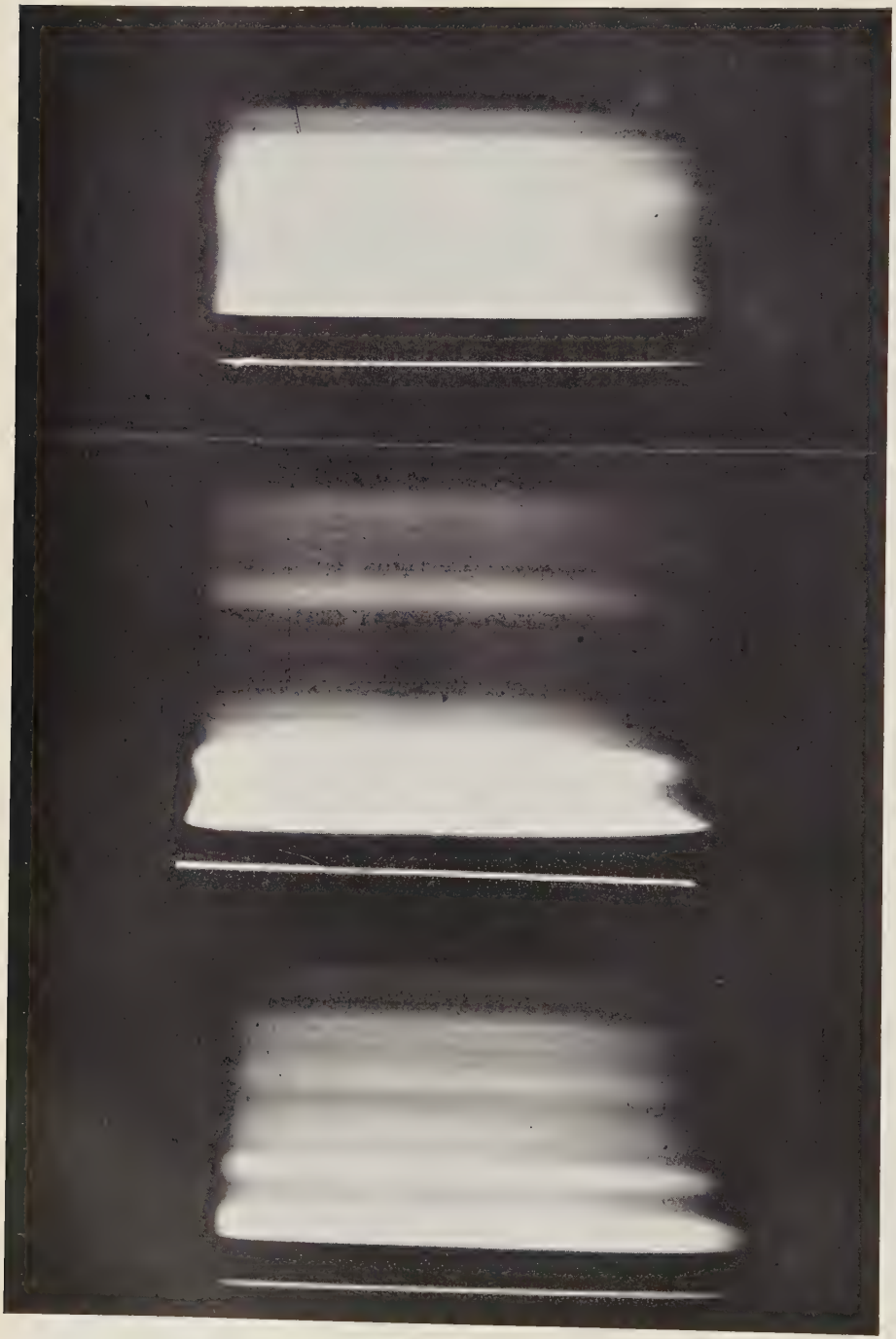

Fig. 4.

b) The output pulses from both crystal devices are amplified and lengthened, as we have said before in *a*). They are applied respectively to the vertical and horizontal oscillograph deflection plates.

If a γ-ray coincidence occurs, the co-operative action of the two pulses displaces the electronic spot from its rest position at a point whose coordinates on the x, y axis of the oscillograph correspond to the amplitude of the pulses applied respectively to the vertical and horizontal deflection plates.

As a coincidence occurs the cathode ray oscillograph is triggered through the driving grid and the spot on the screen is brightened for an extremely short time (1-2 μs) corresponding to the flat top of the pulses.

The relative crowding of points in various regions of the screen, determines the energy of the two coincident γ-rays (*coincidence spectrum with both side discrimination*) ([9]).

In Fig. 3 we can observe the coincidences of the (0.58; 2.62) MeV γ-ray cascade of $^{208}_{82}$Pb ([10]).

3. – Measurements and Experimental Results.

In order to calibrate our γ-ray spectrometer, we have made spectrograms on some radioactive nuclides whose γ-rays have well known energies extending in the interval between 0.58 and 2.62 MeV, that comprises the $^{214}_{84}$Po γ-ray energies.

In Fig. 4 *a*, *b*, *c*, the spectrograms of $^{60}_{27}$Co, RdTh, $^{214}_{84}$Po are shown.

Each spectrogram corresponds to ≈ 500000 pulses.

In Fig. 5 we show the calibration curve of our spectrometer; this was used for energies up to 2.2 MeV: the lack of linearity is sensible only for the highest energies where it does not reach 10% at the limit of the calibration curve.

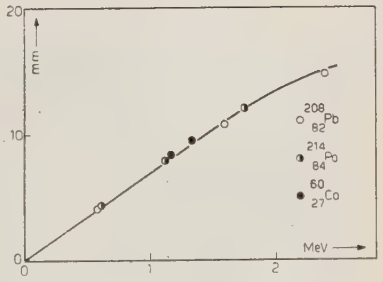

Fig. 5.

With the above apparatus we have obtained the following spectrograms:

Fig. 6 *a* relative to the total coincidences of $^{214}_{84}$Po with one side discrimination;

Fig. 6 *b* relative to the accidental coincidences.

Both spectrograms have been made with the same exposure, diaphragm

([9]) S. C. Curran: *Luminescence and Scintillation Counters* (Butterworths Scientific Publication, 1953).

([10]) F. Oppenheimer: *Proc. Camb. Phyl. Soc.*, **32**, 328 (1936).

and trace brightness; they correspond respectively to $\approx 40\,000$ coincidences for Fig. 6 *a* and $\approx 4\,500$ coincidences for Fig. 6 *b*.

In Fig. 6 *c* we can observe the spectrogram of the coincidences with both side discrimination for the $^{214}_{84}$Po decay; the number of recorded points corresponds to $\approx 55\,000$ coincidences.

In Fig. 6 *d* the total $^{214}_{84}$Po γ-ray spectrum are shown in order to make a direct comparison with the coincidence spectrum (Fig. 6 *a*).

From the Fig. 6 spectrograms we can easily deduce that the 0.61 MeV, the 1.12 MeV and other less intense γ-rays, whose energies are at most 1.7 MeV, belong to a set of cascades.

The crowding of points in Fig. 6 *c* is confined almost exclusively by the photoelectric lines of the 0.61 MeV γ-rays; this indicates that nearly all γ-rays in coincidence are followed by the 0.61 MeV γ-ray which, according to the experimental evidence [5] is the lowest energy γ-ray belonging to the spectrum of $^{214}_{84}$Po.

The results obtained with the photographic method are qualitatively satisfying from the standpoint of energy at least for the more intense γ-rays: but the following problems, however, remain opened if the photographic method only is used:

Fig. 7.

1) to identify the maximum energy γ-ray belonging to a cascade;

2) to know if all the cascade γ-rays are followed by the 0.61 MeV transition; and to identify other types of cascades, if any;

3) to measure the ratio $\sum_s p_s / \sum_n p_n$ between the total number of cascade γ-rays and the total number of all γ-rays emitted by $^{214}_{84}$Po.

In order to solve the above problems we have measured the effective coincidence counting rate N_b versus the bias of the integral discriminators at the input of the coincidence circuit, carefully calibrated in energy of the γ-rays.

In Fig. 7 *a* the experimental points are obtained biasing the discriminator F_1 at a voltage corresponding to the γ-ray energy of 0.51 MeV, while the bias of the discriminator F_2 is varying from $h\nu/mc^2 = 1$ to $h\nu/mc^2 = 3.5$.

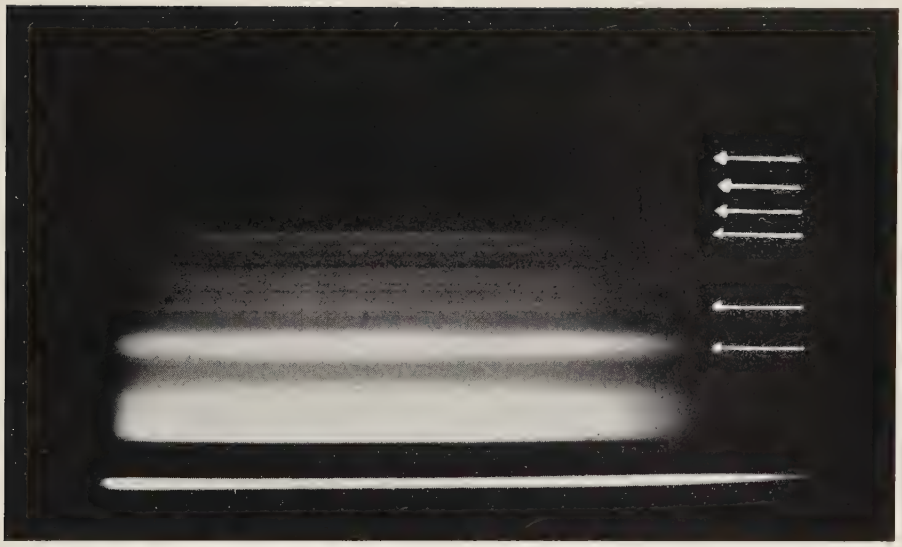

Fig. 6 *a*).

Fig. 6 *b*).

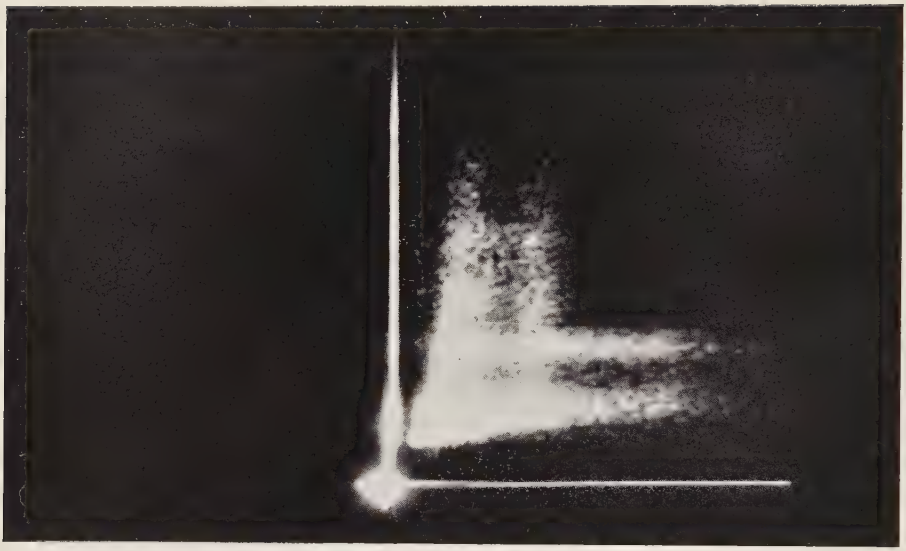

Fig. 6 *c*).

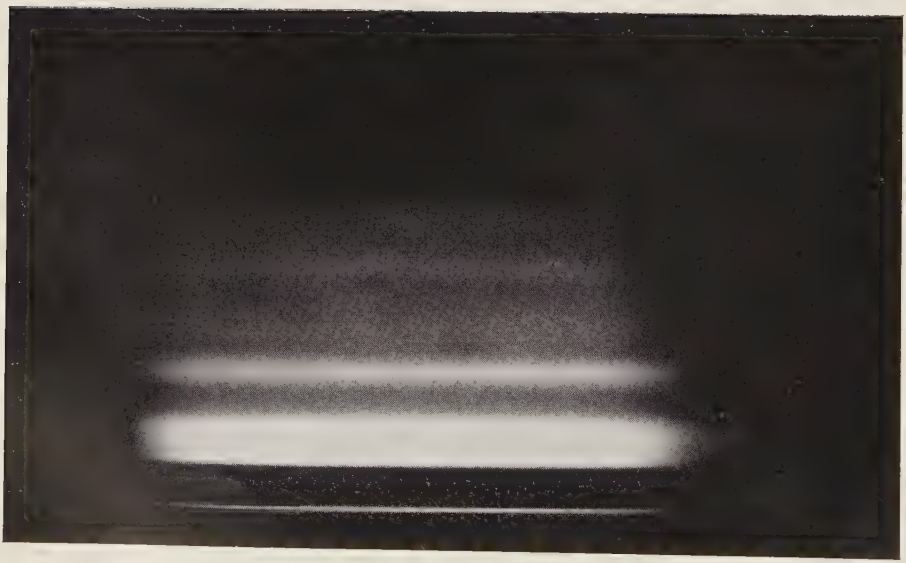

Fig. 6 *d*).

In Fig. 7 *b* the experimental points are obtained biasing the first discriminator to a voltage corresponding to $h\nu/mc^2 = 1.5$ while the second discriminator changes its bias from $h\nu/mc^2 = 1.4$ to $h\nu/mc^2 = 2.8$.

In both Fig. 7 *a*, 7 *b* the experimental points are normalized to the values N_{b_0} relative to the effective coincidence counting rate when the two discriminators are both biased to $h\nu/mc^2 = 1$.

In this figures the experimental points are conveniently corrected for cosmic ray coincidences.

From the above experimental data we can deduce immediately that:

I) a small intensity cascade whose rays have an energy higher than 0.61 MeV but lower (or equal) to 1.30 MeV does exist (see Fig. 7 *b*);

II) all the other cascades have as a common component the 0.61 MeV γ-ray (see Fig. 6 *c*, 7 *a*, 7 *b*);

III) from fig. 7 *a* we can deduce that the maximum energy γ-transition belonging to a cascade is the 1.52 MeV γ-ray;

IV) all other γ-rays with energy higher than 1.60 MeV *do not belong to a cascade*;

V) among the various cascade γ-rays followed by the 0.61 MeV, the 1.12 MeV is the most intense (see Fig. 5 *a*).

To get further and more precise information from the experimental data we have drawn the curves of Fig. 8.

They represent the γ-ray integral cross-section σ versus the discriminator bias (parameter $h\nu/mc^2$) in NaI-Tl crystals (see Appendix).

The curves of Fig. 7 *a* are the theoretical values of N_b/N_{b_0} versus $h\nu/mc^2$, where it is:

$$N_b = \sum_s q_s [\sigma_{1i}\sigma_{2j} + \sigma_{1j}\sigma_{2i}],$$

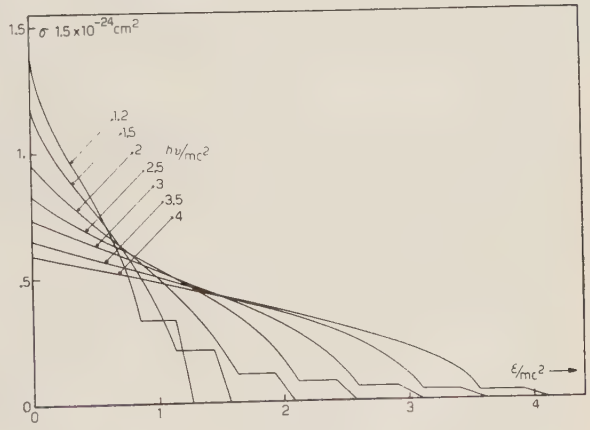

Fig. 8.

and q_s is the cascade relative intensity deduced from the relative intensity of the γ-rays according to G. D. LATYSHEV[3].

The full line represents N_b/N_{b_0} for the cascade (0.76; 1.29) MeV while the dotted line represents the same quantity for the cascade (0.93; 1.29) MeV.

In Fig. 7 *b* the dotted line represents N_b/N_{b_0} for the group of the three cascades:

(1.12; 0.61) MeV, (intensity 49%)
(1.52; 0.61) MeV, (» 14%)
(0.76; 1.29) MeV, (» 14%)

while the full line represents, in good agreement with the experimental data, N_b/N_{b_0} for this group and the following cascade:

(1.38; 0.61) MeV, (intensity 23%).

Actually the 0.61, 0.76, 1.12, 1.29, 1.38, 1.52 MeV rays may be observed in Fig. 6 *a* relative to the total coincidences with one side discrimination and are indicated with small arrows.

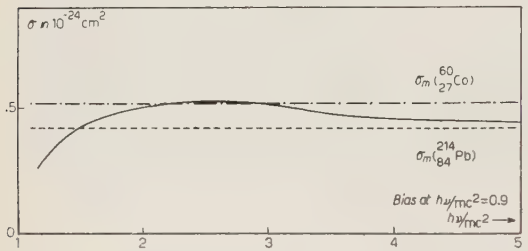

Fig. 9.

In order to give an answer to point 3) (measurement of the ratio: number of cascade γ-rays over total number of γ-rays for each β disintegration process of $^{214}_{83}$Bi) we have operated in the following way.

The two discriminators were biased to a voltage corresponding to 0.45 MeV; in this condition the γ cross-section σ is roughly indipendent, as we can see in Fig. 9, upon the energy of the incident γ-rays in an interval including the $^{214}_{84}$Po γ-rays.

With a weighted mean $\sigma_{m,\mathrm{Po}}$, $\sigma_{m,\mathrm{Co}}$ for $^{214}_{84}$Po and $^{60}_{27}$Co (see Fig. 9), and making use of a standardized $^{60}_{27}$Co source (*) we could determine the number of γ-rays emitted per unit time from our $^{214}_{84}$Po source, i.e. the quantity $I \sum_n p_n$ where I is the source intensity (number of disintegration processes per unit time).

From our measurements we got the value:

$$I \sum_n p_n = (2.50 \pm 0.05) \cdot 10^5 \ \mathrm{s}^{-1} .$$

The above quantity appears in the following expression:

$$\frac{N_b}{N_c} = \frac{n_{12}}{2\tau n_1 n_2} - 1 = \frac{\sum_s p_s \sigma_{si} \sigma_{sj}}{\tau I (\sum_n p_n \sigma_n)^2} = \frac{1}{\tau I \sigma_m^2 \sum_n p_n} \frac{\sum_s p_s \sigma_{si} \sigma_{sj}}{\sum_n p_n} ,$$

(*) With the same standardized $^{60}_{27}$Co source we could verify the efficiency of our coincidence circuit.

where N_b, N_c are respectively the effective and accidental coincidence counting rate, n_1, n_2 are the experimental values of the single counting rate for each discriminator, n_{12} is the value of the total coincidence counting rate, and the other symbols have a meaning already indicated.

For the cascades with the 0.61 MeV γ-ray the product σ_{si}, σ_{sj} has the constant value $0.15 \cdot 10^{-48}$ cm^4, while for the cascade (0.76; 1.29) MeV its value is $0.23 \cdot 10^{-48}$ cm^4.

Making the assumption, according to the data of G. D. LATYSHEV, that the small intensity cascade is the $\approx 14\%$ of the total cascade intensity, the expression:

$$\frac{\sum_s p_s \sigma_{si} \sigma_{sj}}{\sum_n p_n} ,$$

becomes

$$1.075 \frac{\sum_s p_s}{\sum_n p_n} ;$$

therefore we get

$$\frac{\sum_s p_s}{\sum_n p_n} = 0.64 \pm 0.06 ,$$

i.e. the total number of γ-rays belonging to cascades represents $\approx 65\%$ of the total number of γ-rays emitted from $^{214}_{84}$Po.

In Fig. 10 the experimental points represent the ratio N_b/N_c against $h\nu/mc^2$; the full line is the theoretical behaviour of the ratio assuming for the product $I \sum_n p_n$ the experimental value $2.50 \cdot 10^5$ s^{-1} and for $\sum_s p_s / \sum_n p_n$ the value 0.64.

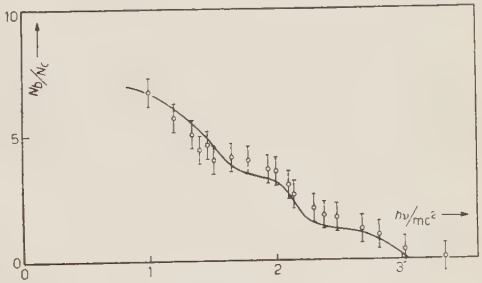

Fig. 10.

4. – Discussion of Experimental Data.

The experimental data we have obtained allow us now to build up a decay scheme of $^{214}_{84}$Po; for this purpose we have to consider the long range α-particles levels and the data concerning the value of the β-branches from $^{214}_{83}$Bi.

According to what has been previously pointed out, the γ-rays higher than 1.60 MeV fall directly to the ground state; and they decay therefore from the following energy levels:

$$2.43 , \quad 2.20 , \quad 2.09 , \quad 1.82 , \quad 1.76 , \quad 1.69 , \quad 1.62 \text{ MeV} .$$

Otherwise, since there is not doubt that the first excited state is the 0.61 MeV level, the cascade (1.12; 0.61) MeV determines a level at 1.73 MeV; recent experimental results ([11]) give just the existence of a small intensity γ-ray of this energy.

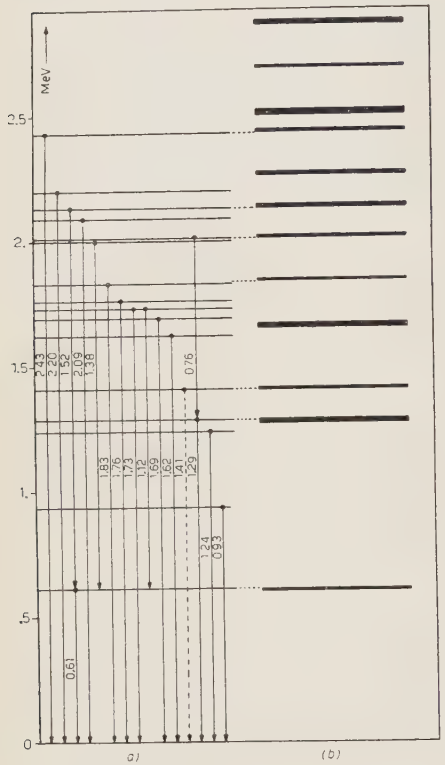

Fig. 11.

The cascades

(1.52; 0.61) MeV

(1.38; 0.61) MeV

(0.76; 1.29) MeV

must decay from the levels

2.13 , 1.99 , 2.06 MeV

and the 0.93 MeV transition, which is not apparently in cascade with any other γ-ray, from a level at 0.93 MeV.

In Fig. 11 *a* we have drawn a decay scheme which is in agreement with our measurements on the γ-ray cascades; in Fig. 11 *b* the levels of the long range α particles are represented, each level being drawn as a narrow strip whose width indicates the probable errors which affect the single measurements according to the results of E. RUTHERFORD and coworkers ([2]).

From the above figure we can get the following conclusions: the *only* γ-rays of

2.42 (*) , 1.82 (*) , 1.29 , 0.61 MeV

and the *only* cascades

(0.76; 1.29) MeV

(1.52; 0.61) MeV

seem to decay, in a good approximation, from levels identified in the long range α-particles measurements ([2]).

([11]) M. MLADJENOVIC and A. HEDGRAN: *Physica*, **18**, 1243 (1952).

(*) More recent measurements give for the γ-rays of 2.42 MeV and 1.82 MeV respectively the values 2.43 MeV and 1.84 MeV ([11]).

All the other long range α-particle levels do not appear to produce any measurable γ-ray transition; inversely *all* the other γ-ray levels, which it seems to be necessary to introduce, do not give rise to any long range α-particles as they have been detected till now; among these we find the 1.76, 1.73, 1.69 MeV levels from which particularly intense γ-ray transitions come out.

We think furthermore that the existence of some levels corresponding to γ-ray transitions with energy nearly equal to α-particle levels, but not included in the relative approximation be of some interest.

According to the proposed scheme the following β-branches would exist:

3.17 MeV decaying to the ground state ([3,6]);

2.56 MeV decaying to the 0.61 MeV level ([12]);

1.40 MeV decaying to the 1.70 MeV group of levels.

Some other β-branches of lower intensity decay to the remaining levels. With the assumption that the 3.17 MeV β-branch forms the 20% of all β-rays from $^{214}_{83}$Bi ([3,6]) and taking into account our experimental value 0.64 of the ratio $\sum_s p_s / \sum_n p_n$ we can easily deduce that $\sum_n p_n = 1.18 \pm 0.05$; while, if we suppose that the intensity of the same β-branch is the 10% of all β-rays from $^{214}_{83}$Bi it would result

$$\sum_n p_n = 1.33 \pm 0.06 .$$

This values are very different from those given by C. D. Ellis and G. D. Latyshev ([3]).

At this point we ought to assign parities and angular momenta to the different levels of our decay scheme, but the known experimental data do not allow us to make this assignement.

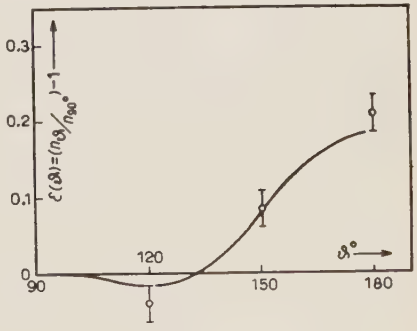

Fig. 12.

However, making use of the data concerning the total angular correlation of the γ-ray cascades ([13]), of the knowledge on the transition types (dipole, quadrupole) and that the 0.61 MeV is a 2+ level ([5]), we can satisfy the experimental curve of the total angular correlation (Fig. 12) with only three types of cascades, which are the fol-

([12]) R. A. Ricci and G. Trivero: *Atti Acc. Lincei* (in press).

([13]) F. Demichelis and R. Malvano: *Nuovo Cimento*, **10**, 1359 (1953); *Phys. Rev.*, **93**, 526 (1954).

lowing ones:

(1.12; 0.61) and (1.52; 0.61) MeV: Quadrupole-quadrupole; 4 – 2 – 0
(1.38; 0.61) MeV : » » ; 2 – 2 – 0
(0.76; 1.29) MeV : Dipole-quadrupole ; 2 – 2 – 0

In order to obtain a confirmation of the above hypothesis it should be necessary, in angular correlation experiments, to isolate each cascade.

We want to express our deep gratitude to Prof. E. PERUCCA, Director of the Institute, for his encouragement and advice.

APPENDIX

In order to calculate the γ-ray cross-section in NaI-Tl crystals, versus the integral discriminator bias, we have taken into account the Compton and the photoelectric cross-section: the pair production cross-section can be disregarded for the energies of $^{214}_{84}$Po γ-rays.

The Compton cross-section is given by the formula

$$\sigma\left(\frac{2\gamma}{2\gamma+1}\right) - \sigma(\alpha) = \pi r_0^2 \left[\frac{\gamma^2 - 2\gamma - 2}{\gamma^3} \log(1-\alpha)(2\gamma+1) + (1-\alpha)\frac{2\gamma+1}{\gamma^3} - \right.$$
$$\left. - \frac{1}{(1-\alpha)\gamma^3} + \frac{1}{2}\frac{(1-\alpha)^2}{\gamma} + \frac{16\gamma^2 + 15\gamma + 4}{2\gamma^2(2\gamma+1)^2}\right],$$

where r_0 is the classical electronic radius; besides it is: $\gamma = h\nu/mc^2$, $\alpha = \varepsilon/\gamma$, ε = energy of the electrons corresponding to the integral discriminator bias.

In order to calculate the photoelectric cross-section, we have used the curve obtained by D. MAEDER and coworkers ([14]); it gives the ratio between the total number of photoelectric processes and the total number of interaction processes in a NaI-Tl crystal of given shape and dimension. The total cross-section versus ε/mc^2 (parameter $h\nu/mc^2$) is drawn in Fig. 8.

([14]) D. MAEDER, R. MÜLLER and V. WINTERSTEIGER: *Helv. Phys. Acta*, **27**, 1, 3 (1954).

RIASSUNTO

È stato ripreso lo studio dello spettro di decadimento del $^{214}_{84}$Po, utilizzando sia il metodo fotografico sia il metodo di conteggio delle coincidenze opportunamente discriminate. Questi metodi hanno condotto alla individuazione delle cascate γ-γ presenti nello spettro di decadimento del $^{214}_{84}$Po. Ciò ci ha concesso di determinare uno schema di decadimento, capace di dar ragione sia delle energie dei raggi γ, già note, sia delle cascate da noi controllate; esso è sensibilmente diverso da quelli proposti per il passato da altri autori.

A V-Event Associated with a Star from which a K-meson is Emitted.

A. Debenedetti, C. M. Garelli, L. Tallone and M. Vigone

Istituto Nazionale di Fisica Nucleare - Sezione di Torino

(ricevuto il 28 Giugno 1954)

Summary. — From a star observed in a stack of stripped emulsions, a K-meson and a neutral particle decaying in flight are emitted. The V-event can be interpreted either as a Λ^0 decay ($Q = 36^{+67}_{-16}$ MeV) or as a θ^0-decay ($Q = 216^{+150}_{-55}$ MeV).

An event consisting of a pair of lightly ionizing tracks was observed in this laboratory during the general scanning of a stack of stripped emulsions, flown at 80 000 ft in the Sardinia Expedition 1953. The vertex of the pair is at a distance of 25 μ from the centre of a star (Fig. 1).

The two tracks could not be found in the following plate.

Ionization and scattering measurements have been carried out. To determine the ionization, we measured the quantity b^*, that is the ratio of the blob number of the track to the blob number of the « plateau ». This last value was obtained using electron tracks from μ-decays.

Scattering measurements have been made following the suggestions of the Bureau of Standards. The scattering constant has been deduced from the theoretical curves given by Voyvodic and Pickup [1]. As we have no calibration for the scattering constant, the standard error in the $p\beta$ has been increased by an additional error of 8%.

Track 1 (Fig. 2) travels 3 130 μ before leaving the plate. From scattering measurements we have $\alpha_{100} = 0{,}075^\circ \pm 0{,}011^\circ$; $p\beta c = 320 \pm 65$ MeV. The ionization value is $b^* = 0.905 \pm 0.028$.

Track 2 escapes from the emulsion after 1 760 μ. Ionization measurements

---

[1] L. Voyvodic and E. Pickup: *Phys. Rev.*, **85**, 91 (1952).

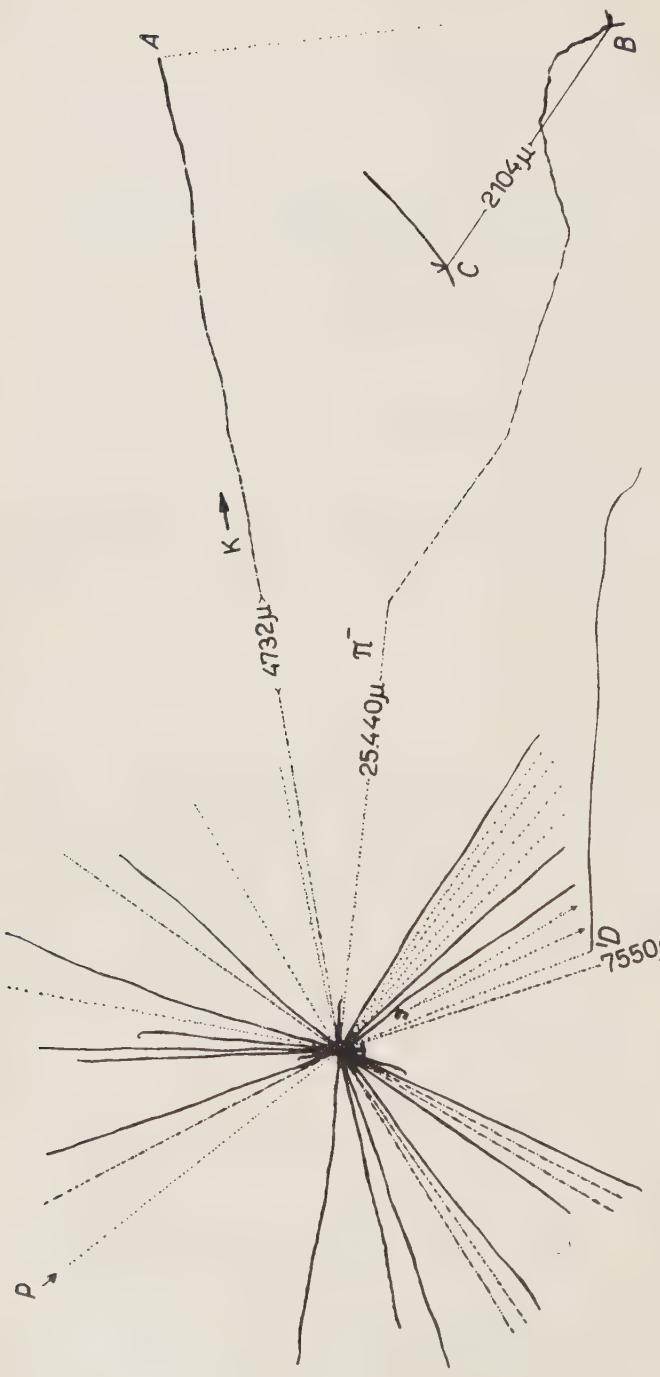

Fig. 1. *Observer*: M. Greco

give $b^* = 0.977 \pm 0.039$. Scattering measurements on track 2 were disturbed by local distortions produced by impurities of the emulsion. The rough estimate obtained, $\alpha_{100} \sim 0.06^\circ$, has never been used in the calculations.

The angle between the two tracks is $16^\circ\,43' \pm 30'$. The direction of motion of neither particle can be determined.

Such an event can be interpreted either as a scattering or as the decay of a neutral particle, emitted from the star. However the first hypothesis does not appear to be likely, because no recoil or slow electron track is visible at the vertex of the pair, whereas the second one is strongly supported by the coplanarity of the two tracks with the centre of the neighbouring star. The assumed direction of motion of a primary neutral particle is at an angle of $40'$ with the plane of the two tracks. As in the calculation of this angle the experimental errors give an uncertainty of $\pm 1^\circ$, we can say that the coplanarity is satisfactorily proved.

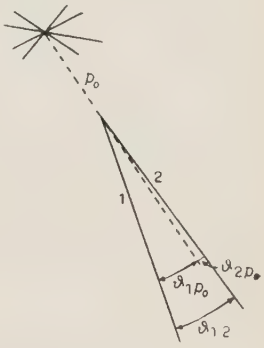

Fig. 2.

To determine the position of the centre of the star, we calculated the intersection points of pairs of relativistic prongs. We obtained that the most probable uncertainty in the position of the centre is $\pm 0.18\ \mu$. Consequently, the error in the direction of the neutral primary p_0 is $\pm 30'$. The direction of each of the tracks 1, 2 has been determined within $\pm 15'$ because the two tracks have a very small angle of dip. Therefore we can have in the angle $\vartheta_{12} = 16^\circ\,43'$ an error of $\pm 30'$, and in both angles $\vartheta_{1p_0} = 14^\circ\,52'$ and $\vartheta_{2p_0} = 1^\circ\,53'$ and error of $\pm 45'$.

We interpret the event as the two-body decay of a neutral particle ejected from the star.

From scattering and ionization measurements, we can say that track 1 is not due to a proton; it can be either an electron or a light meson.

The hypothesis that the V-event is an electron-pair produced by a γ-ray is very improbable:

a) because the angle between the two tracks is too large;
b) for the strong asymmetry of the two momenta;
c) because the interaction length of the γ-rays makes it impossible to consider the V-event as associated with the star.

The abnormal decay $\pi^0 \to \beta^+ + \beta^-$ [2] does not seem to be very probable:

---

[2] We are very grateful to Prof. G. Occhialini, Mrs. C. Occhialini Dilworth, Prof. A. Bonetti, Dr. L. Scarsi, and to Prof. M. Verde for useful discussions on this point.

a) for the geometrical reasons quoted above;

b) because the time of flight of the π^0-meson would be at least 10^7 times larger than the theoretical lifetime;

c) because, within our experimental error, the conservation of momenta would not be verified.

We therefore assume that track 1 is a π-meson. From the experimental data we obtain the momentum of track 1:

$$P_1 = 346 \pm 50 \text{ MeV/c}$$

and from the momentum balance we can calculate the momentum of track 2:

$$P_2 = 2\,700^{+2500}_{-1000} \text{ MeV/c} .$$

The V-event can be interpreted either as a Λ^0 or a θ^0 decay. Using the formulae:

$$M_0^2 = M_1^2 + M_2^2 + 2E_1E_2 - 2P_1P_2 \cos \vartheta_{12}$$

(where E_1, E_2 are total energies),

$$Q = m_0 - (M_1 + M_2)$$

from the scheme:

$$\Lambda^0 \to \mathrm{p} + \pi^- + Q$$

we obtain:

$$Q = 36^{+67}_{-16} \text{ MeV}$$

and from the scheme:

$$\theta^0 \to \pi^+ + \pi^- + Q$$

we find:

$$Q = 216^{+150}_{-55} \text{ MeV} .$$

The values of the energy release are in good agreement with the results of other Authors (3).

(3) M. W. FRIEDLANDER, D. KEEFE, M. G. K. MENON and M. MERLIN: *Phil. Mag.*, **45**, 533 (1954). References to previous work are cited in this paper.
R. W. THOMPSON, A. V. BUSKIRK, C. R. ETTER, C. G. KARZMARK and R. H. REDIKER: *Phys. Rev.*, **90**, 329 (1953); M. YASIN: *Phil. Mag.*, **45**, 413 (1954); *Reports of the Bagnères Conference*, July 1953; *Reports of the Padua Meeting*, April 1954.

The time of flight of both neutral particles is of the order of 10^{-13} s. This figure is appreciably lower than the value $\sim 10^{-10}$ s which has been found in Wilson chamber experiments; however in photographic emulsions there is a strong bias towards V-particles with a short time of flight, because only these events, can be associated with stars.

In order to decide between the two possibilities, it would be necessary to identify particle 2.

From the theoretical ionization curves a particle with a momentum of 2 700 MeV/c should have minimum ionization if it is a proton, and « plateau » ionization if it is a π-meson. Therefore the identification of the track lies in the possibility of distinguishing between the « plateau » and minimum ionization. In our minimum determination care was taken to select electron tracks in the same plate, with the same dip and at the same depth as the tracks studied. Moreover as our plates are rather underdeveloped, the discrimination of the tracks should be more reliable. If the ionization value of track 2, $b^* \sim 1$, were significant, it would give a slight indication in support of the second interpretation.

The star in which the V-evetn originates belongs to the type 27 + 9p. Among the identified prongs there are a K-meson which is studied in a work in press and two negative π-mesons. A prong of one of the σ stars in its turn produces a small star.

An analysis of the parent star is in progress. The event is interesting because it can be either an additional example of a star emitting both a hyperon and a heavy meson ([4,5]), or an example of two heavy mesons ejected from the same star ([4,6]).

It is a pleasure to thank prof. G. Lovera for many useful discussions, and prof. R. Deaglio and prof. G. Wataghin for constant encouragement and interest. We wish also to express our thanks to Mr. M. Greco who found the event described in this paper.

([4]) D. Lal, Y. Pal and B. Peters: *Proc. Ind. Ac. Sci.*, **38**, 398 (1953).

([5]) W. B. Fowler, R. P. Shutt, A. M. Thorndike and W. L. Whittermore: *Phys. Rev.*, **93**, 861 (1954).

([6]) E. Amaldi, G. Baroni, C. Castagnoli, G. Cortini, C. Franzinetti and A. Manfredini: *Nuovo Cimento*, **11**, 207 (1954).

RIASSUNTO

Da una stella osservata in uno stack di « stripped emulsions » vengono emessi un mesone K ed una particella neutra che può essere interpretata sia come una Λ^0 con $Q = 36^{+67}_{-16}$ MeV, sia come una θ^0 con $Q = 216^{+150}_{-55}$ MeV.

An Analysis of Three K-mesons Ejected from Stars.

A. Debenedetti, C. M. Garelli, L. Tallone and M. Vigone

Istituto Nazionale di Fisica Nucleare - Sezione di Torino

(ricevuto il 28 Giugno 1954)

Summary. — In a stack of stripped emulsions three cases of K-meson decays have been found. K_2 and K_3 have a mass of 915 ± 130 m_e; the secondaries cannot be identified. The mass of K_1-meson is 1020 ± 270 m_e (scattering-range) and 1165 ± 130 m_e (ionization-range); its secondary is a light meson with $p\beta = 104 \pm 24$ MeV/c.

In a stack of stripped emulsions flown at 80 000 ft during the Sardinia Expedition 1953, three cases of heavy mesons decaying at rest have been observed. The events have been found during the general scanning of the plates.

Primary Particles.

The masses of the primary mesons have been determined by the following methods:

a) *Scattering-range.* We have used the constant sagitta method [1], and have applied both the dip and relativistic correction. Following the standard method the results are given without correction for the distortion. The value of the sagitta of the proton, determined by calibration through direct measurements, is affected by an error of about 5%. However as its mean value has been checked by measuring the masses of three τ-mesons, the errors indicated for

[1] C. C. Dilworth, S. J. Goldsack and L. Hirschberg: *Nuovo Cimento*, **11**, 113 (1954).

the mass values are only the standard deviations. In all cases, the mean value of the sagitta has been calculated in the various plates traversed; the consistency of the results within the experimental errors, and an indication of the distortion in the plates, given by third differences, are shown in the Appendix.

b) Ionization-range. Following the method recommended by O'CEALLAIGH (2), the calibration has been carried out by measuring the mean gap length of π-meson tracks at approximately the same depth in the same plates. The π-meson line in the log-log plot (see Fig. 1) has been calculated with the least squares method. In the same way we plotted the K-meson lines.

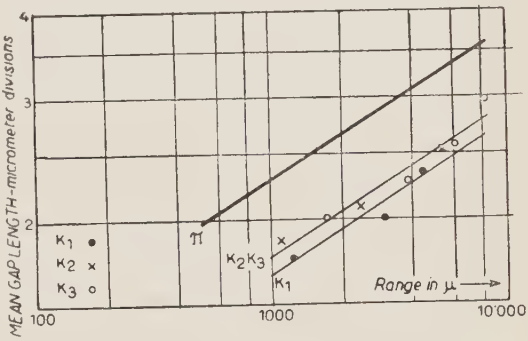

Fig. 1.

K_1 is ejected from a star of the type 27 + 9p. An event interpreted as a V-decay has been observed near the same star (3).

The primary meson travels 5 700 μ in 5 plates before decaying. The sagitta used for the determination of the mass is the mean value over three plates. The fourth plate is strongly distorted; the sagitta calculated from third differences (4), is in fair agreement with the mean value adopted.

The mass value is:

from scattering-range measurements: $M_{K_1} = 1\,020 \pm 270\ m_e$
from ionization-range measurements: $M_{K_1} = 1\,165 \pm 130\ m_e$

K_1-meson is ejected with a velocity $\beta_{emiss} = 0{,}314 \pm 0{,}032$ and its time of flight is $0{,}75 \times 10^{-10}$ s.

K_2 is emitted from a star of the type 22 + 15p; it travels 24 000 μ in 16 emulsions (the range in a plate varies between 1 360 μ and 1 800 μ). As the track passes through a cut edge of the plate, a section of about 3 000 μ could not be measured. Moreover, in the calculations, two bad plates affected

(2) C. O'CEALLAIGH: *Proc. Roy. Soc.* (January 27th 1954); *Proceedings of the Bagnères Conference*, p. 124 (1953).

(3) A. DEBENEDETTI, C. M. GARELLI, L. TALLONE and M. VIGONE: *Nuovo Cimento*, 12, 369 (1954).

(4) B. D'ESPAGNAT: *Journ. de Phys. et le Rad.*, 13, 74 (1952).

by local distortions, have not been taken into account. From scattering-range measurements it follows:

$$M_{K_2} = 911 \pm 146 \text{ m}_e ,$$

and from ionization-range:

$$M_{K_2} = 915 \pm 130 \text{ m}_e .$$

The velocity of emission from the star is $\beta_{emiss} = 0{,}476 \pm 0{,}038$ and the time of flight of the heavy meson is $2{,}26 \times 10^{-10}$ s.

K_3 originates from a star of the type 14 + 4n; it travels 16 400 μ in 9 plates (the range in an emulsion varies between 1 630 μ and 2 250 μ). No plate has been discarded in the calculations. We find:

$M_{K_3} = 915 \pm 145 \text{ m}_e$ from scattering-range
$M_{K_3} = 915 \pm 130 \text{ m}_e$ from ionisation-range
$\beta_{emiss} = 0{,}432 \pm 0{,}036$
time of flight $= 1{,}52 \cdot 10^{-10}$ s .

Secondary Particles.

Our data on the secondaries of K-mesons are unfortunately incomplete. Two of them (K_2 and K_3) have a very large dip and could not be found in the following emulsions so that the $p\beta$ value could not be determined by scattering measurements. We measured the ionisation by blob counting, and we related our value to the number of blobs at the « plateau ».

	True angle with the primary	Angle of dip	Measured range	b^*
K_1	$85^\circ \pm 1^\circ$	29°	2 000 μ	0.974 ± 0.033
K_2	$65^\circ \pm 1^\circ$	45°	500 μ	0.923 ± 0.065
K_3	$125^\circ \pm 1^\circ$	55°	600 μ	0.873 ± 0.058

The secondary of K_1-meson has been measured in 2 emulsions. The value of the scattering angle was determined following the suggestions of the standard method. The scattering constant has been deduced from VOYVODIC and PICKUP's work [5]; the standard error has been increased by 8% because we

[5] L. VOYVODIC and E. PICKUP: *Phys. Rev.*, **85**, 91 (1952).

have no calibration for the scattering constant

$$\alpha_{100} = 0.222^{\circ} \pm 0.035^{\circ}$$

$$p\beta c_{\text{emiss}} = 104 \pm 24 \text{ MeV}$$

nature of the secondary: L-meson

$$\beta_{\text{emiss}} = \begin{cases} 0.782 \pm 0.043 & \text{if a } \mu\text{-meson}, \\ 0.719 \pm 0.048 & \text{if a } \pi\text{-meson}. \end{cases}$$

Conclusions.

We think it reasonable to assume for K_1 meson the decay scheme:

$$K(\mu) \rightarrow \mu + ? + ?$$

In fact, in the cases previously interpreted following the the same scheme of decay (6), the $p\beta$ of the identified μ secondaries varies between 12 MeV/c and 140 MeV/c, whereas no example of π secondary with $p\beta \sim 100$ MeV/c has been found so far.

Nothing can be said about the decay schemes of K_2 and K_3 mesons, because the available data on their secondaries do not allow their identification.

Our thanks are due to Prof. R. Deaglio, Prof. G. Lovera, Prof. G. Wataghin, for their constant interest in this work. The events described in this paper were found by Mr. M. Greco.

Appendix

In Tables I, II, III, the second column gives the mean sagitta value in each plate, calculated from second differences and corrected for dip. In the third column are reported the mean values obtained from third differences.

(6) See: *Proc. Roy. Soc.*, A **221**, Jan. 27th (1954); *Cosmic Ray Conference, Bagnères de Bigorre*, July 1953; *Reports of Padua Meeting*, April 1954 (*Nuovo Cimento* to be published).

TABLE I. – K_1:

Plate no.	d_2 (μ)	d_2 (μ) from d_3
1	0.212 ± 0.078	0.192 ± 0.081
2	0.238 ± 0.038	0.280 ± 0.047
3	0.269 ± 0.049	0.318 ± 0.061
4	0.432 ± 0.085	0.289 ± 0.062
5	few cells	—

TABLE II. – K_2:

Plate no.	d_2 (μ)	d_2 (μ) from d_3
1	few cells	—
2	0.314 ± 0.053	0.341 ± 0.065
3	0.187 ± 0.036	0.225 ± 0.043
4	0.285 ± 0.063	0.323 ± 0.064
5	0.400 ± 0.100	0.315 ± 0.076
6	0.209 ± 0.052	0.185 ± 0.052
7	0.275 ± 0.069	0.306 ± 0.071
8	0.269 ± 0.070	0.245 ± 0.079
9	0.185 ± 0.052	0.240 ± 0.070
10	few cells	—
11	local distortions	—
12	0.369 ± 0.110	0.217 ± 0.061
13	0.306 ± 0.089	0.400 ± 0.120
14	0.280 ± 0.081	0.281 ± 0.089
15	local distortions	—
16	0.196 ± 0.057	0.194 ± 0.058

TABLE III. – K_3:

Plate n o.	d_2 (μ)	d_2 (μ) from d_3
1	0.248 ± 0.028	0.256 ± 0.030
2	0.331 ± 0.056	0.322 ± 0.055
3	0.284 ± 0.056	0.270 ± 0.057
4	0.240 ± 0.052	0.256 ± 0.057
5	0.210 ± 0.049	0.223 ± 0.056
6	0.275 ± 0.070	0.442 ± 0.123
7	0.330 ± 0.087	0.315 ± 0.030
8	0.231 ± 0.060	0.260 ± 0.073
9	few cells	—

The values of the sagitta used for the determination of the mass are:

$$D_{K_1} = 0.256 \pm 0.029 \ \mu,$$
$$D_{K_2} = 0.2685 \pm 0.018 \ \mu,$$
$$D_{K_3} = 0.268 \pm 0.018 \ \mu.$$

These values have been calculated by averaging on the full length of the track and are inclusive of the dip and relativistic corrections.

RIASSUNTO

In uno stack di « stripped emulsions » sono stati trovati tre casi di disintegrazione di mesoni K. K_2 e K_3 hanno una massa di 915 ± 130 m_e; non è stato possibile identificare i secondari. La massa del mesone K_1 è 1020 ± 270 m_e (scattering-range) e 1165 ± 130 m_e (ionizzazione-range); il suo secondario è un mesone leggero con $p\beta = 104 \pm 24$ MeV/c.

IL NUOVO CIMENTO Vol. XII, N. 3 1° Settembre 1954

On Recurrence Relations in Field Theory.

D. J. Candlin

Department of Mathematical Physics, University of Birmingham, England

(ricevuto il 3 Luglio 1954)

Summary. — The relations between propagation functions given by Caianiello are obtained in the interaction representation without the use of the perturbation expansion. They are also derived in the Heisenberg representation by variational methods.

1. – Introduction.

Caianiello ([1,2]) has recently given recurrence relations between propagation functions in quantum field theory, some of which are equivalent to the integral equations of Matthews and Salam ([3]) and of Freese ([4]). In combination with some new equations involving derivatives with respect to the coupling constant, these give an equation placing a condition on the kernel for a single process. In view of the interest of these equations, it may be well to give a derivation which does not rely on the validity of a perturbation expansion.

2. – Interaction Representation.

In the interaction representation, the S-matrix element for a scattering process is

$$(\Psi_f | S | \Psi_i) .$$

([1]) E. R. Caianiello: *Nuovo Cimento*, **10**, 1634 (1953).
([2]) E. R. Caianiello: *Nuovo Cimento*, **11**, 492 (1954).
([3]) P. T. Matthews and A. Salam: *Proc. Roy. Soc.*, A **221**, 128 (1953).
([4]) E. Freese: *Zeits. f. Naturfor.*, 8*a*, 776 (1953).

If χ_i be the correctly normalized Slater wave function of the incoming particles, the initial state vector ([4])

$$|\Psi_i) = \int \mathrm{d}^3x_1 \dots \mathrm{d}^3x_l \, \mathrm{d}^3y_1 \dots \mathrm{d}^3y_m \, \mathrm{d}^3z_1 \dots \mathrm{d}^3z_n \; \chi_i(x; y; z) \cdot \\ \cdot \boldsymbol{\psi}^{(-)}(x_1) \dots \boldsymbol{\psi}^{(-)}(x_l) \bar{\boldsymbol{\psi}}^{(-)}(y_1) \dots \bar{\boldsymbol{\psi}}^{(-)}(y_m) \boldsymbol{\varphi}^{(-)}(z_1) \dots \boldsymbol{\varphi}^{(-)}(z_n) \, |0) \, .$$

All times are to be put equal to the initial time t_i and the $(-)$ denotes that only the negative frequency parts (creation operators) of the operators are to be taken. In fact the product of the negative frequency parts acting on the vacuum may be replaced by the normal product ([5]) of the complete operators acting on the vacuum, for the positive frequency parts acting on the vacuum give zero. This normal product may now be rearranged by the inverse of Wick's theorem ([3]), to give a time-ordered product of the same operators. The contributions to the S-matrix element of terms involving contractions between operators in the initial state will be zero, for they will be proportional to the probability amplitude for an incoming fermion-antifermion pair, or two bosons, to annihilate each other, without any interaction with the rest of the system. This amplitude is zero, for energy and momentum cannot be conserved in the process. Thus, if we express the state $\Psi_f)$ in the same form, the S-matrix element may be written

$$\int\int\int_{t'=t_f} \mathrm{d}^3x' \, \mathrm{d}^3y' \, \mathrm{d}^3z' \int\int\int_{t=t_i} \mathrm{d}^3x \, \mathrm{d}^3y \, \mathrm{d}^3z \, \bar{\chi}_f(x'; y'; z') \; G(x'; y'; z'; x; y; z;) \; \chi_i(x; y; z) \, ,$$

where the x represents all the incoming antifermion coordinates and so on. Here

$$G = (0 \,|\boldsymbol{\psi}(x_1') \dots \bar{\boldsymbol{\psi}}(y_1') \dots \boldsymbol{\varphi}(z_1') \, \boldsymbol{U}(t_f, t_i) \boldsymbol{\psi}(x_1) \dots \bar{\boldsymbol{\psi}}(y_1) \dots \boldsymbol{\varphi}(z_1) \dots |0) \, ,$$

where every $t' = t_f$ and every $t = t_i$. This can be written

$$(1) \qquad G = (0 \,| \, U(t_f, 0) \psi(x_1') \dots \bar{\psi}(y_1') \dots \varphi(z_1') \dots \psi(x_1) \dots \bar{\psi}(y_1) \dots \varphi(z_1) \dots \, U(0, t_i) \, | \, 0),$$

where the italic operators are in the Heisenberg representation,

$$\boldsymbol{O}(t) = U(t, 0) O(t) U^{-1}(t, 0) \, .$$

We may define the function G for arbitrary times as we like, provided it reduces to (1) for $t = t_i$, $t' = t_f$. In fact, we shall put

$$(2) \qquad (0 \,| \, U(t_f, 0) T(\psi(x_1') \dots \bar{\psi}(y_1') \dots \varphi(z_1') \dots \psi(x_1) \dots \bar{\psi}(y_1) \dots \varphi(z_1) \dots) \, (U(0, t_i)) \, | \, 0).$$

([5]) F. J. Dyson: *Phys. Rev.*, **82**, 428 (1951).

To obtain an unambiguous value for (1) we must assume that there are infinitesimal time differences in the initial coordinates, and again in the final ones. (2) may be written

$$G = (-1)^j K\begin{pmatrix} x'_1 \dots x'_{l'} x_1 \dots\dots x_l \\ y'_1 \dots\dots y'_{m'} y_1 \dots y_m \end{pmatrix} \Big| \; z'_1 \dots z'_{n'} z_1 \dots z_n \Big),$$

where

$$j = lm' + \tfrac{1}{2}N(N-1), \qquad N = l + l' = m + m',$$

and

$$(3) \qquad K\begin{pmatrix} x_1 \dots x_N \\ y_1 \dots y_N \end{pmatrix} \Big| \; z_1 \dots z_P \Big) = (0 \,|\, U(t_f, 0) T(\psi(x_1)\bar{\psi}(y_1) \dots \psi(x_N)\bar{\psi}(y_N)\varphi(z_1) \dots \varphi(z_P)) U(0, t_i) \,|\, 0).$$

To obtain those equations for the kernels which do not involve the coupling constant (Caianiello [2], equations (48) (49) (50)), we integrate some equations of Matthews and Salam (reference [3], theorem 2), of which the first is

$$\left(\gamma \frac{\partial}{\partial \xi} + \varkappa\right) T(\psi(\xi)\bar{\psi}(y_1)\psi(x_2)\bar{\psi}(y_2) \dots \psi(x_N)\bar{\psi}(y_N)\varphi(z_1) \dots \varphi(z_P)) =$$

$$= g\gamma(\xi) T(\psi(\xi)\bar{\psi}(y_1)\psi(x_2)\bar{\psi}(y_2) \dots \psi(x_N)\bar{\psi}(y_N)\varphi(\xi)\varphi(z_1) \dots \varphi(z_P)) +$$

$$+ \sum_{k=1}^{N} (-1)^{k-1} \delta(\xi - y_k) T(\psi(x_2)\bar{\psi}(y_2) \dots \psi(x_k)\psi(y_{k-1})\psi(x_{k+1})\psi(y_{k+1}) \dots \psi(x_N)\bar{\psi}(y_N) \cdot$$

$$\cdot \varphi(z_1) \dots \varphi(z_P)),$$

or

$$\left(\gamma \frac{\partial}{\partial \xi} + \varkappa\right) K\begin{pmatrix} \xi\, x_2 \dots x_N \\ y_1 y_2 \dots y_N \end{pmatrix} \Big| \; z_1 \dots z_P \Big) = g\gamma(\xi) K\begin{pmatrix} \xi\, x_2 \dots x_N \\ y_1 y_2 \dots y_N \end{pmatrix} \Big| \; \xi z_1 \dots z_P \Big) +$$

$$+ \sum_{k=1}^{N} (-1)^{k-1} \delta(\xi - y_k) K\begin{pmatrix} x_2 \dots x_k \quad x_{k+1} \dots x_N \\ y_1 \dots y_{k-1}\; y_{k+1} \dots y_N \end{pmatrix} \Big| \; z_1 \dots z_P \Big),$$

by equation (3). If we multiply by $-\frac{1}{2}S_F(x_1, \xi) \equiv s(x_1, \xi)$ and integrate ξ over all space, and from t_i to t_f, we obtain

$$(4) \qquad \left\{ \begin{aligned} K\begin{pmatrix} x_1 \dots x_N \\ y_1 \dots y_N \end{pmatrix} \Big| \; z_1 \dots z_P \Big) &= g \int s(x_1, \xi)\gamma(\xi) K\begin{pmatrix} \xi\, x_1 \dots x_N \\ y_1 y_2 \dots y_N \end{pmatrix} \Big| \; \xi z_1 \dots z_P \Big) \mathrm{d}^4\xi + \\ &+ \sum_{k=1}^{N} (-1)^{k-1} s(x_1, y_k) K\begin{pmatrix} x_2 \dots x_k \quad x_{k+1} \dots x_N \\ y_1 \dots y_{k-1}\; y_{k+1} \dots y_N \end{pmatrix} \Big| \; z_1 \dots z_P \Big) - \\ &- \left(\int_{t_f} - \int_{t_i}\right) s(x_1, \xi)\gamma_4 K\begin{pmatrix} \xi\, x_2 \dots x_N \\ y_1 y_2 \dots y_N \end{pmatrix} \Big| \; z_1 \dots z_P \Big) \mathrm{d}^3\xi, \end{aligned} \right.$$

since $-\frac{1}{2}S_F(x,y)$ is the Feynman-Green function [6] for the operator $i(\gamma\,\partial/\partial x+\varkappa)$. The surface terms are of the form $(f(t_i)-f(t_f))$, which may be transformed to $\int_{-\infty}^{\infty} g(p)(\exp[ipt_i]-\exp[ipt_f])\,\mathrm{d}p$. If we average in the usual way [2] over the initial times we see that only $p=0$ gives a contribution, which is cancelled by that obtained from averaging over final times. Thus we have

$$K\left(\begin{matrix}x_1\dots x_N\\ y_1\dots y_N\end{matrix}\,\middle|\, z_1\dots z_P\right)=g\int s(x_1,\xi)\gamma(\xi)K\left(\begin{matrix}\xi\, x_2\dots x_N\\ y_1 y_2\dots y_N\end{matrix}\quad \xi z_1\dots z_P\right)\mathrm{d}^4\xi+ \tag{5}$$

$$+\sum_{k=1}^{N}(-1)^{k-1}s(x_1,y_k)K\left(\begin{matrix}x_2\dots x_k & x_{k+1}\dots x_N\\ y_1\dots y_{k-1} & y_{k+1}\dots y_N\end{matrix}\,\middle|\, z_1\dots z_P\right).$$

Similarly, using the other equations of MATTHEWS and SALAM,

$$K\left(\begin{matrix}x_1\dots x_N\\ y_1\dots y_N\end{matrix}\,\middle|\, z_1\dots z_P\right)=g\int K\left(\begin{matrix}x_1x_2\dots x_N\quad \xi z_1\dots z_P\\ \xi\, y_2\dots y_N\end{matrix}\right)\gamma(\xi)s(\xi,y_1)\,\mathrm{d}^4\xi+ \tag{6}$$

$$+\sum_{k=1}^{N}(-1)^{k-1}s(x_k,y_1)K\left(\begin{matrix}x_1\dots x_{k-1}x_{k+1}\dots x_N\\ y_2\dots y_k\quad y_{k+1}\dots y_N\end{matrix}\,\middle|\, z_1\dots z_P\right),$$

and

$$K\left(\begin{matrix}x_1\dots x_N\\ y_1\dots y_N\end{matrix}\,\middle|\, z_1\dots z_P\right)=g\int d(z_1,\xi)\,\mathrm{trace}\left\{\gamma(\xi)K\left(\begin{matrix}x_1\dots x_N\xi\\ y_1\dots y_N\xi\end{matrix}\,\middle|\, z_2\dots z_P\right)\right\}d\xi+ \tag{7}$$

$$+\sum_{k=2}^{P}d(z_1,z_k)K\left(\begin{matrix}x_1\dots x_N\\ y_1\dots y_N\end{matrix}\,\middle|\, z_2\dots z_{k-1}\,z_{k+1}\dots z_P\right),$$

where $d(z,z')=\frac{1}{2}\Delta_F(z,z')$ is the Green function for the operator $-i(\Box_z-\mu^2)$. These last three are in fact those equations of CAIANIELLO which do not involve differentiation with respect to the coupling constant.

The differential equation for $U(t,0)$ is

$$i\,\frac{\mathrm{d}U(t,0)}{\mathrm{d}t}=\boldsymbol{H}'(t)\,U(t,0)=ig\int\bar{\boldsymbol{\psi}}(\boldsymbol{r},t)\gamma\boldsymbol{\psi}(\boldsymbol{r},t)\boldsymbol{\varphi}(\boldsymbol{r},t)\mathrm{d}^3\boldsymbol{r}U(t,0)\,,$$

so that

$$i\left(\frac{\mathrm{d}}{\mathrm{d}t}\right)D_gU(t,0)=i\int\bar{\boldsymbol{\psi}}(\boldsymbol{r},t)\gamma\boldsymbol{\psi}(\boldsymbol{r},t)\boldsymbol{\varphi}(\boldsymbol{r},t)\,\mathrm{d}^3\boldsymbol{r}\;U(t,0)+\boldsymbol{H}'(t)D_gU(t,0)\,,$$

where

$$D_g\equiv\mathrm{d}/\mathrm{d}g\,,$$

[6] R. P. FEYNMAN: *Phys. Rev.*, **76**, 749 (1949).

or

$$\frac{\mathrm{d}}{\mathrm{d}t}(U^{-1}D_gU) = U^{-1}\int \boldsymbol{\psi}\gamma\boldsymbol{\psi}\boldsymbol{\varphi}\,\mathrm{d}^3\boldsymbol{r}\,U = \int \overline{\psi}\gamma\psi\varphi\,\mathrm{d}^3\boldsymbol{r}\,,$$

or

$$D_gU = U\int_0^t \overline{\psi}(x)\gamma\psi(x)\varphi(x)\,\mathrm{d}^4x\,.$$

Similarly

$$D_gU^{-1} = \int_0^t \overline{\psi}(x)\gamma\psi(x)\varphi(x)\mathrm{d}^4x\,U^{-1}\,.$$

Hence $D_gO(t) = [O(t), f(t, 0)]$ for any Heisenberg operator, where

$$f(t, t') = \int_{t'}^{t} \overline{\psi}(x)\gamma\psi(x)\varphi(x)\,\mathrm{d}^4x\,.$$

Thus

$$D_g(0\,|\,U(t_f, 0)\prod_{k=1}^{n} O_k(x_k)U^{-1}(t_i, 0)\,|\,0) = (0\,|\,U(t_f, 0)f(t_f, 0)\prod_{k=1}^{n} O_k(x_k)U^{-1}(t_i, 0)\,|\,0) +$$

$$+\sum_{k=1}^{n}(0\,|\,U(t_f, 0)\prod_{p=1}^{k}O_p(x_p)\{f(0, t_k)O_k(x_k) - O_k(x_k)f(t_k, 0)\}\prod_{q=k+1}^{n}O_q(x_q)U^{-1}(t_i, 0)\,|\,0) +$$

$$+(0\,|\,U(t_f, 0)\prod_{k=1}^{n}O_k(x_k)f(0, t_i)U^{-1}(t_i, 0)\,|\,0) =$$

$$= (0\,|\,U(t_f, 0)f(t_f, t_1)O_1(x_1)\ldots O_n(x_n)U^{-1}(t_i, 0)\,|\,0) +$$

$$+(0\,|\,U(t_f, 0)O_1(x_1)f(t_1, t_2)O_2(x_2)\ldots O_n(x_n)U^{-1}(t_i, 0)\,|\,0) +$$

$$+\ldots +$$

$$+(0\,|\,U(t_f, 0)O_1(x_1)\ldots O_n(x_n)f(t_n, t_i)U^{-1}(t_i, 0)\,|\,0)\,,$$

and so

$$D_g(0\,|\,U(t_f, 0)T\{\prod_{k=1}^{n}O_k(x_k)\}U^{-1}(t_i, 0)\,|\,0) =$$

$$= \int_{t_i}^{t_f}\mathrm{d}^4x(0\,|\,U(t_f, 0)T\{\overline{\psi}(x)\gamma\psi(x)\varphi(x)\prod_{k=1}^{n}O_k(x_k)\}U^{-1}(t_i, 0)\,|\,0)\,.$$

In particular, from (3)

$$D_g K\left(\begin{matrix} x_1 \dots x_N \\ y_1 \dots y_N \end{matrix} \middle| \, z_1 \dots z_P\right) = \int_{t_i}^{t_f} \mathrm{d}^4\xi K\left(\begin{matrix} x_1 \dots x_N \xi \\ y_1 \dots y_N \xi \end{matrix} \quad \xi z_1 \dots z_P\right). \tag{8}$$

If we substitute in the right hand side from (5), (6) or (7), treating ξ as x_1, y_1, or z_1 respectively of those equations, we find CIANIELLO's three equations involving the operator $\mathrm{d}/\mathrm{d}g$.

3. – Heisenberg Representation.

The derivation of these equations has been given entirely in the interaction representation, in the sense that physical observables have been identified in terms of interaction representation quantities, and Heisenberg variables were added merely as mathematical tools. It is, however, possible to work throughout in the Heisenberg representation. From (3) the propagator in the interaction representation may be written

$$K = (0f|\, T(\psi(x_1)\overline{\psi}(y_1) \dots \varphi(z_1) \dots)\, |0i), \tag{9}$$

where $|0i) \equiv U(0, -\infty)|0)$ (which is actually the Heisenberg vacuum for incoming particles ([4])) and $|0f) = U^{-1}(\infty, 0)|0)$, the Heisenberg vacuum for outgoing particles. We must now take the interaction interval (t_f, t_i) as $(\infty, -\infty)$ to allow the identification of the interaction representation variables with incoming and outgoing Heisenberg representation variables ([7]).

We now show directly that (9) is the propagator in the Heisenberg representation. If there are sources (SCHWINGER ([8])) η, $\overline{\eta}$ and J of nucleons, antinucleons and mesons present, the probability amplitude that they act in such a way that all particles created are subsequently absorbed is $(0f|0i)$. This may be expanded in a Maclaurin series in the source strengths at all space-time points

$$\begin{aligned}(0f|0i) = (0f|0i)_0 &+ \int K'\left(\begin{matrix} x \\ y \end{matrix}\right) \overline{\eta}(x)\eta(y)\, \mathrm{d}^4x\, \mathrm{d}^4y + \\ &+ \int K'\left(\begin{matrix} x \\ y \end{matrix} \middle| \, z\right) \overline{\eta}(x)\eta(y)J(z)\, \mathrm{d}^4x\, \mathrm{d}^4y\, \mathrm{d}^4z + \\ &+ \int K'\left(\begin{matrix} x_1\, x_2 \\ y_1\, y_2 \end{matrix}\right) \overline{\eta}(x_1)\eta(y_1)\overline{\eta}(x_2)\eta(y_2)\, \mathrm{d}^4x_1 \mathrm{d}^4x_2 \mathrm{d}^4y_1 \mathrm{d}^4y_2 + \\ &+ \text{higher terms.}\end{aligned} \tag{10}$$

([7]) C. N. YANG and D. FELDMAN: *Phys. Rev.*, **79**, 972 (1950).
([8]) J. SCHWINGER: *Proc. Nat. Acad. Sci.*, **37**, 452 (1951).

where $K'\begin{pmatrix} x_1 \dots x_N & z_1 \dots z_P \\ y_1 \dots y_N & \end{pmatrix}$ is the value of the functional derivative $\delta^{2N+P}(0f\,|\,0i)/\delta\bar{\eta}(x_1)\delta\eta(y_1)\dots\delta J(z_1)\dots$, when the sources are put equal to zero. Now SCHWINGER has shown, from the equations of motion including sources, that this coefficient K' is in fact equal to (9), so that we may omit the primes on the K. From (10) we see that for example $K\begin{pmatrix} x_1 & x_2 \\ y_1 & y_2 \end{pmatrix}$ is the probability amplitude for the process in which two δ-function sources and two sinks operate, for the term in which it occurs is the only one proportional to the strengths of the appropriate sources and sinks. Thus it is the Green function, or propagation function, for two nucleons, which is defined in the usual way as the solution for δ-function sources.

The derivation of equations (5), (6) and (7) still stands, for we used no properties of the interaction representation, but the same is not true for equation (8). This, however, can be deduced simply from Schwinger's action principle [8], according to which a change $\delta\mathcal{L}(x)$ in the Lagrangian density produces a change $-i\int(0f\,|\,\delta\mathcal{L}(x)\,|\,0i)\,\mathrm{d}^4x$ in $(0f\,|\,0i)$. We consider the change $\delta\mathcal{L}(x) = i\,\mathrm{d}g\cdot\bar{\psi}(x)\gamma\psi(x)\varphi(x)$ produced in the system by a change $\mathrm{d}g$ in the coupling constant. Then

$$D_g(0f\,|\,0i) = \int (0f\,|\,\bar{\psi}(\xi)\gamma\psi(\xi)\varphi(\xi)\,|\,0i)\,\mathrm{d}^4\xi\,.$$

We may again use the theorem that multiple variations give the matrix element of the T-product of the variations in the Lagrangian density, to obtain (8).

I am greatly indebted to Dr. P. T. MATTHEWS for many helpful discussions, and to Trinity College, Cambridge, for financial support.

RIASSUNTO (*)

Le relazioni fra le funzioni di Green date da CAIANIELLO si deducono nella rappresentazione di interazione senza ricorrere ad uno sviluppo in serie della costante di accoppiamento. Si mostra, inoltre, come, nella rappresentazione di Heisenberg, le stesse relazioni si possano ottenere mediante un procedimento variazionale.

(*) *Traduzione a cura della Redazione.*

IL NUOVO CIMENTO Vol. XII, N. 3 1° Settembre 1954

The Analysis of V° Decays when the Errors of Measurement Are Large.

J. P. Astbury (*)

Istituto di Fisica dell'Università - Roma
Istituto Nazionale di Fisica Nucleare - Sezione di Roma

(ricevuto il 4 Luglio 1954)

Summary. — The identification of V° decays, starting from the now established Q-values for the Λ^0 and θ^0-particles, is discussed. A method of separating Λ^0 and θ^0-particles is described; it demands measurements only of the negative secondary momentum and of the angle between the secondary tracks. Curves are given which facilitate calculations of Q-values. Since, if the errors of measurement are large, standard errors in Q are unreliable, curves are given by means of which the compatibility of any given event with Λ^0 and θ^0-decay may be checked. The effect of instrumental and selection bias on the interpretation of anomalous V° decays is considered.

1. – Introduction.

It is now known that there are at least two types of V°-particle, the Λ^0 and the θ^0-particles. There is evidence indicating that there may be more than two types; other hypothetical types are described briefly later. The decay processes of the Λ^0 and the θ^0-particles are now fairly well established. Comparatively little is known about how the particles are produced, the probability of production as a function of the energy of the particle initiating a nuclear disintegration, of the other shower particles produced and of the nature of the parent nucleus. The order of magnitude of the mean lives of the Λ^0 and θ^0-particles are known; but before the mean lives can be measured with a precision equal to that of known values of the π and μ-mesons, many more observations will be required.

(*) Now at University College, London.

In order to obtain more information about the mean lives and the production of V^0-particles, it is not essential to make the precise measurements which are required for the accurate definition of a decay process. It is necessary only to distinguish the different types of V^0-particle, and desirable, if possible, to determine the momentum of the identified particle. It is therefore possible to take into account a much larger number of events than that used for the definition of a type of decay process. In these notes we discuss the techniques of analysis of these extended data. We take as a starting point the values already established for the energy released in Λ^0 and θ^0-decays.

Knowing these values it is very often possible to distinguish between the two types of decay, even if the errors in momentum measurement are very large. In particular we shall show that it is possible to make a fairly efficient separation without any information about the momentum and ionization of the positive particle.

If θ_+ and θ_-, the angles made by the secondary tracks to the line of flight of the V^0-particle, are known it is very often possible to distinguish between Λ^0 and θ^0-decays by reference only to the ionization of the secondary particles [1]. In this type of analysis, as in many other applications, the parameter α is of fundamental importance [2].

Here we exclude from attention cases where θ_+ and θ_- are measured, and consider only cases in which at least one of the two secondary range momenta are measured, or may be deduced from measurements of range or scattering. In these cases α is of less value; it is defined by two angle measurements, but not by two momentum measurements p_+ and p_- nor by one momentum measurement associated with the angle between the two secondary tracks, φ. The type of separation which we describe here, based on p_- and φ, is best made in terms of a new parameter, a «critical momentum», which we define in the next section. (This critical momentum is connected with the points, S_1 and S_2, defined by PODELANSKI and ARMENTEROS [2]).

We also consider another but related problem. It is generally felt that the Λ^0- and θ^0-particles do not account for all the observed examples of V^0-decay. It is however certain that if some other type of V^0-particle exists, its decays are certainly very rare compared with those of the Λ^0-particle: they will therefore be about as frequent as grossly distorted Λ^0-decays (assuming the errors in measurements are normally distributed). Thus here again we have to assume that we may be dealing with very large errors. In these circumstances it is difficult to be sure that any single event is inconsistent with

[1] See, for example, M. DEUTSCHMANN: *Zeits. f. Naturfor.*, **7a**, 142 (1952); W. B. FRETTER, M. M. MAY and M. P. NAKADA: *Phys. Rev.*, **89**, 168 (1953); D. B. GAYTHER: *Phil. Mag.*, **360**, 570 (1954).

[2] J. PODOLANSKI and R. ARMENTEROS: *Phil. Mag.*, **360**, 13 (1954).

Λ^0- or θ^0-decay. It is preferable to consider together as a group the most inconsistent events, and to see whether they show any common features. These anomalous events form a very highly selected group and we have to appreciate whether any common features which emerge are genuinely representative of a third type of decay, or are merely introduced by the selection criterion.

We define in Fig. 1 some of the terms which we shall use below, referred to the C (Centre of mass) system and the L (Laboratory) system. We shall use an asterisk to denote a quantity measured in the C system. We shall use the symbols e, m and β, with appropriate subscripts, to denote energies, masses and velocities. We shall measure masses and momenta in energy units, with the velocity of light, $c = 1$.

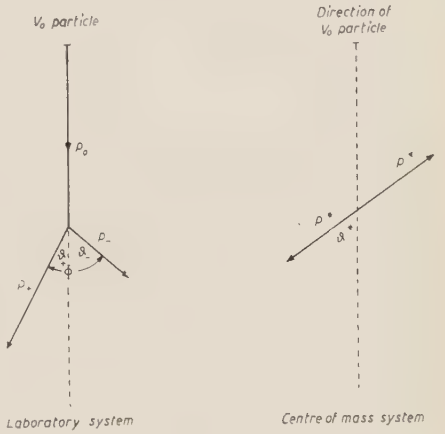

Fig: 1.

We define as a V_1^0-decay any process of the type $V_1^0 \to p^+ + L^- + Q$, where L represents a π or μ-meson. The Λ^0-decay, $\Lambda^0 \to p^+ + \pi^- + 37$ MeV is then a special case of a V_1^0-decay. We define as a V_2^0-decay a process of the type $V_2^0 \to L^+ + L^-$, where a neutral particle may or may not be included among the secondary products. The θ^0-decay, $\theta^0 \to \pi^+ + \pi^- +$ about 210 MeV, is then a special case of V_2^0-decay.

2. – Separation of Λ^0 and θ^0 Particles when the Errors of Measurement are Large.

When the momentum of the positive particle is in the range $7 \cdot 10^8$ eV/c $> p_+ > 10^8$ eV/c separation can be made by the ionization estimate without reference to the momentum of the negative particle. The probability of finding this condition, as a function of the momentum of the neutral particle, is given by the curves in Fig. 2.

If both secondary particles have minimum ionisation an obvious way of classifying a V^0-event is by estimating Q-values for the different assumed decay processes, and comparing the results with the established values; but if the errors of measurement are large, it is exceedingly difficult to estimate the consequent error in the Q-estimate.

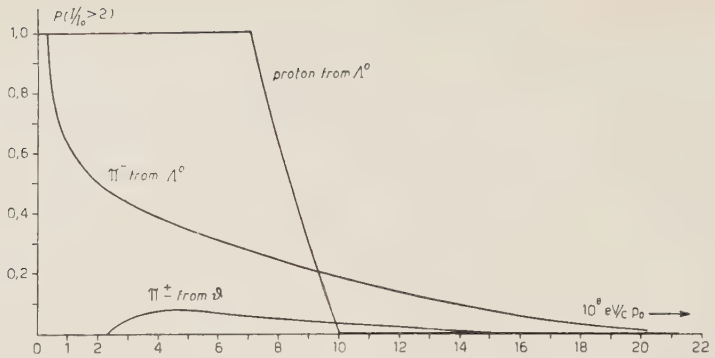

Fig. 2. – The probability $P(I/I_0 > 2)$ that a secondary particle emitted in V^0 decay should have a specific ionization greater than 2 expressed as a function of p_0, the momentum of the primary particle. The curve has been derived from the formula

$$\cos\theta^* = \frac{1}{\beta_0\beta_1^*}\left(\frac{\gamma_1}{\gamma_0\gamma_1^*} - 1\right)$$

by substituting the appropriate values for $\gamma_1\gamma_1^*$ and β_1^* (see Appendix I).

For small errors, following LEIGHTON *et al.* ([3]), we can put

$$\Delta Q = \left[\left(\frac{\partial Q}{\partial p_+}\Delta p_+\right)^2 + \left(\frac{\partial Q}{\partial p_-}\Delta p_-\right)^2 + \left(\frac{\partial Q}{\partial \varphi}\Delta\varphi\right)^2\right]^{\frac{1}{2}}, \tag{1}$$

where

$$\frac{\partial Q}{\partial p_+} = \frac{p_-}{m_0}\left(\frac{\beta_+}{\beta_-} - \cos\varphi\right), \tag{2}$$

$$\frac{\partial Q}{\partial p_-} = \frac{p_+}{m_0}\left(\frac{\beta_-}{\beta_+} - \cos\varphi\right), \tag{3}$$

$$\frac{\partial Q}{\partial \varphi} = \frac{p_+ p_-}{m_0}\sin\varphi\,. \tag{4}$$

In applying these formulae we rely on a number of approximations, which are not valid for large errors. We list below some of these approximations

1) That $\Delta p_+ = -p_+^2\,\Delta(1/p_+)$: in general, errors in $1/p$, rather than p, are normally distributed. This approximation can be avoided by substituting separately the positive and negative errors $+\Delta p_+$ and $-\Delta p_+$ to yield an asymmetric error in Q.

([3]) R. B. LEIGHTON, S. D. WANLASS and C. D. ANDERSON: *Phys. Rev.*, **89**, 148 (1953).

2) That the errors Δp_+ and Δp_- are independent; in practice, if φ is small, there is likely to be a negative correlation of nearly unity.

3) That in determining $\partial Q/\partial p_+$, p_- is accurately known.

4) That $\partial^2 Q/\partial p_+^2$ is zero over the range covered by Δp_+. In fact $\partial^2 Q/\partial p_+^2$ is always positive, so that the positive errors in Q, the « upper limits », are always understimated.

In these circumstances it is preferable, instead of estimating Q-values and errors in Q-values, to calculate directly the errors in measurements that must be assumed before an event can be interpreted by a particular decay-scheme. In practice we find that nearly always the effect of the error in φ is negligible compared with the effect of errors in the momentum measurements. We assume first that one of the momenta can be measured relatively accurately. If we assume a particular decay process — say for example a Λ^0-decay — the value of the other momentum can be calculated from the conservation equations, written generally

$$f(m_0 m_+ m_- p_+ p_- \varphi) = 0 .$$

This is the equation which has been used to determine the Q-values for the Λ^0- and θ^0-decays. Then m_0, the unknown, was derived from the measured values of p_+, p_- and φ and assumed values of m_+ and m_-.

We here assume the three masses to be known, φ and for example p_-, to be measured and will solve the equation for p_+. It is convenient to consider first the special case of the solution $p_+ = 0$ (corresponding to the point S_1 of PODELANSKI and ARMENTEROS). Phenomenologically the V^0 then degenerates into a line, the angle φ must be zero, and p_- has a critical value which we will call P_-. The value of P_- is easily calculated. As $p_+ = 0$ we must have $\beta_+^* = -\beta_0$ and thus $p_0/m_0 = p^*/m_+$. But by conservation of momentum in the L-system we have also $p_0 = p_- = P_-$. Thus

$$P_- = (m_0/m_+)p^* . \tag{5}$$

The critical value of the positive momentum is by the same argument

$$P_+ = (m_0/m_-)p^* . \tag{6}$$

Values of P_- and P_+, are given in Table I.

In the general case, because the errors are symmetrically distributed in the reciprocal momenta, it is convenient to solve for $1/p_+$. The solution is

$$\frac{1}{p_+} = \frac{(1/B)X\cos\varphi \pm (1/\beta_-)(X^2 - \sin^2\varphi)^{\frac{1}{2}}}{m_+(1 - X^2)} , \tag{7}$$

TABLE I.

		$\Lambda^0 \to p^+ + \pi^-$	$\theta^0 \to \pi^+ + \pi^-$	$V_3^0 \to \tau^+ + \pi^-$
p^*	18^8 eV/c	1.0	2.0	1.2
Q	10^8 eV	0.37	2.09	0.59
m_0	10^8 eV/c²	11.15	4.88	6.88
P_+	10^8 eV/c	8.0	7.0	5.9
P_-	10^8 eV/c	1.2	7.0	1.7
Γ		1.31	5.11	1.57
$Y = m_+ m_- \Gamma$ $(10^8$ eV$)^2$		17.2	9.95	10.7

$\Gamma = (1 - B^2)^{-\frac{1}{2}}$ where B is the velocity corresponding to the critical momenta P_+ and P_-.

where $X = P_-/p_-$ is the reciprocal of the negative momentum measured in units of the critical momentum, and B is the value of β corresponding to the

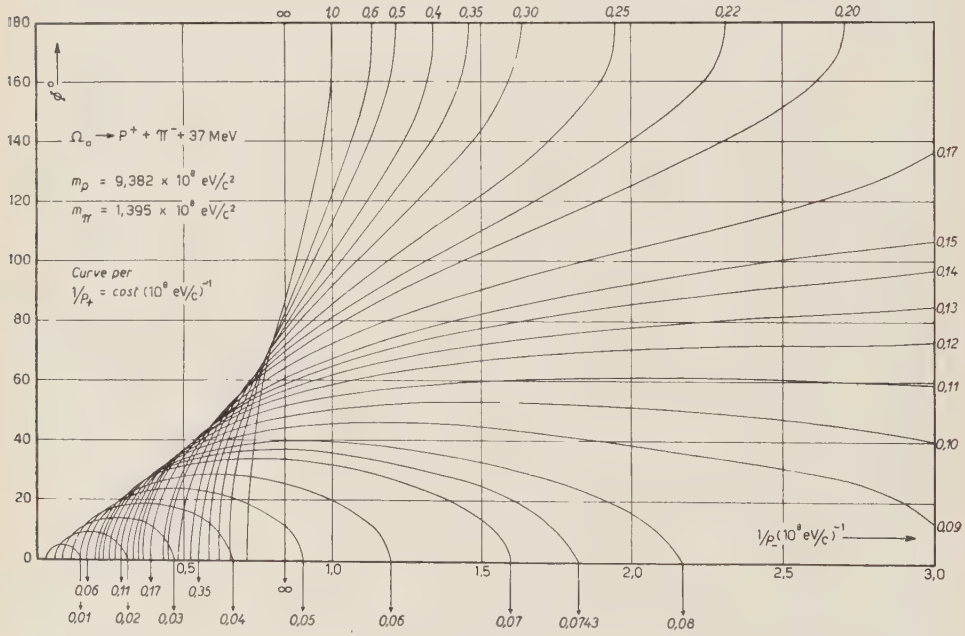

Fig. 3. – Curves of constant $1/p_+$ against $1/p_-$ and φ for the decay process $\Lambda^0 \to p^+ + \pi^+ + 37$ MeV.

critical momenta. (As from equations (5) and (6) $P_-/m_- = P_+/m_+$ the critical velocity is the same for both secondary particles).

In order to evade the labour of frequently solving equation (7), and to make it possible to check the effect of simultaneous errors in the measured values, curves of constant $1/p_+$ have been plotted as functions of $1/p_-$ and φ. These

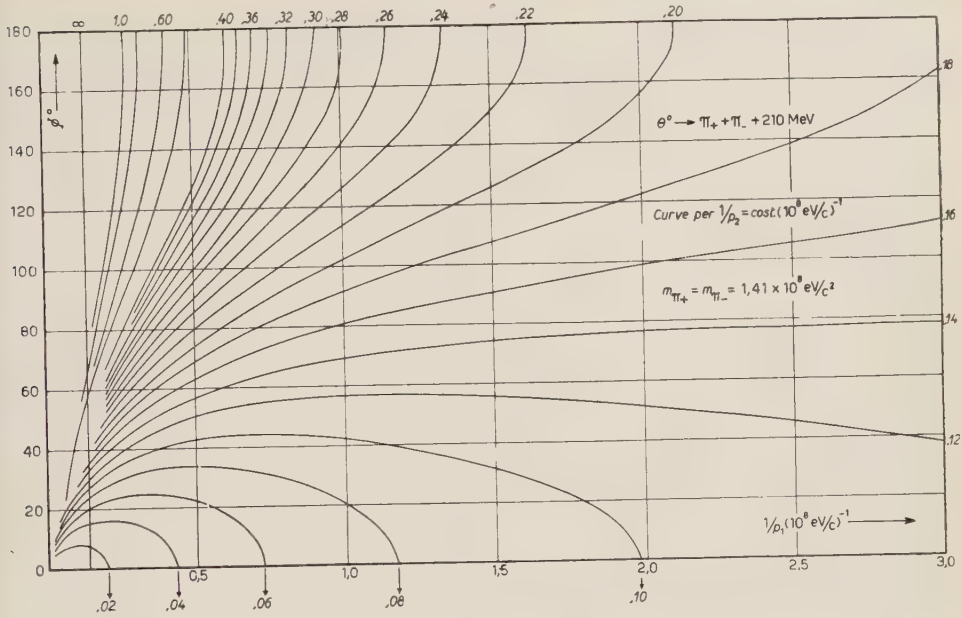

Fig. 4. Curves of constant $1/p_1$ againzt $1/p_2$ and φ for the decay process $\theta \to \pi^+ + \pi^- + 210$ MeV.

curves for the Λ^0- and θ^0-decays, and for the assumed decay process $V_3^0 \to \tau^\pm + \pi^\mp + 60$ MeV are reproduced in Figs. 3, 4 and 5.

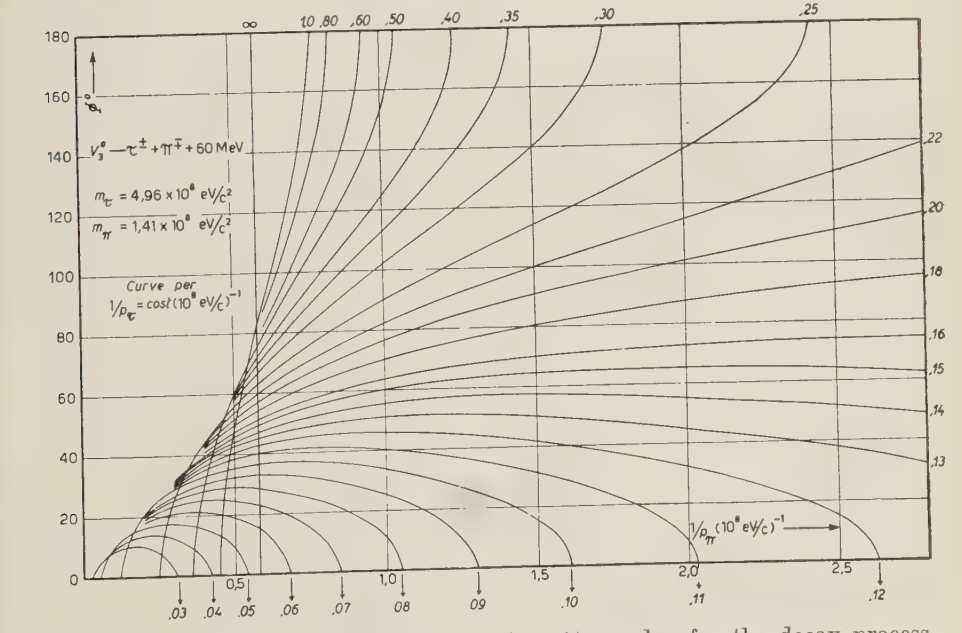

Fig. 5. – Curves of constant $1/p_1$ against $1/p_2$ and φ for the decay process $V_3^0 \to \pi^\pm + \tau^\mp + 60$ MeV.

An example of the use of the curves is provided by Table II, which is reprinted from another paper ([4]). It gives data on 6 events which, interpreted as Λ^0- or θ^0-decays, yield Q-values very different from the accepted values.

TABLE II. – *All reciprocal momenta are in units of* $(10^8\ \mathrm{eV/c})^{-1}$.

Event	Measured values			Correction for Λ^0		Correction for θ^0	
	$1/p_+$	$1/p_-$	φ	$(1/p_+)$	$(1/p_-)$	$(1/p_+)$	$(1/p_-)$
1	2	3	4	5	6	7	8
1	0.53	0.48	64	— 0.39	+ 0.38	— 0.23	— 0.24
2	0.81 ± 0.25	0.57 ± 0.08	61	— 0.31	+ 0.13	+ 1.9	— 0.44
3	0.17	0.125	14	— 0.09	+ 0.14	— 0.09	— 0.08
4	0.15	0.09	19.5	— 0.05	+ 0.22	— 0.02	— 0.03
5 *	—	0.15	41	—	+ 0.36	—	— 0.04
6	0.20 ± 0.05	0.20 ± 0.05	15	— 0.10	+ 0.09	— 0.10	— 0.15

Columns 5 to 8 give the corrections which must be applied to (or the errors that must be assumed in) the measured values if the event is to be interpreted as an Λ^0 or a θ^0 decay.
For a chamber with $MDM = 5 \cdot 10^8$ eV/c the standard error in $1/p$ is 0.02 $(10^8\ \mathrm{eV/c})^{-1}$.

* In event 5 the positive momentum could not be measured. The negative momentum has been adjusted to give the best fit with the observed ionization of the positive particle: 2 to $5 \cdot I/I_0$.

In columns 2, 3 and 4 we give the measured values of $1/p_-$ and φ. We have found from Fig. 3 the corresponding pairs of values, $1/p_-$ and $1/p_+$, consistent with Λ^0-decay which most nearly fit the measurements. The differences between the measured values and those derived from Fig. 3 are given in columns 5 and 6. Similarly in columns 7 and 8 we give the difference between the measured values and those consistent with θ^0-decay, found from Fig. 4. From these figures, and knowing the maximum detectable momentum of the chambers concerned — the reciprocal of $0.02 \cdot (10^8\ \mathrm{eV/c})^{-1}$ — it is possible to make an evaluation of the significance of the discrepancies which is more realistic than that based on the conventional errors in Q-values. It happens that all these events are consistent with the V_3^0-decay scheme. This may be checked from Fig. 5.

3. – Separation by Measurements of p_- and φ.

We see from Figs. 3, 4 and 5 that for low values of $1/p_-$ only a limited range of values of φ is possible; from equation (7) it is clear that a real solution

([4]) J. P. ASTBURY: *Report of the Padua Conference* 1954: to be published in *Nuovo Cimento*.

for $1/p_+$ is only possible if $\sin\varphi$ is less than P_-/p_-. The physical meaning of this is that high values of p_- imply a high velocity for the primary neutral particle, and thus that both secondary particles must be thrown forward in the L-system. This phenomenon can be used as the basis for a method of distinguishing between Λ^0- and θ^0-particles. For the Λ^0-particle $P_- = (m_0|m_-)p^* = 1.2\cdot10^8$ eV/c and thus a Λ^0-decay must satisfy the condition

$$\sin\varphi \leqslant \frac{1.2\cdot10^8 \text{ eV/c}}{p_-} . \tag{8}$$

The corresponding condition for a θ-decay is

$$\sin\varphi \leqslant \frac{7.0\cdot10^8 \text{ eV/c}}{p_-} . \tag{9}$$

Owing to the symmetry of the θ^0-decay there is a high probability that φ will be near the maximum value permitted by (9). Thus nearly all θ^0-decays fail to satisfy inequality (8).

The curve $1/p = (\sin\varphi)/(1.2)\cdot(10^8 \text{ eV/c})^{-1}$ is shown in Fig. 6 (curve A). All Λ^0-decays will lie to the right of this curve. Curve B refers to the θ^0-particle; ninety percent of θ^0-decays will lie to the left of this curve. Thus if a mixture of Λ^0- and θ^0-decays are plotted on Fig. 6 all the events to the left of curve A will be θ^0-decays. The events to the right of line A will comprise all the Λ^0-decays associated with not more than 10% of the θ^0-decays.

This p_- and φ method of separation forms a useful complement to that based on a measurement of p_+ and the ionization of the positive particle. The $p_+ - (I/I_0)_+$ method has the advantage of being absolute (i.e. there is no dilution), but is only applicable for a limited range of p_+:

There is a widespread feeling [5] that the Λ^0- and θ^0-particles do not account for all the observed Λ^0-decays. Data on a number of «anomalous» V^0-decays have been reviewed by ASTBURY [4] who has shown that most of them can be interpreted as distorted Λ^0- or θ^0-decays. If a third type of V^0-particle exists it appears to be rare with respect to Λ^0- and θ^0-particles. It would however be rash to assume the complete absence of V^0-decays other than those produced by Λ^0- and θ^0-particles; it is therefore worth while to consider briefly how the various hypothetical decay processes which have been proposed would be classified by the $p_-\varphi$ method.

LEIGHTON *et al.* [3] have suggested that there may be a decay

$$V_1^0 \rightarrow p^+ + \pi^- + 75 \text{ MeV} ,$$

where the Q-value of about 75 MeV is significantly higher than the common value of about 37 MeV. The critical momentum for the negative particle, P_-,

---

[5] See, for example, *Report of the Bagnères-de-Bigorre Conference* 1953.

for such a process would be 1.9×10^8 eV/c instead of $1.2\cdot10^8$ eV/c for the Λ^0-decay. Thus the corresponding φ_{max} curve can be obtained from curve A in Fig. 6 by reducing the abscissae by the factor 1.2/1.9. The representative points of most θ-decays lie well to the left of curve A, and only 20% would lie to the right of the new curve. ASTBURY (6) found that out of 10 « not Λ^0 »-decays identified by p_- and φ, only one could be interpreted as a high Q V_1^0 type event. If high Q V_1^0-decays exist, they will tend to be classified by the p_-—φ method as Λ^0-decays rather than as θ^0-decays.

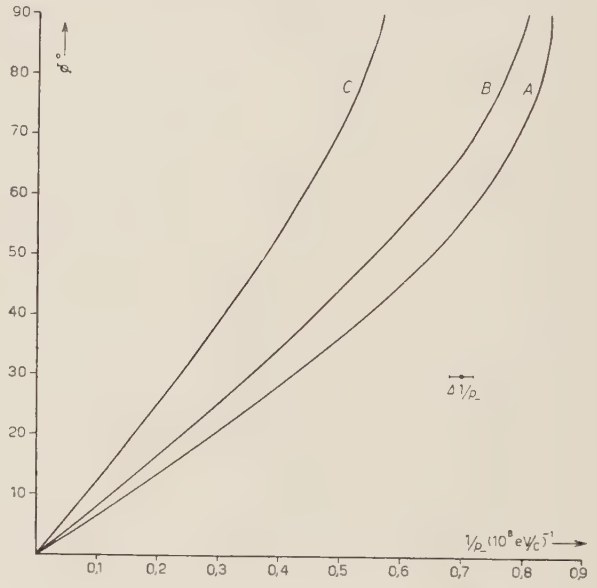

Fig. 6. – Curve A is obtained from the equation

$$\sin\varphi_{max} = \frac{m_0 p^*}{m_+ p_-} = \frac{P_-}{p_-} = \frac{1.2\cdot10^8 \text{ eV/c}}{p_-}$$

for the Λ_0-particle.

The representative points for Λ^0 decays will all lie to right of curve A. The construction of curves B and C is explained in Appendix I. Ninety percent of the representative points for θ^0-decays will lie to the left of curve B; 80% will lie to the left of curve C. The error $\Delta(1/p)$ corresponds to a maximum detectable momentum of $5\cdot10^9$ eV/c.

Most of the anomalous events, if interpreted by the process $V_2^0 \to \pi^+ + \pi^- + Q$ yield Q-values below that (210 MeV) for the θ^0-decay. It will be shown in the next section that the marked preponderance of examples with $Q < 210$ MeV, compared with those with $Q > 210$ MeV, is probably an effect of instrumental bias. But a τ^0-decay, $\tau^0 \to \pi^+ + \pi^- + \pi^0$, would give V_2^0 Q-values below about 80 MeV, and there are one or two accurately measured events which yield low V_2^0 Q-values (7).

(6) J. P. ASTBURY: *Report of Bagnères-de-Bigorre Conference*, p. 52.

(7) R. W. THOMPSON, J. R. BURWELL, H. O. COHN, R. W. HUGGETT, C. J. KARZMARK and Y. B. KIM: *Proceedings of the Fourth Rochester Conference on High Energy Nuclear Physics*, p. 77.

Measurements of p_- and φ are sufficient to define minimum values for Q. These are given, from equation (2), by setting $\beta_+ = \beta_- \cos\varphi$. It is thus always possible to test whether a given event, identified by p_- and φ as «not Λ^0» is consistent with a low Q V_2^0 type of decay. Very few θ^0-decays will have p_- and φ values which are consistent with a τ^0-decay.

Most of the anomalous decays can be interpreted by the process $V_3^0 \to \pi^\pm + \tau^\mp + 60$ MeV. But it appears that the prototype of this process, and the example which is most difficult to reconcile with Λ^0- or θ^0-decay, may be a charged V-decay ([8]). The critical momenta for the assumed V_3^0-decay process are $P_\pi = 1.7 \cdot 10^8$ eV/c and $P_\tau = 5.9 \cdot 10^8$ eV/c. Thus from the $p_- \varphi$ criterion decays of the type $V_3^0 \to \pi^\tau + \tau^-$ would nearly all be classified as θ-decays, whilst most $V_3^0 \to \pi^- + \tau^+$ events would be classified as Λ^0-decays. It will be shown in the next section that in certain circumstances it would be difficult to distinguish V_3^0-decays from Λ^0- and θ^0-decays even when p_+ is fairly accurately measured.

It appears that decays of the type described by COWAN ([9]), viz either *a*) $V^0 \to \pi^+ + \varepsilon^-$ or *b*) $V^0 \to \pi^+ + p^-$, must be rare compared with θ^0-decays. Until either one or other of the two possible processes is confirmed no further comment can be made.

Once an event has been classified as either a Λ^0- or a θ^0-decay, the momentum of the primary particle can be determined. This is most conveniently done by finding first p_+, either by solving equation (7) or by interpolation in the curves of Fig. 3 and 4. The uncertainty introduced by interpolation is usually negligible compared with other errors. A complication is introduced because, for values of $p_- > P_-$, the solution of equation (7) for $1/p_+$ is double-valued. For values of p_- not much greater than P_- one of the two p_+ values is very small, and thus a decision between the two is possible by reference to the ionization of the positive particle. For the Λ^0-particle, as P_+ is relatively low, the ambiguity introduced by the double values is greater than for the θ^0-particle; but PAGE and NEWTH ([10]) found that in their analysis of Λ^0-particles the effect of the ambiguity was not serious.

4. – Anomalous Decays.

We have noted in section 1 that a number of V^0-decays have been reported which yield Q-values apparently inconsistent with the Λ^0- or θ^0-decay process; before we can be certain that these decays are produced by V^0-particles other

([8]) R. B. LEIGHTON: Private communication.
([9]) E. W. COWAN: *Phys. Rev.*, **94**, 161 (1954).
([10]) D. I. PAGE and J. A. NEWTH: *Phil. Mag.*, **3·0**, 38 (1954).

than Λ^0- or θ^0-particles, rather than by distorted Λ^0-decays, we have to detect characteristic common features; moreover we have to be satisfied that any common features which are revealed are not introduced merely by the selection criterion, i.e. by the need to reject from consideration those events which are consistent with Λ^0- or θ^0-decay. The effect of such biasses is discussed in this section.

The Q-value of a decay, assuming given secondary masses, m_+ and m_-, can be derived from the measured quantities by the formula given by LEIGHTON *et al* [3]

$$Q = (m_+ + m_-)\left[\left(1 + \frac{2Q'}{m_+ + m_-}\right)^{\frac{1}{2}} - 1\right], \tag{10}$$

where

$$Q' = \frac{\varepsilon_+\varepsilon_- - p_+p_- \cos\varphi - m_+m_-}{m_+ + m_-} \tag{11}$$

and ε_+ and ε_- are the total energies of the two particles.

In practice, because it is necessary to find the difference between nearly similar quantities, the calculation of Q is rather laborious. LEIGHTON *et al.* have pointed out that for the Λ^0-particle, $Q \approx Q'$. It is convenient to con-

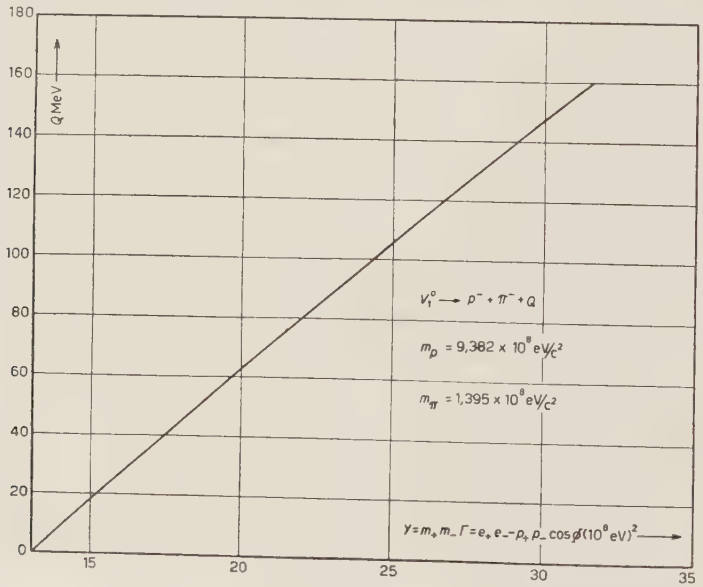

Fig. 7. – Q as a function of Y for the Λ^0-particle. $Y = e_+e_- - p_+p_- \cos\varphi = m_+m_-\Gamma = m_+E_- = m_-E_+$. E_- is the energy corresponding to the critical momentum, P_- of fig. 6, and Γ is the corresponding critical value of $\gamma_- = e_-/m_-$. In the range $30 < Q < 50$ MeV, Q may be calculated from the approximate formula $Q = (0.90Y - 1.173)\cdot 10^8$ eV. The error at 30 and 50 MeV is about 1/10 MeV.

sider a function which is rather simpler than Q'. We define

$$Y = \varepsilon_+\varepsilon_- - p_+p_- \cos\varphi \,. \tag{12}$$

Curves relating Y to Q for different decay processes are given in Figs. 7, 8 and 9. For the Λ^0-particle, in the range $30 < Q < 50$ MeV, Q may be calculated from, $Q = (0.09Y - 1.173)\cdot 10^8$ eV. The error introduced by the use of this approximate formula is less than that due to the uncertainty in the mass of the π-meson.

Since $Q = m_0 - m_+ - m_-$, and since the relation between Y and Q depends only on m_+ and m_-, Y is a function only of the rest masses. It is therefore invariant to a change in the frame of reference, and may be calculated in the C system. We thus have

$$Y = \varepsilon_+^*\varepsilon_-^* + p^{*2} \,. \tag{13}$$

As Y is a constant for a given decay process, its value may be also calculated from any convenient values of the momenta in the L system. As above we choose $p_+ = 0$, and thus have from (12)

$$Y = m_+E_- \,, \tag{14}$$

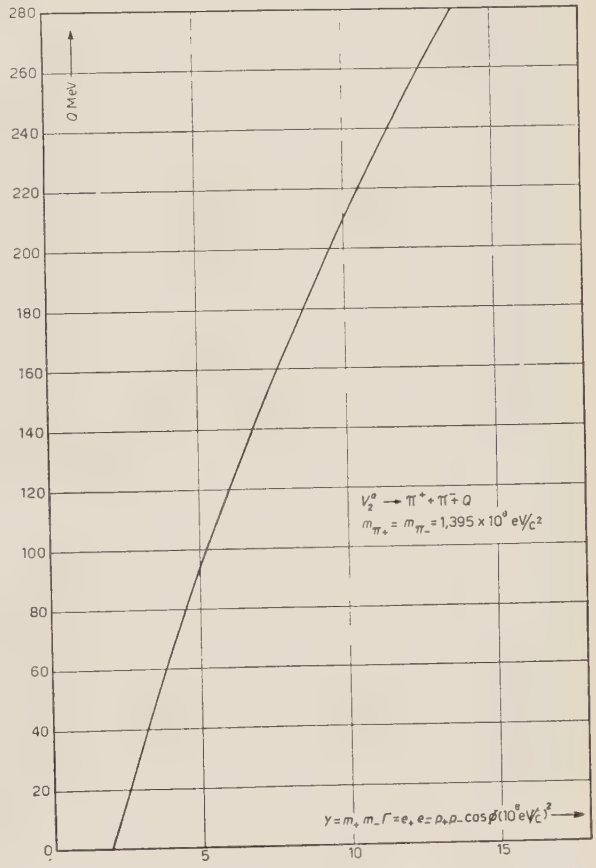

Fig. 8. – Q as a function of Y for the θ^0-particle.

where E_- is the energy corresponding to the critical momentum. Alternatively we can use the more symmetrical relation

$$Y = m_+m_-\Gamma \,, \tag{15}$$

where $\Gamma = E_-/m_-$ is the critical value of $\gamma_- = e_-/m_-$. (By similar reasoning $\Gamma = E_+/m_+$).

The function Y enables Q-values to be calculated rapidly. It is more convenient than Q for analytical treatment. As a first illustration of its use we will show that there is, in most chambers, an instrumental bias against measuring Q-values much greater than 200 MeV for the decay process $V_2^0 \rightarrow \pi^+ + \pi^-$.

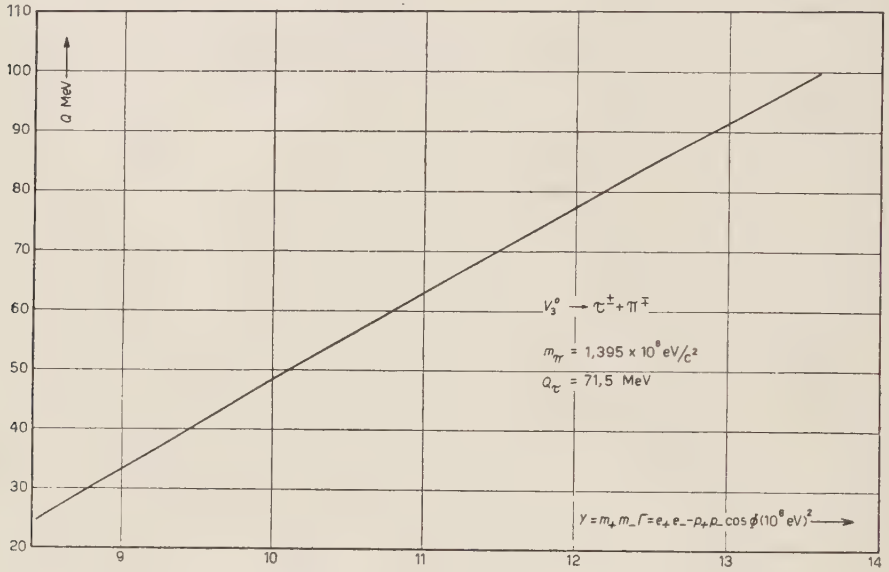

Fig. 9. – Q as a function of Y for the V_3^0-particle.

In the Jungfraujoch chamber (which has a maximum detectable momentum not significantly different from that of BUTLER and his collaborators [11], and those described by LEIGHTON *et al.* [3], the only accurate measurements of magnetic curvature are those leading to momenta less that $5 \cdot 10^8$ eV/c [12]. For any given angle φ this maximum value for accurate measurements defines a maximum accurate Q value which can be recorded. We can find easily the value of φ corresponding to this maximum momentum value ($5 \cdot 10^8$ eV/c) for the two secondary particles and to a V_2^0 Q-value of 210 MeV. From Fig. 8, for $Q = 210$ MeV, $Y = 10 \cdot (10^8\ \mathrm{eV})^2$. Then from equation (12) we have

$$\begin{aligned} 10 &= (m_\pi^2 + 5^2)^{\frac{1}{2}}(m_\pi^2 + 5^2)^{\frac{1}{2}} - 5 \cdot 5 \cdot \cos\varphi \\ &= m_\pi^2 + 25(1 - \cos\varphi) \end{aligned}$$

whence

$$\cos\varphi = 1 - \frac{8}{25}$$

[11] K. H. BARKER: *Report of Bagngres-de-Bigorre Conference* (1953), p. 2.

[12] J. S. BUCHANAN, W. A. COOPER, D. D. MILLAR and J. A. NEWTH: *Phil. Mag* (in the press).

or

$$\varphi = 47^\circ .$$

Thus in these conditions of maximum detectable momentum an accurate V_2^0 Q-value greater than 210 MeV can only be measured when φ is greater than 47°. But with large angle decays there is a marked bias against finding secondary tracks which are long enough for accurate measurement. Thus the fact that nearly all anomalous decays yield V_2^0 Q-values below 210 MeV is not in itself a convincing demonstration in favour of a V_2^0 type of decay with a low Q-value (the above argument does not of course apply to chambers such as that of THOMPSON and his collaborators in which the maximum detectable momentum is very high).

The use of the function Y is not essential for the above discussion. With a little extra arithmetic we could have proceeded directly from Q. Alternatively we could have read the value of φ, corresponding to $p_- = p_- = 5 \cdot 10^8$ eV/c and $Q = 210$ MeV, directly from the curves in Fig. 4. But when we have to compare Q-values assuming different decay processes for the same event Y introduces a substantial simplification in the argument.

We call Q_1 the value of Q for a given event calculated assuming a Λ^0-decay, Q_2 the value for the same event assuming a $V_2^0 \to \pi^+ + \pi^-$ decay and Q_3 the value for a decay of type $V_3^0 \to \tau^- + \pi^-$. We will call Y_1, Y_2 and Y_3 the corresponding values of Y. We then have

$$(16) \qquad \begin{cases} Y_1 = e_p e_- - p_+ p_- \cos\varphi \\ Y_2 = e_\pi e_- - p_+ p_- \cos\varphi \\ Y_3 = e_\tau e_- - p_+ p_- \cos\varphi \end{cases}$$

where e_p, e_π and e_τ are the energies of the positive particle assumed to be a proton, a π-meson and a τ-meson respectively.

By combining equations (16) we obtain

$$(17) \qquad Y_2 = Y_1 - e_- (e_p - e_\pi)$$

The term $e_p - e_\pi$ depends on p_+, m_p and m_π. As p_+ increases it approaches the asymptotic value,

$$(18) \qquad (\varepsilon_p - \varepsilon_\pi)_{p_+ \to \infty} = \frac{m_p^2 - m_\pi^2}{2 p_+} = \frac{43}{p_+} \cdot 10^8 \text{ eV/c} ,$$

when p_+ is in units of 10^8 eV/c. We now introduce the approximation that $e_p - e_\pi$ is equal to this asymptotic value; we consider later the error intro-

duced by the approximation. We then have from equation (17)

$$Y_2 = Y_1 - 43\ e_-/p_+ . \tag{19}$$

From equation (19) and Figs. 7 and 8 we can now predict Q_2 corresponding to any given value of Q_1, i.e. the Q-value for an event interpreted as a V_2^0-decay, corresponding to its Q-value were it interpreted as a V_1^0-decay. We consider for an example an event which, assuming a large error of measurement, is compatible with the Λ^0-decay process, — say yielding a Λ^0 Q-value in the range $20 < Q_1 < 60$ MeV. From Fig. 7 we see that the corresponding range of Y_1 is $15 < Y_1 < 20 \cdot (10^8\ \mathrm{eV})^2$. The corresponding value of Y_2, from equation (19), lies in the range, $15 - 43\ e_-/p_+ < Y_2 < 20 - 43\ e_-/p_+$. This range of Y_2 and the associated range of Q_2, is plotted in Fig. 10 as a function of e_-/p_+. It is defined by the lines E and F. The lines C and D of the same

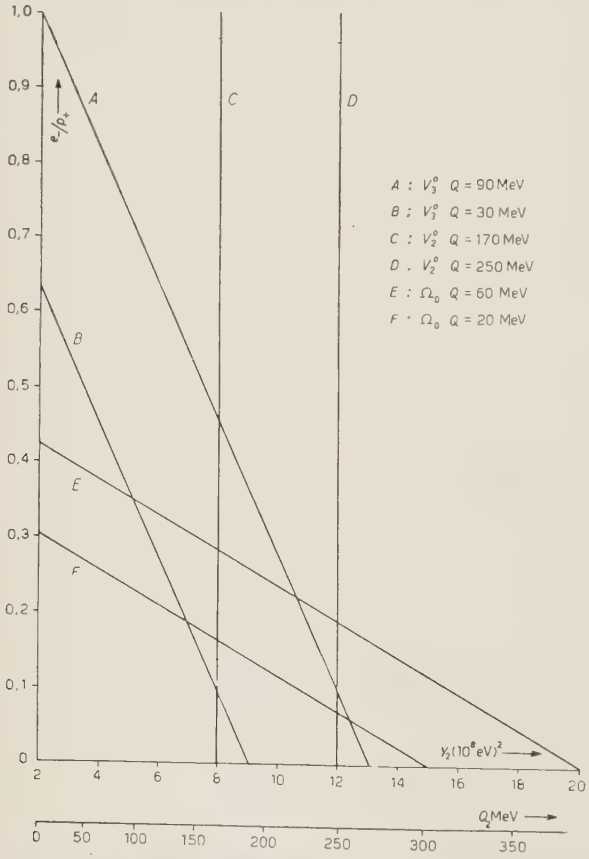

Fig. 10. – Here we consider three types of V^0-decay, Λ^0, θ^0 and the hypothetical process $V_3^0 \to \tau^+ + \pi^-$ (N.B. Not $V_3^0 \to \to \tau^- + \pi^+$). For any given V^0 event Q-values corresponding to these three processes can be calculated. These Q-values differ from each other because of the different masses assumed for the positive secondary particle; but they are not independent because they all depend on the same values of p_+p_- and φ. For high values of p_+ the correlation can be expressed as a function only of the ratio e_-/p_+. For example, line A represents events which, if interpreted as V_3^0-particles, would yield a Q-value of 90 MeV. The position of a given event on this line is defined by the ordinate e_-/p_+; the corresponding abscissa gives the Q-value which would be obtained if the event were to be interpreted as a V_2^0-decay. The space to the right of line D (events which give $Q_2 > 250$ MeV if interpreted as V_2^0-particles) is theoretically infinite. In practice, as is shown in the text, it is severely limited by chamber geometry.

figure define the range of V_2^0 Q-values for an event which, assuming a large error in measurement, can be interpreted as a θ^0-decay. The lines A and B have been derived in a manner exactly analogous to that used for lines E and F but corresponding to a decay process $V_3^0 \to \tau^+ + \pi^- + 60$ MeV instead of $\Lambda^0 \to p^+ + \pi^- + 37$ MeV.

An event which yields a V_2^0 Q-value too low to be consistent with θ-decay, and a V_1^0 Q-value too high to be consistent with Λ^0-decay, would lie on Fig. 10 in the space to the left of line C and above line E. However such events were produced many of them would be expected to lie between lines A and B, and thus be consistent with the assumed decay process $V_3^0 \to \tau^+ + \pi^-$. This shows that in interpreting anomalous decays we have to be careful in assuming that an apparent peak in Q-values is genuinely due to a new particle, and is not produced by a spurious effect introduced by the selection criteria.

In passing, it is interesting to note from Fig. 10 that in certain circumstances it is extremely difficult to discriminate between, Λ^0, θ^0 and V_3^0-decays.

The error introduced by the approximation of putting $e_-(e_\nu - e_\pi)$ equal to the asymptotic value 43 e_-/p_+ is 5% at $p_+ = 2 \cdot 10^9$ eV/c and 20% at $p_+ = 10^9$ eV/c. The error in the corresponding approximation for the V_3^0-decay, that $e_-(e_\tau - e_\pi) = 22\, e_-/p_+$, is 5% at $p_+ = 10^9$ eV/c. This error has little effect on the preceeding argument for the following reasons: 1) we are not concerned with precise values; we are illustrating only a trend; 2) when the error becomes large, i.e. when p_+ is low, identification is possible by ionization. 3) If the exact expression were applied the line E would be displaced to the right. The line B would also be displaced to the right, but by a smaller amount. Thus the arguments developed above would not be essentially altered.

5. – Conclusions.

1) Curves have been presented by means of which it is possible to determine the errors in measurement which must be assumed before a given V^0-event can be interpreted as a Λ^0, θ^0 or V_3^0-decay.

2) It has been shown that a fairly efficient separation of Λ^0 and θ^0-particles can be made by reference only to the angle between the secondary tracks and the momentum of the negative particle. All two body V^0-decays must satisfy the condition $p_- < P_- \operatorname{cosec} \varphi$. The critical momentum P_- is a constant for a given decay process, $P_- = (m_0/m_+)p^*$. For the Λ^0-particle $P_- = 1.2 \cdot 10^8$ eV/c, so for all Λ^0-decays $p_- < 1.2 \operatorname{cosec} \varphi \cdot 10^8$ eV/c. For the θ^0-particle P_- is much higher, and 90% of θ^0-decays will have $p_- > 1.2 \operatorname{cosec} \varphi \cdot 10^8$ eV/c.

3) Another constant for a given decay scheme has been introduced, $Y = m_+ E_-$, where E_- is the energy corresponding to the critical momentum P_-.

The value of Υ for a given event is more easily calculated than Q. Curves have been given relating Υ to Q for the Λ^0, θ^0 and V_3^0-decay processes. For the Λ^0-particle $Q = 0.09\Upsilon - 1.173 \cdot 10^8$ eV, with an error which, in the range $30 < Q < 50$ MeV, is negligible.

It has been shown by examples that the constant Υ, being more amenable than Q to analytical treatment, is useful for discussing selection and instrumental biasses.

Acknowledgements.

This work was started when I was at the University of Manchester. I am very much obliged to Professor P. M. S. BLACKETT for his interest and encouragement, and to my colleagues of the Jungfraujoch and Pic-du-Midi groups.

I am very grateful to Miss P. MILES and Signor S. MARTELLUCCI for the help which they have given me in carrying out the computations.

I have had the benefit of many valuable discussions, in particular with Dr. B. BRUNELLI, Prof. C. FRANZINETTI Dr. J. PODOLANSKI and Dr. E. ZAVATTINI.

I am glad to have this opportunity of thanking Professor E. AMALDI for his advice and for the facilities which he has given me, and to record the pleasure which I have had in working with him, Professor C. BALLARIO and their colleagues of the University of Rome.

APPENDIX I

a) The probability that $p_- \sin\varphi$ be less than a given value.

We have shown in section 3 that for the Λ_0-decay $p_- \sin\varphi$, must be less than $1.2 \cdot 10^8$ eV/c. We require to find the probability that $p_- \sin\varphi$ for a θ^0-decay should be less than $1.2 \cdot 10^8$ eV/c. We are interested only in values of φ less than 90^o.

Thus, using the symbol P to denote a probability, and working in units of 10^8 eV/c,

$$P(p_- \sin\varphi < 1.2) < P(p_- \sin\theta_- < 1.2)$$
$$< P(\sin\theta^* < 1.2/p^*) .$$

For the θ^0-decay p^* is $2 \cdot 10^8$ eV/c so that substituting this value and converting to $\cos\theta^*$ we find

$$P(p_- \sin\varphi < 1.2) < P(\cos\theta^* > 0.80)$$

(a more detailed discussion shows that the alternative solution, $-0.8 > \cos\theta^* > -1.0$, can be neglected).

Assuming isotropic emission in the C system, the probability that θ^* lies between θ_1^* and θ_2^* is

$$P(\theta_1^* < \theta^* < \theta_2^*) = \tfrac{1}{2}(\cos\theta_1^* - \cos\theta_2^*)\,. \tag{20}$$

Therefore

$$P(p_- \sin\varphi < 1.2) < \tfrac{1}{2}(1 - 0.80) < 10\,\%.$$

Thus less than 10% of the points representing θ^0-decays will lie to the left of curve A in Fig. 9.

In drawing curve B, no approximations have been used; for different values of γ_0 corresponding values of p_- and φ have been calculated from the equations

$$\cot\theta_+ = \gamma_0(\beta_0/\beta_+^*)\,\mathrm{cosec}\,\theta^* + \gamma_0\cot\theta^*\,,$$

$$\cot\theta_- = \gamma_0(\beta_0/\beta_-^*)\,\mathrm{cosec}\,\theta^* - \gamma_0\cot\theta^*\,,$$

$$p_- = p^*\sin\theta^*\,\mathrm{cosec}\,\theta_-\,,$$

$$\varphi = \theta_+ + \theta_-\,.$$

Values of $\mathrm{cosec}\,\theta^*$ and $\cot\theta^*$ corresponding to $\cos\theta^* = 0.80$ (10% probaility) have been substituted in these equations.

b) The probability that the ionization of a secondary particle should be greater than a given value.

The energy of a secondary particle in the L system is,

$$\varepsilon_1 = \varepsilon_1^* + \beta_0 p^*\cos\theta^*\,,$$

whence

$$\cos\theta^* = \frac{1}{\beta_0\beta_1^*}\left(\frac{\gamma_1}{\gamma_0\gamma_1^*} - 1\right). \tag{21}$$

The specific ionisation of a particle is about 2 if $\gamma = 1.25$. This value of γ_1 and the appropriate constants, γ_1^* and β_1^*, have been substituted in equation (20), to derive the curves given in Fig. 2.

RIASSUNTO (*)

Si discute l'identificazione dei decadimenti V^0 a partire dai valori ora stabiliti dei Q per le particelle Λ^0 e θ^0. Si descrive un metodo per la separazione delle particelle Λ^0 e θ^0, che richiede solo misure dell'impulso del secondario negativo e dell'angolo fra le tracce dei secondari. Si danno curve che facilitano il calcolo dei valori di Q. Poichè, se gli errori di misura sono grandi, gli errori « standard » nei valori di Q non sono attendibili, si danno curve per mezzo delle quali è possibile verificare se i singoli eventi possono interpretarsi come decadimenti Λ^0 o θ^0. Riguardo ai decadimenti V^0 anomali, si tiene conto dell'influenza delle deviazioni strumentali ed ai criteri usati nella selezione degli eventi.

(*) *Traduzione a cura della Redazione.*

On the Decay Scheme of $^{212}_{84}$Po(ThC′).

F. Demichelis

Istituto di Fisica Sperimentale del Politecnico - Torino

(Ricevuto il 7 Luglio 1954)

Summary. — In a previous paper an incomplete correspondence between the γ levels and the long range α-particles levels for the nuclide $^{214}_{84}$Po has been noticed. Now I accomplished an analogous research for the nuclide $^{212}_{84}$Po. Also in this case, from the experimental determination of the γ-γ cascades, I was able to obtain a new level scheme of this nuclide. The partial lack of correspondence between γ levels and long range α levels is existing again. In conclusion this fact must be considered a general property for the radioactive nuclides emitting long range α-particles.

Two natural radioactive nuclides $^{214}_{84}$Po of the uranium series and $^{212}_{84}$Po of the thorium series, emit in their disintegration, groups of long range α-particles (1).

These nuclides $^{214}_{84}$Po and $^{212}_{84}$Po are β-decay products; $^{214}_{84}$Po comes from $^{214}_{83}$Bi (99.96%, half-life $T = 19.7$ minutes), $^{212}_{84}$Po comes from $^{212}_{83}$Bi (66%, $T = 60.5$ minutes).

The decay scheme of $^{214}_{84}$Po is particularly complex.

It must take into account: the γ-rays of different energies corresponding to the transition from the excited states to the ground state of $^{214}_{84}$Po; the existence at the same time of twelve groups of long range α-particles.

Very recently F. Demichelis and R. Malvano (2) have proposed a new

---

(1) E. Rutherford, W. B. Lewis and B. V. Bowden: *Proc. Roy. Soc.*, A **142**, 347 (1933); S. Rosenblum and M. Valadres: *Compt. Rend.*, **194**, 967 (1932); W. B. Lewis and B. V. Bowden: *Proc. Roy. Soc.*, A **145**, 235 (1934); W. B. Holloway and M. S. Livingston: *Phys. Rev.*, **54**, 18 (1938); W. Y. Chang and T. Coor: *Phys. Rev.*, **174**, 1196 (1948); A. Rytz: *Compt. Rend.*, **233**, 790 (1951); G. H. Briggs: *Rev. Mod. Phys.*, **26**, 1 (1954).

(2) F. Demichelis and R. Malvano: *Nuovo Cimento*, **12**, 358 (1954).

decay scheme for $^{214}_{84}$Po, as suggested by their experimental researches on the γ-γ cascades.

On the other hand the decay scheme of $^{212}_{84}$Po appears by far a simpler one: only three groups of long range α-particles are certain.

In spite of this the building up of this scheme is not a simple task because $^{212}_{84}$Po decays into $^{208}_{82}$Pb with a half-life of $\approx 10^{-7}$ s only; in its turn the $^{208}_{82}$Pb falls to the ground state emitting a very intense γ-γ cascade whose rays have respective energies of 0.58 and 2.62 MeV. This cascade interferes on the purity of the experimental results on $^{212}_{84}$Po.

Previous experiments ([3]) have made known the energies and the intensities of γ-rays from $^{212}_{84}$Po.

In Table I is reported the γ-ray spectrum of $^{212}_{84}$Po and $^{208}_{82}$Pb.

TABLE I.

Transition	Energy per photon MeV	Intensity J	Intensity L_1	Intensity L_2
$^{212}_{83}Bi \rightarrow ^{212}_{84}Po$	0.73	37	—	—
	0.83	38	—	—
	1.03	11	—	—
	1.35	9	3.6	10.0
	1.50	—	3.7	6.5
	1.60	14	10.0	11.0
	1.80	14	6.2	6.5
	2.20	—	5.05	10.0
$^{212}_{84}Po \rightarrow ^{208}_{82}Pb$	0.58	101	—	—
	2.62	100 (assumed)	100.00 (assumed)	100.00 (assumed)

J: A. JOHANSSON: *Arkiv Mat. Astron. Fysik*, **34** A, 9, 1 (1947).
L_1: G. D. LATYSHEV: *Rev. Mod. Phys.*, **19**, 132 (1947).
L_2: G. D. LATYSHEV: *Rev. Mod. Phys.*, **19**, 132 (1947).

On the basis of these γ-ray energies, and of the long range α-particles, several authors ([3]) have suggested a decay scheme of $^{212}_{84}$Po.

But these suggestion do not quite agree with each other; not even the several authors suppose the same γ-γ cascades to set up their schemes.

([3]) F. OPPENHEIMER: *Proc. Camb. Phyl. Soc.*, **32**, 328 (1936); D. G. E. MARTIN and H. O. W. RICHARDSON: *Proc. Phys. Soc.*, A **63**, 223 (1950); A. JOHANSSON: *Arkiv Mat. Astron. Fysik*, **34** A, 9, 1 (1947); G. D. LATYSHEV: *Rev. Mod. Phys.*, **19**, 132 (1947).

No doubt a direct knowledge of the really existing γ-γ cascades, would bring us to the selection of the best scheme.

This has been the purpose of this research.

The experimental apparatus was fundamentally the same as in the preceeding experiments on $^{214}_{84}$Po [2].

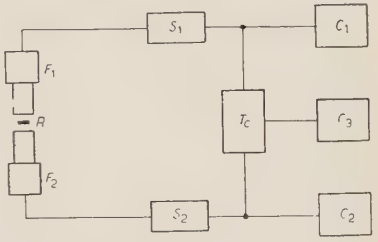

Fig. 1.

F_1 and F_2 (see Fig. 1) are two scintillation receivers (NaI(Tl) crystals-RCA 5819 photomultipliers) mounted so as to act as proportional counters for γ-rays. R is the radioactive source.

The pulses from the scintillation receivers are first amplified and next applied to the coincidence circuit T_c through two pulse shapers S_1 and S_2. These shapers act also as integral discriminators.

C_1 and C_2 count the total number of γ-rays detected by F_1 and F_2; C_3 counts the total number of coincidences.

In a first set of measurements one pulse shaper was constantly biased to a voltage corresponding to the energy $h\nu = 0.65$ MeV, while the other pulse shaper was biased to a variable voltage corresponding to energies from $h\nu = 0.60$ MeV to $h\nu = 1.70$ MeV.

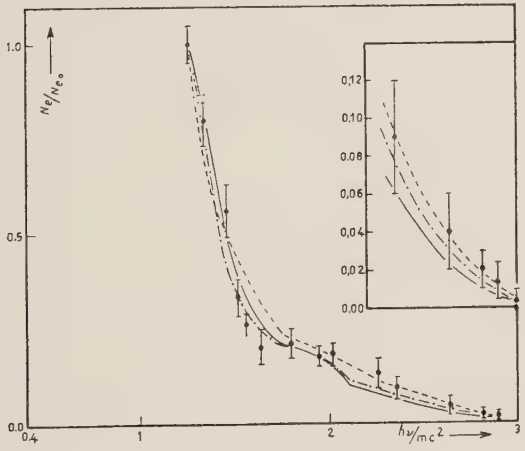

Fig. 2.

The experimental points are shown in Fig. 2, where $h\nu/mc^2$ is represented on the x-axis while on the y-axis is represented the ratio N_e/N_{e_0} between the effective coincidences N_e and the effective coincidences N_{e_0} obtained with a bias of F_1 corresponding to $h\nu = 0.65$ MeV.

In a second set of measurements, one pulse shaper was constantly biased to a voltage corresponding to $h\nu = \approx 0.78$ MeV, while the other pulse shaper was biased to a variable voltage corresponding to energies from $h\nu = 0.75$ MeV to $h\nu = 1.50$ MeV.

The experimental points are represented in Fig. 3 (same quantities on the axes as in Fig. 2).

Diagram of Fig. 2 shows us that at least one γ-γ cascade is existing.

One of the γ-rays in the cascade has an energy lower (or equal) to 1.50 MeV and another cascade γ-ray has an energy higher than 0.65 MeV.

From Fig. 3 we must deduce that there exists also another γ-γ cascade; one of the γ-rays of this cascade has an energy lower (or equal) to 1.35 MeV and the other γ-ray has an energy higher than 0.80 MeV.

Evidently the bias of the pulse shapers and the end of the experimental points in Fig. 2 and 3 give only an approximate value of the γ-ray energy; on the other hand we know already the energies of the γ-rays (see Table I).

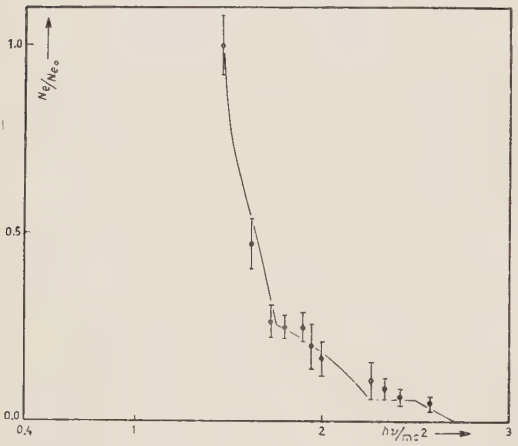

Fig. 3.

The experimental points of Fig. 3 allow an easier theoretical interpretation; indeed the full line is the theoretical curve of the γ-γ cascade (1.35; 0.83) MeV as a function of the γ-rays integral cross-section in our NaI(Tl) crystals ([2,4]). The agreement between the experimental points and the full line, shows the existence of this cascade and this only.

The experimental points of Fig. 2 must include the coincidences from said cascade and at least another one.

The dotted line, Fig. 2, represents the theoretical curve of the two following cascades:

a) (1.50; 0.73) MeV,

b) (1.35; 0.83) MeV.

This curve is calculated taking into account the intensities of the γ-rays as given by G. D. LATYSHEV (see L_1 in Table I). The agreement with the experimental data cannot be considered sufficient in the neighborhood of 1.60 MeV. Nor an advantage can be reached through an acceptable modification of these intensities.

The full line, Fig. 2, is obtained considering the two cascades *a*) and *b*), using the same intensities as that used for the dotted line, and the following

([4]) D. MAEDER, R. MÜLLER and V. WINTERSTEIGER: *Helv. Phys. Acta*, **27** 1, 3, (1954).

cascade:

c) (1.03; 0.73) MeV,

with the intensity given by A. JOHANSSON (see J in Table I).

The dotted-dashed line, Fig. 2, is obtained considering the same cascades *a*), *b*), *c*) with the following intensities:

cascade *a*): intensity L_2, Table I;

cascade *b*): intensity L_1, Table I;

cascade *c*): the same intensity as cascade *a*).

Although the experimental uncertainties do not allow a safe choice among the different groups of admissible intensities, the dotted-dashed line seems the best theoretical one, and it shows the existence of cascades *a*), *b*) and *c*).

In conclusion and according to our experimental results on the γ-ray cascades the decay scheme should be represented as in Fig. 4*a*.

Fig. 4*b* represents the energy levels as deduced from long range α-particles; in this scheme the dotted level corresponds to a not surely established group of long range α-particles (1).

We can deduce, from Fig. 4*a*, 4*b*, that in $^{212}_{84}$Po only three groups of long range α-particles do exist for certain; two α-levels and the uncertain one, correspond to γ-ray levels. On the other hand there are γ-ray levels corresponding to no α-level known so far.

This conclusion was necessary to state the general validity of the analogous conclusion already notified for $^{214}_{81}$Po (2).

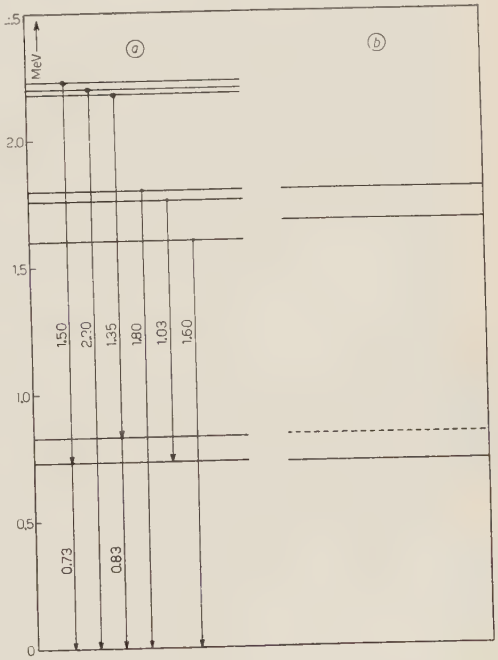

Fig. 4 *a-b*.

The lack of an agreement between the two schemes of Fig. 4*a*, 4*b* is a general property of the nuclides emitting long range α-particles.

I wish to express my deep gratitude to Prof. E. PERUCCA for his constant interest and stimulating help.

RIASSUNTO

In un lavoro precedente era stato notato, per il nuclide $^{214}_{84}Po$, l'incompleto accordo tra i livelli energetici dedotti dallo spettro di raggi γ e i livelli energetici individuati dalle particelle α di lungo percorso. Ora ho compiuto analogo studio sul nuclide $^{212}_{84}Po$ e, valendomi della determinazione sperimentale delle cascate γ-γ da questo emesse, ho potuto giungere allo schema dei livelli γ del $^{212}_{84}Po$. Di nuovo è risultato il disaccordo parziale ma sensibile tra i livelli γ e i livelli α. Questo fatto deve quindi considerarsi proprietà comune ai nuclidi radioattivi emettenti particelle α di lungo percorso finora noti.

On the Dependence of the Decay Times of Space Charges by the Static Characteristic in Intermittent Discharges.

D. Brini, O. Rimondi and P. Veronesi

Istituto di Fisica dell'Università - Bologna

(ricevuto il 10 Luglio 1954)

Summary. — The results of some measurements on the decay times of space charges and their dependence on the static characteristic of the tube and the external circuit are reported. The results show a dependence of such times on the external circuit, but stress the existence of a true decay time of the space charges, which is not influenced by the external circuit and is dependent only on the static characteristic of the tube. Moreover, an empirical method for the calculation of the decay times of space charges, is given.

1. – In a previous paper [1], dedicated to the measurement of the decay time of space charges in conditions of intermittent discharges we had the occasion to formulate a general picture of such phenomena in relation to the static characteristic of the tube. We then described the phenomena, supposing that the starting potential of the intermittent discharges at the end of the first kind would correspond to the potential in which the transition from Townsend's phase to that of subnormal glow takes place, and equally, that the starting potential of the intermittent discharges at the beginning of the second kind would correspond to the potential in which the subnormal glow phase begins. Moreover in such a picture it was also possible to explain the phenomenon of intermittent group discharges, due to the instable tract of the static characteristic between Townsend's phase and the glow one. With the purpose of verifying experimentally and defining quantitatively the hypothesis formulated by us in the previous paper, we have carried out a series of measurements , the results of which are here set out.

[1] D. Brini and P. Veronesi: *Nuovo Cimento*, **10**, 1662 (1953).

2. – For the measurements of the times τ_1, and τ_0, respectively the charge times of the capacity, for the discharges at the end of the first kind and the beginning of the second kind, we used the apparatus already described in the above-mentioned paper. As discharge tubes, the use of the commercial tubes, viz, OB3(VR90), OC3(VR105), OD3(VR150), 85A1, 150C, ST100, STV140, 991 and 4687 was found convenient. The behaviour of these tubes was investigated by many authors (2); EDWARDS studied (3) recently their employement in relaxation oscillations.

The behaviour of these tubes differs from type to type, and, for tubes of the same type, from tube to tube. Our preliminary experiments carried out to select tubes gave the results shown in Table I.

TABLE I.

Type of Tube	No. of Tubes Tested	No. of Tubes which showed 1st and 2nd kinds	No. of Tubes which showed 1st kind only	No. of Tubes which did not show intermittent discharges
OB3	10	10	0	0
OC3	10	2	8	0
OD3	10	1	8	1
85A1	1	1	0	0
150C	1	0	0	1
ST100	10	0	10	0
STV140	5	4	1	0
991	5	5	0	0
4687	1	1	0	0

The advantage in the use of these discharge tubes, in respect to the experimental tube used by us in the preceding experiments, lies in the fact that the characteristics of the tubes proved to be more stable and the measurements more reproducible. In this connexion one can say that, if the tube is made to function in continuous discharge for about half-an-hour, the measurements of the times showed themselves to be satisfactorily reproducible, even at a long-term distance.

3. – As our first aim we decided to put into evidence the dependence of the times τ_1 and τ_0 on the external circuit. Assuming E as a parameter, we measured

(2) G. M. KIRKPATRICK: *Proc. I.R.E.*, **35**, 485 (1947); F. V. HUNT and R. W. HICKMAN: *Rev. Sci. Instr.*, **10**, 6 (1939).

(3) P. L. EDWARDS: *Proc. I.R.E.*, **41**, 1756 (1953).

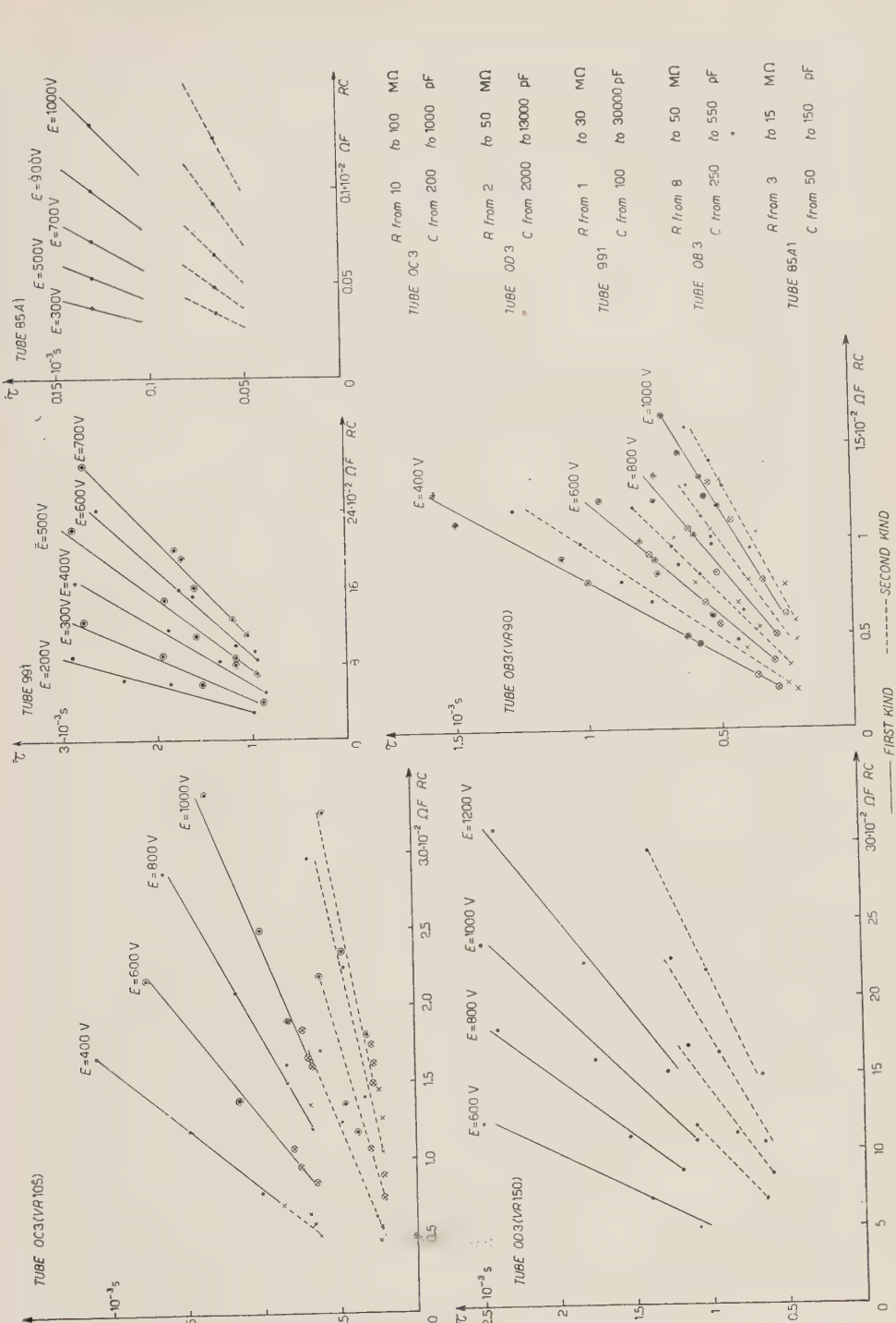

TUBE OC3 R from 10 to 100 MΩ C from 200 to 1000 pF

TUBE 003 R from 2 to 50 MΩ C from 2000 to 13000 pF

TUBE 991 R from 1 to 30 MΩ C from 100 to 30000 pF

TUBE OB3 R from 8 to 50 MΩ C from 250 to 550 pF

TUBE 85A1 R from 3 to 15 MΩ C from 50 to 150 pF

Fig. 1.

such times as a dependence of the product RC: τ_1 and τ_0 were determined, as reciprocals respectively of the frequencies at the end of the first kind and the beginning of the second, corrected by the discharge time. The precision of the measurements was 10%. The results obtained for different types of tubes are shown in Fig. 1. It must be remembered, as VALLE has already shown [4], that the product RC is always obtained for one pair of values of R and C which satisfy the condition $RC = \text{cost}$. Beside the curves represented in Fig. 1, the orders of magnitude used of the values of R and C can also be found. The results quoted show that τ_1 and τ_0 depend on the external circuit, but that for every tube there exists a minimum value sufficiently well defined both for τ_1 and τ_0, which does not depend on the external circuit. Measurements carried out on different tubes of one type showed that these times are always approximately the same, and that the curves which give τ_1 and τ_0 as a function of RC have always the same behaviour with small deviations parallel to the RC axis.

Some of the tubes used by us, such as OB3 and OC3, showed two different values of τ_1 and τ_0, for the same E and R. The smallest of the two different values of τ_1 was obtained when the frequency at the end of the first kind was found as the superior limit of the frequency of the first kind; the greater value was obtained when the frequency at the end of the first kind was reached by surpassing the inferior limit of the frequency of the second kind. Both the values of τ_1 in the diagrams of Fig. 1 are to be found on the same representative straight line; the first are indicated by a little cross. Similarly, the smallest of the two different values of τ_0 was obtained when the initial frequency of the second kind was arrived at at the transition from the discharges of the first kind to those of the second; the greater was obtained when the initial frequency of the second kind was reached as the inferior limit of the frequency of the second kind. These results are also characterized by the fact that, with these types of tubes, group discharges were not present; with tubes in whith it was only possible to determine one value of τ_1 and τ_0 in the same condition of R and E, group discharges between those of the first and second kind were almost always present.

The determination of the static characteristics showed that, for the tubes which presented two different values of τ_1 and τ_0, hysteresis at the transition from Townsend's phase to that of the subnormal glow and vice versa was present, as is shown schematically in Fig. 2. It was not possible to observe any hysteresis in the tubes which presented one value of τ_1 and τ_0. It is reasonable to admit then that the phenomena of hysteresis are also present in conditions of intermittent discharges: the transition from the first to the second kind takes place by jumps between the point T_A and G_A of the static

[4] G. VALLE: *Phys. Zeits.*, 13, 473 (1942).

characteristic, while that from the second to the first kind takes place instead by jumps between the points G_B and T_B of the static characteristic. Further measurements, to be reported in the following paragraph, confirm this hypothesis.

The bringing to light of the static characteristic has also revealed that in the tubes which presented group discharges, the difference between the maximum current of Townsend's phase and the minimum current of the subnormal glow phase is noteworthy, the difference being very small in the tubes in which the group discharges did not take place.

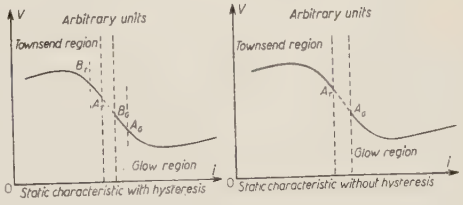

Fig. 2.

4. – A series of measurements was carried out to determine the height of the oscillation pulses and the values of the starting potential in the conditions of intermittent discharges at the end of the first kind and the beginning of the second kind. The measurements were carried out by sending the output pulse of the tube to a cathode follower, and from this to a dyode rectifier. The results obtained show that in each case, and independently of the external circuit, the starting potential of the discharges at the end of the first kind always assumes the same value, which value corresponds exactly to what, on the static characteristic, takes place at the end of Townsend's phase. Similarly the starting potential of the discharges at the beginning of the second kind always assumes the same value, which value corresponds to what, on the static characteristic, takes place at the beginning of the glow phase.

The determination of the height of the pulses which were obtained with a normal circuit height pulse meter or by varying the bias of the dyode in the above mentioned circuit until the whole pulse had passed, permitted us too to measure the exhaustion potential of the discharges. It was thus possible to see that, in conditions of periodic discharges at the end of the first kind and beginning of the second kind, the starting potential of the discharges remains constant, while the exhaustion one varies. In the conditions in which we measured the minimum values of τ_1 and τ_0, the exhaustion potential was not strongly dependent on the external circuit. These results were obtained both in the tubes which did not show hysteresis and in those which demonstrated it.

5. – Many attempts were made to formulate adequate expressions for τ_c and τ_d, which represent the charge and discharge times of the capacity, as a function of the circuit constants and of the characteristics of the tube. In

each case a beginning was made with the circuit equation, giving the conductivity respectively of $\lambda_c(V)$ and $\lambda_d(V)$, as functions of the instantaneous applied potential. The integration of the differential equation which describes the condition of the functioning of the circuit leads to the following two expressions:

$$(1) \qquad \tau_c = RC\int_M^A \frac{\mathrm{d}V}{R\lambda_c(V)V-(E-V)}\,, \quad \tau_d = RC\int_A^M \frac{\mathrm{d}V}{R\lambda_d(V)V-(E-V)}\,,$$

where M and A are the minimum and maximum values of the potential applied to the tube in a condition of intermittent discharges and for a certain condition of functioning, and V is the instantaneous value of such a potential.

VALLE solved the relation (1), supposing λ_c and λ_d constant for every definite discharge condition, but variable with the different external circuit conditions, which are compatible with the intermittent discharges. This hypothesis gives us the following expressions of τ_c and τ_d:

$$(2) \qquad \tau_c = \frac{RC}{R\lambda_c+1}\ln\frac{E-M(R\lambda_c+1)}{E-A(R\lambda_c+1)}\,, \qquad \tau_d = \frac{RC}{R\lambda_d+1}\ln\frac{E-A(R\lambda_d+1)}{E-M(R\lambda_d+1)}\,.$$

We took up the problem again, referring however only to the intermittent discharge conditions at the end of the first kind and the beginning of the second kind. In this case, as we have already had occasion to mention, the terms of the problem are much more clearly defined. To determine the dependence of λ_c upon the potential, we supposed that during a time interval corresponding to the capacity charge, a decrease in the current of the discharge tube represented by

$$(3) \qquad \mathrm{d}i = -Ki\,\mathrm{d}V\,,$$

could be assumed. This assumption is reasonable enough and leads to the expression for i of

$$(4) \qquad i = i_M \exp\left[-K(V-M)\right],$$

where K has the value of

$$K = \frac{1}{A-M}\ln\frac{i_M}{i_A}\,,$$

and where i_M and i_A are respectively the currents corresponding to the M and A potentials applied to the tube.

From (4) it can immediately be seen that

$$\lambda_c = \frac{i_M \exp\left[-\frac{k}{V}(V-M)\right]}{} = \frac{E-M}{RV}\exp\left[-K(V-M)\right], \tag{5}$$

where we put for i_M the corresponding expression

$$i_M = \frac{E-M}{R}.$$

Substituting (5) in the first expression of (1) and indicating as usual the two values of τ_c corresponding respectively to the end of the first kind and the beginning of the second kind with τ_1 and τ_0, it is immediately obvious that

$$\left|\begin{array}{l} \tau_1 = RC_1 \displaystyle\int_{M_1}^{T} \frac{dV}{(E-M_1)\exp\left[-K_1(V-M_1)\right]-(E-V)}, \\ \\ \tau_0 = RC_0 \displaystyle\int_{M_0}^{G} \frac{dV}{(E-M)\exp\left[-K_0(V-M_0)\right]-(E-V)}, \end{array}\right. \tag{6}$$

where T and G are the starting discharge potentials at the end of the first kind and the beginning of the second. Rather than to resolve the integral (6) which is somewhat complicated, it is possible to determine, in a semiempirical manner, an expression of τ_1 and τ_0 as a function of the parameters of the circuit.

In fact it is easy to see that the mean value $\bar{i}$ of the current in the time interval in which V rises from M to A is expressed by

$$\bar{i} = \frac{1}{A-M}\int_M^A i_M \exp\left[-K(V-M)\right]dV = \frac{i_M}{(A-M)K}\left[1-\exp\left[-K(A-M)\right]\right],$$

from which, taking into account the expression of K, we have

$$\bar{i} = \frac{i_M}{\ln\frac{i_M}{i_A}}\left(1-\frac{i_A}{i_M}\right).$$

Remembering the expression of i_M, the mean current can be represented by the relation

$$\bar{i} = \frac{E-M}{R\ln\frac{E-M}{Ri_A}}\left(1-\frac{Ri_A}{E-M}\right). \tag{7}$$

Considering that in the capacity charge phase the current in the tube has the constant value $\bar{i}$, the equation of the circuit in such a condition becomes

$$C\,\mathrm{d}V + \bar{i}\,\mathrm{d}t = \frac{E - V}{R}\,, \tag{8}$$

which, integrated between M and A, gives

$$\tau_c = RC \ln \frac{E - M - v}{E - A - v}\,, \tag{9}$$

were we put

$$v = R\bar{i}\,.$$

With convenient substitutions, it is immediately evident that

$$\tau_1 = RC_1 \ln \frac{E - M_1 - v_T}{E - T - v_T}\,, \qquad \tau_0 = RC_0 \ln \frac{E - M_0 - v_G}{E - G - v_G}\,, \tag{10}$$

where

$$v_T = R\bar{i}_T\,, \qquad v_G = R\bar{i}_G\,;$$

$\bar{i}_T$ and $\bar{i}_G$ being the mean values of the current in the discharge conditions at the end of the first kind and beginning of the second.

The expressions (10) are somewhat simple ones, in good agreement with the experimental facts.

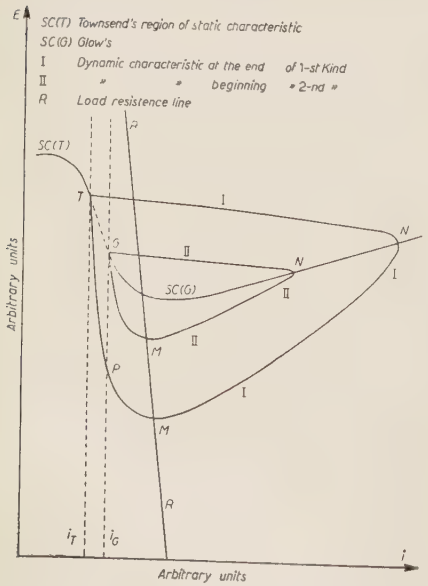

Fig. 3.

In Table II for purposes of comparison, the experimental data and those calculated by means of (10) for the tubes OD3 and OC3 for the two values of E are reported. It is easy to see that the agreement is good, which permits us to hold that the supposed expression (3) is correct.

6. – We are now able to define a true decay time τ^* of the space charges. An approximate valuation of such a time consists in assuming the smallest of all the values of τ_1 as τ^*, which is also independent of the external conditions of the circuit. Observing Fig. 3, in which the static characteristic of a tube and the dynamic ones corre-

TABLE II. – *Tube* OD3 *first and second kind.*

E (V)	R (MΩ)	C_1 (pF)	τ_1 (ms)	T (V)	$T - M_1$ (V)	i_T (μA)	τ_1 calc (ms)	C_0 (pF)	τ_0 (ms)	G (V)	$G - M_0$ (V)	i_G (μA)	τ_0 calc (ms)
	25	2 000	1.1	144	3.7	4.5	0.9	—	—	—	—	—	—
600	20	3 450	1.4	144	4.4	4.5	1.2	3 400	0.65	142	1.6	10	0.73
	15	8 000	2.5	144	5.2	4.5	2.4	7 650	1.1	142	1.7	10	1
	40	2 650	1.1	144	4.5	4.5	1	2 600	0.65	142	1.6	10	0.65
1 000	30	5 570	1.8	144	4.9	4.5	1.7	5 400	0.95	142	1.8	10	0.9
	25	9 600	2.5	144	5.2	4.5	2.4	9 100	1.25	142	1.8	10	1.1

Tube OC3 *first kind.*

E (V)	R (MΩ)	C_1 (pF)		τ_1 (ms)		T (V)		$T - M_1$ (V)		i_T (μA)		τ_1 calc (ms)	
	40	—	130	—	0.6	—	120	1	12	—	3	—	0.65
	30	290	200	1	0.65	122	120	16	13	2.5	3	1.1	0.7
400	25	500	260	1.5	0.7	122	120	19	14	2.5	3	1.7	0.75
	20	850	360	2.1	0.9	122	120	22	15	2.5	3	2.4	0.8
	80	190	150	0.8	0.6	122	120	14	13	2.5	3	0.7	0.65
800	70	300	190	1.1	0.6	122	120	16	13	2.5	3	1.1	0.65
	60	490	250	1.6	0.7	122	120	19.5	14.5	2.5	3	1.8	0.8

TABLE III.

TUBE OD3					TUBE OC3				
E (V)	τ_1 (ms)	τ_0 (ms)	$\tau_1 - \tau_0$ (ms)	τ^* (ms)	E (V)	τ_1 (ms)	τ_0 (ms)	$\tau_1 - \tau_0$ (ms)	τ^* (ms)
600	1.1	0.65	0.45	0.39	400	0.6	0.2	0.4	0.21
800	1.2	0.6	0.60	0.41	600	0.6	0.2	0.4	0.19
1 000	1.1	0.65	0.45	0.40	800	0.6	0.2	0.4	0.19
1 200	1.2	0.7	0.5	0.42	1 000	0.7	0.3	0.4	0.18

sponding to the end of the first kind and the beginning of the second are reported schematically, it is easy to see that such a value of τ^* represents a superior valuation for the decay time of the space charges. In fact the interval of the dynamic characteristic included between M and P takes place in the glow region in which the space charges are still present. Analogously it is possible to make a more approximate valuation of τ^* by assuming

$$\tau^* = \tau_1 - \tau_0 .$$

The exact calculation was made by evaluing the time in which the PT interval of the dynamic characteristic was covered, and by considering, among all the characteristics corresponding to the end of the discharges of the first kind, those for which τ_1 is the smallest.

Since the current in P has a value of i_G and depends on the static characteristic of the tube, it can be seen from (4) that

$$i_G = i_{M_1} \exp\left[-K(P - M_1)\right],$$

from which we have

$$P = M_1 + \frac{1}{K_1} \ln \frac{i_{M_1}}{i_G} .$$

It follows immediately that

$$\tau^* = RC_1 \left[\int_{M_1}^{T} \frac{\mathrm{d}V}{(E - M_1) \exp\left[-K_1(V - M_1)\right] - (E - V)} - \int_{M_1}^{P} \frac{\mathrm{d}V}{(E - M_1) \exp\left[-K_1(V - M_1)\right] - (E - V)} \right] .$$

To follow up the calculations it is convenient in this case also to proceed with the assumption previously formulated on the behaviour of i, and to determine a mean current between P and T expressed by

$$\bar{i}^* = \frac{i_G}{\ln \frac{i_G}{i_T}} \left(1 - \frac{i_T}{i_G}\right) . \tag{11}$$

In analogy to our previous development, we shall obtain

$$\tau^* = RC_1 \ln \frac{E - P - v^*}{E - T - v^*} , \tag{12}$$

where

$$v^* = R\bar{i}^* .$$

Table III shows the results of the calculations, which are reported together, for purposes of comparison, with those corresponding to τ_1 and $\tau_1 - \tau_0$.

7. – We should here like to make some observations of a qualitative nature on the elementary processes which take place during intermittent discharges, limiting ourselves to the conditions already mentioned of the discharges at the end of the first kind and beginning of the second kind.

Observing the dynamic characteristics I and II of Fig. 3, it can be seen that only at the points T, G and N there is a correspondence between the values of the current i and those of the potential V applied to the tube. Such points however do not correspond to conditions of equilibrium of the discharge, since the line of resistance does not pass either of them. Nevertheless at the points T and G above-mentioned the relations

$$(13) \qquad \mu = \gamma\left(\exp\left[\int_0^l \alpha \mathrm{d}x\right] - 1\right) = 1\,, \qquad \mu = \gamma\left(\exp\left[\int_0^d \alpha \mathrm{d}x\right] - 1\right) = 1\,,$$

must exist, where l represents the length of the discharge tube, which in Townsend's phase is entirely interested in the elementary processes, while d is the cathode space in which such processes are essentially developed in the glow phase. Evidently at the points N two relations will be valid analogous to the second of (13), where in this case for d the values corresponding to the two conditions N will be taken. The intervals TN and GN of the characteristics I and II correspond to the condition $\mu > 1$. Moreover, during the time in which the interval TN is covered, the formation of the space charge before the cathode on the characteristic I and the rapid deformation of the field in the interior of the tube take place. In the intervals NM of the characteristics, these must be $\mu < 1$, which decreases in such a way as to reduce the space charge which was formed in N. In fact, in this interval of the dynamic characteristic, it can be admitted that all the elementary processes take place and are developed in the cathode space. Point N having been passed, the discharge develops in such a way that, for every avalanche of positive n ions which reach the cathode, a number of γn electrons are freed, which will give rise to multiplication processes in the cathode space. The reduction, however, of the space charge provokes a diminution of the cathode field, in consequence of which the coefficient α decreases. Let us assume for α the known expression

$$\alpha = \frac{1}{\lambda} \exp\left[-\frac{V_i}{E\lambda}\right],$$

where λ is the mean free path of the electrons, V_i the ionization potential of the gas and E the field within which the electrons move. According to von

ENGEL and STEENBECK (5) it is

$$4\pi\varrho d = E\,,$$

from which it is immediately apparent that a reduction of ϱ also reduces α. The equivalent resistance of the tube reaches its minimum value in N and then increases, albeit slowly, along the interval NM.

In the caracteristic intervals MT and MG, we have a weakening of the luminosity of the discharge, and the front of the glow moves towards the interior (6). In these intervals μ begin to grow again in order to reach the value l in T and G. In fact with the reduction of the space charge the cathode field diminishes, but, contemporaneously with the diminution of ionization in the cathode space, there is an increase in ionization in the rest of the tube with a prevalence of the increase over the diminution.

In the conditions at the beginning of the second kind, the potential reaches the value G before the space charge has completely disappeared, and when its value corresponds to the beginning value of the glow phase. In the case, however, of the discharges at the end of the first kind, we have the total disappearance of the space charges, the potential reaching the value T when the current in the tube assumes the value of that at the end of Townsend's phase.

Our results, of course, are related to commercial tubes in which the geometrical arrangement of the electrodes is very irregular. Tubes with a rigorous geometry could permit a better verification of our conclusions.

Our thanks are due to Mr. L. PARISINI and Dr. T. LANZARINI for help given in the measurements.

(5) v. ENGEL and STEENBECK: *Elektrische Gasentladungen* (Berlin, 1934), p. 71.
(6) M. J. DRUYSTEYN: *Zeits. f. Phys.*, **57**, 292 (1929).

RIASSUNTO (*)

Si riportano i risultati di alcune misure dei tempi di decadimento delle cariche spaziali e della loro dipendenza dalla caratteristica statica del tubo e dal circuito esterno. I risultati mostrano la dipendenza di tali tempi dal circuito esterno, ma fanno risaltare l'esistenza di un vero tempo di decadimento delle cariche spaziali che non è influenzato dal circuito esterno e dipende solo dalla caratteristica statica del tubo. Si dà inoltre un metodo empirico per il calcolo dei tempi di decadimento delle cariche spaziali.

(*) *Traduzione a cura della Redazione.*

IL NUOVO CIMENTO Vol. XII, N. 3 1° Settembre 1954

Nucleon Polarization Resulting from π-Meson Production.

B. T. Feld

Istituto di Fisica dell'Università - Padova (*)
Istituto Nazionale di Fisica Nucleare - Sezione di Padova

(ricevuto il 12 Luglio 1954)

Summary. — In this paper we derive the polarization of the nucleons resulting from the three «fundamental,» meson-nucleon reactions $\pi + \mathcal{N} \to \mathcal{N}' + \pi'$, $\gamma + \mathcal{N} \to \mathcal{N}' + \pi'$, $\pi + \mathrm{D} \to \mathcal{N} + \mathcal{N}'$. It is shown that the observed angular distributions of these reactions permit of two types of solutions — a «Fermi» solution, in which the important interaction is in the meson-nucleon intermediate state of $J = \frac{3}{2}+$, $T = \frac{3}{2}$; and a «Yang» solution, which requires a strong interaction in the state $J = \frac{1}{2}+$, $T = \frac{3}{2}$. These solutions can be distinguished on the basis of the polarization of the recoil nucleons. Tables are given for the predicted polarizations in the second and third of the above reactions (the first has previously been discussed by Fermi). The greatest difference between the two solutions is predicted in the photoproduction of neutral mesons. However, the kinematics of the reactions are such that the most likely case for detection of the polarized nucleons is the third of the above reactions; in this case, however, the difference between the predicted polarizations for the two solutions is only in the sign.

1. – Introduction.

Recent experiments have demonstrated the practicability of the production and detection of polarized fast neutrons (1) and protons (2). In view of these developments, a new tool is now becoming available for the study of reactions

(*) On leave from the Physics Department, M.I.T., Cambridge, Mass., U.S.A.. This work was started while the author was a guest of the Istituto di Fisica, Università di Roma.

(1) L. F. Wouters: *Phys. Rev.*, **84**, 1069 (1951).

(2) C. L. Oxley, W. F. Cartwright, J. Rouvina, E. Baskir, D. Klein, J. Ring and W. Skillman: *Phys. Rev.*, **91**, 419 (1953); O. Chamberlain, E. Segrè, R. Tripp, C. Wiegand and T. Ypsilantis: *Phys. Rev.*, **93**, 1430 (1954); J. Marshall, L. Marshall and H. G. de Carvalho: *Phys. Rev.*, **93**, 1431 (1954).

involving π-mesons and nucleons through the investigation of the polarization of the nucleons involved in the various reactions. This possibility was first pointed out by FERMI [3], who showed that the recoil nucleons, resulting from the meson-scattering reaction

$$\pi + \mathcal{N} \to \mathcal{N}' + \pi' , \tag{1}$$

are expected to be strongly polarized. In particular, as demonstrated by FERMI, a study of the polarization of the recoil nucleons in reaction (1) could provide a means for distinguishing between the « Fermi » and « Yang » solutions for the phase shifts involved in meson-nucleon scattering.

Another application of the use of polarized nucleons has been discussed by MARSHAK and MESSIAH [4]. They considered the reaction

$$\mathrm{P} + \mathrm{P} \to \mathrm{D} + \pi^+ \tag{2}$$

and showed that a « right-left asymmetry » would be expected if the above reaction were induced by polarized protons, provided that an appreciable part of the reaction cross-section results from an interaction of the two protons in the ${}^3P_1$-state, leading to the emission of mesons with $l = 0$. (The angular distribution of reaction (2), $\sim 0.2 + \cos^2\theta$, indicates that the major fraction of the mesons are emitted in the p-state).

In this paper, we consider the polarization of the nucleons resulting from the inverse of reaction (2)

$$\pi^+ + \mathrm{D} \to \mathrm{P} + \mathrm{P}' \tag{2'}$$

as well as from the photoproduction of π-mesons

$$\gamma + \mathcal{N} \to \mathcal{N}' + \pi . \tag{3}$$

In particular, we are concerned with the possible use of the study of nucleon polarization to distinguish between the « Fermi »- and the « Yang »-types of interpretations of these reactions, since it is not possible to distinguish between these possibilities on the basis of the available observations on the angular distributions alone.

2. – Outline of the Theory.

The computation of the polarization of the nucleons in the reactions of interest follows, essentially, along the same lines as outlined by FERMI [3] for reaction (1). We consider the bombarding particle, incident along the posi-

---

[3] E. FERMI: *Phys. Rev.*, **91**, 947 (1953).

[4] R. E. MARSHAK and A. M. L. MESSIAH: *Nuovo Cimento*, **11**, 337 (1954).

tive z-direction, as reacting with a target nucleon at the origin. Characterizing the possible states of polarization of the initial (bombarding plus target) particles by the indices a_i, and those of the reaction products by b_j, the reaction amplitudes $q(a_i, b_j)$ are obtained, following conventional reaction theory [5], as a summation

$$q(a_i, b_j) = \sum_k q_k(a_i, b_j) \tag{4}$$

over the amplitudes for the various possible intermediate states, k, allowed by the requirements of conservation of angular momentum and parity. The partial amplitudes may be written

$$q_k(a_i, b_j) = C(a_i; l, m_l|k)C(k|b_j; l', m_{l'})a_k Y^{m_{l'}}(\theta, \varphi)\,, \tag{5}$$

where l, m_l; l', $m_{l'}$ are, respectively, the incident and product orbital angular momentum quantum numbers, the C's are the appropriate Clebsch-Gordon coefficients, $Y^{m_{l'}}$ is a spherical harmonic, and a_k is proportional to the matrix element connecting the initial and final states through the intermediate state k. In writing equation (5) we have included various phase and proportionality factors, which depend on l and l', in the a_k's. The basic simplification achieved by choosing the direction of the incident particle or quantum for the z-axis is that $m_l = 0$ for incident particles while, for quanta, $m_l = \pm 1$.

To obtain the cross-section for the production of the products in the state of polarization b_j, in the case that the initial system is unpolarized, we must average the reaction intensities, $I(a_i, b_j) = |q(a_i, b_j)|^2$ over the initial states

$$I(b_j) = \frac{1}{N} \sum_{i=1}^{N} I(a_i, b_j)\,. \tag{6}$$

For the case of initial polarization, equation (6) is replaced by the appropriate weighted average. (The total cross-section is obtained by a further summation over the final polarizations b_j.)

Since there are, in general, two reaction products, the intensities $I(b_j)$ correspond to states in which both reaction products are polarized. If we are only interested in the polarization of one of the products, the appropriate cross-section is obtained by an additional sum

$$I'(b_j) = \sum_{j'} I(b_{j'}) \tag{7}$$

over those final states j' in which the product of interest has the required polarization. This problem does not arise in the case of reactions (1), (2)

---

[5] J. M. Blatt and V. F. Weisskopf: *Theoretical Nuclear Physics* (New York 1952).

and (3) since the π-meson, having zero spin, can be emitted in only one state of polarization. It does, however, arise for reaction (2′) if we are interested in experiments in which the polarization of only one of the product nucleons is observed.

The computation outlined above will, however, when carried out along the lines of conventional reaction theory, lead to the result that the product nucleons are unpolarized i.e., $I'(b_1) = I'(b_2)$, where b_1 and b_2 correspond to nucleons polarized parallel and antiparallel to the z-direction, respectively. The reason for this is that there can be no polarization in the plane containing the directions of the incident and product particles (the z-axis, being taken as the direction of the incident particle, always lies in this plane) since there can be no change of the angular momentum in this plane; polarization implies a preference for imparting angular momentum in one direction. Polarization, then, if it is to be found, must be sought in a direction perpendicular to the plane of scattering.

It is convenient to consider the polarization along the x-axis ($\varphi = 0$). To do this, we note that for a nucleon (spin $\frac{1}{2}$) the amplitudes for polarization in the $\pm x$-direction may be written in terms of the amplitudes for polarization in the $\pm z$-direction, as follows

$$q(a_i, c_\pm) = \sqrt{\tfrac{1}{2}}\,[q(a_i, b_1) \pm q(a_i\, b_2)]\,. \tag{8}$$

(In equation (8), the angular momenta of the incident and of the undetected product particles are still characterized by their components along the z-axis.) The evaluation of the cross-section for the production of polarized nucleons then follows according to the method outlined above, by use of equations (4)-(7). The results may be written

$$\frac{\mathrm{d}\sigma}{\mathrm{d}\Omega}(c_\pm) = \frac{1}{2}\,\overline{\frac{\mathrm{d}\sigma}{\mathrm{d}\Omega}} \pm A \sin\varphi\,, \tag{9}$$

in which $\overline{\mathrm{d}\sigma/\mathrm{d}\Omega} \equiv \mathrm{d}\sigma/\mathrm{d}\Omega(c_+) + \mathrm{d}\sigma/\mathrm{d}\Omega(c_-)$ is the differential cross-section for the reaction. It is convenient to define the polarization, corresponding to scattering in the y-z plane ($\varphi = 90°$), as

$$P(\theta) \equiv 2A \Big/ \overline{\frac{\mathrm{d}\sigma}{\mathrm{d}\Omega}}\,. \tag{10}$$

The existence of a polarization term in equation (9) depends on an interference between the amplitude θ corresponding to different intermediate states. Thus, if only one state is involved in the reaction in question, the resulting nucleons will be unpolarized.

In the following, the results of the calculations will be stated without further detailed derivation. The details of the calculations will be given in an article to be presented for future publication in this journal.

3. – Discussion of the Reactions:

3·1. *Meson-Nucleon Scattering.* – For incident meson energies up to ~ 200 MeV, it has been found possible to express the observed angular distributions for reactions (1) as

$$\overline{\mathrm{d}\sigma/\mathrm{d}\Omega} = A_0 + A_1 \cos\theta + A_2 \cos^2\theta \,. \tag{11}$$

This implies that meson angular momenta $l = 0$ and 1 only are involved in the scattering, at least to the accuracy of the present experiments (6). Thus, it is necessary to consider only three intermediate states of angular momentum, $J = \frac{1}{2}$, negative parity (s-wave mesons) (*)(7) $J = \frac{1}{2}$ and $\frac{3}{2}$ positive parity (p-wave mesons). Writing for the matrix elements in these states, respectively, a_0, a_1, a_2, we obtain

$$\frac{4}{\lambda_\pi^2}\overline{\frac{\mathrm{d}\sigma}{\mathrm{d}\Omega}} = \left[|a_0|^2 + |a_2 - a_1|^2\right] + 2\,\mathrm{Re}\left\{a_0^*(2a_2 + a_1)\right\}\cos\theta + \left[|2a_2 + a_1|^2 - |a_2 - a_1|^2\right]\cos^2\theta \,, \tag{12}$$

$$\frac{4}{\lambda_\pi^2} A = 2Im\left\{a_0^*(a_2 - a_1)\sin\theta + (2a_2 + a_1)^*(a_2 - a_1)\sin\theta\cos\theta\right\}. \tag{13}$$

As is well known, the hypothesis of « charge-independence » implies the existence of another good quantum number, the isotopic spin which for the meson-nucleon system can have two values $T = \frac{3}{2}$ and $\frac{1}{2}$. Thus, each of the matrix elements becomes two, and the various scattering and charge-exchange reactions can all be described in terms of six independent parameters, by methods already extensively described in the literature (8).

Since FERMI (3) has already discussed the predicted nucleon polarization in detail, including numerical examples, we shall confine ourselves here to a few qualitative observations. For the purposes of our present review, the important aspect of the existing measurements is that they allow of two possible interpretations. In one, the « Fermi » solution, the predominant scattering arises from an intermediate state of $J = T = \frac{3}{2}$. In the second, the « Yang » solution, the most important scattering is in the state $J = \frac{1}{2}$, $T = \frac{3}{2}$.

---

(6) H. L. ANDERSON, E. FERMI, R. MARTIN and D. E. NAGLE: *Phys. Rev.*, **91**, 155 (1953); E. FERMI, M. GLICKSMAN, R. MARTIN and D. NAGLE: *Phys. Rev.*, **92**, 161 (1953).

(*) The π-meson, being pseudoscalar, has negative intrinsic parity.

(7) W. K. H. PANOFSKY, R. L. AAMODT and J. HADLEY: *Phys. Rev.*, **81**, 565 (1951).

(8) E. M. HENLEY, M. A. RUDERMAN and J. STEINBERGER: *Annual Review of Nuclear Science*, Vol. **3** (Stanford, Calif., 1953).

In both solutions, p-wave scattering predominates. There is, however, an important qualitative difference between these solutions: a « Fermi » solution is possible in which there is relatively little contribution from the $J=\frac{1}{2}^+$ term, while the « Yang » solution always requires an appreciable $J=\frac{3}{2}^+$ contribution. This difference gives rise to a major difference in the predicted polarizations. Thus, for an extreme « Fermi » solution, $a_1 \approx 0$, and the entire polarization comes from the first term in equation (13), $2I_m\{a_0^* a_2 \sin\theta\}$. On the other hand. for the « Yang » solution, the second term, which can be written as $6I_m\{a_2 a_1^* \sin\theta\cos\theta\}$, is significant, while the first term decreases in importance, as well as reversing its sign. It should be possible to observe the dependence of P on the angle of meson emission, θ, even if its absolute sign cannot be determined.

3·2. *Photomeson Production.* – If we confine ourselves to those intermediate states which lead to the emission of mesons with $l=0$ or 1, reaction (3) involves four possibilities: electric dipole absorption to $J=\frac{1}{2}$, negative parity, followed by the emission of s-mesons; magnetic dipole absorption to $J=\frac{1}{2}$ or $J=\frac{3}{2}$, or electric quadrupole absorption to $J=\frac{3}{2}$, all positive parity and all followed by emission of p-mesons. Application of the theory outlined above (*), yields

$$(14)\qquad \frac{8}{\lambda_\gamma^2}\frac{\overline{\mathrm{d}\sigma}}{\mathrm{d}\Omega} = \Big[|a_{\frac{1}{2}}^{ED}|^2 + |a_{\frac{1}{2}}^{MD}|^2 + \frac{5}{2}|a_{\frac{3}{2}}^{MD}|^2 + \frac{3}{2}|a_{\frac{3}{2}}^{EQ}|^2 + \\ + \mathrm{Re}\{a_{\frac{1}{2}}^{MD*}(a_{\frac{3}{2}}^{MD} + \sqrt{3}\,a_{\frac{3}{2}}^{EQ}) - \sqrt{3}\,a_{\frac{3}{2}}^{MD*}a_{\frac{3}{2}}^{EQ}\}\Big] + \\ + 2\,\mathrm{Re}\{a_{\frac{1}{2}}^{ED*}(-a_{\frac{1}{2}}^{MD} + a_{\frac{3}{2}}^{MD} + \sqrt{3}\,a_{\frac{3}{2}}^{EQ})\}\cos\theta + \\ + \Big[-\frac{3}{2}|a_{\frac{3}{2}}^{MD}|^2 + \frac{3}{2}|a_{\frac{3}{2}}^{EQ}|^2 - 3\mathrm{Re}\{a_{\frac{1}{2}}^{MD*}(a_{\frac{3}{2}}^{MD} + \sqrt{3}\,a_{\frac{3}{2}}^{EQ}) - \sqrt{3}\,a_{\frac{3}{2}}^{MD*}a_{\frac{3}{2}}^{EQ}\}\Big]\cos^2\theta.$$

$$(15)\qquad \frac{8}{\lambda_\gamma^2}A = \frac{1}{2}I_m\{a_{\frac{1}{2}}^{ED*}(2a_{\frac{1}{2}}^{MD} + a_{\frac{3}{2}}^{MD} + \sqrt{3}\,a_{\frac{3}{2}}^{EQ})\sin\theta + \\ + 3a_{\frac{3}{2}}^{MD}(a_{\frac{3}{2}}^{MD} + \sqrt{3}\,a_{\frac{3}{2}}^{EQ})^*\sin\theta\cos\theta\}.$$

Since most of the available experimental material concerns the reaction

$$(3a)\qquad \gamma + \mathrm{P} \to \mathrm{N} + \pi^+,$$

(*) The phase and proportionality factors required in equation (5) are somewhat different for photon absorption than for particles. These have been applied so that the matrix elements can be written $a_k = A_k e^{i\alpha_k}$, with all A_k and a_k real.

we consider this reaction first. Owing to the overabundance of parameters (each of the matrix elements, being complex, provides two), a unique fit is not possible. However, these parameters are not entirely arbitrary in their energy dependence (9) and, as is the case with the scattering reaction (1), two types of « fits » are suggested by the data (*). One, a « Fermi-type » solution, assumes $a_{\frac{1}{2}}^{MD} \approx 0$. The second, of the « Yang »-type, requires $|a_{\frac{1}{2}}^{MD}| > |a_{\frac{3}{2}}^{MD}|$. In both solutions, the most important contribution below $E_\gamma \approx 250$ MeV comes from the electric dipole term and both require an appreciable electric quadrupole contribution above $E_\gamma \approx 300$ MeV. The results of these fittings are summarized in Table I where the various columns abbreviate equations (14) and (15) as follows,

$$\overline{\mathrm{d}\sigma/\mathrm{d}\Omega} = A_0 + A_1 \cos\theta + A_2 \cos^2\theta \,, \tag{14'}$$

$$2A = B_1 \sin\theta + B_2 \sin\theta \cos\theta \,. \tag{15'}$$

As may be seen from the table, the polarizations, as defined by equation (10), are quite appreciable for both the « Fermi » and « Yang » types of solutions. Actually, our method of arriving at the « Yang » solution overestimates the polarization effects, since we have neglected, in equation (14), the terms proportional to $|a_{\frac{3}{2}}^{MD}|^2$ and $|a_{\frac{3}{2}}^{EQ}|^2$. However, the effect of these terms can be shown to be comparatively small, $< 30\%$ on A_0 and A_2, so that the polarizations are not grossly overestimated, and the trends are certainly those shown in Table I.

TABLE I. – *Angular Distributions and Polarizations in* $\gamma + \mathrm{P} \to \mathrm{N} + \pi^+$.

E_γ (MeV)	$\frac{A_1}{A_0}$	$-\frac{A_2}{A_0}$	« Fermi » Solution (*)			« Yang » Solution			
			$-B_1/A_0 = -P(90°)$	$-P$ (45°)	$-P$ (135°)	$B_1/A_0 = P(90°)$	B_2/A_0	P (45°)	P (135°)
200	0.24	0.14	0.24	0.22	0.15	0.80	0.02	0.75	0.50
240	0.24	0.32	0.30	0.31	0.21	0.95	0.08	1.05	0.63
280	0.25	0.40	0.27	0.31	0.20	0.80	0.22	1.08	0.47
320	0.06	0.36	0.30	0.28	0.25	0.82	0.37	0.98	0.45
360	−0.20	0.23	0.34	0.24	0.33	0.86	0.63	0.89	0.40
400	−0.46	0.08	0.34	0.19	0.38	0.85	1.05	0.88	0.12
450	−0.89	−0.13	0.27	0.11	0.45	0.60	0.87	0.51	−0.03

(*) $B_2 \approx 0$. The angle shown is that of emission of the meson in the c.m. system.

(9) K. A. BRUECKNER and K. M. WATSON: *Phys. Rev.*, **86**, 923 (1952); B. T. FELD: *Phys. Rev.*, **89**, 330 (1953).

(*) The fitting of the data on the photoproduction of mesons is discussed by the author in a Letter to the Editor submitted to the *Physical Review* and, in greater detail, in an article in preparation for this Journal.

In addition to a difference in the signs of the polarizations predicted for the two solutions, there are appreacible differences in the energy and angular dependences which might make it possible to distinguish between them. However, in view of the present rather primative state of the art of polarization measurements, especially as applied to fast neutrons, it may prove to be rather difficult in practice to perform experiments of the requisite accuracy.

The situation is quite different for the second reaction

(3*b*) $$\gamma + \mathrm{P} \rightarrow \mathrm{P} + \pi^0 .$$

Here the experimental evidence is relatively scanty, but sufficient to permit the following general observations:

a) At least up to $E_\gamma \approx 300$ MeV, the electric dipole absorption appears to be negligible. Even at higher energies, the asymmetry in the angular distributions is not very great.

b) The assumption of « charge independence » and of the importance of the $T = \frac{3}{2}$ intermediate state predicts that the remaining three matrix elements are proportional to the corresponding matrix elements for reaction (3*a*) the constant of proportionality being $\sqrt{2}$. On this assumption, coupled with the assumption $a_{\frac{1}{2}}^{ED} \approx 0$, the parameters used to fit reaction (3*a*) yield a qualitative fit to the data on reaction (3*b*), although they predict a cross-section which, at 90°, is somewhat too large, possibly by as much as a factor of 2 at some energies. The origins of this discrepancy are, at present, obscure, and it is not out of the question that they may be experimental.

TABLE II. – *Angular Distributions and Polarizations in* $\gamma + \mathrm{P} \rightarrow \mathrm{P} + \pi_0$:

E_γ (MeV)	$-A_2/A_0$	« Yang » Solution (*)	
		B_2/A_0	$P(45°) = -P(135°)$
200	0.67	0.09	0.07
240	0.59	0.14	0.10
280	0.62	0.29	0.21
320	0.45	0.48	0.31
360	0.31	0.83	0.49
400	0.10	1.4	0.73
450	−0.17	1.3	0.61

(*) For the « Fermi » solution, $P(\theta) \approx 0$.

Nevertheless, assuming a solution as outlined above, the predicted polarizations are as shown in Table II. The important qualitative feature is that

there is no polarization for the « Fermi » solution, since $a_{\frac{1}{2}}^{ED} \approx a_{\frac{1}{2}}^{MD} \approx 0$ in equation (15). The « Yang » solution, on the other hand, predicts appreciable polarization effect for the recoil protons.

It is rather difficult, in view of the uncertainties in the existing angular distribution data for reaction (3*b*), to estimate an upper limit to the possible proton polarizations predicted for the « Fermi » solution. At energies $E_\gamma <$ 300 MeV, the data indicate that possible asymmetries could hardly lead to values of $P(\theta)$ greater than a few percent. At $E_\gamma \approx 400$ MeV, the experiments indicate an angular asymmetry which, at most, would lead to $P\ (90°) < 0.10$.

TABLE III. – *Kinematics* (*) *of* $\gamma + \mathcal{N} \to \mathcal{N}' + \pi$.

E_γ (MeV)	$\theta_{cm} = 45°$		$\theta_{cm} = 90°$		$\theta_{cm} = 135°$	
	$E_{\mathcal{N}'}$ (MeV)	θ (deg)	$E_{\mathcal{N}'}$ (MeV)	θ (deg)	$E_{\mathcal{N}'}$ (MeV)	θ (deg)
200	7.5	41.6	21.5	33.4	35.6	17.6
240	10.2	50.3	32.4	37.4	54.6	19.2
280	13.5	55.0	44.3	39.3	75.2	19.9
320	17.1	57.7	57.0	40.3	97.0	20.2
360	21.1	58.4	70.3	40.5	119.3	20.3
400	25.6	59.1	84.1	40.7	142.0	20.4
450	31.6	59.9	102.3	40.8	173.1	20.4

(*) The mass difference between π^+ and π^0 is neglected in this table, which has been calculated for reaction (3 *b*).

Table III gives the laboratory energies and angles of the protons or neutrons for which the polarizations are indicated in Tables I and II.

Table III indicates that the observation of polarization of the recoil nucleon from reactions (3*a*) and (3*b*) will not be easy, from the experimental point of view, since the nucleon energies are rather small and the angles of emission of the nucleons, in the laboratory system, are relatively weakly dependent on the photon energy. The major difficulty arises from the fact that the available photon sources all yield « Bremsstrahlung » energy distributions, so that all photon energies are simultaneously present in the photon beams. Thus, the degree of specification of the energy of the photons responsible for the nucleons detected depends on the available resolution in both the angle and energy of the emitted nucleons.

3·3. *Meson Absorption by Deuterium.* – The third of the « fundamental » meson-nucleon reactions, reaction (2), involves two nucleons and is, corres-

pondingly, somewhat more complicated (*). The polarization of the product deuterons has been discussed by WATSON and RICHMAN [10], while the effects of the use of polarized protons in reaction (2) have been discussed by MARSHAK and MESSIAH [4].

We consider the inverse, reaction (2′), for which the theory is essentially the same as for reaction (2), the differences being dictated by the principle of detailed balancing [11]. Thus, the polarization of the recoil protons is given by essentially the same expression as was derived by MARSHAK and MESSIAH [4] for the asymmetry in reaction (2) resulting from polarized protons (+). In deriving these results, we confine ourselves to mesons with $l \leqslant 1$, in which case there are three intermediate states involved: $J = 1^-$, induced by s-wave mesons and resulting in nucleons in the ${}^3P_1$ state; $J = 0^+$, due to p-wave mesons and yielding nucleons in the state ${}^1S_0$; and $J = 2^+$, due to p-wave mesons and yielding nucleons in the ${}^1D_2$ state. Calling the amplitudes for these processes $a_1 = \sqrt{\frac{2}{3}}\, Be^{i\delta_1}$, $a_0 = Ae^{i\delta_0}$, and $a_2 = \sqrt{\frac{2}{5}}\, Ce^{i\delta_2}$, respectively,

$$\frac{12}{\lambda\!\!\!^{-2}_\pi}\frac{\mathrm{d}\sigma}{\mathrm{d}\Omega} = (2B^2 + D^2) + 3(E^2 - A^2)\cos^2\theta\,, \tag{16}$$

$$\frac{12}{\lambda\!\!\!^{-2}_\pi}\Delta = BD\sin(\delta_1 - \delta)\sin\theta\,, \tag{17}$$

where

$$De^{i\delta} \equiv a_0 - \sqrt{\tfrac{5}{2}}\, a_2\,, \tag{18a}$$

$$E^2 \equiv |a_0 + \sqrt{\tfrac{5}{2}}\, a_1|^2\,. \tag{18b}$$

Thus,

$$P(\theta) = \frac{2BD\sin(\delta_1 - \delta)\sin\theta}{2B^2 + D^2 + 3(E^2 - A^2)\cos^2\theta}\,. \tag{19}$$

It is clear that $P_{\max}$ occurs for $\theta = 90^\circ$

$$P(90^\circ) = \frac{2BD\sin(\delta_1 - \delta)}{2B^2 + D^2} \equiv Q\sin(\delta_1 - \delta) \tag{19a}$$

and that the maximum polarization at 90° occurs for $2B^2 = D^2$, with $Q = \pm 0.707$. Now, as has been pointed out by MARSHAK and MESSIAH [4], the existence of

(*) In order to keep the theory relatively simple, we confine ourselves to the « two-body » reactions involving the deuteron.

[10] K. M. WATSON and C. RICHMAN: *Phys. Rev.*, **83**, 1256 (1951).

[11] R. E. MARSHAK: *Meson Physics* (New York, 1952).

(+) Indeed, these authors performed their calculations for the inverse of reaction (2) i.e., reaction (2′).

an appreciable polarization depends on the existence of an appreciable s-wave meson absorption.

In principal, the cross-section for s-wave meson absorption can be obtained from a simple extension of the experiments of PANOFSKY and co-workers [7] on the capture of π^--mesons in deuterium and hydrogen. Actually, the only datum still lacking is a measurement of the relative rates of capture of π^--mesons by the two nuclei [12]. Assuming that these rates are equal, and using the available low-energy data on reaction (2′) [8] as a measure of the strength of the p-wave meson absorption, application of the principal of detailed balancing to the capture data [13] yields the values of B^2/D^2, inversely proportional to the square of the meson c.m. momentum, as shown in column 2 of Table IV. Also shown, in Table IV column 3, are the corresponding values of Q, defined by equation (19a), as well as the appropriate parameters corresponding to the « Fermi »- and « Yang »-type solutions for this reaction (column 4 and 5) (see below).

TABLE IV. – *Nucleon Polarization in* $\pi + D \to \mathcal{N} + \mathcal{N}'$.

E_π (MeV)	B^2/D^2	$\lvert Q\rvert$	R (Fermi)	R (Yang)
20	0.50	0.71	0.17	0.33
50	0.11	0.55	0.05	0.28
100	0.055	0.42	0.026	0.25

The fact that there are two solutions results, again, from the quadratic nature of the dependence of the angular distribution, equation (16), on the parameters. In calculating the factors of columns 4 and 5, Table IV, we have taken for the experimentally observed angular distribution

$$W(\theta) \approx 1 + 3\cos^2\theta\,. \tag{20}$$

From equation (16), this gives, according to our notation for the amplitudes,

$$[C^2 + A^2 - 2AC\cos(\delta_2 - \delta_0)](1 + 2B^2/D^2) = C^2 + 2AC\cos(\delta_2 - \delta_0)\,. \tag{21}$$

The « Fermi » solution assumes $C^2 \gg A^2 \approx 0$, giving

$$R\,(\text{Fermi}) \equiv (A/C)\cos(\delta_2 - \delta_0) \approx \frac{B^2/D^2}{2(1 + B^2/D^2)}\,. \tag{22}$$

This type of solution would result if the reaction proceeded through an intermediate state in which one of the nucleons is excited in a state of $J = T = \frac{3}{2}$,

(12) For an estimate, see K. BRUECKNER, R. SERBER and K. WATSON, *Phys. Rev.* **81**, 575 (1951).

(13) H. L. ANDERSON and E. FERMI, *Phys. Rev.*, **86**, 794 (1952).

positive parity, assuming that the two nucleons remain, in the intermediate state, in a state of relative orbital angular momentum 0.

The « Yang » solution, on the other hand, assumes $A^2 \gg C^2 \approx 0$. It would result from the excitation of one of the nucleons into a state of $J = \frac{1}{2}^+$, $T = \frac{3}{2}$, with

$$R\,(\text{Yang}) \equiv (C/A)\cos(\delta_0 - \delta_2) \approx \frac{(1 + 2B^2/D^2)}{4(1 + B^2/D^2)}\,. \tag{23}$$

As can be seen from equations (16)–(19), the magnitudes of the predicted nucleon polarization parameter are the same for both solutions. The difference, as may be seen from equation (18*a*), lies in the sign of Q, which is negative for the « Fermi » solution and positive for the « Yang » solution (*).

TABLE V. – *Kinematics of* $\pi + \mathrm{D} \to \mathcal{N} + \mathcal{N}'$.

θ_{mc} (deg)	$P/P(90°)$	$E_\pi = 25$ MeV		$E_\pi = 50$ MeV		$E_\pi = 100$ MeV	
		$E_{\mathcal{N}}$(MeV)	$\theta_{\mathcal{N}}$(deg)	$E_{\mathcal{N}}$(MeV)	$\theta_{\mathcal{N}}$(deg)	$E_{\mathcal{N}}$(MeV)	$\theta_{\mathcal{N}}$(deg)
30	0.154	97	27.1	117	26.2	157	25.0
45	0.283	94	40.9	113	39.5	150	37.8
60	0.495	91	54.8	107	53.1	141	50.9
90	1.000	82	83.8	94	81.5	119	78.5

The kinematical situation, with regard to the detection of the polarization, is somewhat more favourable for reaction (2′) than for the other reactions. It is summarized in Table V, for which we have assumed the angular distribution of equation (20).

4. – Conclusions.

In the preceding discussion, we have summarized the nucleon polarizations expected in the fundamental meson-nucleon interactions. In all three of the reactions considered — scattering by nucleons, photoproduction by nucleons, and absorption by deuterons we have seen that the polarizations are quite appreciable.

The experimental information available for all three reactions permits of two types of solutions. One, the « Fermi »-type, assumes that the most im-

(*) If, as is anticipated, $\delta > \delta_1$ for both solutions, the sign of the polarization will be opposite to that of Q, according to equation (19*a*).

portant intermediate state of the meson-nucleon system is that of angular momentum $J = \frac{3}{2}^+$ and isotopic spin $T = \frac{3}{2}$, involving mesons in the p state. The second, the « Yang »-type solution, differs from the first in that the important meson-nucleon reaction is in a state of angular momentum $J = \frac{1}{2}^+$. These two solutions predict different nucleon polarizations.

In the cases of meson scattering and of the photoproduction of positive mesons from hydrogen the differences are both in the sign of the polarizations and in their angular dependences. The photoproduction of neutral mesons on hydrogen seems to present the most favorable case for a decision between the two possible solutions allowed by the angular distributions, since only the « Yang » solution predicts appreciable nucleon polarization. However, for both the scattering and photoproduction reactions, the kinematics are such as to render the detection of the polarization difficult; this is especially true of the photoproduction.

For the deuteron-absorption reactions, on the other hand, the kinematics are much more favorable for the detection of the polarization. Here, however, the differentiation between the « Fermi » and « Yang » solutions depends on the possibility of detecting the sign of the nucleon polarization.

The author is pleased to acknowledge his profound indebtedness to the John Simon Guggenheim Memorial Foundation for financial support, to the Massachusetts Institute of Technology for the grant of an Educational Leave of Absence, and to the Universities of Rome and Padua for their generous hospitality.

RIASSUNTO (*)

Nel presente lavoro deriviamo la polarizzazione dei nucleoni risultanti da tre « fondamentali » reazioni mesone-nucleone: $\pi + N \to N' + \pi'$, $\gamma + N \to N' + \pi'$, $\pi + D \to N + N'$. Si dimostra che le distribuzioni angolari di queste reazioni osservate consentono due tipi di soluzioni — una soluzione di « Fermi » in cui l'interazione importante avviene nello stato mesone-nucleone intermedio con $J = \frac{3}{2}^+$, $T = \frac{3}{2}$; e una soluzione di « Yang » che richiede una forte interazione nello stato $J = \frac{1}{2}^+$, $T = \frac{3}{2}$. Queste soluzioni possono distinguersi in base alla polarizzazione dei nucleoni di rinculo. Si danno tabelle delle polarizzazioni previste nella seconda e la terza delle reazioni sopra indicate (la prima è stata già precedentemente discussa da Fermi). La massima differenza fra le due soluzioni si prevede per la fotoproduzione di mesoni neutri. Le cinematiche delle reazioni sono, tuttavia, tali che la maggior facilità di rivelare i nucleoni polarizzati è offerta dalla terza delle reazioni di cui sopra: in questo caso, però, la differenza tra le polarizzazioni previste è solo nel segno.

(*) *Traduzione a cura della Redazione.*

High-Energy Expansions of Phase Shifts.

E. Corinaldesi
Dublin Institute for Advanced Studies

(ricevuto il 17 Luglio 1954)

Summary. — The phase shifts of the Klein-Gordon and of the Dirac equation are developed in powers of the inverse of the momentum, following a method based on the iteration of an integral equation. The expansion is found to be possible only under somewhat restrictive conditions for the potential. A procedure is suggested by which, if the phase shifts for a certain potential are given, those for a large family of other potentials can be calculated by series expansions in powers of the inverse of the momentum. This method is seen to be rapidly convergent for small values of the angular momentum, and is relevant to recent calculations on the scattering of high-energy electrons by nuclei.

1. – Introductions.

Experiments on scattering of high energy electrons, recently performed by Hofstadter, Fechter and McIntyre [1] have aroused considerable interest in view of the possibility of deriving information on the charge distribution in an atomic nucleus. To this purpose, a theoretical investigation was first carried out by the use of the Born approximation [2], and the impression gained was that the experimental data could best be fitted when the nuclear model adopted was one with a concentration of charge in the centre. Subsequently, exact numerical calculations of the angular distribution were performed [3,4] which proved, not only that, at energies of about 150 MeV, the Born approx-

[1] R. Hofstadter, H. R. Fechter and J. A. McIntyre: *Phys. Rev.*, **92**, 978 (1953).

[2] L. I. Schiff: *Phys. Rev.*, **92**, 988 (1953).

[3] D. R. Yennie, R. N. Wilson and D. G. Ravenhall: *Phys. Rev.*, **92**, 1325 (1953).

[4] S. Brenner, G. E. Brown and L. R. B.Elton: *Phil. Mag.*, **45**, 524 (1954).

imation is not reliable, but also that nuclear models with a non-peaked charge distribution could as well lead to satisfactory agreement with the experiments.

The non-reliability of the Born approximation has been proved, of course, only for the particular energies for which the exact calculations have been carried out. The possibility of improvement at higher energy cannot be excluded. In this respect, the writer has criticized [5] the argument based on the fact [6] that the phase shifts at infinite energy, for which an exact formula is known, differ from those yielded by the Born approximation. In fact, the angular distribution at infinite energy is an ambiguous expression in both cases. In order to resolve this ambiguity, it appears necessary to know more about the energy dependence of the phase shifts in the « extreme relativistic » region. This has originated the present note, which deals with the derivation of the expansion of the phase shift $\eta_l(k)$ in powers of the inverse of the momentum k [7], subject to the assumption that the angular momentum l be much smaller than k [8]. For $l \neq 0$ it is found that the expansion can be carried up to an arbitrary order in $1/k$ only on condition that the potential $V(r)$ and all its derivatives vanish for $r = 0$. There is no such restriction for $l = 0$. Although no conclusion concerning the original problem of the Born approximation can be reached on the basis of the results given here [8], yet these may perhaps be important in themselves, being an instrument for the actual evaluation of the phase shifts. In fact, it will be shown that, once the phase shifts have been calculated for a certain nuclear model, our formulae make it possible rapidly to evaluate those for an entire family of nuclear charge distributions, all obtained from the original one by altering the charge density, while preserving the value of the total charge. We hope that this may be of help when modern computing devices are not available, or, in any case, as a labour saving procedure or for checking purposes.

2. – Preliminaries.

The equations to be studied are of the form

$$\psi_l'' + \left(k^2 - \frac{\gamma}{r^2}\right)\psi_l = U\psi_l\,, \tag{1}$$

where $\gamma = l(l+1)$, $U(r)$ is an effective energy-dependent potential, and k is the momentum [7]. If $V(r)$ denotes the actual potential and $E = \sqrt{k^2+1}$

[5] E. Corinaldesi: *Nuovo Cimento*, **11**, 200 (1954).
[6] G. Parzen: *Phys. Rev.*, **80**, 261 (1950).
[7] We use a system of units in which $\hbar = c = m = 1$.
[8] The case when l is comparable with k remains to be investigated.

the energy, it is

$$U = 2EV - V^2 \tag{2a}$$

for the Klein-Gordon equation, and

$$U = 2EV - V^2 - \frac{l+1}{r}\frac{\alpha'}{\alpha} + \frac{3}{4}\frac{\alpha'^2}{\alpha^2} - \frac{1}{2}\frac{\alpha''}{\alpha}\,, \tag{2b}$$

with $\alpha = E - V + 1$ for the Dirac equation.

We denote by $f_l(\pm k, r)$ [9] two independent solutions of eq. (1) with the asymptotic behaviour

$$\lim_{r\to\infty} \exp[\pm ikr] f_l(\pm k, r) = 1\,, \tag{3}$$

and

$$f_l(\pm k) = (2l+1) \lim_{r\to 0} r^l f_l(\pm k, r)\,. \tag{4}$$

The physically interesting solution $\varphi_l(E, r)$ with the boundary condition

$$\lim_{r\to 0} \frac{\varphi_l(E, r)}{r^{l+1}} = 1 \tag{5}$$

can be constructed from $f_l(\pm k, r)$ as

$$\varphi_l(E, r) = \frac{1}{2ik}\left[f_l(k) f_l(-k, r) - f_l(-k) f_l(k, r)\right]. \tag{6}$$

Eq. (1) for $f_l(+k, r)$, with the boundary condition (3), is equivalent to the integral equation

$$f_l(+k, r) = F_l(+k, r) - \int_r^\infty G_l(r, \varrho) U(\varrho) f_l(+k, \varrho)\, \mathrm{d}\varrho\,. \tag{7}$$

Here $F_l(+k, r)$ is a solution of the homogeneous equation

$$\Psi_l'' + \left(k^2 - \frac{\gamma}{r^2}\right)\Psi_l = 0 \tag{8}$$

with the asymptotic behaviour

$$\lim_{r\to\infty} \exp[ikr] F_l(+k, r) = 1\,. \tag{9}$$

[9] In doing this we follow R. Jost: *Helv. Phys. Acta*, **20**, 256 (1947).

The solution of eq. (8) which for $r \to \infty$ behaves like

$$\Phi_l(k, r) \sim \frac{1}{k} \sin\left(kr - \frac{l\pi}{2}\right), \tag{10}$$

has also to be considered. The kernel $G_l(r, \varrho)$, which must satisfy the conditions

$$G_l(r, r) = 0\,, \qquad \left(\frac{\partial G_l(r, \varrho)}{\partial r}\right)_{r=\varrho} = 1 \tag{11}$$

is then explicitly given by

$$G_l(r, \varrho) = i^l\left[\Phi_l(k, r) F_l(+k, \varrho) - \Phi_l(k, \varrho) F_l(+k, r)\right]. \tag{12}$$

The functions $F_l(+k, r)$ and $\Phi_l(k, r)$ can be expressed in terms of Bessel functions ([10]),

$$F_l(+k, r) = \frac{1}{i^{l+1}} \sqrt{\frac{\pi k r}{2}}\, H^{(2)}_{l+\frac{1}{2}}(kr), \tag{13a}$$

$$\Phi_l(k, r) = \sqrt{\frac{\pi r}{2k}}\, I_{l+\frac{1}{2}}(kr)\,, \tag{13b}$$

so that

$$G_l(r, \varrho) = \frac{\pi}{2i} \sqrt{r\varrho}\left[I_{l+\frac{1}{2}}(kr)\, H^{(2)}_{l+\frac{1}{2}}(k\varrho) - I_{l+\frac{1}{2}}(k\varrho) H^{(2)}_{l+\frac{1}{2}}(kr)\right]. \tag{14}$$

It is now convenient to introduce the new function

$$g_l(z, r) = \frac{f_l(+k, r)}{F_l(+k, r)}\,, \tag{15}$$

with $z = 2ik$. This satisfies the integral equation

$$g_l(z, r) = 1 + \int_r^\infty K_l(r, \varrho) U(\varrho) g_l(z, \varrho)\, \mathrm{d}\varrho \tag{16}$$

with

$$K_l(r, \varrho) = -\frac{G_l(r, \varrho) F_l(+k, \varrho)}{F_l(+k, r)}\,. \tag{17}$$

Note that, while $G_l(r, \varrho)$ is simply antisymmetric in r and ϱ, $K_l(r, \varrho)$ has no special symmetry properties.

([10]) Cf. e.g. A. SOMMERFELD: *Partial Differential Equations* (New York, 1949), p. 84.

Finally the phase shift $\eta_l(k)$ is defined by

$$\exp\left[2i\left(\eta_l(k)-\frac{l\pi}{2}\right)\right]=\frac{f_l(k)}{f_l(-k)}=\frac{g_l(z,0)F_l(k,0)}{g_l(-z,0)F_l(-k,0)}\,, \tag{18}$$

or, using eq. (13a) and the actual form of the Hankel function,

$$\exp\left[2i\eta_l(k)\right]=\frac{g_l(z,0)}{g_l(-z,0)}\,. \tag{19}$$

3. – Expansion of $g_l(z, r)$.

In order to develop $\eta_l(k)$ in powers of $1/k$, the expansion of $g_l(z, r)$ in powers of $1/z$ ($z=2ik$) must first be obtained. We prefer to derive the latter by the use of the integral equation (16), although one could undoubtedly proceed directly from eq. (1). Our approach may have a special appeal in view of the employment of some technical devices which have become familiar in quantum field theory. By iterating eq. (16) we obtain

$$g_l(z,r)= \tag{20}$$

$$=1+\sum_{n=1}^{\infty}\int_r^{\infty}\mathrm{d}r_1\int_{r_1}^{\infty}\mathrm{d}r_2\ldots\int_{r_{n-1}}^{\infty}\mathrm{d}r_n\,K_l(r,r_1)K(r_1,r_2)\ldots K(r_{n-1},r_n)U(r_1)\ldots U(r_n).$$

From eqs. (12), (13) and (17), and by using the well-known asymptotic expansion of the Bessel functions for large values of the argument ([10]), $K_l(r, \varrho)$ can be evaluated as a power series of $1/z$. In this paper we consider terms up to $1/z^4$, and $g_l(z, r)$ will be finally computed also in the same approximation, the extension to any power of $1/z$ being immediate, though possibly laborious. Thus we find

$$K_l(r,\varrho)=\frac{1}{z}\left(1-L_l(\varrho,r)\right)\,, \tag{21}$$

with

$$L_l(\varrho,r)=\left[-\frac{2\gamma}{z^2\varrho^2}+\frac{6\gamma(\gamma-2)}{z^4\varrho^4}\ldots\right]- \tag{22}$$

$$-\left[1+\frac{2\gamma}{z}\left(\frac{1}{\varrho}-\frac{1}{r}\right)+\frac{2\gamma}{z^2}\left(\frac{\gamma-1}{\varrho^2}+\frac{\gamma}{r^2}-\frac{2\gamma}{r\varrho}\right)\ldots\right]\exp\left[-z(\varrho-r)\right].$$

In the first square bracket we neglect terms of order higher than $1/z^4$, while in the second, for reasons which will become apparent later on, we already drop a term in $1/z^3$ which has the property of vanishing for $\varrho=r$.

The assumption is made that z has a small positive real part, i.e. that k has a negative imaginary part, so that the iterated expression (20) may converge. This can now be written in the form

$$g_l(z, r) = 1 + \sum_{n=1}^{\infty} \frac{1}{z^n} \int_r^{\infty} U(1, n) + \sum_{n=1}^{\infty} \frac{1}{z^n} \int_r^{\infty} U(1, n) \sum_{i=1}^{n} L_l(r_i, r_{i-1}) - \tag{23}$$

$$+ \sum_{n=2}^{\infty} \frac{1}{z^n} \int_r^{\infty} U(1, n) \sum_{i=1}^{n-1} L_l(r_i, r_{i-1}) \sum_{j=i+1}^{n} L_l(r_j, r_{j-1}) + (L^3) + (L^4) + \ldots$$

with $r_0 \equiv r$ and the abbreviation

$$\int_r^{\infty} U(1, n) \equiv \int_r^{\infty} \mathrm{d}r_1 \int_{r_1}^{\infty} \mathrm{d}r_2 \ldots \int_{r_{n-1}}^{\infty} \mathrm{d}r_n U(r_1) \ldots U(r_n) .$$

(L^3), (L^4)... denote summations with three, four... L factors. The advantage of (23) lies in the fact that a term of the type (L^n) can, at most, be of the order $1/z^n$, as it is easy to see from the form of $L_l(\varrho, r)$ together with the remark that U/z, according to $(2a, b)$, tends to a finite limit for $|z| \to \infty$. In this respect, it is also important to notice that exponentials $\exp[-z(r_i - r_{i-1})]$, deriving from $\exp[-z(\varrho - r)]$ in eq. (22), in eq. (23) will always appear integrated from r_{i-1} to ∞. Thus, by a series of partial integrations, it is possible to separate out a sum of powers of $1/z$ not involving the exponential ($\exp[-z(r_i - r_{i-1})] = 1$ at the lower limit of integration $r_i = r_{i-1}$!), plus an integral containing $\exp[-z(r_i - r_{i-1})]$ multiplied by the highest power of $1/z$ to have been extracted. In order to illustrate our method we shall now explicitly evaluate $g_l(z, r)$ up to $1/z^2$, although the final results will eventually be given up to $1/z^4$.

We introduce the notation

$$\left| \begin{array}{l} A_i(r) = \dfrac{1}{z^i} \displaystyle\int_r^{\infty} (U(\varrho))^i \, \mathrm{d}\varrho , \\ \\ B_{ij}(r) = \dfrac{1}{z^i} \displaystyle\int_r^{\infty} \dfrac{(U(\varrho))^i}{\varrho^j} \, \mathrm{d}\varrho . \end{array} \right. \tag{24}$$

The first two terms of (23) can then be combined together to give

$$1 + \sum_{n=1}^{\infty} \frac{1}{z^n} \int_r^{\infty} U(1, n) = 1 + \sum_{n=1}^{\infty} \frac{1}{n!} (A_1(r))^n = \exp(A_1(r)) . \tag{25}$$

We consider now the summation which contains the function L_l only linearly:

$$(26)\qquad (L) = \sum_{n=1}^{\infty} \frac{1}{z^n} \int^{n} U(1, n) \sum_{i=1}^{n} L_i(r_i, r_{i-1}) =$$

$$= \sum_{n=1}^{\infty} \frac{1}{z^n} \int^{n} U(1, n) L_l(r_1, r) + \sum_{n=2}^{\infty} \frac{1}{z^n} \int^{n} U(1, n) \sum_{i=2}^{n} L_i(r_i, r_{i-1}) .$$

Changing the order of summation in the second term to $\sum_{i=2}^{\infty} \sum_{n=i}^{\infty}$ we get

$$(27)\quad (L) = -\frac{1}{z} \int_{r}^{\infty} U(\varrho) L_l(\varrho, r) \exp\left[A_1(\varrho)\right] \mathrm{d}\varrho + \sum_{i=2}^{\infty} \frac{1}{z^i} \int^{i} U(1, i) L_l(r_i, r_{i-1}) \exp\left[A_1(r_i)\right].$$

The second term of (27) can be treated by observing that the identity

$$(28)\quad \sum_{i=2}^{\infty} \frac{1}{z^i} \int^{i} U(1, i) \varphi(r_i, r_{i-1}) = \frac{1}{z^2} \int_{r}^{\infty} \mathrm{d}\varrho \int_{\varrho}^{\infty} \mathrm{d}\varrho' U(\varrho) U(\varrho') \varphi(\varrho', \varrho) \exp\left[A_1(r) - A_1(\varrho)\right],$$

holds, as can easily be shown by carrying out the substitution $r_i \to r_1$, $r_{i-1} \to r_2 \ldots$, $r_2 \to r_{i-1}$, $r_1 \to r_i$. Thus finally we have

$$(29)\qquad (L) = \frac{1}{z} \int_{r}^{\infty} U(\varrho) L_l(\varrho, r) \exp\left[A_1(\varrho)\right] \mathrm{d}\varrho +$$

$$+ \frac{1}{z^2} \int_{r}^{\infty} \mathrm{d}\varrho \int_{\varrho}^{\infty} \mathrm{d}\varrho' U(\varrho) U(\varrho') L_l(\varrho', \varrho) \exp\left[A_1(r) + A_1(\varrho') - A_1(\varrho)\right].$$

Substituting in this equation the expression (22) for L_l correct to $1/z^2$, and performing a double partial integration of the exponential $\exp\left[-z(\varrho' - \varrho)\right]$, we find, correct to the second order in $1/z$,

$$(30)\qquad (L) = \left[\frac{1}{z}\left(-\frac{U}{z} - A_2\right) + \frac{1}{z^2}\left(-\frac{U'}{z} + \frac{3U^2}{2z^2} + A_3 - 2\gamma B_{12}\right) + \ldots\right] \exp\left[A_1\right].$$

In this formula and in the following the argument of U, A_i, ect., is assumed to be r when not otherwise indicated. Finally

$$(31)\qquad (L^2) = \sum_{n=2}^{\infty} \frac{1}{z^n} \int^{n} U(1, n) \sum_{i=1}^{n-1} L_i(r_i, r_{i-1}) \sum_{j=i+1}^{n} L_l(r_j, r_{j-1}) ,$$

can be expressed in terms of (L) by suitably changing the order of summation of the indices i and n:

$$(L^2) = \sum_{i=1}^{\infty} \frac{1}{z^i} \int_r^{\infty} U(1, i) L_l(r_i, r_{i-1}) (L)_{r_i}, \tag{32}$$

where $(L)_{r_i}$ denotes (L) with r replaced by r_i. This shows that in the procedure described use is made at each step of the results of previous steps. By inserting the actual expression for L_l, and by performing a partial integration, we get, in our approximation,

$$(L^2) = \left| \frac{1}{z^2} \left(\frac{U^2}{z^2} + A_2 \frac{U}{z} + A_3 + \frac{1}{2} A_2^2 \right) + \ldots \right| \exp[A_1]. \tag{33}$$

The sum of (25), (30) and (33) gives the first three terms of an expansion of $g_l(z, r)$ in powers of $1/z$; not yet, however, a consistent expansion, as U/z itself, as given by (2*a*) or (2*b*), should also be developed. This will be done at the last stage. Here we give the results that would have been found if we had pushed the expansion one step further and evaluated the $1/z^4$ terms as well. The numerous contributions which are obtained can be shown to be equivalent to the expression [11]

$$\begin{aligned} g_l(z, r) = \exp \Big[& A_1 + \frac{1}{z} \left(- \frac{U}{z} - A_2 \right) + \frac{1}{z^2} \left(- \frac{U'}{z} + \frac{2U^2}{z^2} + 2A_3 - 2\gamma B_{12} \right) + \\ & + \frac{1}{z^3} \left(- \frac{U''}{z} + \frac{5UU'}{z^2} - \frac{16U^3}{3z^3} + \frac{4\gamma U}{r^2 z} - 5A_4 + 6\gamma B_{22} - \frac{1}{z^2} \int_r^{\infty} U(\varrho) U''(\varrho) \, \mathrm{d}\varrho \right) + \\ & + \frac{1}{z^4} \left(- \frac{U'''}{z} + \frac{7UU''}{z^2} - \frac{25U^2U'}{z^3} + \frac{11U'^2}{2z^2} + \frac{16U^4}{z^4} - \frac{16\gamma U^2}{r^2 z^2} + \frac{6\gamma U'}{r^2 z} - \right. \\ & - \frac{8\gamma U}{r^3 z} + 14A_5 + 6\gamma(\gamma - 2) B_{14} - 20\gamma B_{32} - \frac{1}{z^2} \int_r^{\infty} U(\varrho) U'''(\varrho) \mathrm{d}\varrho + \\ & \left. + \frac{5}{z^3} \int_r^{\infty} U(\varrho)^2 U''(\varrho) \mathrm{d}\varrho \right) + \ldots \Big]. \end{aligned} \tag{34}$$

[11] It is not difficult to verify directly that (34) is a solution of (1), (15) to the accuracy of $1/z^4$.

This is particularly handy for the evaluation of $\eta_l(k)$. [In fact, from (19) and (34) and the fact that U is an even function of z, we have [12]

$$(35)\qquad i\eta_l(k) = \Big[A_1 + \frac{1}{z}(-A_2) + \frac{1}{z^2}\Big(-\frac{U'}{z} + 2A_3 - 2\gamma B_{12}\Big) +$$

$$+ \frac{1}{z^3}\Big(\frac{5UU'}{z^2} - 5A_4 + 6\gamma B_{22} - \frac{1}{z^2}\int_r^\infty U(\varrho)U''(\varrho)\,\mathrm{d}\varrho\Big) +$$

$$+ \frac{1}{z^4}\Big(-\frac{U'''}{z} - \frac{25U^2U'}{z^3} + \frac{6\gamma U'}{r^2 z} - \frac{8\gamma U}{r^3 z} + 14A_5 + 6\gamma(\gamma-2)B_{14} - 20\gamma B_{32} +$$

$$+ \frac{5}{z^3}\int_r^\infty U(\varrho)^2U''(\varrho)\,\mathrm{d}\varrho\Big) + \ldots\Big|_{r=0}.$$

For this expression to be meaningful, suitable conditions must be satisfied by the function $U(r)$. Firstly, $U(r)$ must decrease sufficiently rapidly for large r so that the integrals A_1, etc., converge. It is easy to see that this requires that the potential $V(r)$ occurring in (2a, b) should decrease at large distances more rapidly than the Coulomb potential. Secondly, $U(r)$ and all its derivatives up to a sufficiently high order must vanish for $r = 0$. The higher l and the order of approximation, the greater number of derivatives of $U(r)$ must vanish. Rigorously, for the expansion to be possible to any order in $1/z$ and for any l, the derivative of $U(r)$ of an arbitrarily large order should be zero for $r = 0$. It is interesting to point out that these restrictions do not apply to the case $l = 0$. The phase shift $\eta_0(k)$ is therefore an analytic function of $1/k$ in the neighborhood of $k = \infty$, for any $U(r)$ which is continuous and differentiable at $r = 0$ and vanishes sufficiently rapidly at infinity.

Finally, here is the complete formula for the expansion of the phase shift of the Dirac equation, obtained by developing (2b) and substituting into (35):

$$(36)\qquad \eta_l(k) = -\mu_1^0 - \frac{1}{2k^2}(\mu_1^0 + (l+1)\mu_{01}^1 + \gamma\mu_1^2) -$$

$$- \frac{1}{2k^3}\Big(\mu_2^0 + \frac{3}{4}\mu_{101}^0 + \frac{3}{4}\mu_{02}^0 - (l+1)\mu_{01}^1 + 2(l+1)\mu_{11}^1 + \gamma\mu_2^2 + \frac{1}{2}V'(0) + \frac{3}{4}V(0)V'(0)\Big) +$$

$$+ \frac{1}{8k^4}\Big(\mu_1^0 - 4\mu_3^0 + 6\mu_{101}^0 + 6\mu_{02}^0 - 10\mu_{12}^0 - 5\mu_{201}^0 - 2(l+1)\mu_{01}^1 + 12(l+1)\mu_{11}^1 -$$

$$- 12(l+1)\mu_{21}^1 - 2\gamma\mu_1^2 - 3\gamma(\gamma-2)\mu_1^4 - 4\gamma\mu_3^2 - \gamma\mu_{001}^2 - 2\gamma(l+1)\mu_{01}^3 +$$

$$+ \Big[-5V(r)^2V'(r) - \frac{(l+1)V''(r)}{r} + \frac{(l+1)V'(r)}{r^2} - \frac{3\gamma V'(r)}{r^2} + \frac{4\gamma V(r)}{r^3}\Big]_{r=0}\Big) + \ldots$$

[12] When U/z is developed in powers of $1/k$, it is found that the zero order term is $-iV$ for both (2a) and (2b). Hence from (35) one finds $\eta_l(\infty) = -\int_0^\infty V(\varrho)\,\mathrm{d}\varrho$, a result given some years ago by PARZEN [6].

with the notation

$$\mu^m_{abc\ldots} \equiv \int_0^\infty \frac{1}{\varrho^m} V(\varrho)^a V'(\varrho)^b V''(\varrho)^c \ldots \mathrm{d}\varrho\,, \tag{37}$$

so that for instance

$$\mu^1_{101} \equiv \int_0^\infty \frac{V(\varrho)V''(\varrho)}{\varrho}\,\mathrm{d}\varrho\,, \qquad \mu^0_2 \equiv \int_0^\infty (V(\varrho))^2 \mathrm{d}\varrho\,, \text{ etc..}$$

4. – Applications.

Due to the restrictions to which V must be subjected for eq. (36) to have any sense, it is doubtful whether this expansion can in general be of much use for the evaluation of the phase shifts. For instance it could not be applied directly to the case of scattering of electrons by a nucleus, since $V(r)$ would be $-Ze^2/r$ at large distances (thus $\int_0^\infty V(\varrho)\,\mathrm{d}\varrho$ would diverge), and would in general not vanish at the origin (being for instance given by $Ze^2(r^2 - 3R^2)/2R^3$ for $r < R$ in the case of a square nuclear charge distribution of radius R). However, eq. (36) comes to be very handy in all cases when the phase shifts are already known for a certain potential V, and those for a modified potential $V + \delta V$ are required, δV being a function which decreases more rapidly than $1/r$ at infinity and vanishes at the origin with a sufficient number of its derivatives. In fact, the difference $\delta\eta_l(k)$ of the phase shifts for the two nuclear models described by V and $V + \delta V$ would be free from the divergence difficulty of $\int_0^\infty V(\varrho)\,\mathrm{d}\varrho$ at the upper limit, since $\int_0^\infty \delta V(\varrho)\,\mathrm{d}\varrho$ would be convergent by assumption, and also from any possible difficulty at $r = 0$, if δV is suitably restricted. It is not difficult to think of functions which would satisfy this requirement. E.g., $\delta V = \exp[-a/r]f(r)$ $(a > 0)$ would vanish with all its derivatives at the origin, and decrease sufficiently rapidly at infinity if $f(r)$ did so. It is clear that the condition $\int_0^\infty \delta\varrho(r)\, r^2\,\mathrm{d}r = 0$ with

$$\delta\varrho = -\frac{1}{4\pi r^2}\frac{\mathrm{d}}{\mathrm{d}r}\left(r^2\,\frac{\mathrm{d}\delta V}{\mathrm{d}r}\right)$$

must be satisfied by each proposed nuclear model if the total nuclear charge has to be preserved. It is possible that the condition that δV and its derivatives should vanish at $r = 0$ may in some cases be even too restrictive. For instance, eq. (36) can be used in order to calculate the difference of the phase shifts for scattering of 125 MeV electrons by Mercury nuclei ($Z = 80$)

described as square charge distributions of radius $R_1 = 1.4A^{\frac{1}{3}} \cdot 10^{-13}$ cm and $R_2 = 1.2A^{\frac{1}{3}} \cdot 10^{-13}$ cm respectively. One finds $\delta\eta_0(k) = 0.08580$, where from the results of BRENNER, BROWN and ELTON (4) one gets the figure 0.08566 accurate to the fifth decimal place. The error committed by using the series expansion (36) arrested at the $1/k^4$ term is therefore 1.6 per thousand. If the series had been arrested at the $1/k^2$ term, one would have found the figure 0.08412, i.e. an error of 1.7 per cent. This points to a satisfactory rapidity of convergence. For $l > 0$, $\delta\eta_l(k)$ for the two models in question is divergent. If, however, we tentatively use the trick of introducing convergence factors $\exp[-a_1/r]$ and $\exp[-a_2/r]$ into the integrals occurring in the expansion (36) as applied to the two models, while letting a_1 and a_2 eventually tend to zero in such a way that the divergent parts cancel in the difference $\delta\eta_l(k)$, we would still find, surprisingly enough, reasonable results. Thus we have $\delta\eta_1(k) = = 0.07398$, to be compared with the value 0.07442 from BRENNER *et al.*, the error being now 6 per thousand (i.e. larger than in the case of $\delta\eta_0(k)$) and $\delta\eta_2(k) = 0.05685$, against the value 0.05383 according to the above authors, the error having grown to 5 per cent. It seems therefore that the numerical convergence of the series would become worse with increasing l, an eventuality naturally to be expected.

Acknowledgements.

The author is indebted to Prof. R. PEIERLS for a stimulating discussion, and to Profs. W. HEITLER and E. SCHRÖDINGER for their encouragement.

RIASSUNTO

Gli spostamenti di fase delle equazioni di Klein-Gordon e di Dirac vengono sviluppati in serie di potenze dell'inverso del momento, seguendo un metodo basato sull'iterazione di una equazione integrale. Lo sviluppo risulta possibile soltanto per una classe piuttosto ristretta di potenziali. Si suggerisce un procedimento in base al quale, se si conoscono gli spostamenti di fase relativi ad un certo potenziale, quelli per una vasta famiglia di altri potenziali possono essere calcolati sotto forma di sviluppi in serie di potenze dell'inverso del momento. Questo metodo converge con rapidità se il momento angolare non è troppo elevato, e può essere utile per lo studio dello scattering di elettroni d'alta energia da parte di nuclei.

Note to the Solution of the Schrödinger Equation for Finite Systems.

T. TIETZ

Nicolas Copernicus University - Torún (Poland)

(ricevuto il 14 Giugno 1954)

This note deals with the number of the eigenvalue of the Schrödinger equation of finite systems. Lastly R. B. DINGLE [1] considered the solution of the Schrödinger equation for finite systems, which deals with the formulation of a number of different methods applicable to problems of these types. I hope that my note may also be of interest for the discussed problems. In this note I determine the number of eigenvalues of the Schrödinger equation.

A. RUBINOWICZ [2] has shown that the solution of the eigenvalue problem belonging to the self adjoint differential equation

$$\frac{\mathrm{d}}{\mathrm{d}x}\left(p\,\frac{\mathrm{d}f}{\mathrm{d}x}\right)-(q-\lambda\varrho)f=0, \tag{1}$$

and obtainable by Sommerfeld's polynomial method [3] are given by

$$f=p^{-\frac{1}{2}}\,\mathcal{P}\,. \tag{2}$$

The function $\mathcal{P}$ is here either of the form

$$\mathcal{P}=\xi^{\alpha}\exp\left[-\xi/2\right]{}_1F_1(a',c',\xi) \tag{3}$$

or of the form

$$\mathcal{P}=\xi^{\alpha}(1-\xi)^{\gamma}\,{}_2F_1(a,b,c,\xi) \tag{4}$$

where

$$\xi=\varkappa x^{h}\,,$$

${}_1F_1$ and ${}_2F_1$ are the confluent and the ordinary hypergeometric functions h is a positive integer and α, γ, $\varkappa$. are the constants. The number of positive and negative

(1) R. B. DINGLE: *Proc. Camb. Soc.*, A **49**, 103 (1953).
(2) A. RUBINOWICZ: *Proc. Phys. Soc.*, A **63**, 766-768 (1950).
(3) A. SOMMERFELD: *Atombau und Spectrallinien*, II. (Braunschweig, 1939).

zeros of the confluent hypergeometric function ${}_1F_1(a', c', \xi)$ and the ordinary hypergeometric function ${}_2F_1(a, b, c, \xi)$ are known for all possible real sets of parameters (a', c') and (a, b, c). This problem in case of ${}_1F_1$ was examined by A. KIENAST ([4]), F. G. TRICOMI ([5]), H. SKOVGAARD ([6]) and by the author ([7]). The author of this paper has shown that, taking into consideration the proof of which use was made by A. HURWITZ to determine positive zeros of the ordinary hypergeometric function ${}_2F_1(a, b, c, \xi)$. Out of this proof one can also determine the positive and negative zeros of the confluent hypergeometric function. In this mode there was formed the unite method for determination of the number of zeros for ${}_2F_1(a, b, c, \xi)$ and ${}_1F_1(a', c', \xi)$. From the above mentioned proof after H. SKOVGAARD and the author. only in the following cases ${}_1F_1(a', c', \xi)$ has real positive simple zeros

$$
(5)\quad \begin{cases} 1) & -n \leqslant a' < -n+1\,, & c' > 0 \\ 2) & -(n+m) \leqslant a' < -(n+m)+1\,, & -m < c' < -m+1 \\ 3) & a' > 0\,, & -n < c' < -n+1 \\ 4) & -m < a' < -m+1\,, & -(n+m) < c' < -(n+m)+1 \end{cases}
$$

(m a positive integer).

In the cases (5.1) and (5.2) ${}_1F_1(a', c', \xi)$ has exactly n zeros, in the cases (5.3) and (5.4) ${}_1F_1(a', c', \xi)$ has no positive zeros if n is even, but one positive zero if n is odd.

In case of the ordinary hypergeometric series after F. KLEIN ([8]) and A. HURWITZ ([9]) the ordinary hypergeometric function ${}_2F_1(a, b, c, \xi)$ has $\mathcal{N}$ zeros only in the following cases

(6)

	a	b	c	$\mathcal{N}$
I	+	+	−	$\dfrac{1-(-1)^{\nu}}{2}$
II	+	−	+	μ
III	+	−	−	$\mu-\nu$ for $\mu \geqslant \nu$; $\dfrac{1-(-1)^{\mu+\nu}}{2}$ for $\mu \leqslant \nu$
IV	−	−	−	$\dfrac{1-(-1^{+\lambda+\mu+\nu})}{2}$

([4]) A. KIENAST: *Untersuchungen über die Lösungen der D-Gl Denkschr., Schweiz. naturforsch. Ges.*, **57**, 247 (1921).

([5]) F. G. TRICOMI: *Math. Z.*, **52**, 669 (1950).

([6]) H. SKOVGAARD: *Math. Z.*, **58**, 448 (1953).

([7]) To be published shortly.

([8]) F. KLEIN: *Math. Annalen*, **37**, 573 (1890).

([9]) A. HURWITZ: *Math. Annalen*, **38**, 435 (1891).

In the case where a is negative λ is the first number of the sequence 1, 2, 3,... for which the number $a+\lambda$ is positive so that in the sequence

$$a\,,\quad a+1\,,\quad a+2\,,\quad \ldots\,,\quad a+\lambda-1\,,\quad a+\lambda\,, \tag{7}$$

the expression $a+\lambda-1$ is the last negative number. The corresponding meaning have μ and ν for the reason of b and c.

E.g. in case of radial function of a non relativistic one electron atom

$$\frac{1}{x^2}\frac{\mathrm{d}}{\mathrm{d}x}\left(x^2\frac{\mathrm{d}f}{\mathrm{d}x}\right)+\left[\frac{2m}{\hbar^2}\left(E+\frac{Ze^2}{x}\right)-\frac{l(l+1)}{x^2}\right]f=0\,, \tag{8}$$

the eigenfunctions of (8) are given by

$$f=x^l\exp\left[-\xi/2\right]{}_1F_1(-\alpha,\,2l+2,\,\xi)\,, \tag{9}$$

where

$$\xi=\varkappa x\,,\qquad \frac{2mE}{\hbar^2}=-\frac{\varkappa^2}{4}\,,\qquad a_1=\frac{\hbar^2}{me^2Z}\,,$$

$$\varkappa=2/(\alpha+l+1)a_1\,,$$

we see that only in case of (5.1) we have zeros

$$-n\leqslant-\alpha<-n+1\,. \tag{11}$$

If $x\to\infty$ we obtain the known formula for eigenvalues. More details will be published later on.

We wish to express to our gratitude to Prof. Dr. R. B. Dingle for studying the complete manuscript and for his criticism before publication.

Pseudoscalar Nuclear Field and Polarization.

M. Verde

Istituto di Fisica dell'Università - Torino
Istituto Nazionale di Fisica Nucleare - Sezione di Torino

(ricevuto il 21 Luglio 1954)

The experiments made recently in the field of nuclear physics have shown two new features which seem to us of extreme interest. The first of these consists in the remarkable fact that the nuclei are sources of a pseudoscalar field (t.i. of a field which change sign by improper Lorentz transformations) the particles of which are the well known π-mesons. The second one concerns the strong azimuthal dependence of the differential cross-section in the scattering of a nucleon by a nucleus. It is characteristic of these azimuthal asymmetries of being important at low energies (several MeV) as well as at high energies (several hundreds of MeV).

Experiments have in this way proved the existence of an important spin-orbit interaction when a nucleon happens to come near a nucleus.

One indication of this type, certainly less direct, came already from the shell model of nuclei. This valuable model has drawn our attention on the efficiency of a central field in nuclei. One postulates besides, a strong phenomenological spin-orbit coupling, at it is not possible to assume it as due to a relativistic effect of the type of a Thomas precession in a scalar field, which comes out to be too small.

It is now tempting to assume the nuclear field of the shell model as a pseudoscalar field and to reduce the strong polarization in the scattering of nucleons, to their usual pseudoscalar or pseudovector interaction with this kind of field.

We will here anticipate some results of the collisions theory of a Dirac particle in a given static field which is pseudoscalar and has a spherical symmetry.

It is a characteristic feature of a pseudoscalar interaction with a pseudoscalar field that a remarkable azimuthal dependence of the differential cross-sections is effective at the high as at the low energies.

Being the total angular momentum and the parity costants of motion, we shall characterize the phases δ with the corrispondent quantum numbers. To a given j correspond two configurations with opposite parity, the orbital momentum being, $l = j \pm \frac{1}{2}$.

It is possible to prove that:

$$\sin \delta_j^{\pm} = \pm \int_0^{\infty} \frac{V}{\hbar c} (G_j^{\pm} F_j^0 + F_j^{\pm} G_j^0) \, \mathrm{d}r,$$

where the signs $\pm$ are related to the two parities $l = j \pm \frac{1}{2}$, and:

$$F_j^0 = \sqrt{\frac{\pi kr}{2}}\, J_j(kr)\,, \qquad G_j^0 = -\sqrt{\frac{\pi kr}{2}}\, J_{j+1}(kr)\,.$$

The two radial eigenfunctions F and G have the asymptotic behaviour:

$$F_j^{\pm} \simeq \cos\left(kr - \frac{j+\frac{1}{2}}{2}\pi + \delta_j^{\pm}\right),$$

$$G_j^{\pm} \simeq -\sin\left(kr - \frac{j+\frac{1}{2}}{2}\pi + \delta_j^{\pm}\right),$$

and are solutions of the following system of differential equations:

$$\begin{pmatrix} k & D_+ \\ -D_- & k \end{pmatrix}\begin{pmatrix} F_j^{\pm} \\ G_j^{\pm} \end{pmatrix} = \mp\frac{V}{\hbar c}\begin{pmatrix} 0 & 1 \\ 1 & 0 \end{pmatrix}\begin{pmatrix} F_j^{\pm} \\ G_j^{\pm} \end{pmatrix}.$$

$\hbar k$ is the momentum of the incident particle and:

$$D_{\pm} = \frac{\partial}{\partial r} \pm \frac{j+\frac{1}{2}}{r}\,.$$

$V(r)$ is a scalar interaction of spherical symmetry. The pseudoscalar nature of the field has been lost in the passage to the equations for the radial components. With a pseudoscalar field the only matrix elements different from zero are those between two states of opposite parity. It is just the contrary of what happens with a scalar field.

In order to make a comparison with the collision of a Dirac particle in a scalar field, we give here the correspondent formulas for the phases:

$$\sin\delta_j^+ = -\int_0^{\infty}\frac{V}{\hbar c}\left(\eta F_j^0 F_j^+ - \frac{1}{\eta}G_j^0 G_j^+\right)\mathrm{d}r\,,$$

$$\sin\delta_j^- = -\int_0^{\infty}\frac{V}{\hbar c}\left(-\frac{1}{\eta}F_j^0 F_j^- + \eta G_j^0 G_j^-\right)\mathrm{d}r\,, \qquad \eta = (E+Mc^2)/pc,$$

E being the energy of the incoming particles, M their reduced mass. $F_j^{\pm}$ and $G_j^{\pm}$ have the same asymptotic behaviour as the case discussed before, they must however satisfy the systems:

$$\begin{pmatrix} k & D_+ \\ -D_- & k \end{pmatrix}\begin{pmatrix} F^+ \\ G^+ \end{pmatrix} = \frac{V}{\hbar c}\begin{pmatrix} \eta & 0 \\ 0 & -1/\eta \end{pmatrix}\begin{pmatrix} F^+ \\ G^+ \end{pmatrix},$$

respectively

$$\begin{pmatrix} k & D_+ \\ -D_- & k \end{pmatrix} \begin{pmatrix} F^- \\ G^- \end{pmatrix} = \frac{V}{\hbar c} \begin{pmatrix} -1/\eta & 0 \\ 0 & \eta \end{pmatrix} \begin{pmatrix} F^- \\ G^- \end{pmatrix}.$$

At low energies:

$$\frac{\eta}{\hbar c} = \frac{2M}{\hbar^2} \frac{1}{k} \left(1 + \frac{\beta^2}{4}\right), \qquad \frac{1}{\eta \hbar c} = \frac{2M}{\hbar^2} \frac{1}{k} \frac{\beta^2}{4},$$

where

$$\beta = v/c .$$

It is easy to understand from the examination of the formulas given above that at high energies the pseudoscalar and the scalar field show appreciable azimuthal effects, whereas at low energies the pseudoscalar field only continues to have the same property.

If the interaction is weak enough to justify the use of Born's approximation, one has:

$$\sin \delta_l^+ = -\pi \int_0^\infty \frac{V}{\hbar c} \cdot (kr) \cdot J_{l-\frac{1}{2}}(kr) \cdot J_{l+\frac{1}{2}}(kr)\, \mathrm{d}r \qquad j = l + \tfrac{1}{2}$$

$$\sin \delta_l^- = +\pi \int_0^\infty \frac{V}{\hbar c} \cdot (kr) \cdot J_{l+\frac{3}{2}}(kr) J_{l+\frac{1}{2}}(kr)\, \mathrm{d}r \qquad j = l - \tfrac{1}{2}$$

for the pseudoscalar field, and:

$$\sin \delta_l^+ = \sin \delta_l^- = -\frac{1}{k} \frac{2M}{\hbar^2} \int_0^\infty V \cdot \left(\frac{\pi kr}{2}\right) \cdot J^2_{l+\frac{1}{2}}(kr)\, \mathrm{d}r,$$

for the scalar field. (We have here omitted terms in $\beta^2/4$).

The difference $\sin \delta_l^+ - \sin \delta_l^-$ is zero in the second case and is equal to $-(2l+1)\pi \int_0^\infty \frac{V}{\hbar c} J^2_{l+\frac{1}{2}}(kr)\, \mathrm{d}r$ in the first one.

We wish briefly to mention that the eventual importance of the pseudovector coupling is effective as a fourth component of a vectorial field and does not produce appreciable azimuthal effects.

The extensive account of the above considerations and theory with some applications to special field $V(r)$ will be given soon.

IL NUOVO CIMENTO Vol. XII, N. 3 1° Settembre 1954

On the Ground State of the Mesonic Atom.

M. Suffczyński

Institute of Theoretical Physics - Warsaw, Polonia

(ricevuto il 23 Luglio 1954)

The proton charge distribution inside the heavy nuclei influences the energy levels of the μ-mesonic atoms. Fitch and Rainwater [1] have calculated these energy levels for the uniform charge distribution. Assuming nuclear radius (*) $R=1.3\cdot A^{\frac{1}{3}}$ they have obtained the transition energies smaller than measured in their X-ray studies of the mesonic atoms [1,2].

There is some experimental evidence that the proton charge distribution is peaked at the centre of the nucleus [2-4]. Especially good fit with the electron scattering experiments [3] gives the exponential charge distribution $\varrho(r)=(Ze/2a^3)\cdot\exp[-r/a]$, which gives the potential energy

$$V(r) = -Ze^2\left\{\frac{1}{r}-\left(\frac{1}{r}+\frac{1}{2a}\right)\exp[-r/a]\right\}, \tag{1}$$

for the meson. In order to find the energy of the ground state of the mesonic atom with exponential charge distribution numerical integration has been undertaken of the Dirac equations

$$\begin{cases} \dfrac{\mathrm{d}\psi_1}{dr} = (k-1)\dfrac{\psi_1}{r} - \psi_2(E'-V)/\hbar c\,, \\ \dfrac{\mathrm{d}\psi_2}{\mathrm{d}r} = (k+1)\dfrac{\psi_2}{r} + \psi_1(E'-V+2\mu c^2)/\hbar c\,. \end{cases} \tag{2}$$

for $k=-1$ (i.e. for $1s_{\frac{1}{2}}$ state), for potential (1) with $Z=82$ (Pb). The meson mass was assumed to be $\mu=207$ electron masses [5]. Atomic constants were taken from [6].

The length a was chosen firstly equal to the Compton wavelength of the meson, that is 1 865 (I), and secondly, 1.1 times smaller, that is 1 696 (II), approximately.

---

(1) V. L. Fitch and J. Rainwater: *Phys. Rev.*, **92**, 789 (1953).
(*) All lengths here are expressed in units 10^{-13} cm.
(2) R. Hooper and E. M. Henley: *Phys. Rev.*, **92**, 801 (1953).
(3) R. Hofstadter, H. R. Fechter and J. A. Mc Intyre: *Phys. Rev.*, **92**, 978 (1953).
(4) L. I. Schiff: *Phys. Rev.*, **92**, 988 (1953).
(5) F. M. Smith, W. Birnbaum and W. H. Barkas: *Phys. Rev.*, **91**, 765 (1953).
(6) J. W. M. Du Mond and E. R. Cohen: *Rev. Mod. Phys.*, **25**, 691 (1953).

The energy E' of the ground state turned out to be

$$-10.260 < E' < -10.255 \text{ MeV} \qquad \text{for} \quad a = 1\,865 \quad \text{(I)},$$

$$-10.757 < E' < -10.750 \text{ MeV} \qquad \text{for} \quad a = 1\,696 \quad \text{(II)}.$$

Assuming for the moment that the energy of a higher state is the same for either exponential as for the uniform charge distribution since higher states are not so seriously affected by the charge distribution as the ground state, we could take the energy of $2p_{\frac{3}{2}}$ state from the calculation of FITCH and RAINWATER. Then the $2p_{\frac{3}{2}} \to 1s_{\frac{1}{2}}$ transition energy would be about 5.6 MeV in case (I) and 6.1 MeV in case (II), whereas the value found experimentally in Pb is 6.02 MeV. There is reason therefore to believe that the value of a for Pb should lie between (I) and (II).

On analyzing the electron scattering experiments SCHIFF [4] allows a to lie between 1.6 and 2.9, but apparently the value given [3] as the best for exponential charge distribution in Pb, namely 2.36, would be poor for the calculation of the mesonic energy levels.

Details of this work will be given in *Acta Physica Polonica*.

I thank Prof. J. WERLE and M. DANYSZ for valuable discussions.

On the Renormalization Technique in Quantum Electrodynamics.

B. Ferretti

Istituto di Fisica e Scuola di perfezionamento in Fisica Nucleare dell'Università - Roma
Istituto Nazionale di Fisica Nucleare - Sezione di Roma

(ricevuto il 2 Agosto 1954)

In a previous paper [1] it has been shown that the fundamentals of the general renormalization method developed by Dyson [2], and the idea itself of the Feynman graphs, suitably generalized, are by no means limited to the use of a power expansion of the electric charge, but may be applied without any essential modification in a way in principle much more general, using the idea of increasing the charge from zero to the actual value by a succession of infinitesimal steps.

The method of renormalization outlined in [1] although in principle perhaps sufficiently sound, does appear all but quite simple for practical purposes.

In this letter a result is presented by which the renormalization procedure described in the preceding paper is prooved to be sufficiently simple when suitably performed.

The most cumbersome task in the renormalization is the elimination of the so called « overlapping divergencies ». These divergencies can be treated by the Salam prescription [3] both in conventional (power series) and infinitesimal step techniques [1].

The overlapping divergencies appear when considering the kernels $\Sigma^*(p)$, $\Pi^*(p)$ of Dysons integral equations, for either electron and photon propagators (ref. [2]. eq. (63), (64)).

Let us consider the kernel $\Sigma^*(p)$. This may be *always* be put under the form:

$$\Sigma^*(p) = \sum_{n=1}^{\infty} \psi_n \,, \tag{1}$$

ψ_n corresponding to the set of the graphs of Salam's category $[n]$ (see [1], Appendix 4).

Now the terms ψ_n may be expressed in the following form:

$$\psi_n(p) = \int \mathrm{d}t_1 \int \mathrm{d}t_2 \ldots \int \mathrm{d}t_{n-2} \int \mathrm{d}\tau_2 \int \mathrm{d}\tau_1 \gamma D'_F(t_1) S'_F(p-t_1) T(p-t_1, p-t_2, t_1, t_2) \cdot \tag{2}$$

$$\cdot D'_F(t_2) S'_F(p-t_2) T(p-t_2, p-t_3, t_2, t_3) \ldots T(p-\tau_2, p-\tau_1, \tau_2, \tau_1) D'_F(\tau_1) S'_F(p-\tau_1) \gamma +$$

$$+ \text{renormalization terms following Salam's prescription.}$$

[1] B. Ferretti: *Nuovo Cimento*, **10**, 1079 (1953).
[2] F. J. Dyson: *Phys. Rev.*, **75**, 1736 (1949).
[3] A. Salam: *Phys. Rev.*, **82**, 217 (1951).

where the function $T(p-t_1, p-t_2, t_1, t_2)$ corresponds to the sum of all the possible different graphs with two external electronics lines of momentum $p-t_1$, $p-t_2$, and two photon lines of momentum t_1, t_2, such that the lines $p-t_1$, t_1, cannot be separated from the lines $p-t_2$, t_2 with less than three cuts [1].

Now putting:

$$\psi_n(p) = \int \mathrm{d}t_1 \int \mathrm{d}t_2 \ldots \int \mathrm{d}\tau_2 \int \mathrm{d}\tau_1 \, \gamma \Phi_n(p, t_1, t_2 \ldots \tau_2, \tau_1)\gamma \,, \qquad n \geqslant 4, \tag{3}$$

the following result holds:

$$\begin{aligned} \Phi_n(p, t_1, t_2 \ldots \tau_2, \tau_1) = {} & U^0(t_1, t_2)\Phi_{n-1}(p, t_2 \ldots \tau_2, \tau_1) + \\ & + \Phi_{n-1}(p, t_1, t_2 \ldots \tau_2) \cdot U^0(\tau_2, \tau_1) - \\ & - U^0(t_1, t_2)\Phi_{n-2}(p, t_2 \ldots \tau_2)U^0(\tau_2, \tau_1) + \\ & + U(t_1, t_2)B_n U(\tau_2, \tau_1) \,, \end{aligned} \tag{4}$$

where

$$U^0(t_1, t_2) = S'_F(p_0 - t_1)D'_F(t_1)[T(p_0 - t_1, p_0 - t_2, t_1, t_2) - T(p_0 - t_1, p_0, t_1, 0)] \tag{5}$$

being

$$\gamma_\mu p_{0\mu} + ik = 0 \tag{5'}$$

and where

$$\begin{aligned} U(t_1, t_2) = {} & S'_F(p - t_1)D'_F(t_1)T(p - t_1, p - t_2, t_1, t_2) - \\ & - S'_F(p_0 - t_1)D'_F(t_1)T(p_0 - t_1, p_0 - t_2, t_1, t_2) \end{aligned} \tag{6}$$

and

$$B_n = S'_F(p - t_2)D'_F(t_2)T(p - t_2, p - t_3, t_2, t_3) \ldots S'_F(p - \tau_2)D'_F(\tau_2) \,. \tag{6'}$$

Now it should be noted that $\int \mathrm{d}t_1 \ldots \int \mathrm{d}\tau_1 U(t_1, t_2)B_n U(\tau_2, \tau_1)$ is convergent at inspection [1], and therefore, keeping into account (5), the relation (4) gives the formal proof that if the prescription of Salam gives convergent results for $n-1$, it does so for n. But this is not the main interest of the recurrency relation (4).

Putting indeed:

$$\psi(t_1, t_2, \tau_2, \tau_1) = \sum_4^\infty \int \mathrm{d}t_3 \ldots \int \mathrm{d}t_{n-2} \, \Phi_n(t_1, t_2 \ldots \tau_2, \tau_1) \,, \tag{7}$$

we have

$$\Sigma^* = \sum_1^4 \psi_i + \int \mathrm{d}t_1 \int \mathrm{d}t_2 \int \mathrm{d}\tau_2 \int \mathrm{d}\tau_1 \, \psi \,. \tag{1'}$$

Using then the relation (4) we easily get

$$\begin{aligned} \psi = {} & \frac{\Phi_4 + \int \mathrm{d}t_3 \, \Phi_5[1 - U^0(t_1, t_2) - U^0(\tau_2, \tau_1)]}{1 - U^0(t_1, t_2) - U^0(\tau_2, \tau_1) + U^0(t_1, t_2)U^0(\tau_2, \tau_1)} + \\ & + \frac{U(t_1, t_2)S'_F(p - t_2)D'_F(t_2)B'S'_F(p - \tau_2)D'_F(\tau_2)U(\tau_2, \tau_1)}{1 - U^0(t_1, t_2) - U^0(\tau_2, \tau_1) + U^0(t_1, t_2)U^0(\tau_2, \tau_1)} \,, \end{aligned} \tag{8}$$

where

$$(8') \qquad \begin{cases} S'_F(p-t_2)D'_F(t_2)\mathcal{B}'S'_F(p-\tau_2)D'_F(\tau_2) = \sum_{n=\sigma}^{\infty} B_n \\ S'_F(p-t_2)D'_F(t_2)\mathcal{B}S'_F(p-\tau_2)D'_F(\tau_2) = \sum_{n=4}^{\infty} B_n , \end{cases}$$

and $\mathcal{B}$ is a function corresponding to the sum of all possible different graphs with external electron lines $p-t_2$, $p-\tau_2$ and photon lines t_2, τ_2 such that the lines $p-t_2$, t_2 cannot be separated from $p-\tau_2$, τ_2, with less than two cuts.

In the relations (1′) and (8) all the diverging integrations have disappeared and the renormalization procedure which in reference [1] appeared to imply in every infinitesimal step an infinite number of operations, can be performed in a closed manner.

A similar result holds for the photon kernel $\Pi^*(p)$; the vertex parts are treated in an even simpler way.

I have the pleasure to thank Dr. CAIANIELLO for interesting discussions on these topics.

Sul metodo delle emulsioni nucleari nello studio della componente neutronica della radiazione cosmica.

M. Curatolo, M. M. Indovina Addario, D. Palumbo e M. Santangelo

Istituto di Fisica dell'Università - Palermo

(ricevuto il 4 Agosto 1954)

Desiderando studiare la componente neutronica della radiazione cosmica col metodo delle emulsioni nucleari, recentemente usato da Kaplan e Yagoda [1] e da Eugster [2], abbiamo cominciato col misurare il flusso dei neutroni cosmici a due diverse quote, per conoscere le difficoltà che si presentano nell'applicazione di tale metodo.

Con una soluzione al 15% di borato di litio, usando il procedimento detto per « assorbimento » [1], abbiamo caricato delle lastre Ilford C_2, spesse 200 μ, e le abbiamo esposte, contemporaneamente, alla radiazione cosmica entro blocchi di paraffina, aventi le dimensioni di $20 \times 20 \times 20$ cm, al livello del mare (Palermo) e a 4500 m s.l.d.m. (Capanna Margherita). Dopo l'esposizione, durata 43 giorni al livello del mare e 15 in montagna, le lastre sono state sviluppate nel seguente modo:

1) pre-immersione in H_2O distillata; tempo 40 min; da temperatura ambiente a 5 °C;

2) sviluppo freddo: D 19 diluito 1 a 4; tempo 45 min; temperatura 5 °C;

3) sviluppo secco caldo: tempo 20 min; temperatura 18 °C;

4) lavaggio in 5% solfato anidro di sodio; tempo 15 min; temperatura 5 °C;

5) bagno di frenaggio: 2% di acido acetico e 5% di solfato anidro di sodio; tempo 40 min; temperatura 5 °C;

6) fissaggio: 400 g di iposolfito, 2,5 g di solfito di sodio, 1000 cm³ di H_2O distillata; temperatura 6 °C; tempo fino a schiarimento delle lastre.

Quindi le lastre sono state tenute per un tempo uguale in una soluzione costituita da fissaggio sempre più diluito e dal 5% di solfato di sodio;

7) lavaggio in acqua corrente per 6 ore;

8) immersione per 6 ore in una soluzione contenente il 30% di alcool e il 5% di glicerina; quindi sono state asciugate a bassa temperatura in ambiente umido.

[1] H. Kaplan e H. Yagoda: *Rev. Sci. Instr.*, **23**, 155 (1952).

[2] J. Eugester: *Rev. Sci. Instr.*, **25**, 5(1954).

Usando un obiettivo ad immersione con un campo di 95 μ di diametro, sono state misurate tutte le tracce aventi entrambi gli estremi nell'emulsione, proiezione orizzontale superiore a 4.5 μ ed inferiore a 50 μ. Queste tracce sono quindi state divise in due gruppi in base alla loro lunghezza effettiva: quelle aventi lunghezza effettiva compresa fra 5 e 10 μ sono state attribuite alla reazione $^{10}B(n, \alpha)^7Li$; quelle aventi lunghezza effettiva compresa fra 37 e 48 μ alla reazione $^6Li(n, \alpha)^3H$. Il massimo e il minimo range per i due gruppi sono stati stabiliti in base alle misure fatte da Szteinsznaider [3], e tenendo conto della precisione colla quale noi possiamo misurare la proiezione orizzontale e quella verticale di una traccia.

Le tracce dovute ad impurità radioattive non possono avere alterato i nostri risultati, perchè in una lastra Ilford C_2 la lunghezza minima di una traccia, originata da una sostanza radioattiva, è di 14 μ; inoltre le sostanze radioattive, che possono dare origine a tracce di lunghezza effettiva compresa fra 37 e 48 μ, avendo una vita media molto breve, all'osservazione si presentano non come tracce singole ma come stelle.

Il numero di tracce, trovato sperimentalmente, deve essere opportunamente corretto per tener conto:

a) del numero di tracce perdute per difetto di proiezione;

b) del numero di tracce perdute perchè uscite fuori dall'emulsione;

c) dell'eventuale accorciamento delle tracce per azione del fading.

Le prime due correzioni si apportano prendendo come numero di tracce vere, N, quello dato dalla formula

$$(1) \qquad N = n \Big/ \left(1 - \frac{a}{2t}\sqrt{1 - \frac{x_0^2}{a^2}}\right)\sqrt{1 - \frac{x_0^2}{a^2}}$$

nella quale n è il numero di tracce lette, x_0 la minima proiezione orizzontale osservata, t lo spessore dell'emulsione, a la lunghezza media dell'intervallo di range considerato. La (1) è stata dedotta nell'ipotesi che tutte le tracce abbiano la stessa lunghezza effettiva a. Il valore di tale fattore di correzione $1/f$, per diversi valori di a, è dato in tabella I.

Tabella I.

x_0 in micron	5,5	6,5	7,5	8,5	9,5	42,5
$1/f$	1,77	1,41	1,27	1,2	1,16	1,12

In base al numero di mg di B e di Li contenuti in un cm^3 di emulsione secca [1], alla percentuale di ^{10}B e di ^6Li, ed al valore delle sezioni d'urto delle due reazioni, abbiamo calcolato il valore del rapporto fra il numero di tracce per cm^2 dovute alla reazione $^{10}B(n, \alpha)$ e il numero di tracce per cm^2 dovute alla reazione $^6Li(n, \alpha)$, ed abbiamo trovato 17,5. Calcolando poi il valore di tale rapporto coi dati sperimentali ottenuti da diverse lastre, abbiamo trovato un valore medio di 14. La differenza fra il valore sperimentale e quello dedotto in base ai dati di Kaplan e di Yagoda [1] può essere attribuita a piccole diversità nel processo di caricamento; questo rende evidente la necessità di una preventiva taratura delle lastre con una sorgente di neutroni, ogni volta che si carica un gruppo di lastre.

Volendo tener conto della distribuzione gaussiana delle tracce, la (1) fornisce per la distribuzione osservata

$$(2) \qquad dn = \frac{N}{h\sqrt{\pi}}\sqrt{1 - \frac{x_0^2}{a^2}} \cdot \left(1 - \frac{a}{2t}\sqrt{1 - \frac{x_0^2}{a^2}}\right)\exp\left[-\frac{(a - \bar{a})^2}{h^2}\right].$$

[3] Szteinsznaider: *Journ. de Phys. et le Rad.*, **14**, 468 (1953).

dove $\bar{a}$ è la lunghezza media delle tracce ed h il parametro di precisione della gaussiana.

La distribuzione delle lunghezze effettive delle tracce (valori osservati corretti) della reazione $^{10}B(n, \alpha)$ nei vari intervalli di range, osservata nelle lastre esposte al l.d.m., è data in fig. 1, quella osservata nelle lastre esposte a 4500 m s.l.d.m. è data in fig. 2. Come si vede la distribuzione rappresentata dalla (2)

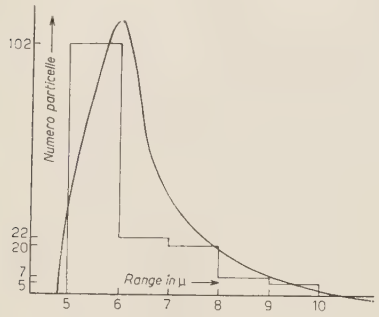

Fig. 1.

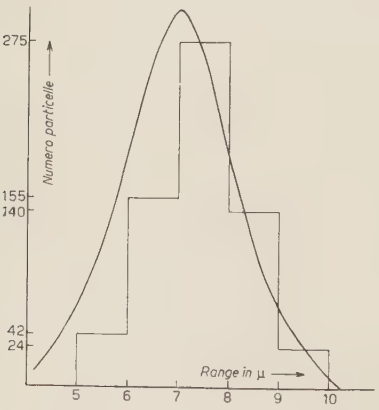

Fig. 2.

è in accordo abbastanza buono con quella delle tracce della reazione $^{10}B(n, \alpha)$ osservate nelle lastre esposte a 4500 m; l'accordo è meno buono per le tracce della medesima reazione osservate nelle lastre esposte al livello del mare. Abbiamo pensato che questo potesse essere attribuito al fading; infatti nelle lastre esposte al livello del mare, il fading ha sicuramente fatto sentire la sua azione, sia per il lungo tempo d'esposizione, sia perchè in tale periodo non è stato possibile eliminare l'umidità dall'ambiente a 4° C nel quale si trovavano le lastre. Ammettendo che l'effetto del fading consista in un accorciamento delle tracce la (2) diventa

$$(3) \qquad dn = \frac{N\lambda}{h\sqrt{\pi}} \sqrt{1 - \frac{x_0^2}{a^2}} \cdot \left(1 - \frac{a}{2t}\sqrt{1 - \frac{x_0^2}{a^2}}\right) \exp\left[-\frac{(\lambda a' - \bar{a})^2}{h^2}\right].$$

dove $\lambda \ll 1$ è il fattore di fading, cioè quel numero per il quale occorre moltiplicare la lunghezza osservata a' di una traccia per avere la lunghezza $(a = a'\lambda)$ prima del fading. Il termine $(a/2t)\sqrt{1-(x_0^2/a^2)}$ è trascurabile nel caso delle tracce della reazione $^{10}B(n, \alpha)$ e per $t = 200$ μ.

I valori di h e di λ sono da determinare; per far questo si prenda la (2) e la si integri per due diversi intervalli di range, il rapporto di questi due integrali deve essere uguale al rapporto fra il numero (non corretto) delle particelle osservate nei due intervalli considerati di range; in tal modo si ricava $h = 1$. Ripetendo lo stesso procedimento, con l'equazione (3) si trova $\lambda = 1{,}2$. Con tali valori di λ la (3) rappresenta abbastanza bene la distribuzione sperimentale di fig. 1. Solamente le tracce della radiazione $^{10}B(n, \alpha)$, osservate al livello del mare, sono state corrette per il fading in tal modo; nessuna correzione è stata apportata alle tracce della reazione $^{6}Li(n, \alpha)$, osservate alla medesima altezza, perchè su tali tracce l'azione del fading non è avvertibile, essendo molto più lunghe e mancando il taglio sulle proiezioni orizzontali.

In tabella II diamo il flusso dei neutroni alle due altezze; tale flusso è stato

TABELLA II.

Flusso dei neutroni d. cm^{-2}	Dalla reazione $^{10}B(n, \alpha)$	Dalla reazione $^{6}Li(n, \alpha)$
Livello del mare (Palermo)	$18,3 \pm 0,5$	$43,5 \pm 0,8$
4550 m s.l.d.m. (Monte Rosa)	$267,5 \pm 4,2$	$539 \pm 6,2$
Flusso dei neutroni d. cm^{-2} a 4550 m / Flusso dei neutroni d. cm^{-2} al l.d.m.	$14,6 \pm 0,6$	$12,4 \pm 0,36$

calcolato con il numero dei neutroni per cm^2 ricavato dai valori sperimentali. Il flusso dei neutroni calcolato coi dati ottenuti dalla reazione $^{10}B(n, \alpha)$ non è uguale a quello calcolato coi dati ottenuti dalla reazione $^{6}Li(n, \alpha)$; questo perchè nel calcolo del flusso abbiamo usato il numero di mg di Li e di B per cm^3 di emulsione secca dato da KAPLAN e da YAGODA [1]. Ma il valore del rapporto tra il flusso dei neutroni alle due altezze, calcolato coi dati ottenuti dalla reazione $^{10}B(n, \alpha)$, è abbastanza in accordo col valore del rapporto, calcolato coi dati ottenuti dalla reazione $^{6}Li(n, \alpha)$; entrambi questi valori sono in buon accordo con quanto hanno trovato altri autori [1,4]. Il numero dei neutroni ricavato dai valori sperimentali è stato corretto per i neutroni termici atmosferici, che hanno colpito le lastre nel periodo di tempo trascorso tra il caricamento e l'esposizione in paraffina; tale correzione è stata fatta con il valore dato da KAPLAN e YAGODA [1] del flusso dei neutroni termici atmosferici al livello del mare.

Dai nostri dati si ricava un l.c.m. di 158 ± 5 g·cm^{-2} per la radiazione che genera i neutroni. Tale valore è in accordo con quello trovato da altri autori [1,5], ed è uguale al l.c.m. della radiazione che genera le disintegrazioni nucleari; i neutroni da noi registrati, avendo un'energia compresa fra 2 e 15 MeV, debbono essere generati nelle disintegrazioni nucleari che avvengono nelle immediate vicinanze dell'apparato sperimentale e nella paraffina stessa.

Dato che i risultati trovati sono in accordo con quelli di altri autori, che eseguono le loro ricerche con altri metodi, possiamo dire che la componente neutronica può essere studiata anche col metodo delle lastre per ricerche nucleari caricate con borato di litio. È però necessario fare una taratura preventiva delle lastre con una sorgente di neutroni d'intensità nota e mettersi in condizioni tali da rendere minimo il fading.

[4] C. C. MONTGOMERY e A. R. TOBEY: *Phys. Rev.*, **75**, 1478 (1949).

[5] J. A. SIMPSON: *Phys. Rev.*, **83**, 1175 (1951).

Decadimento in quiete di una particella di massa iperprotonica.

C. Castagnoli, G. Cortini e A. Manfredini

Istituto di Fisica dell'Università - Roma
Istituto Nazionale di Fisica Nucleare - Sezione di Roma

(ricevuto il 6 Agosto 1954)

Nel corso dell'esplorazione di un pacco di lastre fotografiche esposte durante la spedizione internazionale di Cagliari dell'estate 1953, abbiamo trovato un evento in cui una particelle uscente da una stella $p(17,3)10$, dopo un percorso di 1250 μ in un'unica lastra, si riduce in quiete e dal suo punto di arresto parte una particella di massa certamente maggiore della massa del mesone π. Questa particella secondaria si arresta dopo aver percorso 1675 ± 37 μ, in due lastre. L'errore sul percorso comprende lo «straggling» e l'errore di taratura da cui è affetta la misura del potere frenante delle nostre emulsioni; l'errore sperimentale di misura risulta trascurabile perchè la traccia è inclinata in media sul piano della lastra di soli $\sim 10°$. La distorsione è stata misurata, e la relativa correzione sul percorso (già computata nel dato sopra citato) ammonta a 26 μ. I punti di partenza e di arrivo della traccia secondaria non rivelano il minimo indizio di fenomeni nucleari di qualsiasi tipo.

La massa della particella primaria risulta, in base alle misure:

a) di scattering [1]: $M_p = 2800^{+1500}_{-900}\ m_e$

b) di lacune [2]: $M_p = 2670 \pm 500\ m_e$

La somiglianza di questo evento con quelli descritti da Bonetti *et al.* [3] e da Baldo *et al.* [4], in particolare la concordanza del percorso del secondario, suggerisce immediatamente la interpretazione

$$Y^+ \to P + \pi^0 + Q\,,$$

proposta dagli autori citati. Accettata tale ipotesi, utilizzando la relazione energia-percorso, che attualmente sembra la migliore [5] e il più recente valore della massa del mesone π^0 [6], dal percorso del secondario si deduce:

$$Q = 117.0 \pm 1.3\ \text{MeV}\,.$$

Le misure di massa eseguite sulla particella secondaria con il metodo dello

[1] C. C. Dilworth, S. J. Goldsack e L. Hirschberg: *Nuovo Cimento*, **11**, 113 (1954).

[2] G. Baroni e C. Castagnoli: *Congresso di Padova*, Aprile 1954.

[3] A. Bonetti, R. Levi Setti, M. Panetti e G. Tomasini: *Nuovo Cimento*, **10**, 1736 (1953).

[4] M. Baldo, G. Belliboni, M. Ceccarelli e B. Vitale: *Congresso di Padova*, Aprile 1954.

[5] G. Baroni, C. Castagnoli, G. Cortini, C. Franzinetti e A. Manfredini: *Comunicato al Secretariat on Stand. of Measur. in Phot. Em.*, Ginevra.

[6] W. Chinowsky e J. Steinberger: *Phys. Rev.*, **93**, 586 (1954).

scattering a sagitta costante e con il metodo delle lacune danno sicura indicazione di una massa superiore a quella del mesone. La sua sicura identificazione con un protone rende però necessario un esteso lavoro di taratura sulla lastra in cui l'evento ha luogo (e nella quale il secondario svolge gran parte del suo percorso), taratura attualmente in corso.

È interessante osservare che tra le tracce associate con la stella da cui ha origine l'evento ora discusso è stato identificato un mesone K che si ferma in emulsione dopo un percorso di 2.20 mm (in 3 lastre) e decade in una particella al minimo di ionizzazione. Entrambe le tracce sono inclinate. La misura di scattering sul primario indica che la massa è inferiore a quella del protone.

La produzione in coppia di mesoni K ed iperoni, prevista, ad esempio, dalle teorie di NAMBU *et al.* [7] e PAIS [8] è già stata osservata in lastre esposte ai raggi cosmici da LAL *et al.* [9] in due casi, ed in altri due da DAHANAYAKE *et al.* [10].

Poichè negli esperimenti di Brookhaven [11] è stata decisivamente confermata l'esistenza della reazione

$$\pi^- + P \rightarrow Y + K \quad (\pi^- \text{ da } 1{,}37 \text{ GeV})$$

seguendo l'analisi di DAHANAYAKE *et al.* è legittimo interpretare la produzione della coppia di particelle instabili da noi osservata come una reazione del tipo

$$\pi + N \rightarrow K + Y \quad (N = \text{nucleone}).$$

Resta così confermato che molto spesso gli Y e K creati nelle stelle di alta energia sono prodotti in associazione.

[7] Y. NAMBU, K. NISHIJNA e Y. YAMAGUCHI: *Prog. Theor. Phys.*, **6**, 615 (1951).

[8] A. PAIS: *Phys. Rev.*, **86**, 663 (1952).

[9] D. LAL, YASH PAL e B. PETERS: *Proc. Ind. Acad. Sci.*, **38**, 398 (1953).

[10] C. DAHANAYAKE, P. E. FRANCOIS, Y. FUJIMOTO, P. IREDALE, C. Y. WADDINGTON e M. YASIN: Comunicazione privata.

[11] W. B. FOWLER, R. P. SHUTT, M. THORNDIKE e W. L. WITTEMORE: *Phys. Rev.*, **93**, 861 (1954).

An Unstable Fragment and a Positive τ-Meson Emitted in a Nuclear Disintegration.

A. Debenedetti, C. M. Garelli, L. Tallone and M. Vigone
Istituto Nazionale di Fisica Nucleare - Sezione di Torino

(ricevuto l'8 Agosto 1954)

Considerable evidence of the delayed disintegration of unstable fragments has been collected so far from observations in nuclear plates [1]. To our knowledge, in four cases a π-meson has been observed among the disintegration products. In the event described by Bonetti *et al.* [2], the experimental data are consistent with the assumption of the disintegration of an excited triton, following the scheme:

$$(1) \qquad {}_1^3\mathrm{H}^* \rightarrow {}_2^3\mathrm{He} + \pi^- + Q$$

$$Q = 41.7 \pm 1 \text{ MeV}.$$

An event which can be interpreted with the same scheme of decay was observed in this laboratory during the general scanning of a stack of stripped emulsions, flown at 89000 ft in the Sardinia Expedition 1953.

The unstable particle (track *f*, Fig. 1) is ejected from a star of the type $21+7\mathrm{p}_s$. It travels 1490 μ in two plates, and appears to disintegrate at rest in two charged particles (tracks *a*, *b*, Fig. 2). The heavily ionizing track *a* is emitted nearly in the backward direction, and has a range of 9 μ; the fast one, *b*, is ejected in the opposite direction, and has a ionisation of 1.7 the « plateau ». It travels 14 plates and escapes from the stack after a range of 17300 μ. The two lines tangent to the track are collinear within the experimental errors. The uncertainty of 2° is due to the short range of the black track. The two tracks are contained in a plane nearly perpendicular to the plane of the emulsion and their direction makes an angle of 20° with the direction of the parent particle. The geometry of the event suggests the hypothesis of a two body decay.

From the analysis of δ-rays we find that the primary particle is singly charged.

Scattering-range measurements with constant sagitta [3] give for the mass of

[1] See: *Reports of Padua meeting*, April 1954, *Nuovo Cimento* (to be published).

[2] A. Bonetti, R. Levi Setti, M. Panetti, L. Scarsi e G. Tommasini: *Nuovo Cimento*, **11**, 210 e 330 (1954).

[3] C. Dilworth, S. J. Goldsack, M. Hirschberg: *Nuovo Cimento*, **11**, 113 (1954).

the parent particle the value:

$$M_f = 4\,830 \pm 1\,400 \text{ m}_e .$$

The distortion has been checked by third differences, and has been found unimportant.

We also carried out ionisation-range measurements. For this purpose, we made the calibration on proton tracks coming to rest in the same plate at approximately the same depth and with the same angle of dip. The mass value obtained is

$$M_f = 5\,300 \pm 900 \text{ m}_e .$$

Therefore the primary particle is a particle of mass number 3, and charge 1, that is a $^3_1$H-nucleus.

On the fast secondary we made ionisation and scattering measurements. In the first 2 mm of the track from the point of emission, we have the following values:

$$\alpha_{100} = 0.636^\circ \pm 0.06^\circ$$

$$b^* = 1.70 \pm 0.08 .$$

From these results we conclude that the particle is a light meson.

Fig. 1.

The charge conservation requires the light meson to be negatively charged. Consequently the other disintegration product must have a charge +2. For this reason and from the value of the primary mass, we deduce that the hypothesis of a disintegration represented by the scheme (1) appears to be likely According to this assumption, the fast secondary is a π-meson. We carried out scattering measurements on the full length of the track. These measurements

have been made following the suggestions of the Bureau of Standards; the scattering constant has been obtained from the curves given by VOYVODIC and PICKUP (4); the standard error on the $p\beta$ has been increased by 8% because we have no calibration for the scattering constant. The momentum of emission can be deduced from the mean angle of scattering in various sections of the track, making use of the range-energy relation A good consistency is obtained between the values thus calculated. We find:

$$E_\pi = 40.2 \pm 6 \text{ MeV},$$

$$p_\pi = 113.3 \pm 8 \text{ MeV/c}.$$

Moreover ionisation-measurements have been performed on the various sections of the track. The calibration has been made by determining the ionisation-range plot for a large number of π-mesons tracks. We obtain:

$$E_\pi = 39.6 \pm 3 \text{ MeV},$$

$$p_\pi = 112.4 \pm 5 \text{ MeV/c}.$$

The weighted mean of the two results is therefore:

$$E_\pi = 39.8 \pm 4 \text{ MeV},$$

$$p_\pi = 112.4 \pm 5 \text{ MeV/c}.$$

The energy of the heavy secondary can be deduced both from its range and from the conservation of momentum. We find:

$$E_{^3_2\text{He}} = 2.66 \pm 0.7 \text{ MeV}$$

(from the range-energy relation)

$$E_{^3_2\text{He}} = 2.26 \pm 0.26 \text{ MeV}$$

(from the momentum balance).

The good agreement between these figures strongly supports our assumptions.

The energy release of the disintegration is:

$$Q = 42.06 \pm 4.2 \text{ MeV}.$$

Conclusions.

Our present data confirm the hypothesis that an excited $^3_1$H nucleus may be ejected in nuclear interactions: in such an excited state, it is assumed that the last neutron of the nucleus is replaced by a Λ^0 particle.

The quantity Δ:

$$\Delta = m_{^3_2\text{He}} + m_{\pi^-} + Q - m_{^3_1\text{H}} - (m_{\Lambda^0} - m_n)$$

has in the present case the value:

$$\Delta = 6.0 \pm 4.2 \text{ MeV},$$

if we take for the Λ^0 mass the best estimate given by FRIEDLANDER *et al.* (5):

$$m_{\Lambda^0} = 2181 \pm 1 \text{ m}_e.$$

The binding energy of the Λ^0 turns out to be: $B = 0.24 \pm 4$ MeV.

The time of flight of the fragment is:

$$\tau = 4 \cdot 10^{-11} \text{ s}.$$

From the same star a positive τ-meson is ejected. It travels 17 mm in 10 plates. Two of the three π-mesons emitted come

Charge		Range	Number of plates
π_1	—	14130 ± 150 μ	6
π_2	+	6050 ± 250 μ	11
π_3	+	10700 ± 200 μ	11

(4) L. VOYVODIC e E. PICKUP: *Phys. Rev.*, **85**, 91 (1952).

(5) M. W. FRIEDLANDER, D. KEEFE, M. G. K. MENON e M. MERLIN: *Phil. Mag.*, **45**, 553 (1954).

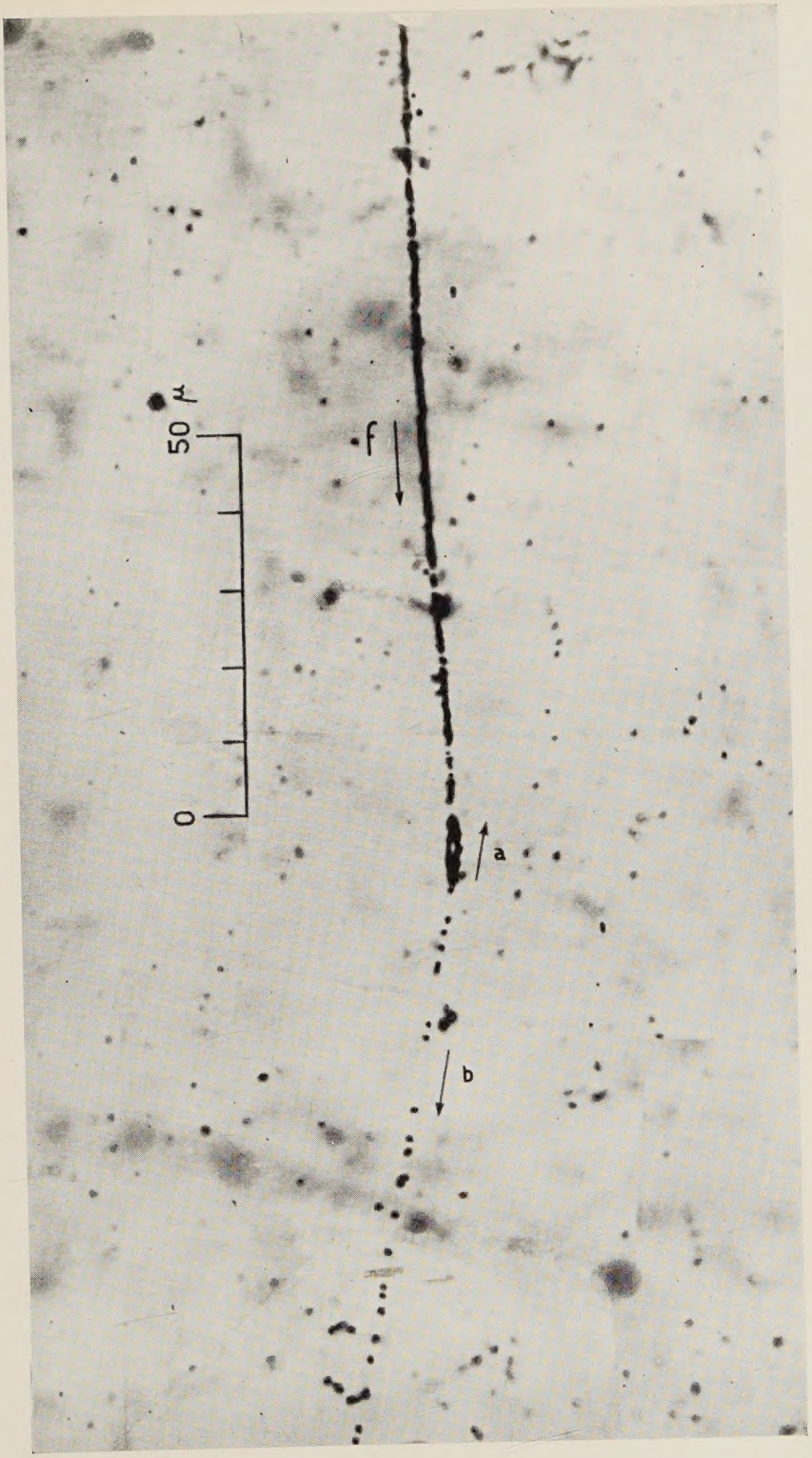

Fig. 2.

to rest in the emulsion and suffer $\pi \to \mu \to e$ decay. The negative one, after 14 130 μ, gives rise to a two pronged star before the end of its range.

The energy of π_1-meson has been deduced both from momentum balance and from direct scattering measurements.

The values obtained are the following:

	From Range	From momentum balance	From scattering measurements
E_{π_1}	—	30.7 ± 1.5 MeV	30.8 ± 6 MeV
E_{π_2}	17.06 ± 0.85 MeV	—	—
E_{π_3}	23.61 ± 0.84 MeV	—	—

The angles are:

$$\varphi_{\pi_2\pi_3} = 102^\circ\, 50' \pm 30'$$

$$\varphi_{\pi_1\pi_3} = 133^\circ\, 35' \pm 30'$$

$$\varphi_{\pi_1\pi_2} = 123^\circ\, 34' \pm 30'$$

The energy of π_2 and π_3 has been calculated from the range using the relation [5]:

$$E = kR^{0,568}\left(\frac{m_\pi}{m_p}\right)^{0,432}$$

k has been determined from range measurements of μ coming from $\pi \to \mu$ decay,

The Q-value of the τ-meson is:

$$Q = 71.4 \pm 3.2 \text{ MeV}.$$

This is the second example of a star emitting two heavy particles observed in our laboratory [6]. An analysis of these events is in progress.

We are indebted to Professors R. Deaglio, G. Lovera and G. Wataghin for helpful discussions.

The event studied in this paper was found by Miss T. Sappia and Mr. M. Greco, whom we wish to thank for the photograph.

[6] A. Debenedetti, C. M. Garelli, L. Tallone e M. Vigone: *Nuovo Cimento*, **12**, 369 (1954).

ERRATA-CORRIGE

E. Corinaldesi – **Construction of Potentials from Phase Shift and Binding Energies of Relativistic Equations**, *Nuovo Cimento*, **11**, 468 (1954).

The factors $-2i$ in eqs. (30) and (A 10), and $i/2$ in eq. (31) should be omitted, being due to an oversight.

Direttore responsabile: G. POLVANI

Tipografia Compositori - Bologna

Questo fascicolo è stato licenziato dai torchi il 23-VIII-1954.